THE QUARTERLY JOURNAL OF MECHANICS AND APPLIED MATHEMATICS

VOLUME VIII
1955

OXFORD
AT THE CLARENDON PRESS

Oxford University Press, Amen House, London E.C.4
GLASGOW NEW YORK TORONTO MELBOURNE WELLINGTON
BOMBAY CALCUTTA MADRAS KARACHI CAPE TOWN IBADAN
Geoffrey Cumberlege, Publisher to the University

PRINTED IN GREAT BRITAIN
AT THE UNIVERSITY PRESS, OXFORD
BY CHARLES BATEY, PRINTER TO THE UNIVERSITY

THE CHARACTER OF THE EQUILIBRIUM OF AN INCOMPRESSIBLE FLUID SPHERE OF VARIABLE DENSITY AND VISCOSITY SUBJECT TO RADIAL ACCELERATION

By S. CHANDRASEKHAR

(*Yerkes Observatory and Institute for Nuclear Studies, University of Chicago*)

[Received 13 April 1954]

SUMMARY

This paper is devoted to a consideration of the following problem: An incompressible fluid sphere, in which the density and the viscosity are functions of the distance r from the centre only, is subject to a radial acceleration $-\gamma r$, where γ is a function of r: to determine the manner of initial development of an infinitesimal disturbance. By analysing the disturbance in spherical harmonics, the mathematical problem is reduced to one in characteristic values in a fourth-order differential equation and a variational principle characterizing the solution is enunciated. The particular case of a sphere of radius R and density ρ_1 embedded in a medium of a different density ρ_2 (but of the same kinematic viscosity ν) is considered in some detail; and it is shown that the character of the equilibrium depends on the sign of $\gamma_R(\rho_2-\rho_1)$ and the magnitude of $\mathfrak{G} = \gamma_R R^4/\nu^2$. If $\gamma_R(\rho_2-\rho_1) > 0$, the situation is unstable and the mode of maximum instability is $l = 1$ for all $\mathfrak{G} < 230$; for larger values of $\mathfrak{G}$ it shifts progressively to higher harmonics. In the case $\gamma_R(\rho_2-\rho_1) > 0$ the results of both an exact calculation and an approximate calculation (based on the variational principle) are given and contrasted. In the case $\gamma_R(\rho_2-\rho_1) < 0$ when the situation is stable, the manner of decay of the disturbance is briefly discussed in terms of an approximate theory only.

1. Introduction

The character of the equilibrium of an incompressible heavy fluid of variable density stratified in parallel planes has been the subject of investigations by Rayleigh (**1**), Harrison (**2**), Lamb (**3**), Chandrasekhar (**4**), and Hide (**5**). But the related problem of the equilibrium of an incompressible fluid sphere of variable density and viscosity does not seem to have attracted any attention, though as an example of a problem in hydrodynamic stability it has a definite interest. The problem recently arose in connexion with certain geophysical and astrophysical questions; and the solution (on a certain approximation) is presented here with a view to those applications.

2. The equations of the problem

A static state in which an incompressible fluid subject to radial acceleration is arranged in concentric shells and the pressure p and the density ρ are functions of the distance r from the centre only is clearly a kinematically

realizable one. The character of the equilibrium of this static state can be analysed by supposing that there is a slight disturbance and then following its further evolution. Let the actual density at any point x_i $(i = 1, 2, 3)$ following the disturbance be $\rho+\delta\rho$, where $\delta\rho$ is a function of x_i and the time t. Let δp be the corresponding increment in the pressure; δp will also be a function of x_i and t. Finally, let u_i $(i = 1, 2, 3)$ denote the components of the velocity; u_i (like $\delta\rho$ and δp) will be considered as a small quantity of the first order.

In formulating the relevant equations of motion we shall make the simplifying assumption that the changes in the prevailing field of force caused by the disturbance can be ignored. In the case of a fluid sphere in equilibrium under its own gravitation this assumption will be justified only if the variations in the initial density distribution over the relevant distances are small compared with the mean density: in other words, the theory we shall present will provide the asymptotically correct solution *either* when the variations in density become very small *or* when the order of the spherical harmonic disturbance considered becomes very large (cf. Cowling (**6**) and Ledoux (**7**)). Alternatively, the theory may also be considered as applying when the prevailing field of force is of 'external origin' such as a source of intense radiation at the centre. Equally, the theory will also apply to a spherical shell of fluid subject to an acceleration (caused by an 'explosion' (say) at the centre) which impinges on the surrounding medium.

On the assumption made in the foregoing paragraph, the equations of motion and continuity in Cartesian tensor notation are

$$\rho\frac{\partial u_i}{\partial t} = -\frac{\partial}{\partial x_i}\delta p+\frac{\partial}{\partial x_k}p_{ik}-g_i\,\delta\rho \tag{1}$$

and

$$\frac{\partial u_i}{\partial x_i} = 0, \tag{2}$$

where (in accordance with the assumption) the acceleration g_i (unaffected by the disturbance) is of the form

$$g_i = \gamma(r)x_i; \tag{3}$$

$\gamma(r)$, as the notation implies, is a function of r only. Also, in equation (1), p_{ik} is the viscous stress tensor given by

$$p_{ik} = \mu\left(\frac{\partial u_k}{\partial x_i}+\frac{\partial u_i}{\partial x_k}\right), \tag{4}$$

where μ (which is a function of r) denotes the coefficient of viscosity. In addition to equations (1) and (2) we have the equation

$$\frac{\partial}{\partial t}\delta\rho+u_i\frac{\partial\rho}{\partial x_i} = 0, \tag{5}$$

which ensures that the density of every element of liquid remains unchanged.

Inserting equation (4) in equation (1) and making use of the solenoidal character of u_i, we find

$$\rho\frac{\partial u_i}{\partial t} = -\frac{\partial}{\partial x_i}\delta p+\mu\nabla^2 u_i+\left(\frac{\partial u_k}{\partial x_i}+\frac{\partial u_i}{\partial x_k}\right)\frac{\partial \mu}{\partial x_k}-\gamma\,\delta\rho\, x_i; \tag{6}$$

or, since

$$\frac{\partial \mu}{\partial x_k} = \frac{x_k}{r}\frac{d\mu}{dr}, \tag{7}$$

we have

$$\rho\frac{\partial u_i}{\partial t} = -\frac{\partial}{\partial x_i}\delta p+\mu\nabla^2 u_i+\frac{x_k}{r}\left(\frac{\partial u_i}{\partial x_k}+\frac{\partial u_k}{\partial x_i}\right)\frac{d\mu}{dr}-\gamma x_i\,\delta\rho. \tag{8}$$

Similarly, equation (5) can be rewritten in the form

$$\frac{\partial}{\partial t}\delta\rho+u_r\frac{d\rho}{dr} = 0, \tag{9}$$

where

$$u_r = u_i x_i/r \tag{10}$$

is the radial component of the velocity.

We shall seek solutions of equations (8) and (9) whose dependence on t is given by the factor

$$e^{nt} \tag{11}$$

where n is a constant. For solutions having this dependence on time, equations (8) and (9) become

$$\frac{\partial}{\partial x_i}\delta p = -(n\rho u_i+\gamma x_i\,\delta\rho)+\mu\nabla^2 u_i+\frac{x_k}{r}\left(\frac{\partial u_i}{\partial x_k}+\frac{\partial u_k}{\partial x_i}\right)\frac{d\mu}{dr}, \tag{12}$$

and

$$\delta\rho = -\frac{u_r}{n}\frac{d\rho}{dr}. \tag{13}$$

Multiplying equation (12) by x_i/r and remembering that

$$x_i\frac{\partial}{\partial x_i} = r\frac{\partial}{\partial r}, \tag{14}$$

we get

$$\frac{\partial}{\partial r}\delta p = -(n\rho u_r+\gamma r\,\delta\rho)+\frac{\mu}{r}x_i\,\nabla^2 u_i+2\frac{d\mu}{dr}\frac{x_i x_k}{r^2}\frac{\partial u_i}{\partial x_k}; \tag{15}$$

or, since

$$\frac{x_i x_k}{r^2}\frac{\partial u_i}{\partial x_k} = \frac{1}{r^2}\left(x_k\frac{\partial}{\partial x_k}u_i x_i-u_i x_i\right) = \frac{1}{r}\left\{\frac{\partial}{\partial r}(ru_r)-u_r\right\} = \frac{\partial u_r}{\partial r}, \tag{16}$$

and the operations of x_i and ∇^2 are permutable when applied to a solenoidal vector, we have

$$\frac{\partial}{\partial r}\delta p = -(n\rho u_r+\gamma r\,\delta\rho)+\frac{\mu}{r}\nabla^2(ru_r)+2\frac{d\mu}{dr}\frac{\partial u_r}{\partial r}. \tag{17}$$

Next, taking the divergence of equation (12), we get

$$\nabla^2 \delta p = -\left\{nu_r \frac{d\rho}{dr} + 3\gamma\,\delta\rho + r\frac{\partial}{\partial r}(\gamma\,\delta\rho)\right\} + \frac{1}{r}\frac{d\mu}{dr}\nabla^2(ru_r) + \\ + \frac{\partial}{\partial x_i}\left\{\frac{x_k}{r}\left(\frac{\partial u_i}{\partial x_k} + \frac{\partial u_k}{\partial x_i}\right)\frac{d\mu}{dr}\right\}. \quad (18)$$

Again, using the solenoidal property of u_i, we can reduce the last term on the right-hand side of equation (18) in the manner (cf. equation (16))

$$\frac{\partial}{\partial x_i}\left\{\frac{1}{r}\frac{d\mu}{dr}x_k\left(\frac{\partial u_i}{\partial x_k} + \frac{\partial u_k}{\partial x_i}\right)\right\}$$
$$= \frac{2}{r}\frac{d}{dr}\left(\frac{1}{r}\frac{d\mu}{dr}\right)x_i x_k \frac{\partial u_i}{\partial x_k} + \frac{1}{r}\frac{d\mu}{dr}\left\{\delta_{ik}\left(\frac{\partial u_i}{\partial x_k} + \frac{\partial u_k}{\partial x_i}\right) + x_k \nabla^2 u_k\right\}$$
$$= 2r\frac{d}{dr}\left(\frac{1}{r}\frac{d\mu}{dr}\right)\frac{\partial u_r}{\partial r} + \frac{1}{r}\frac{d\mu}{dr}\nabla^2(ru_r). \quad (19)$$

Hence

$$\nabla^2 \delta p = -\left\{nu_r \frac{d\rho}{dr} + 3\gamma\,\delta\rho + r\frac{\partial}{\partial r}(\gamma\,\delta\rho)\right\} + \frac{2}{r}\frac{d\mu}{dr}\nabla^2(ru_r) + 2r\frac{d}{dr}\left(\frac{1}{r}\frac{d\mu}{dr}\right)\frac{\partial u_r}{\partial r}. \quad (20)$$

Equations (13), (17), and (20) are the basic equations of this theory.

3. The equation for determining the rate of growth of a spherical harmonic disturbance of order l

We shall seek solutions of equations (13), (17), and (20) which are of the forms

$$\delta p = \varpi Y_l(\vartheta, \varphi), \qquad \delta\rho = \sigma Y_l(\vartheta, \varphi), \quad \text{and} \quad u_r = wY_l(\vartheta, \varphi), \quad (21)$$

where $Y_l(\vartheta, \varphi)$ is a spherical harmonic of order l and ϖ, σ, and w are functions of r only. For solutions of this form, the equations reduce to

$$\left\{\frac{d^2}{dr^2} + \frac{2}{r}\frac{d}{dr} - \frac{l(l+1)}{r^2}\right\}\varpi = -\left\{nw\frac{d\rho}{dr} + 3\gamma\sigma + r\frac{d}{dr}(\gamma\sigma)\right\} + \\ + \frac{2}{r}\frac{d\mu}{dr}\left\{\frac{d^2}{dr^2} + \frac{2}{r}\frac{d}{dr} - \frac{l(l+1)}{r^2}\right\}(rw) + 2r\frac{d}{dr}\left(\frac{1}{r}\frac{d\mu}{dr}\right)\frac{dw}{dr}, \quad (22)$$

$$\frac{d\varpi}{dr} = -(n\rho w + \gamma r\sigma) + \frac{\mu}{r}\left\{\frac{d^2}{dr^2} + \frac{2}{r}\frac{d}{dr} - \frac{l(l+1)}{r^2}\right\}(rw) + 2\frac{d\mu}{dr}\frac{dw}{dr} \quad (23)$$

and

$$\sigma = -\frac{w}{n}\frac{d\rho}{dr}. \quad (24)$$

Letting

$$F = \left\{\frac{d^2}{dr^2} + \frac{2}{r}\frac{d}{dr} - \frac{l(l+1)}{r^2}\right\}(rw), \quad (25)$$

we shall rewrite equations (22) and (23) as

$$\frac{d}{dr}\left(r^2\frac{d\varpi}{dr}\right)-l(l+1)\varpi = -\left\{nr^2w\frac{d\rho}{dr}+\frac{d}{dr}(r^3\gamma\sigma)\right\}+2r\frac{d\mu}{dr}F+2r^3\frac{d}{dr}\left(\frac{1}{r}\frac{d\mu}{dr}\right)\frac{dw}{dr} \tag{26}$$

and

$$\frac{d\varpi}{dr} = -(n\rho w+\gamma r\sigma)+\frac{\mu}{r}F+2\frac{d\mu}{dr}\frac{dw}{dr}. \tag{27}$$

By differentiating equation (26) with respect to r and eliminating $d\varpi/dr$ between the resulting equation and equation (27), we obtain

$$\begin{aligned}\frac{d^2}{dr^2}\left\{r^2\left[-(n\rho w+\gamma r\sigma)+\frac{\mu}{r}F+2\frac{d\mu}{dr}\frac{dw}{dr}\right]\right\}&-\\ -l(l+1)\left\{-(n\rho w+\gamma r\sigma)+\frac{\mu}{r}F+2\frac{d\mu}{dr}\frac{dw}{dr}\right\}&+\\ +\frac{d}{dr}\left\{nr^2w\frac{d\rho}{dr}+\frac{d}{dr}(r^3\gamma\sigma)-2r\frac{d\mu}{dr}F-2\left(r^2\frac{d^2\mu}{dr^2}-r\frac{d\mu}{dr}\right)\frac{dw}{dr}\right\} &= 0.\end{aligned} \tag{28}$$

After some further reductions equation (28) can be brought to the form

$$\begin{aligned}-n\frac{d}{dr}\left\{\rho\frac{d}{dr}(r^2w)\right\}+\frac{d}{dr}\left\{\mu\frac{d}{dr}(rF)\right\}+\frac{d}{dr}\left\{rF\frac{d\mu}{dr}\right\}&-\\ -2\frac{d}{dr}\left\{\frac{d\mu}{dr}\left[r\frac{dw}{dr}+2w-l(l+1)w\right]\right\}&+\\ +l(l+1)\left\{n\rho w-\frac{\mu}{r}F-2\frac{d\mu}{dr}\frac{dw}{dr}\right\} &= -l(l+1)\gamma r\sigma.\end{aligned} \tag{29}$$

Now it can be readily verified that

$$rF-2\left\{r\frac{dw}{dr}+2w-l(l+1)w\right\} = r\left\{\frac{d^2W}{dr^2}+(l+2)(l-1)\frac{W}{r^2}\right\}, \tag{30}$$

where

$$W = rw. \tag{31}$$

Substituting from equations (24) and (30) in equation (29) we finally obtain, after some rearrangement of the terms:

$$\begin{aligned}\frac{d}{dr}\left\{\rho\frac{d}{dr}(rW)-\frac{\mu}{n}\frac{d}{dr}(rF)\right\}&-\\ -\frac{1}{n}\frac{d}{dr}\left\{r\frac{d\mu}{dr}\left[\frac{d^2W}{dr^2}+(l+2)(l-1)\frac{W}{r^2}\right]\right\}&-\frac{l(l+1)}{r}\left(\rho W-\frac{\mu}{n}F\right)\\ &= -\frac{l(l+1)}{n^2}\left\{\gamma W\frac{d\rho}{dr}+2n\frac{d\mu}{dr}\frac{dw}{dr}\right\},\end{aligned} \tag{32}$$

where it may be recalled that

$$F = \left\{\frac{d^2}{dr^2}+\frac{2}{r}\frac{d}{dr}-\frac{l(l+1)}{r^2}\right\}W. \tag{33}$$

Equations (32) and (33) together represent a fourth-order differential equation for W. In seeking a solution of these equations we must satisfy certain conditions at the centre and on the bounding sphere. At the centre we must clearly require that none of the physical quantities has any singularity; this requires in particular that (cf. equation (31))

$$W \to 0 \quad \text{as } r \to 0. \tag{34}$$

And on the bounding sphere we must have

$$W = 0 \text{ and either } \frac{dW}{dr} \text{ or } \frac{d^2W}{dr^2} = 0 \text{ (on the bounding sphere)}, \tag{35}$$

depending on whether the bounding surface is rigid or free† (cf. Jeffreys and Bland (**8**); and Chandrasekhar (**9**)). The requirement that a solution of equations (32) and (33) satisfies the foregoing boundary conditions will determine a sequence of possible values for n; and the sign and the magnitude of the real part of n will decide whether or not the initial state is stable for a spherical harmonic disturbance of order l and will determine the rate of decay (or growth) of the disturbance.

4. A fluid sphere of constant density and viscosity in an infinite medium of different density and viscosity

We shall first apply the equation derived in the preceding section to the case when a fluid sphere of radius R, density ρ_1, and viscosity μ_1 is embedded in an infinite medium of density ρ_2 and viscosity μ_2. In each of the two regions of constant ρ and μ, equation (32) reduces to

$$\rho\frac{d^2}{dr^2}(rW)-\frac{\mu}{n}\frac{d^2}{dr^2}(rF)-\frac{l(l+1)}{r}\left(\rho W-\frac{\mu}{n}F\right)=0, \tag{36}$$

where, for the present, we are suppressing the subscripts distinguishing the two regions.

Equation (36) can be written alternatively in the form

$$\left\{\frac{d^2}{dr^2}+\frac{2}{r}\frac{d}{dr}-\frac{l(l+1)}{r^2}\right\}\left(W-\frac{\nu}{n}F\right)=0, \tag{37}$$

where $\nu = \mu/\rho$ denotes the coefficient of kinematic viscosity. The general solution of this equation is

$$W-\frac{\nu}{n}F = A_1 r^l + A_2 r^{-(l+1)}, \tag{38}$$

† In the present connexion a free bounding surface is equivalent to an interface with a frictionless surface.

where A_1 and A_2 are constants of integration. Using this solution in equation (33) we have

$$\left\{\frac{d^2}{dr^2}+\frac{2}{r}\frac{d}{dr}-\frac{l(l+1)}{r^2}\right\}W = \frac{n}{\nu}\{W-A_1 r^l-A_2 r^{-(l+1)}\}. \tag{39}$$

A particular integral of this equation is clearly

$$W = A_1 r^l+A_2 r^{-(l+1)}, \tag{40}$$

while the complementary function is a linear combination of the integrals

$$\frac{1}{\sqrt{r}}I_{l+\frac{1}{2}}\{r\sqrt{(n/\nu)}\} \quad \text{and} \quad \frac{1}{\sqrt{r}}K_{l+\frac{1}{2}}\{r\sqrt{(n/\nu)}\}, \tag{41}$$

where $I_{l+\frac{1}{2}}$ and $K_{l+\frac{1}{2}}$ are the Bessel functions of the two kinds for a purely imaginary argument. (Strictly speaking, we should, without 'prejudice', express the complementary function as a linear combination of $J_{l+\frac{1}{2}}$ and $J_{-(l+\frac{1}{2})}$ with the argument $r\sqrt{(-n/\nu)}$ and allow n to be complex; but we are expressing the solution as a linear combination of $I_{l+\frac{1}{2}}$ and $K_{l+\frac{1}{2}}$ with the argument $r\sqrt{(n/\nu)}$ since we shall be particularly interested in the unstable case when n is real and positive.) The general solution of equation (37) is therefore

$$W = A_1 r^l+A_2 r^{-(l+1)}+\frac{B_1}{\sqrt{r}}I_{l+\frac{1}{2}}\{r\sqrt{(n/\nu)}\}+\frac{B_2}{\sqrt{r}}K_{l+\frac{1}{2}}\{r\sqrt{(n/\nu)}\}, \tag{42}$$

where B_1 and B_2 are further constants of integration.

Since W must vanish both when $r \to 0$ (in the 'core') and when $r \to \infty$ (in the 'mantle') we can write

$$W_1 = A_1 r^l+\frac{B_1}{\sqrt{r}}I_{l+\frac{1}{2}}\{r\sqrt{(n/\nu_1)}\} \quad (r \leqslant R) \tag{43}$$

and

$$W_2 = A_2 r^{-(l+1)}+\frac{B_2}{\sqrt{r}}K_{l+\frac{1}{2}}\{r\sqrt{(n/\nu_2)}\} \quad (r \geqslant R), \tag{44}$$

as the solutions appropriate for the core and the mantle respectively.

On the interface ($r = R$) the components of the velocity as well as the tangential viscous stresses should be continuous. These conditions require (cf. Jeffreys and Bland (**8**)) that

$$W, \quad \frac{dW}{dr}, \quad \text{and} \quad \mu\left\{r^2\frac{d^2W}{dr^2}+(l+2)(l-1)W\right\} \tag{45}$$

are continuous on the interface $r = R$.

A further boundary condition is obtained by integrating equation (32) across the interface $r = R$ between $r = R+\epsilon$ and $r = R-\epsilon$ ($\epsilon > 0$)

and then letting $\epsilon \to 0$. In view of the continuity conditions (45) this limiting process leads to

$$\rho_2\left[\frac{d}{dr}\left\{r\left(W_2-\frac{\nu_2}{n}F_2\right)\right\}\right]_{r=R}-\rho_1\left[\frac{d}{dr}\left\{r\left(W_1-\frac{\nu_1}{n}F_1\right)\right\}\right]_{r=R}$$
$$= -\frac{l(l+1)}{n^2}\left\{\gamma_R(\rho_2-\rho_1)[W]_R+2n(\mu_2-\mu_1)\left[\frac{dw}{dr}\right]_R\right\}, \tag{46}$$

where $[W]_R$ and $[dw/dr]_R$ are the common values of W_1 and W_2 and similarly of dw_1/dr and dw_2/dr at $r = R$.

Since (cf. equation (38))

$$\frac{d}{dr}\left\{r\left(W-\frac{\nu}{n}F\right)\right\} = (l+1)A_1 r^l - lA_2 r^{-(l+1)}, \tag{47}$$

an equivalent form of the boundary condition (46) as applied to the solutions (43) and (44) is

$$(l+1)\rho_1 A_1 R^l + l\rho_2 A_2 R^{-(l+1)} = \frac{l(l+1)}{n^2}\left\{\gamma_R(\rho_2-\rho_1)[W]_R+2n(\mu_2-\mu_1)\left[\frac{dw}{dr}\right]_R\right\}. \tag{48}$$

In applying the boundary conditions (45) and (48) to the solutions (43) and (44), it is convenient to measure r in units of R. Writing

$$q_1 = \sqrt{(nR^2/\nu_1)} \quad \text{and} \quad q_2 = \sqrt{(nR^2/\nu_2)}, \tag{49}$$

we can express the solutions for W_1 and W_2 in the forms

$$W_1 = A_1 r^l + \frac{B_1}{\sqrt{r}} I_{l+\frac{1}{2}}(q_1 r) \quad (r \leqslant 1) \tag{50}$$

and

$$W_2 = A_2 r^{-(l+1)} + \frac{B_2}{\sqrt{r}} K_{l+\frac{1}{2}}(q_2 r) \quad (r \geqslant 1). \tag{51}$$

Now applying the boundary conditions (45) and (48) to the foregoing solutions we find

$$A_1 + B_1 I_{l+\frac{1}{2}}(q_1) = A_2 + B_2 K_{l+\frac{1}{2}}(q_2) \quad (= [W]_1), \tag{52}$$

$$lA_1 + B_1\{q_1 I'_{l+\frac{1}{2}}(q_1) - \tfrac{1}{2}I_{l+\frac{1}{2}}(q_1)\} = -(l+1)A_2 + B_2\{q_2 K'_{l+\frac{1}{2}}(q_2) - \tfrac{1}{2}K_{l+\frac{1}{2}}(q_2)\}, \tag{53}$$

$$\mu_1[2(l^2-1)A_1 + B_1\{-2q_1 I'_{l+\frac{1}{2}}(q_1) + (q_1^2+2l^2+2l-1)I_{l+\frac{1}{2}}(q_1)\}]$$
$$= \mu_2[2l(l+2)A_2 + B_2\{-2q_2 K'_{l+\frac{1}{2}}(q_2) + (q_2^2+2l^2+2l-1)K_{l+\frac{1}{2}}(q_2)\}], \tag{54}$$

and (cf. equations (48), (52), and (53))

$$(l+1)\rho_1 A_1 + l\rho_2 A_2$$
$$= \frac{l(l+1)}{2n^2}\gamma_R(\rho_2-\rho_1)\{A_1 + B_1 I_{l+\frac{1}{2}}(q_1) + A_2 + B_2 K_{l+\frac{1}{2}}(q_2)\} +$$
$$+ \frac{l(l+1)}{nR^2}(\mu_2-\mu_1)\{(l-1)A_1 + B_1[q_1 I'_{l+\frac{1}{2}}(q_1) - \tfrac{3}{2}I_{l+\frac{1}{2}}(q_1)] -$$
$$-(l+2)A_2 + B_2[q_2 K'_{l+\frac{1}{2}}(q_2) - \tfrac{3}{2}K_{l+\frac{1}{2}}(q_2)]\}, \tag{55}$$

where primes denote differentiation with respect to the argument of the Bessel functions. Introducing the abbreviations

$$\alpha_1 = \frac{\rho_1}{\rho_1+\rho_2}, \qquad \alpha_2 = \frac{\rho_2}{\rho_1+\rho_2} \quad (\alpha_1+\alpha_2 = 1), \tag{56}$$

$$\left.\begin{aligned} \Re &= \frac{l(l+1)}{n^2}\frac{\rho_1-\rho_2}{\rho_1+\rho_2}\gamma_R = \frac{1}{n^2}\gamma_R\, l(l+1)(\alpha_1-\alpha_2) \\ \text{and} \qquad C &= \frac{l(l+1)}{nR^2}\frac{\mu_1-\mu_2}{\rho_1+\rho_2} = \frac{1}{nR^2}l(l+1)(\alpha_1\nu_1-\alpha_2\nu_2) \end{aligned}\right\} \tag{57}$$

we can rewrite equations (52)–(55) in the form

$$A_1+I_{l+\frac{1}{2}}(q_1)B_1-A_2-K_{l+\frac{1}{2}}(q_2)B_2 = 0, \tag{58}$$

$$lA_1+[q_1 I'_{l+\frac{1}{2}}(q_1)-\tfrac{1}{2}I_{l+\frac{1}{2}}(q_1)]B_1+(l+1)A_2+ \\ +[-q_2 K'_{l+\frac{1}{2}}(q_2)+\tfrac{1}{2}K_{l+\frac{1}{2}}(q_2)]B_2 = 0, \tag{59}$$

$$2\alpha_1\nu_1(l^2-1)A_1+\alpha_1\nu_1\{-2q_1 I'_{l+\frac{1}{2}}(q_1)+(q_1^2+2l^2+2l-1)I_{l+\frac{1}{2}}(q_1)\}B_1- \\ -2\alpha_2\nu_2 l(l+2)A_2-\alpha_2\nu_2\{-2q_2 K'_{l+\frac{1}{2}}(q_2)+(q_2^2+2l^2+2l-1)K_{l+\frac{1}{2}}(q_2)\}B_2 = 0 \tag{60}$$

and

$$[(l+1)\alpha_1+\tfrac{1}{2}\Re+(l-1)C]A_1+\{\tfrac{1}{2}\Re I_{l+\frac{1}{2}}(q_1)+C[q_1 I'_{l+\frac{1}{2}}(q_1)-\tfrac{3}{2}I_{l+\frac{1}{2}}(q_1)]\}B_1+ \\ +[l\alpha_2+\tfrac{1}{2}\Re-(l+2)C]A_2+\{\tfrac{1}{2}\Re K_{l+\frac{1}{2}}(q_2)+C[q_2 K'_{l+\frac{1}{2}}(q_2)-\tfrac{3}{2}K_{l+\frac{1}{2}}(q_2)]\}B_2 = 0. \tag{61}$$

The foregoing equations represent a system of linear homogeneous equations for the constants A_1, B_1, A_2, and B_2; and the determinant of the system must vanish if we are to have a non-trivial solution. By equating the determinant of equations (58)–(61) to zero we shall obtain the required characteristic equation for determining n.

5. The case $\nu_1 = \nu_2$

In the further discussion of equations (58)–(61) we shall restrict ourselves to the case when the kinematic viscosities of the two fluids are the same, i.e. when

$$\nu_1 = \nu_2. \tag{62}$$

This assumption simplifies the characteristic equation considerably; but one would not expect the essential features of the problem to be obscured by this simplifying assumption (cf. Chandrasekhar (**4**) and Hide (**5**) for the parallel discussion of the plane problem).

When $\nu_1 = \nu_2$, $\qquad q_1 = q_2 = \sqrt{(nR^2/\nu)} = q$ (say), $\hfill (63)$

and we find that the determinant of equations (58)–(61) can be reduced to

one of third order by adding or subtracting suitable multiples of the different rows (and columns) from other rows (and columns). Thus we find

$$\begin{vmatrix} qI_{l+\frac{3}{2}} & 2l+1 & qK_{l-\frac{1}{2}} \\ \alpha_1 q(-2I_{l+\frac{3}{2}}+qI_{l+\frac{1}{2}}) & 2[\alpha_1(l^2-1)-\alpha_2 l(l+2)] & -\alpha_2 q(2K_{l-\frac{1}{2}}+qK_{l+\frac{1}{2}}) \\ -(l+1)\alpha_1 I_{l+\frac{1}{2}}+qCI_{l+\frac{3}{2}} & (l+1)\alpha_1+l\alpha_2+\Re-3C & -l\alpha_2 K_{l+\frac{1}{2}}-qCK_{l-\frac{1}{2}} \end{vmatrix} = 0, \tag{64}$$

where the argument of all the Bessel functions is now q. In reducing the determinant of equations (58)–(61) to the foregoing, one must make use of the various recurrence relations satisfied by the Bessel functions.

On expanding the determinant (64) we find after some straightforward but lengthy reductions that

$$\begin{aligned} l(l+1)(\alpha_2-\alpha_1)\frac{\mathfrak{G}}{q^4} &= (l+1)\alpha_1+l\alpha_2+ \\ &+\frac{1}{q^2}\Big[2(\alpha_2-\alpha_1)(2l+1)q\{\alpha_2 lI_{l+\frac{3}{2}}K_{l+\frac{1}{2}}-\alpha_1(l^2-1)I_{l+\frac{1}{2}}K_{l-\frac{1}{2}}\}- \\ &\quad -4(\alpha_2-\alpha_1)^2 l(l^2-1)(l+2)I_{l+\frac{3}{2}}K_{l-\frac{1}{2}}+\alpha_1\alpha_2(2l+1)^2q^2I_{l+\frac{1}{2}}K_{l+\frac{1}{2}}\Big]\times \\ &\quad \times\{q(\alpha_1 I_{l+\frac{1}{2}}K_{l-\frac{1}{2}}+\alpha_2 I_{l+\frac{3}{2}}K_{l+\frac{1}{2}})+2(\alpha_2-\alpha_1)I_{l+\frac{3}{2}}K_{l-\frac{1}{2}}\}^{-1}, \end{aligned} \tag{65}$$

where

$$\mathfrak{G} = \gamma_R R^4/\nu^2 \tag{66}$$

is a 'Grashoff' number.

Equation (65) determines $\mathfrak{G}$ as a function of q for each specified l and given α_1 and α_2 ($= 1-\alpha_1$). On the other hand, according to equation (63)

$$\frac{n}{\sqrt{\gamma_R}} = q^2\frac{\nu}{R^2\sqrt{\gamma_R}} = \frac{q^2}{\sqrt{\mathfrak{G}}}; \tag{67}$$

thus $q^2/\sqrt{\mathfrak{G}}$ gives n in units of $\sqrt{\gamma_R}$. Hence, the $(q, \mathfrak{G}; l)$-relation which is directly given by equation (65) can be transformed into an $(n, \mathfrak{G}; l)$-relation; and using this last relation we can determine the dependence of n on l for given $\mathfrak{G}$ and thus complete the solution of the problem.

6. The mode of maximum instability for the case $\nu_1 = \nu_2$ and $\rho_2 > \rho_1$: an illustrative example

When $\rho_2 > \rho_1$ and $\alpha_2 > \alpha_1$, equation (65) determines a $(q, \mathfrak{G})$-relation which for q real and positive is monotonic increasing; thus as q increases from zero to infinity, $\mathfrak{G}$ also increases from zero to infinity. According to equation (67), $n > 0$ and the situation considered is unstable, so we should expect that for a given $\mathfrak{G}$ there will be a mode of maximum instability.

The modes of maximum instability for various assigned values of $\mathfrak{G}$ and $\alpha_2-\alpha_1 = 0{\cdot}1$ were determined in the following manner.

By using the recent tabulation by the Royal Society (**10**) of the spherical Bessel functions for purely imaginary arguments, the $(q, \mathfrak{G})$-relations were determined for $l = 1, 2, \ldots, 9$ and for q in the range $(0, 10)$. Then, by interpolating in these relations, the values of q (and thence the values of n) were determined (for each l) at which $\mathfrak{G}$ had assigned values. The results of such calculations are summarized in Table 1 and are further illustrated in Fig. 1.

TABLE I

The $(n/\sqrt{\gamma_R}, l)$-relation for $\alpha_2-\alpha_1 = 0{\cdot}1$ and for various values of $\mathfrak{G}$. The mode of maximum instability is in bold type in each case

l \ $\mathfrak{G}$	10	100	200	400	600	800	1000	2000	3000
1	**0·106**	**0·195**	**0·221**	0·245	0·258	0·266	0·272	0·290	0·298
2	0·073	0·178	0·218	**0·258**	**0·280**	**0·295**	**0·306**	0·337	0·354
3	0·052	0·146	0·190	0·238	0·267	0·288	0·303	**0·348**	**0·372**
4	0·040	0·119	0·161	0·211	0·243	0·266	0·285	0·341	0·372
5	0·032	0·100	0·137	0·184	0·217	0·241	0·261	0·324	0·361
6	0·027	0·085	0·118	0·162	0·193	0·217	0·236	0·303	0·343
7	0·023	0·074	0·103	0·143	0·172	0·195	0·214	0·280	0·323
8	0·021	0·065	0·092	0·128	0·154	0·176	0·194	0·259	0·302
9	0·018	0·059	0·082	0·115	0·140	0·160	0·177	0·239	0·282

l \ $\mathfrak{G}$	4000	5000	6000	8000	10000	15000	20000	25000	30000
1	0·304	0·308	0·311	0·316	0·319	0·324	0·328	0·331	0·333
2	0·364	0·372	0·378	0·387	0·394	0·404	0·411	0·416	0·420
3	0·388	0·400	0·409	0·423	0·433	0·450	0·460	0·468	0·474
4	**0·393**	**0·409**	**0·421**	0·440	0·453	0·476	0·491	0·501	0·510
5	0·386	0·405	0·420	**0·444**	**0·460**	0·490	0·508	0·522	0·533
6	0·372	0·394	0·412	0·439	0·459	**0·494**	0·517	0·534	0·547
7	0·354	0·378	0·397	0·428	0·451	0·492	**0·518**	**0·538**	0·554
8	0·334	0·359	0·380	0·413	0·439	0·484	0·515	0·538	**0·555**
9	0·314	0·340	0·362	0·397	0·424	0·473	0·507	0·532	0·552

From the results given in Table 1 it is apparent that for $\mathfrak{G}$ less than a certain critical value in the neighbourhood of 200 the mode of maximum instability always occurs for $l = 1$. It is found that

$$n/\sqrt{\gamma_R} = 0{\cdot}226 \quad \text{for } l = 1 \text{ and } l = 2 \quad \text{when } \mathfrak{G} = 230; \tag{68}$$

the critical value of $\mathfrak{G}$ is therefore more nearly 230. For $\mathfrak{G} > 230$ the mode of maximum instability shifts to higher l's.

7. A variational principle

The discussion in the preceding sections of the character of the instability of a fluid sphere of constant density embedded in a medium of a different density but the same kinematic viscosity makes it clear that an investigation of the problem under even slightly more general conditions is likely to

be very troublesome. However, it appears that as in the case of the plane problem (cf. Hide (**5**)) the essential features of the physical problem in the present case can be equally inferred from an approximate theory based on a variational principle. We shall now deduce this principle.

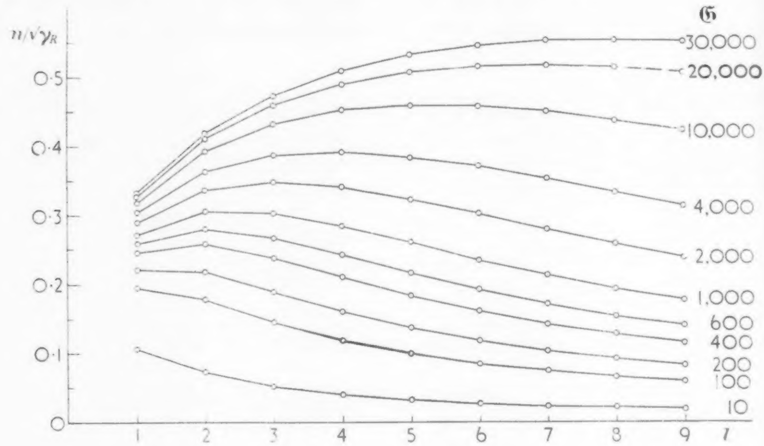

Fig. 1. The (n, l)-relation for various values of 𝔊 $(= \gamma_R R^4/\nu^2)$. The values of 𝔊 to which the various curves refer are indicated.

The equation to be solved is (cf. equations (24) and (29))

$$-n\frac{d}{dr}\left\{\rho\frac{d}{dr}(rW)\right\}+\frac{d^2}{dr^2}(\mu rF)-2\frac{d}{dr}\left\{\frac{1}{r}\frac{d\mu}{dr}\frac{d}{dr}(rW)\right\}+$$
$$+2l(l+1)\frac{d}{dr}\left(\frac{d\mu}{dr}\frac{W}{r}\right)+l(l+1)\left\{n\rho\frac{W}{r}-\frac{\mu}{r}F-2\frac{d\mu}{dr}\frac{d}{dr}\left(\frac{W}{r}\right)\right\}$$
$$=\frac{l(l+1)}{n}\gamma\frac{d\rho}{dr}W. \qquad (69)$$

This can be further simplified to the form

$$-n\frac{d}{dr}\left\{\rho\frac{d}{dr}(rW)\right\}+l(l+1)n\rho\frac{W}{r}-\frac{l(l+1)}{n}\gamma\frac{d\rho}{dr}W+$$
$$+\frac{d^2}{dr^2}(\mu rF)-2\frac{d}{dr}\left\{\frac{1}{r}\frac{d\mu}{dr}\frac{d}{dr}(rW)\right\}+2l(l+1)\frac{1}{r}\frac{d^2\mu}{dr^2}W-l(l+1)\frac{\mu}{r}F=0, \qquad (70)$$

where it may be recalled that F is given by equation (33). And the boundary conditions with respect to which equation (70) must be solved are that

$$W \text{ and } \textit{either } \frac{dW}{dr} \textit{ or } \frac{d^2W}{dr^2} \text{ vanish on the bounding surfaces.} \qquad (71)$$

As we have already stated, the requirement that a solution of equation (70) satisfies the conditions (71) on the bounding surfaces will lead to a determinate sequence of possible values for n. Let n_i and n_j denote two of these characteristic values; and let the solutions belonging to these characteristic values be distinguished by subscripts i and j respectively.

Now consider equation (70) for the characteristic value n_i and after multiplying it by rW_j (belonging to n_j) integrate over the range of r (which we shall assume to be $R_1 \leqslant r \leqslant R_2$). We obtain after one or more integrations by parts:

$$n_i \int\limits_{R_1}^{R_2} \rho\left\{\frac{d}{dr}(rW_i)\frac{d}{dr}(rW_j)+l(l+1)W_i W_j\right\} dr - \frac{l(l+1)}{n_i}\int\limits_{R_1}^{R_2} \frac{d\rho}{dr} r\gamma W_i W_j\, dr$$

$$= -2\int\limits_{R_1}^{R_2} \frac{1}{r}\frac{d\mu}{dr}\frac{d}{dr}(rW_i)\frac{d}{dr}(rW_j)\, dr - 2l(l+1)\int\limits_{R_1}^{R_2} \frac{d^2\mu}{dr^2} W_i W_j\, dr -$$

$$- \int\limits_{R_1}^{R_2} rW_j \frac{d^2}{dr^2}(\mu r F_i)\, dr + l(l+1)\int\limits_{R_1}^{R_2} \mu F_i W_j\, dr. \quad (72)$$

After two successive integrations by parts we find that

$$\int\limits_{R_1}^{R_2} rW_j \frac{d^2}{dr^2}(\mu r F_i)\, dr = -\left[\mu r F_i \frac{d}{dr}(rW_j)\right]_{R_1}^{R_2} + \int\limits_{R_1}^{R_2} \mu r F_i \frac{d^2}{dr^2}(rW_j)\, dr. \quad (73)$$

Now $$\frac{d}{dr}(rW) = r\frac{dW}{dr} \quad \text{on a bounding surface.} \quad (74)$$

If the bounding surface is rigid, this vanishes. On the other hand, if the bounding surface is free, $d^2W/dr^2 = 0$ and (cf. equation (33))

$$F = \frac{2}{r}\frac{dW}{dr} \quad \text{on a free bounding surface.} \quad (75)$$

Hence in all cases we may write

$$\int\limits_{R_1}^{R_2} rW_j \frac{d^2}{dr^2}(\mu r F_i)\, dr = -\left[2\mu r \frac{dW_i}{dr}\frac{dW_j}{dr}\right]_{R_1}^{R_2} + \int\limits_{R_1}^{R_2} \mu r F_i \frac{d^2}{dr^2}(rW_j)\, dr. \quad (76)$$

Using the foregoing result in equation (72) and substituting further for F_i

in accordance with equation (33), we obtain after some rearrangement of the terms:

$$n_i \int_{R_1}^{R_2} \rho\left\{\frac{d}{dr}(rW_i)\frac{d}{dr}(rW_j)+l(l+1)W_i W_j\right\} dr - \frac{l(l+1)}{n_i}\int_{R_1}^{R_2} \frac{d\rho}{dr} r\gamma W_i W_j\, dr$$

$$= -2\int_{R_1}^{R_2} \frac{1}{r}\frac{d\mu}{dr}\frac{d}{dr}(rW_i)\frac{d}{dr}(rW_j)\, dr - 2l(l+1)\int_{R_1}^{R_2} \frac{d^2\mu}{dr^2} W_i W_j\, dr -$$

$$-l^2(l+1)^2\int_{R_1}^{R_2} \frac{\mu}{r^2} W_i W_j\, dr + \left[2\mu r\frac{dW_i}{dr}\frac{dW_j}{dr}\right]_{R_1}^{R_2} -$$

$$-\int_{R_1}^{R_2} \mu\frac{d^2}{dr^2}(rW_i)\frac{d^2}{dr^2}(rW_j)\, dr + l(l+1)\int_{R_1}^{R_2} \frac{\mu}{r}\left\{W_i\frac{d^2}{dr^2}(rW_j)+W_j\frac{d^2}{dr^2}(rW_i)\right\} dr. \tag{77}$$

Rewriting the last integral on the right-hand side of equation (77) in the manner

$$\int_{R_1}^{R_2} \mu\left\{\frac{d^2}{dr^2}(W_i W_j) - 2\frac{dW_i}{dr}\frac{dW_j}{dr} + \frac{2}{r}\frac{d}{dr}(W_i W_j)\right\} dr, \tag{78}$$

we can transform it by further integration by parts into

$$\int_{R_1}^{R_2} \frac{d^2\mu}{dr^2} W_i W_j\, dr - 2\int_{R_1}^{R_2} \mu\frac{dW_i}{dr}\frac{dW_j}{dr}\, dr - 2\int_{R_1}^{R_2} W_i W_j\left(\frac{1}{r}\frac{d\mu}{dr} - \frac{\mu}{r^2}\right) dr. \tag{79}$$

Thus, we finally obtain

$$n_i \int_{R_1}^{R_2} \rho\left\{\frac{d}{dr}(rW_i)\frac{d}{dr}(rW_j)+l(l+1)W_i W_j\right\} dr - \frac{l(l+1)}{n_i}\int_{R_1}^{R_2} \frac{d\rho}{dr} r\gamma W_i W_j\, dr$$

$$= \left[2\mu r\frac{dW_i}{dr}\frac{dW_j}{dr}\right]_{R_1}^{R_2} -$$

$$-\int_{R_1}^{R_2} \mu\left\{\frac{d^2}{dr^2}(rW_i)\frac{d^2}{dr^2}(rW_j) + 2l(l+1)\frac{dW_i}{dr}\frac{dW_j}{dr} + l(l^2-1)(l+2)\frac{W_i W_j}{r^2}\right\} dr -$$

$$-2\int_{R_1}^{R_2} \frac{1}{r}\frac{d\mu}{dr}\left\{\frac{d}{dr}(rW_i)\frac{d}{dr}(rW_j)+l(l+1)W_i W_j\right\} dr - l(l+1)\int_{R_1}^{R_2} \frac{d^2\mu}{dr^2} W_i W_j\, dr. \tag{80}$$

Interchanging i and j in equation (80) and subtracting the resulting equation from it, we obtain

$$(n_i - n_j)\left[\int\limits_{R_1}^{R_2} \rho\left\{\frac{d}{dr}(rW_i)\frac{d}{dr}(rW_j)+l(l+1)W_i W_j\right\} dr + \frac{1}{n_i n_j}\int\limits_{R_1}^{R_2} \frac{d\rho}{dr} r\gamma W_i W_j\, dr\right] = 0. \tag{81}$$

Hence, if $n_i \neq n_j$,

$$\int\limits_{R_1}^{R_2} \rho\left\{\frac{d}{dr}(rW_i)\frac{d}{dr}(rW_j)+l(l+1)W_i W_j\right\} dr + \frac{1}{n_i n_j}\int\limits_{R_1}^{R_2} \frac{d\rho}{dr} r\gamma W_i W_j\, dr = 0 \quad (i \neq j). \tag{82}$$

If n_i should be complex, we can suppose that n_i and n_j are complex conjugates and we deduce from equation (82) that

$$\int\limits_{R_1}^{R_2} \rho\left\{\left|\frac{d}{dr}(rW)\right|^2 + l(l+1)|W|^2\right\} dr + \frac{1}{|n|^2}\int\limits_{R_1}^{R_2} \frac{d\rho}{dr} r\gamma |W|^2\, dr = 0, \tag{83}$$

a relation which cannot be true if $\gamma\, d\rho/dr$ is everywhere positive.

Returning to equation (80) and setting $i = j$, we get (on further suppressing the subscripts)

$$n\int\limits_{R_1}^{R_2} \rho\left\{\left[\frac{d}{dr}(rW)\right]^2 + l(l+1)W^2\right\} dr - \frac{l(l+1)}{n}\int\limits_{R_1}^{R_2} \frac{d\rho}{dr} r\gamma W^2\, dr$$

$$= -\int\limits_{R_1}^{R_2} \mu\left\{\left[\frac{d^2}{dr^2}(rW)\right]^2 + 2l(l+1)\left(\frac{dW}{dr}\right)^2 + l(l^2-1)(l+2)\frac{W^2}{r^2}\right\} dr -$$

$$-2\int\limits_{R_1}^{R_2} \frac{1}{r}\frac{d\mu}{dr}\left\{\left[\frac{d}{dr}(rW)\right]^2 + l(l+1)W^2\right\} dr -$$

$$-l(l+1)\int\limits_{R_1}^{R_2} \frac{d^2\mu}{dr^2} W^2\, dr + 2\left[\mu r\left(\frac{dW}{dr}\right)^2\right]_{R_1}^{R_2}. \tag{84}$$

This last equation provides the basis for a convenient variational procedure for determining n. For, by considering the effect on n (determined in accordance with equation (84)) of an arbitrary variation δW in W compatible only with the boundary conditions on W, we find after some straight-

forward but lengthy reductions that

$$-2\left[\!\!\left[\int\limits_{R_1}^{R_2}\rho\left\{\left[\frac{d}{dr}(rW)\right]^2+l(l+1)W^2\right\}dr+\frac{l(l+1)}{n^2}\int\limits_{R_1}^{R_2}\frac{d\rho}{dr}r\gamma W^2\,dr\right]\!\!\right]\delta n$$

$$=\int\limits_{R_1}^{R_2} r\,\delta W\left\{-n\frac{d}{dr}\left[\rho\frac{d}{dr}(rW)\right]+l(l+1)n\rho\frac{W}{r}-\frac{l(l+1)}{n}\gamma\frac{d\rho}{dr}W+\right.$$

$$\left.+\frac{d^2}{dr^2}(\mu rF)-2\frac{d}{dr}\left[\frac{1}{r}\frac{d\mu}{dr}\frac{d}{dr}(rW)\right]+2l(l+1)\frac{1}{r}\frac{d^2\mu}{dr^2}W-l(l+1)\frac{\mu}{r}F\right\}dr. \qquad (85)$$

It will be observed that the quantity which appears as a factor of δW under the integral sign on the right-hand side of equation (85) vanishes if equation (70) governing W is satisfied. Hence a necessary and sufficient condition for δn to be zero to the first order for all small arbitrary variations in W which are compatible with the boundary conditions is that W be a solution of the characteristic-value problem. Accordingly, equation (84) provides the basis for the determination of n by a variational procedure.

8. Illustration of the use of the variational principle

We shall illustrate the use of the variational principle derived in section 7 by reconsidering on its basis the problem which has been exactly solved in sections 4–6. However, in applying equation (84) to this case, in which discontinuities in ρ and μ occur at $r = R$, we must be careful to make allowance for them by dividing the range of integration into three intervals, 0 to $R-\epsilon$, $R-\epsilon$ to $R+\epsilon$, and finally $R+\epsilon$ to ∞, where $\epsilon > 0$, and then passing to the limit $\epsilon = 0$. By this limiting process we readily derive from equation (84) that for the case considered in section 4,

$$n\left[\!\!\left[\rho_1\int\limits_0^1\left\{\left[\frac{d}{dr}(rW_1)\right]^2+l(l+1)W_1^2\right\}dr+\rho_2\int\limits_1^\infty\left\{\left[\frac{d}{dr}(rW_2)\right]^2+l(l+1)W_2^2\right\}dr\right]\!\!\right]+$$

$$+\frac{1}{R^2}\left[\!\!\left[\mu_1\int\limits_0^1\left\{\left[\frac{d^2}{dr^2}(rW_1)\right]^2+2l(l+1)\left(\frac{dW_1}{dr}\right)^2+l(l^2-1)(l+2)\frac{W_1^2}{r^2}\right\}dr+\right.\right.$$

$$\left.\left.+\mu_2\int\limits_1^\infty\left\{\left[\frac{d^2}{dr^2}(rW_2)\right]^2+2l(l+1)\left(\frac{dW_2}{dr}\right)^2+l(l^2-1)(l+2)\frac{W_2^2}{r^2}\right\}dr\right]\!\!\right]-$$

$$-\frac{l(l+1)}{n}\gamma_R(\rho_2-\rho_1)[W^2]_1+\frac{2}{R^2}(\mu_2-\mu_1)\left[\left\{\frac{d}{dr}(rW)\right\}^2+l(l+1)W^2\right]_1=0, \qquad (86)$$

where r is measured in units of R. In equation (86) the symbol $[\;]_1$ denotes

the common value, at $r = 1$, of the quantity in the brackets (which is continuous at the interface).

In the absence of viscosity the solution for W appropriate to the problem on hand is (cf. equation (38))

$$W = W_1 = r^l \quad (r \leqslant 1)$$

and

$$W = W_2 = r^{-(l+1)} \quad (r \geqslant 1). \tag{87}$$

This solution does not have a continuous derivative at $r = 1$. Nevertheless, from Hide's experience with the plane problem (**5**) we can expect that the use of this solution (valid only in the absence of viscosity) as a 'trial' function in the variational expression for n will lead to the correct dependence of n on the parameters of the problem. However, in the present instance (in contrast to the plane problem) the discontinuity in the derivative of W affects one of the terms in equation (86), namely the term which occurs as the factor of $(\mu_2 - \mu_1)$. Thus,

$$\left[\left\{\frac{d}{dr}(rW_1)\right\}^2 + l(l+1)W_1^2\right]_1 = (l+1)(2l+1), \tag{88}$$

while

$$\left[\left\{\frac{d}{dr}(rW_2)\right\}^2 + l(l+1)W_2^2\right]_1 = l(2l+1). \tag{89}$$

In using equation (86) in conjunction with (87) we shall take the average of the two foregoing values for the term in question. (This is admittedly a crude procedure, but it will presently appear that this term is only of secondary importance in the equation which we shall derive (equation (90) below) for n.) In this manner we find from equation (86) that

$$[(l+1)\alpha_1 + l\alpha_2]n^2 + \frac{1}{R^2}\{2l(l+1)[(l+1)\alpha_1\nu_1 + l\alpha_2\nu_2] + (2l+1)^2(\alpha_2\nu_2 - \alpha_1\nu_1)\}n - \\ - l(l+1)\gamma_R(\alpha_2 - \alpha_1) = 0, \tag{90}$$

where α_1 and α_2 have the meanings given in (56).

The two terms in the quantity in braces in (90) are approximately in the ratio $l(l+1):(2l+1)(\alpha_2 - \alpha_1)$; the second term can therefore be neglected for $|\alpha_2 - \alpha_1| \leqslant 0{\cdot}1$, and in all cases for large values of l.

(i) *The case* $\nu_1 = \nu_2$. To see how much reliance we may place on deductions based on (90) (and therefore on results derived from the variational procedure quite generally) we shall consider the case of equal kinematic viscosities for which we have the results of an exact calculation (Table 1).

For $\nu_1 = \nu_2$ equation (90) becomes

$$n^2 + \frac{\nu}{R^2}\left\{2l(l+1) + (\alpha_2 - \alpha_1)\frac{(2l+1)^2}{l+\alpha_1}\right\}n - (\alpha_2 - \alpha_1)\gamma_R\frac{l(l+1)}{l+\alpha_1} = 0, \tag{91}$$

or, alternatively,

$$\left(\frac{n}{\sqrt{\gamma_R}}\right)^2+\frac{1}{\sqrt{\mathfrak{G}}}\left\{2l(l+1)+(\alpha_2-\alpha_1)\frac{(2l+1)^2}{l+\alpha_1}\right\}\frac{n}{\sqrt{\gamma_R}}-(\alpha_2-\alpha_1)\frac{l(l+1)}{l+\alpha_1}=0. \tag{92}$$

Hence

$$\frac{n}{\sqrt{\gamma_R}}=-\frac{1}{\sqrt{\mathfrak{G}}}\left\{l(l+1)+(\alpha_2-\alpha_1)\frac{(2l+1)^2}{2(l+\alpha_1)}\right\}\pm$$
$$\pm\left[\frac{1}{\mathfrak{G}}\left\{l(l+1)+(\alpha_2-\alpha_1)\frac{(2l+1)^2}{2(l+\alpha_1)}\right\}^2+(\alpha_2-\alpha_1)\frac{l(l+1)}{l+\alpha_1}\right]^{\frac{1}{2}}. \tag{93}$$

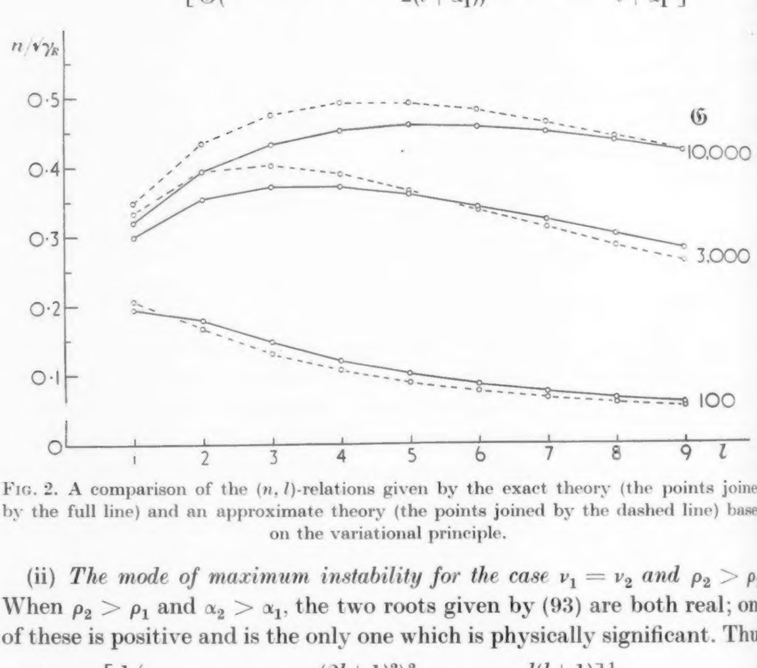

FIG. 2. A comparison of the (n, l)-relations given by the exact theory (the points joined by the full line) and an approximate theory (the points joined by the dashed line) based on the variational principle.

(ii) *The mode of maximum instability for the case $\nu_1 = \nu_2$ and $\rho_2 > \rho_1$.* When $\rho_2 > \rho_1$ and $\alpha_2 > \alpha_1$, the two roots given by (93) are both real; one of these is positive and is the only one which is physically significant. Thus

$$\frac{n}{\sqrt{\gamma_R}}=\left[\frac{1}{\mathfrak{G}}\left\{l(l+1)+(\alpha_2-\alpha_1)\frac{(2l+1)^2}{2(l+\alpha_1)}\right\}^2+(\alpha_2-\alpha_1)\frac{l(l+1)}{l+\alpha_1}\right]^{\frac{1}{2}}-$$
$$-\frac{1}{\sqrt{\mathfrak{G}}}\left\{l(l+1)+(\alpha_2-\alpha_1)\frac{(2l+1)^2}{2(l+\alpha_1)}\right\}; \tag{94}$$

and since n is positive the situation considered is an unstable one.

The values of n derived from (94) for various values of l and $\mathfrak{G}$ are plotted in Fig. 2 (the points joined by the dashed lines) along with the results of the exact calculations (the points joined by the full lines). From a comparison of the two sets of curves it is apparent that the approximate

theory predicts qualitatively the correct dependence of n on l and $\mathfrak{G}$; and the quantitative agreement is not unsatisfactory.

From equation (94) it follows in particular that, for sufficiently large l,

$$\frac{n}{\sqrt{\gamma_R}} \to \frac{\alpha_2-\alpha_1}{2l}\sqrt{\mathfrak{G}} \quad (l \to \infty); \tag{95}$$

thus $n \to 0$ as $l \to \infty$ and this is in agreement with what one should expect on physical grounds.

(iii) *The manner of decay in the case* $\nu_1 = \nu_2$ *and* $\rho_2 < \rho_1$. For $\rho_2 < \rho_1$ and $\alpha_2 < \alpha_1$ both the roots given by (93) have negative real parts: the situation considered is therefore a stable one. However, depending on the value of $\mathfrak{G}$, n can be complex for the lower modes. To see this clearly we shall neglect the terms in $(2l+1)^2(\alpha_2-\alpha_1)/2(l+\alpha_1)$ in equation (93): this, as we have seen, is permissible so long as we do not consider $|\alpha_2-\alpha_1| > 0{\cdot}1$. With this additional approximation we can now write

$$\frac{n}{\sqrt{\gamma_R}} = -\frac{l(l+1)}{\sqrt{\mathfrak{G}}} \pm \left[\frac{l^2(l+1)^2}{\mathfrak{G}} - (\alpha_1-\alpha_2)\frac{l(l+1)}{l+\alpha_1}\right]^{\frac{1}{2}}. \tag{96}$$

The condition for complex roots is therefore

$$\frac{l^2(l+1)^2}{\mathfrak{G}} < \frac{l(l+1)}{l+\alpha_1}(\alpha_1-\alpha_2), \tag{97}$$

or

$$\mathfrak{G} > \frac{l(l+1)(l+\alpha_1)}{\alpha_1-\alpha_2}. \tag{98}$$

From (98) it follows that for a given $\mathfrak{G}$ all modes beyond a certain l (say l_*) will decay aperiodically; and this aperiodic decay can take place at one of two alternative rates. And all modes with $l < l_*$ will be damped periodically. However, if $\mathfrak{G} < 2(1+\alpha_1)/(\alpha_1-\alpha_2)$, then all modes (including $l = 1$) will decay aperiodically. Thus for $\alpha_1-\alpha_2 = 0{\cdot}1$ all modes will decay aperiodically for $\mathfrak{G} < 29$; while for $\mathfrak{G} > 29$ one or more of the lower modes will decay periodically: e.g. for $\mathfrak{G} = 1000$ the modes $l = 1$, 2, 3, and 4 will be damped periodically and all the higher modes will be damped aperiodically. This behaviour of the solution in the stable case has certain similarities to the plane problem (cf. Chandrasekhar (**4**) and Hide (**5**)).

9. Concluding remarks

While this is clearly not the place to go into any detailed geophysical or other applications of the theory presented here, a brief comparison of the manner in which instability arises under the circumstances considered in this paper and under the analogous circumstances of thermal instability might be of some interest. For a fluid sphere heated within, it is known

(cf. Jeffreys and Bland (**8**) and Chandrasekhar (**9**)) that the mode of instability which is easiest to excite is $l = 1$; in spherical shells this shifts to harmonics of higher orders. On the other hand, if the instability is that caused by an overlying material of higher density, then the order of the harmonic in which the instability will manifest itself will depend on the value of $\mathfrak{G}$. But one general result can be stated: as long as $\mathfrak{G} < 230$ the mode of maximum instability will always be $l = 1$. This condition on $\mathfrak{G}$ is essentially a condition for a sufficiently high viscosity. For the condition $\mathfrak{G} < 230$ is equivalent to (cf. equation (66))

$$\nu > R^2\sqrt{(\gamma_R/230)}. \tag{99}$$

If the acceleration on the heavier material causing the instability is that due to the gravitational attraction of the mass interior to R, then,

$$\gamma_R = \tfrac{4}{3}\pi\rho_1 G, \tag{100}$$

where G denotes the constant of gravitation. Hence in this case

$$\nu > (\tfrac{4}{3}\pi\rho_1 G/230)^{\frac{1}{2}} R^2. \tag{101}$$

Choosing $$\rho_1 = 10 \text{ gm./cm.}^2 \text{ and } R = 5\times 10^8 \text{ cm.} \tag{102}$$
as 'typical' values, we find

$$\nu > 2{\cdot}8\times 10^{13} \text{ cm.}^2/\text{sec.} \tag{103}$$

Now it has been variously estimated that the viscosity of the material of the earth's mantle is 10^{22}–10^{23}. This value is larger than (103) by a very large margin. And one might conclude from this that if the viscosity of the earth's mantle should at some time (in the process of cooling?) have 'passed' through the value (103) before reaching its present high value and *if* an instability of the kind considered in this paper should have arisen, then the mode $l = 1$ should be exhibited as the last surviving feature. But before one can be certain of such conclusions it is important that the basic theory be extended and generalized along several directions: and this it is hoped to do in the near future.

In conclusion I should like to acknowledge my indebtedness to Miss Donna Elbert, who carried out all the numerical calculations pertaining to this paper.

The research reported in this paper has in part been supported by the Geophysics Research Directorate of the Air Force Cambridge Research Center, Air Research and Development Command, under Contract AF 19(604)–299 with the University of Chicago.

REFERENCES

1. LORD RAYLEIGH, *Proc. Lond. Math. Soc.* **14** (1883), 170–7 (also *Scientific Papers*, **2**, 200–7).
2. W. J. HARRISON, *Proc. Lond. Math. Soc.* **6** (1908), 396–405.
3. H. LAMB, *Hydrodynamics*, 6th edn. (Cambridge, 1931); see particularly pp. 370–9.
4. S. CHANDRASEKHAR, *Proc. Camb. Phil. Soc.* (in the press).
5. R. HIDE, ibid. (in the press).
6. T. G. COWLING, *Month. Not. R. Astr. Soc.* **101** (1941), 367–75.
7. P. LEDOUX, *Astrophys. J.* **114** (1951), 373–84.
8. H. JEFFREYS and M. E. M. BLAND, *Month. Not. R. Astr. Soc. Geophys. Suppl.* **6** (1951), 148–58.
9. S. CHANDRASEKHAR, *Phil. Mag.* (7) **43** (1953), 1317–29; also *Phil. Mag.* (7) **44** (1953), 233–41 and 1129–30.
10. C. W. JONES, *A Short Table for the Bessel Functions $I_{n+\frac{1}{2}}(x)$ and $(2/\pi)K_{n+\frac{1}{2}}(x)$* (Cambridge, 1952). (Prepared on behalf of the Mathematical Tables Committee of the Royal Society.)

A SOURCE IN A ROTATING FLUID

By S. N. BARUA (*Fitzwilliam House, Cambridge*)

[Received 21 January 1954]

SUMMARY

The flow due to a source placed on the axis of rotation in an otherwise uniformly rotating fluid is discussed. In the ultimate state the irrotational flow due to the source is confined to the region inside a cylindrical discontinuity surface which has a bulge in the neighbourhood of the source, the surface being symmetrical abo , the axis of rotation.

1. Introduction

THE effect of placing a weak spherical source in a rotating incompressible fluid has recently been studied by Stewartson (**1**). He neglected the inertia terms in the equations of motion and, in order to devise a problem analogous to that presented by a source, assumed that the fluid was slowly emitted from the surface of a sphere of radius a. The solution thus obtained involved the existence of vorticity immediately outside the sphere. The whole of the fluid leaving the sphere $x^2+y^2+z^2 = a^2$, the axis of x being the axis of uniform rotation of the fluid before any discharge from the source, was ultimately confined to a cylinder circumscribing it, and the cylinder was consequently filled with the fluid possessing vorticity. This vorticity becomes infinite near the cylindrical surface $y^2+z^2 = a^2$. It is clear that a point-source produces a flow which is irrotational, so that Stewartson's problem bears no relation to that of a point-source. In Stewartson's problem the spherical source produces a perturbation which involves a reduction in transverse velocity relative to fixed axes; but since at the cylindrical surface the perturbation-velocity becomes infinite, it is obvious that the whole solution breaks down there. For these reasons an attempt has been made to calculate the ultimate flow from a source in a rotating fluid. It will be supposed that the discharge starts from the source when the fluid outside is rotating uniformly about an axis and that it forces a passage for itself in both directions along the axis, as these are the regions of low pressure. Rings of particles in the outer fluid preserve their circulation as they expand. When the ultimate steady state is attained the fluid outside the irrotational region can have no axial velocity. For this reason the circumferential velocity must be a function of r (the distance of a point from the axis) only. Since the fluid issuing from the source must extend to infinity along the axis, this circumferential velocity must be that which

corresponds to a central expansion to the radius a which the column of fluid from the source ultimately attains. This velocity does not agree with that obtained by Stewartson and it could not be expected to do so. Our conception of the ultimate state is as indicated in Fig. 1, and our object is to determine the shape of the vortex sheet which separates the rotational fluid from the irrotational stream emanating from the source and to find out the ultimate velocity of the latter.

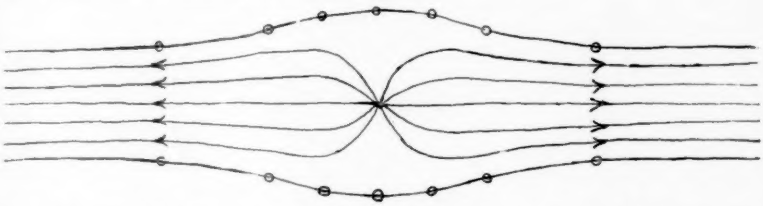

FIG. 1. A section of the discontinuity-surface and the irrotational motion due to the source. (The plotted points on the discontinuity-surface are the results of the numerical calculation shown in Table 1.)

In what follows we shall first obtain an equation relating the maximum diameter $2b$ of the discontinuity-surface to its diameter $2a$ at infinity. This equation is indeterminate, but using a 'variational principle' analogous to that used in hydraulics, we shall obtain definite values for a and b in terms of W, the source output, and Ω, the angular velocity with which the fluid was rotating before any discharge from the source. The measure of the deformation from the cylindrical form at all other points of the bulge will then be obtained by approximating the inside pressure at those points of the discontinuity-surface to that at corresponding points on an impervious infinite cylinder of radius a due to a source of same output W placed on the axis.

2. Calculation of the velocity of the fluid outside the vortex sheet

We shall assume that before the source began to emit fluid and thus produce a vortex sheet, the liquid was rotating with the angular velocity Ω about the axis of x. As the source is supposed to be placed on this axis at $x = 0$, the vortex sheet will be symmetrical about the axis of x as well as about the plane $x = 0$. Near the source there must exist a bulge in the vortex sheet. At a very large distance from the source this bulge will almost vanish. Let us denote the distance of the discontinuity surface from the axis of rotation at a very large distance from the source by a. The equation of continuity may be written as

$$\pi r^2 - \pi a^2 = \pi r'^2$$

or

$$r^2 - a^2 = r'^2, \tag{1}$$

where r' and r denote distances of a particle of fluid from the axis of rotation before and after the spreading out of the vortex sheet. The disturbance is symmetrical about the axis of rotation and the circulation is constant.

Therefore $$\Omega r'^2 = vr,$$

where v is the velocity outside the vortex sheet at a distance r from the axis.

Hence $$v = \frac{\Omega r'^2}{r},$$

or, using (1), $$v = \frac{\Omega(r^2-a^2)}{r}. \tag{2}$$

This velocity vanishes on the discontinuity surface at a large distance from the source, because there $r = a$.

3. Determination of the maximum deformation at the bulge

For the motion of the fluid outside the discontinuity surface the pressure equation may be written as

$$\frac{dp}{dr} = \rho\frac{v^2}{r},$$

or, using (2), $$\frac{dp}{dr} = \rho\frac{\Omega^2(r^2-a^2)^2}{r^3};$$

here p and ρ denote respectively the pressure and the uniform density of the fluid.

Integrating the above expression and denoting the pressure outside at the point of maximum deformation at the bulge by $(p_b)_0$ and that at infinity by $(p_a)_0$ we get

$$(p_b)_0-(p_a)_0 = \int_a^b \rho\Omega^2\frac{(r^2-a^2)^2}{r^3}\,dr$$

$$= \tfrac{1}{2}\rho\Omega^2\left[b^2-\frac{a^4}{b^2}-4a^2\log(b/a)\right], \tag{3}$$

where $2b$ denotes the maximum diameter at the bulge.

Now the velocity of the fluid inside the discontinuity-surface is obviously zero at a point of maximum deformation of the bulge; because from symmetry of the flow, the point must be a stagnation point. Therefore, denoting the pressure at the above point and at infinity by $(p_b)_i$ and $(p_a)_i$ respectively, we write from Bernoulli's equation,

$$(p_b)_i-(p_a)_i = \tfrac{1}{2}\rho\frac{W^2}{4\pi^2a^4}, \tag{4}$$

where W is the total output of the source. Here the density of the fluid coming out of the source has been taken to be the same as that of the fluid outside the vortex sheet.

Since the pressure must be continuous across the discontinuity surface, we must have

$$b^2 - \frac{a^4}{b^2} - 4a^2 \log(b/a) = \frac{W^2}{4\pi^2 a^4 \Omega^2}. \tag{5}$$

Equation (5) contains two unknown quantities a and b, and gives a series of possible values of a and b. The problem is indeterminate without further information. We shall now use a 'Variational Principle'† and the hypothesis that of all the values of b only that for which $(db/da) = 0$ need be adopted, so that corresponding to a small variation in the value of a at infinity, there will be no change in the value of b. By differentiating (5) with respect to a and making use of the above hypothesis, we get

$$a^3\left[b^2 - \frac{2a^4}{b^2} - 6a^2 \log(b/a) + a^2\right] = 0$$

or

$$(b/a)^2 - 2(b/a)^{-2} - 6 \log(b/a) + 1 = 0. \tag{6}$$

On solving this equation we get

$$b/a = 1 \quad \text{or} \quad 1{\cdot}679 \text{ nearly}. \tag{7}$$

We reject the value $b/a = 1$ since substitution in (5) would make a infinitely large, and this is physically impossible in the case under consideration. Taking $b/a = 1{\cdot}679$ we get from (5)

$$a^3 = 1{\cdot}598 \frac{W}{2\pi\Omega}. \tag{8}$$

Therefore the velocity at infinity is given by

$$q = \frac{W}{2\pi a^2},$$

or, using (8),

$$q = 0{\cdot}7316\left(\frac{W\Omega^2}{2\pi}\right)^{\frac{1}{3}}. \tag{9}$$

Thus, when the total output of the source W and the angular velocity Ω are known, the velocity of the fluid at infinity can be determined from (9).

4. Velocity potential due to a source inside a cylinder

Let us now consider an infinite circular cylinder of radius a with a source of total output W placed on the axis. Denoting the velocity potential of

† Mr. T. Brooke Benjamin informed the author that a number of problems in hydraulics, which were otherwise indeterminate, could be solved with the help of a 'Variational Principle'.

the motion due to the source inside the cylinder by ϕ, the boundary conditions may be written as

$$\text{(i)} \quad \left(\frac{\partial \phi}{\partial r}\right)_{r=a} = 0$$

$$\text{(ii)} \quad \left(\frac{\partial \phi}{\partial x}\right)_{x=0} = F(r),$$

where x is measured from the source along the axis of the cylinder; $F(r)$ is a function of r, the distance from the axis of the cylinder and will be defined later. We therefore seek a solution of

$$\nabla^2\phi \equiv \left(\frac{\partial^2}{\partial r^2}+\frac{1}{r}\frac{\partial}{\partial r}+\frac{\partial^2}{\partial x^2}\right)\phi = 0$$

subject to the above boundary conditions. Because of the symmetry of the motion about the plane $x = 0$, a knowledge of the solution for ϕ for $x > 0$ will be sufficient for our purpose. Let us take for $x > 0$

$$\phi = A_0 x + \sum A_n e^{-k_n x} J_0(k_n r),$$

where $J_0(k_n r)$ is the Bessel function of the order zero and k_n is an arbitrary parameter.

From the boundary condition (i)

$$0 = \left(\frac{\partial \phi}{\partial r}\right)_{r=a} = \sum A_n e^{-k_n x} J_0'(k_n a) k_n$$

$$= -\sum A_n k_n e^{-k_n x} J_1(k_n a).$$

This condition can be satisfied by choosing the arbitrary parameter $k_n = \alpha_n/a$, where α_n is the nth zero of $J_1(k_n a)$. Hence

$$\phi = A_0 x + \sum A_n c^{-\alpha_n x/a} J_0(\alpha_n r/a).$$

The boundary condition (ii) gives that

$$\left(\frac{\partial \phi}{\partial x}\right)_{x=0} = A_0 - \sum A_n(\alpha_n/a) J_0(\alpha_n r/a)$$

$$= F(r).$$

Let us now choose

$$F(r) = U_0 \quad \text{for } r < c$$

$$= 0 \quad \text{for } r > c;$$

physically this means that the liquid is flowing out through a hole of radius c in the plane $x = 0$. Since the amount of fluid that is flowing out through any cross-section of the cylinder must be equal to that flowing in through the hole, $A_0 = U_0 c^2/a^2$, and therefore the above condition may be written as

$$\sum A_n(\alpha_n/a) J_0(\alpha_n r/a) = U_0 c^2/a^2 - F(r).$$

Using Dini's expansion of Bessel functions (**2**), we may write

$$A_n \alpha_n/a = \frac{2}{J_0^2(\alpha_n)} \int_0^a \left[U_0 \frac{c^2}{a^2} - F(r)\right] \frac{r}{a} J_0(\alpha_n r/a) \frac{dr}{a}$$

$$= \frac{2U_0}{a^2 J_0^2(\alpha_n)} \left[\int_0^c \left(\frac{c^2}{a^2}-1\right) r J_0(\alpha_n r/a)\, dr + \int_c^a \frac{c^2}{a^2} r J_0(\alpha_n r/a)\, dr\right]$$

$$= \frac{2U_0}{a^2 J_0^2(\alpha_n)} \left[\left(\frac{c^2}{a^2}-1\right) \frac{ac}{\alpha_n} J_1(\alpha_n c/a) - \frac{c^2}{a^2}\frac{ac}{\alpha_n} J_1(\alpha_n c/a)\right]$$

$$= -\frac{2U_0 c}{J_0^2(\alpha_n) a \alpha_n} J_1(\alpha_n c/a).$$

Therefore

$$\phi = U_0\left[\frac{c^2}{a^2}x - 2c \sum \frac{J_1(\alpha_n c/a)}{\alpha_n^2 J_0^2(\alpha_n)} e^{-\alpha_n x/a} J_0(\alpha_n r/a)\right]. \tag{10}$$

Let us now assume that the radius of the hole c in the plane $x = 0$ tends to zero in such a way that

$$U_0 \pi c^2 = \tfrac{1}{2} W$$

or

$$U_0 = \frac{W}{2\pi c^2},$$

where W is the total output of the source. Since $J_1(\alpha_n c/a)$ tends to $\alpha_n c/a$ as c tends to zero, the expression for ϕ may be written as

$$\phi = \frac{W}{2\pi a^2}\left[x - 2a \sum \frac{1}{\alpha_n J_0(\alpha_n)} e^{-\alpha_n x/a} J_0(\alpha_n r/a)\right]. \tag{11}$$

This is the velocity potential of the motion of fluid in the region $x > 0$ due to a source of total output W placed on $x = 0$ at the axis inside an infinite cylinder of radius a.

5. Determination of the deformation

Let us denote the pressure just inside and outside the discontinuity surface at any point by p_i and p_0 respectively. If d denotes the measure of deformation from the cylindrical form of the discontinuity surface,

$$p_0 - (p_a)_0 = \int_a^{a+d} \rho\Omega^2 \frac{(r^2-a^2)^2}{r^3}\, dr$$

$$= \tfrac{1}{2}\rho\Omega^2\left[(a+d)^2 - a^4(a+d)^{-2} - 4a^2 \log\left(\frac{a+d}{a}\right)\right].$$

Let us now assume that the inside pressure on the discontinuity surface is very nearly the same as that on a circular cylinder of radius a due to a source of same output W placed on the axis. Then

$$p_i-(p_a)_i = -\tfrac{1}{2}\rho\left[\left(\frac{\partial\phi}{\partial x}\right)^2_{r=a} - \frac{W^2}{4\pi^2a^4}\right]$$

where ϕ is given by (11). Therefore

$$p_i-(p_a)_i = \tfrac{1}{2}\rho\frac{W^2}{4\pi^2a^4}\left[1-\left(1+2\sum\frac{e^{-\alpha_n x/a}}{J_0(\alpha_n)}\right)^2\right]$$
$$= -\tfrac{1}{2}\rho\frac{W^2}{\pi^2a^4}\left[\sum\frac{e^{-\alpha_n x/a}}{J_0(\alpha_n)}+\left(\sum\frac{e^{-\alpha_n x/a}}{J_0(\alpha_n)}\right)^2\right].$$

Equating the pressure inside with that outside, we get

$$(a+d)^2-a^4(a+d)^{-2}-4a^2\log\left(\frac{a+d}{a}\right)$$
$$= -\frac{W^2}{\pi^2\Omega^2a^4}\left[\sum\frac{e^{-\alpha_n x/a}}{J_0(\alpha_n)}+\left(\sum\frac{e^{-\alpha_n x/a}}{J_0(\alpha_n)}\right)^2\right]$$

or $$\left(\frac{a+d}{a}\right)^2-\left(\frac{a+d}{a}\right)^{-2}-4\log\left(\frac{a+d}{a}\right)$$
$$= -\frac{W^2}{\pi^2\Omega^2a^6}\left[\sum\frac{e^{-\alpha_n x/a}}{J_0(\alpha_n)}+\left(\sum\frac{e^{-\alpha_n x/a}}{J_0(\alpha_n)}\right)^2\right].$$

But, from (8), $$\frac{W^2}{4\pi^2\Omega^2a^6} = 0{\cdot}3918.$$

Therefore

$$\left(\frac{a+d}{a}\right)^2-\left(\frac{a+d}{a}\right)^{-2}-4\log\left(\frac{a+d}{a}\right)$$
$$= -1{\cdot}5672\left[\sum\frac{e^{-\alpha_n x/a}}{J_0(\alpha_n)}+\left(\sum\frac{e^{-\alpha_n x/a}}{J_0(\alpha_n)}\right)^2\right]. \quad (12)$$

This equation has been solved numerically for different values of the axial distance. The solutions are given in the tabulated form below.

TABLE 1

x/a	$\sum\frac{e^{-\alpha_n x/a}}{J_0(\alpha_n)}$	d/a
0	$-0{\cdot}5$	0·68
$\frac{1}{2}$	$-0{\cdot}2845$	0·62
1	$-0{\cdot}5106\times10^{-1}$	0·35
2	$-0{\cdot}1191\times10^{-2}$	0·09

The results are illustrated in Fig. 1.

Finally, the author wishes to thank Sir Geoffrey Taylor, F.R.S., for his interest and guidance during the course of this work.

REFERENCES

1. K. Stewartson, *Quart. J. Mech. and Applied Math.* **4** (1953), 45.
2. G. N. Watson, *Theory of Bessel Functions* (Cambridge, 1922), 597.

NOTE ON TEST FUNCTIONS FOR STABILITY

By W. J. DUNCAN (*Department of Aeronautics and Fluid Mechanics in the University of Glasgow*)

[Received 29 April 1954]

SUMMARY

Simple relations are established between the determinantal forms of the test functions of a given polynomial and of certain related polynomials. These relations are applied to the computation of the test functions and, in particular, of the critical test determinant. It is shown that when the characteristic equation can be factorized, as when certain couplings are absent, the critical test determinant contains an irrelevant factor which is the eliminant of a pair of algebraic equations.

1. Introduction

THIS note is concerned with the test functions for the stability of dynamical systems whose equations of motion are linear with constant coefficients. These are functions of the coefficients of the determinantal or characteristic equation of the system and were first given by Routh (**1, 2**); the necessary and sufficient conditions for stability when the characteristic equation is of the nth degree are that the n test functions shall all be positive, it being understood that the equation is written with the coefficient of the highest power of the unknown positive. Equivalent conditions were later given by Hurwitz (**3**) and Frazer (**4**) in the form that n test determinants $T_1,\ldots, T_n$ shall all be positive. Let the characteristic equation be

$$p_n\lambda^n+p_{n-1}\lambda^{n-1}+\ldots+p_1\lambda+p_0 = 0, \tag{1.1}$$

where p_n is positive. Then

$$T_1 = p_{n-1}, \tag{1.2}$$

$$T_2 = \begin{vmatrix} p_{n-1} & p_n \\ p_{n-3} & p_{n-2} \end{vmatrix}, \tag{1.3}$$

$$T_3 = \begin{vmatrix} p_{n-1} & p_n & 0 \\ p_{n-3} & p_{n-2} & p_{n-1} \\ p_{n-5} & p_{n-4} & p_{n-3} \end{vmatrix}, \tag{1.4}$$

and so on, where a zero is to be substituted for a coefficient when its suffix is negative or exceeds n. It can easily be shown that

$$T_n = p_0 T_{n-1}, \tag{1.5}$$

so the effective conditions are that $T_1,\ldots, T_{n-1}$ and p_0 shall all be positive.

It appears that $p_0 > 0$ and $T_{n-1} > 0$ are *critical criteria for stability* (**4, 5**) since the first occurrence of instability in a system which is completely stable in a basic state must be indicated by the failure of one or the other of these two criteria. The critical condition $T_{n-1} = 0$ is of special importance since, for example, it determines the critical speeds for the flutter of aircraft.

It is shown here that there are simple relations between the test functions of a given polynomial and those of certain related polynomials. These relations can be applied usefully in the computation of test functions. By aid of them it is shown, for example, that the critical test function T_{2m-1} for a characteristic equation of degree $2m$ can be made to depend on the test function T_{2m-3} for a related equation of degree $(2m-2)$. By repeated use of this transformation T_{2m-1} is made to depend on the test function T_3 for a quartic and this is very easily computed. It is also shown that when the characteristic equation can be factorized, as when certain couplings are absent, the critical test function contains an irrelevant factor which is the eliminant of a pair of algebraic equations.

2. Test functions of related polynomials

We shall begin by taking a sextic equation and consider equations of other degrees later. Accordingly the equation under discussion is

$$f(\lambda) \equiv p_6\lambda^6+p_5\lambda^5+p_4\lambda^4+p_3\lambda^3+p_2\lambda^2+p_1\lambda+p_0 = 0 \tag{2.1}$$

and we consider the polynomial

$$F(\lambda) \equiv P_6\lambda^6+P_5\lambda^5+P_4\lambda^4+P_3\lambda^3+P_2\lambda^2+P_1\lambda+P_0 \tag{2.2}$$

obtained from $f(\lambda)$ by adding the sextic

$$(p_5\lambda^4+p_3\lambda^2+p_1)(a\lambda^2+b\lambda+c), \tag{2.3}$$

where a, b, and c are arbitrary constants. The coefficients of (2.2) are accordingly given by

$$P_6 = p_6+ap_5 \tag{2.4}$$

$$P_5 = (1+b)p_5 \tag{2.5}$$

$$P_4 = p_4+ap_3+cp_5 \tag{2.6}$$

$$P_3 = (1+b)p_3 \tag{2.7}$$

$$P_2 = p_2+ap_1+cp_3 \tag{2.8}$$

$$P_1 = (1+b)p_1 \tag{2.9}$$

$$P_0 = p_0+cp_1. \tag{2.10}$$

The penultimate and critical test function for $F(\lambda)$ is T'_5, where

$$T'_5 = \begin{vmatrix} P_5 & P_6 & 0 & 0 & 0 \\ P_3 & P_4 & P_5 & P_6 & 0 \\ P_1 & P_2 & P_3 & P_4 & P_5 \\ 0 & P_0 & P_1 & P_2 & P_3 \\ 0 & 0 & 0 & P_0 & P_1 \end{vmatrix} \tag{2.11}$$

$$= (1+b)^3 \begin{vmatrix} p_5 & p_6+ap_5 & 0 & 0 & 0 \\ p_3 & p_4+ap_3+cp_5 & p_5 & p_6+ap_5 & 0 \\ p_1 & p_2+ap_1+cp_3 & p_3 & p_4+ap_3+cp_5 & p_5 \\ 0 & p_0+cp_1 & p_1 & p_2+ap_1+cp_3 & p_3 \\ 0 & 0 & 0 & p_0+cp_1 & p_1 \end{vmatrix} \tag{2.12}$$

on substitution from equations (2.4) to (2.10). In the last determinant:

subtract from the 2nd column the 1st column multiplied by a and the 3rd column multiplied by c

subtract from the 4th column the 3rd column multiplied by a and the 5th column multiplied by c.

Equation (2.12) now becomes

$$T'_5 = (1+b)^3 T_5, \tag{2.13}$$

where T_5 is the penultimate test function for the original polynomial $f(\lambda)$. Similarly we find that the other test functions of odd order are given by

$$T'_3 = (1+b)^2 T_3 \tag{2.14}$$

$$T'_1 = (1+b) T_1. \tag{2.15}$$

Next,

$$T'_2 = \begin{vmatrix} P_5 & P_6 \\ P_3 & P_4 \end{vmatrix} = (1+b) \begin{vmatrix} p_5 & p_6+ap_5 \\ p_3 & p_4+ap_3+cp_5 \end{vmatrix}$$

$$= (1+b) \begin{vmatrix} p_5 & p_6 \\ p_3 & p_4+cp_5 \end{vmatrix}$$

$$= (1+b)T_2 + c(1+b)p_5^2. \tag{2.16}$$

In a similar manner we obtain

$$T'_4 = (1+b)^2 T_4 + c(1+b)^2 p_3 T_3 - c(1+b)^2 p_1 p_5 T_2 + c(1+b)^2 p_0 p_5^3. \tag{2.17}$$

On account of the importance of the critical test function T_5, equation (2.13) is the most interesting of these relations. We see that all the test functions of odd order are unchanged when b is zero.

Take now a polynomial of general *even* degree $2n$. The equation from which we start is

$$f(\lambda) \equiv p_{2n}\lambda^{2n} + p_{2n-1}\lambda^{2n-1} + \ldots + p_1\lambda + p_0 = 0, \tag{2.18}$$

and we consider the test functions of the polynomial $F(\lambda)$ obtained from $f(\lambda)$ by adding

$$(p_{2n-1}\lambda^{2n-2}+p_{2n-3}\lambda^{2n-4}+...+p_1)(a\lambda^2+b\lambda+c), \tag{2.19}$$

where a, b, and c are arbitrary constants. The coefficients of $F(\lambda)$ are therefore given by

$$P_{2r+1} = (1+b)p_{2r+1}, \tag{2.20}$$

$$P_{2r} = p_{2r}+ap_{2r-1}+cp_{2r+1}, \tag{2.21}$$

where a zero must be substituted for the coefficient p when its suffix is negative or greater than $2n$. Hence we find by the method used for the sextic that the critical penultimate test function for $F(\lambda)$ is

$$T'_{2n-1} = (1+b)^n T_{2n-1}, \tag{2.22}$$

while the general test function of odd order is

$$T'_{2r-1} = (1+b)^r T_{2r-1}. \tag{2.23}$$

The test functions of even order are given by equations which are the generalizations of (2.16) and (2.17). All the test functions of odd order are unchanged when b is zero.

Polynomials of odd degree are of less importance in technical applications than those of even degree and they cannot here be treated in exactly the same manner. Let us take the equation

$$f(\lambda) \equiv p_{2n+1}\lambda^{2n+1}+p_{2n}\lambda^{2n}+...+p_1\lambda+p_0 = 0 \tag{2.24}$$

and consider the function $F(\lambda)$ obtained from $f(\lambda)$ by adding

$$(p_{2n}\lambda^{2n}+p_{2n-2}\lambda^{2n-2}+...+p_0)(b\lambda+c), \tag{2.25}$$

where b and c are arbitrary constants. We now find that the penultimate and critical test function for the modified polynomial is

$$T'_{2n} = (1+c)^n T_{2n} \tag{2.26}$$

while the general test function of even order is

$$T'_{2r} = (1+c)^r T_{2r}. \tag{2.27}$$

Hence all the test functions of even order are unaltered when c is zero. Those of odd order are given by equations similar to (2.16) and (2.17) which can easily be obtained in any given case.

An explanation of the simple relations (2.22) and (2.26) concerning the penultimate test function can be based on an argument which will be exemplified by the case where the polynomial is of even degree $2n$. It is known (4) that T_{2n-1} is a form of the eliminant of the equations

$$p_{2n}\lambda^{2n}+p_{2n-2}\lambda^{2n-2}+...+p_0 = 0, \tag{2.28}$$

$$p_{2n-1}\lambda^{2n-2}+p_{2n-3}\lambda^{2n-4}+...+p_1 = 0 \tag{2.29}$$

and the vanishing of T_{2n-1} is the condition that the equations shall have a common root. Suppose then that T_{2n-1} is zero so that (2.28) and (2.29) are simultaneously satisfied by $\lambda = \pm\beta$, say. Then $f(\lambda)$ has the pair of roots $\pm\beta$ since we obtain

$$f(\lambda) = 0$$

when we multiply (2.29) by λ and add it to (2.28). But we see from (2.19) that $F(\lambda)$ is also satisfied by $\lambda = \pm\beta$, whatever may be the values of a, b, and c. Consequently T'_{2n-1} is zero, i.e. T'_{2n-1} and T_{2n-1} necessarily vanish simultaneously. We conclude that T'_{2n-1} must contain T_{2n-1} as a factor and we should expect the coefficient to depend on a, b, and c; in fact the coefficient depends only on b, as already shown.

3. Test functions when the characteristic equation can be factorized

Let us consider a dynamical system having $(m+n)$ degrees of freedom whose characteristic determinant can be represented in the partitioned form

$$\Delta(\lambda) \equiv \begin{vmatrix} \Delta_{11}(\lambda) & \Delta_{12}(\lambda) \\ 0 & \Delta_{22}(\lambda) \end{vmatrix} = 0, \tag{3.1}$$

where $\Delta_{11}(\lambda)$ is the characteristic matrix of the first subsystem in isolation, $\Delta_{22}(\lambda)$ is that of the second subsystem in isolation, while $\Delta_{12}(\lambda)$ represents coupling agencies; it is to be noted that the system is degenerate since $\Delta_{21}(\lambda)$ is zero. The first subsystem has m degrees of freedom, so

$$|\Delta_{11}(\lambda)| = 0$$

is an equation of degree $2m$ and the second subsystem has n degrees of freedom, so

$$|\Delta_{22}(\lambda)| = 0$$

is an equation of degree $2n$. It follows that

$$\Delta(\lambda) \equiv |\Delta_{11}(\lambda)| \times |\Delta_{22}(\lambda)| = 0 \tag{3.2}$$

is an equation of degree $2(m+n)$. Now the complete system reaches a critical state when either of the subsystems does so. Consequently the penultimate test function $T_{2m+2n-1}$ must contain the product $T_{2m-1}T_{2n-1}$ as a factor. We shall show, however, that there is another factor in $T_{2m+2n-1}$. For a system with m degrees of freedom each coefficient in the characteristic equation is of degree m in the dynamical coefficients (inertias, stiffnesses, damping coefficients) and the critical test function T_{2m-1} is thus of degree $m(2m-1)$ in these coefficients. Similarly $T_{2m+2n-1}$ is of degree

$$(m+n)(2m+2n-1)$$

in the dynamical coefficients whereas the product $T_{2m-1}T_{2n-1}$ is of degree

$$m(2m-1)+n(2n-1) = 2(m^2+n^2)-(m+n).$$

The difference of these numbers is D, the degree of the further factor in $T_{2m+2n-1}$. Thus

$$D = (m+n)(2m+2n-1)-2(m^2+n^2)+(m+n)$$
$$= 4mn. \tag{3.3}$$

We have now to consider the nature of this factor, and the key lies in the fact (**5**) that for an equation in λ of degree r the penultimate test function is given by

$$T_{r-1} = (-1)^{r(r-1)/2} p_r^{r-1}\,\Pi, \tag{3.4}$$

where Π is the continued product of the sums of the roots taken in pairs. This shows that the penultimate test function for the equation (3.2) can vanish in three distinct ways:

(i) The equation $$|\Delta_{11}(\lambda)| = 0 \tag{3.5}$$ has a pair of equal and opposite roots. When this occurs T_{2m-1} vanishes.

(ii) The equation $$|\Delta_{22}(\lambda)| = 0 \tag{3.6}$$ has a pair of equal and opposite roots. When this occurs T_{2n-1} vanishes.

(iii) Equations (3.5) and (3.6) have equal and opposite roots. This is indicated by the vanishing of the eliminant E_{12} of the equations

$$\left.\begin{aligned}|\Delta_{11}(\lambda)| &= 0\\ |\Delta_{22}(-\lambda)| &= 0\end{aligned}\right\}. \tag{3.7}$$

Consequently $T_{2m+2n-1}$ contains E_{12} as a factor and E_{12} can be written in such a way that

$$T_{2m+2n-1} = E_{12}\,T_{2m-1}\,T_{2n-1}. \tag{3.8}$$

We shall now give a very simple illustration of the foregoing. Let

$$\Delta(\lambda) \equiv \begin{vmatrix} A_{11}\lambda^2+B_{11}\lambda+C_{11} & A_{12}\lambda^2+B_{12}\lambda+C_{12} \\ 0 & A_{22}\lambda^2+B_{22}\lambda+C_{22} \end{vmatrix} = 0. \tag{3.9}$$

Here the two factors of $\Delta(\lambda)$ are quadratics whose penultimate test functions T_1 are B_{11} and B_{22}. E_{12} is the eliminant of

$$\left.\begin{aligned}A_{11}\lambda^2+B_{11}\lambda+C_{11} &= 0\\ A_{22}\lambda^2-B_{22}\lambda+C_{22} &= 0\end{aligned}\right\} \tag{3.10}$$

which can be written

$$E_{12} = (A_{11}B_{22}+A_{22}B_{11})(B_{11}C_{22}+B_{22}C_{11})+(A_{11}C_{22}-A_{22}C_{11})^2. \tag{3.11}$$

It can easily be verified that the penultimate test function for the quartic equation (3.9) is given by

$$T_3 = B_{11}B_{22}E_{12}. \tag{3.12}$$

4. Computation of test functions

The results obtained in § 2 can be applied in the computation of test functions and we shall begin with the case of the sextic equation (2.1). Let us put

$$\left.\begin{aligned} b &= 0 \\ a &= -p_6/p_5 \\ c &= -p_0/p_1 \end{aligned}\right\}. \tag{4.1}$$

Then we have by (2.4) and (2.10) that

$$P_0 = P_6 = 0. \tag{4.2}$$

Accordingly the expressions for the test functions of the modified polynomial become

$$T_1' = P_5 \tag{4.3}$$

$$T_2' = P_5 P_4 \tag{4.4}$$

$$T_3' = P_5(P_3 P_4 - P_2 P_5) \tag{4.5}$$

$$T_4' = P_5(P_2 P_3 P_4 - P_1 P_4^2 - P_5 P_2^2) \tag{4.6}$$

$$T_5' = P_1 T_4'. \tag{4.7}$$

Also equations (2.13) to (2.17) yield

$$T_1 = T_1' \tag{4.8}$$

$$T_2 = T_2' - cp_5^2 \tag{4.9}$$

$$T_3 = T_3' \tag{4.10}$$

$$T_4 = T_4' - cp_3 T_3 + cp_1 p_5 T_2 - cp_0 p_5^3 \tag{4.11}$$

$$T_5 = T_5'. \tag{4.12}$$

When interest is confined to the critical test function T_5 the computation by the application of (4.6), (4.7), and (4.12) is particularly easy. Another scheme of calculation for the test functions of the sextic will be found in reference (**6**). It may be noted that the expression within brackets in (4.6) is the test function T_3 for the quartic

$$P_5 \lambda^4 + P_4 \lambda^3 + P_3 \lambda^2 + P_2 \lambda + P_1 = 0. \tag{4.13}$$

Hence we have, in effect, expressed T_5 for the sextic in terms of T_3 for a related quartic.

We shall now take the octic equation and confine the work to the computation of the critical test function T_7. We put $b = 0$, $a = -p_8/p_7$, and $c = -p_0/p_1$, so that $P_8 = P_0 = 0$. Then by (2.23)

$$T_7 = T_7' = P_1 P_7 \begin{vmatrix} P_6 & P_7 & 0 & 0 & 0 \\ P_4 & P_5 & P_6 & P_7 & 0 \\ P_2 & P_3 & P_4 & P_5 & P_6 \\ 0 & P_1 & P_2 & P_3 & P_4 \\ 0 & 0 & 0 & P_1 & P_2 \end{vmatrix}. \tag{4.14}$$

The fifth-order determinant in the last equation can be dealt with by either of the following procedures:

(*a*) Subtract the 1st column $\times P_7/P_6$ from the 2nd column and the 5th column $\times P_1/P_2$ from the 4th column. The determinant is then expressed in terms of another of the third order.

(*b*) Treat the fifth-order determinant as the test function T_5 of the sextic equation

$$P_7\lambda^6+P_6\lambda^5+P_5\lambda^4+P_4\lambda^3+P_3\lambda^2+P_2\lambda+P_1 = 0 \qquad (4.15)$$

and use the scheme of calculation already given for the sextic.

Another method for calculating the test functions of the octic is given in reference (**7**).

Equations of even degree higher than the eighth can be treated by an extension of the process given here. Thus T_9 for an equation of the tenth degree is expressed in terms of T_7 for an octic and this in terms of T_5 for a sextic. Finally, T_5 is expressed in terms of T_3 for a quartic and so computed with ease.

REFERENCES

1. E. J. Routh, *A Treatise on the Stability of a Given State of Motion* (Macmillan, 1877).
2. —— *Advanced Rigid Dynamics* (Macmillan).
3. A. Hurwitz, 'Über die Bedingungen, unter welchen eine Gleichung nur Wurzeln mit negativen reelen Theilen besitzt', *Math. Annalen*, **46** (1895), 273–84.
4. R. A. Frazer and W. J. Duncan, 'On the criteria for the stability of small motions', *Proc. Roy. Soc.* A, **124** (1929), 642.
5. W. J. Duncan, *The Principles of the Control and Stability of Aircraft* (Cambridge, 1952).
6. —— 'Stability criteria, with special reference to the sextic equation'. *J. Roy. Aero. Soc.*, June 1954, 431.
7. —— 'Stability criteria for the octic equation', ibid., Sept. 1954, 649.

A METHOD OF CALCULATING THE NORMAL MODES OF AN AIRCRAFT

By B. A. HUNN (*late Hawker Aircraft Ltd.*)

[Received 26 November 1953]

SUMMARY

In order to calculate the critical speeds at which an aircraft will flutter it is first necessary to determine the manner in which the vibration will take place. This mode of vibration is generally obtained by assuming it to be expressible in terms of some of the aircraft normal modes.

On a projected design it is therefore necessary to calculate the free space normal modes of the aircraft which will be required for the flutter calculation. A method of simplifying this calculation has already been proposed by the author (**1**), and now that this has been applied successfully some attempt has been made to amplify and justify the technique. This is given here although the justification is not attempted on a general basis. Throughout, where possible and convenient, the various points raised are illustrated by numerical examples based largely on the uniform cantilever beam theory.

1. Introduction

In order to calculate modes of vibration of a structure it is necessary to know how it deforms under any arbitrary system of applied loads. This requires, in turn, a complete elastic analysis which is known to be theoretically possible provided the strains are of sufficiently small size to permit linear superposition (**2**). What in theory is possible in practice turns out to be extremely difficult when complete aircraft structures are considered, and it generally happens that some simplified approach such as 'Engineer's Theory' must be employed. This simplification necessarily introduces small local errors in the analysis which, though insignificant from the point of view of the structural engineer, can become quite important in the determination of the higher modes of vibration of the aircraft.

The discrete mass method for calculating normal modes finds wide acceptance in the aircraft industry and involves the construction of a dynamical model (in the mathematical sense) in which the continuous mass distribution is replaced by point masses attached to a light framework whose elastic properties are those of the structure. However, the construction of the model does not seem to be governed by any rigorous rules of procedure except in so far as the number of point masses is related to the number of modes required. It seems intuitively obvious, though, that their distribution ought to follow broadly that of the continuous structure; for example, a uniform beam is better represented by a set of equal masses equally spaced

rather than the same number concentrated in groups. The distribution ought also to follow the trends indicated by the elastic analysis; for example, it would be wasteful to use a large number of masses in those regions where the motion would be small, i.e. near the root of a cantilever beam.

These remarks indicate that the whole procedure is governed by intuition and expediency. Indeed, one overriding consideration is the extent of the computations made necessary by a detailed model, which is roughly proportional to the square of the number of point masses used. It follows that the general tendency is to use the minimum detail in constructing such models. If one accepts the statement by Minhinnick (**3**) that four times as many masses should be used as the number of modes required, hardly more than the first three modes of any structure can be calculated using a desk machine. If, instead of a simple structure, a complete aircraft be considered, then to obtain the first three modes adequately probably more than forty masses would be necessary. Even on electronic digital computers more than twice this number would involve, not only a lengthy and probably expensive programming, but also considerable basic elastic analysis.

In solving the mode problem using the discrete mass method it is usual to determine iteratively the characteristic roots and vectors of a matrix whose size is determined by the number of point masses used on the model. The way in which successive roots are extracted from such matrices depends upon a linear manipulation of the columns and rows so that the order is reduced by one after each root is found, when desk machines are used (**4**). On digital machines the actual characteristic roots can be evaluated, which, on substitution back into the matrix, give sets of homogeneous simultaneous equations whose solutions are the characteristic vectors. In either case it can be shown that the modes, in order, depend to an increasing extent upon the accuracy of the elements of the matrix. It would be safe to say that if the fundamental mode were required to a 10 per cent. accuracy then a similar accuracy must be obtained in the elements of the matrix, and if the same accuracy were required of the first overtone, this accuracy must be improved to 1 per cent. If one bears in mind the simplifications imposed by Engineer's Theory, it would seem difficult to ensure such an accuracy as would permit the calculation of any mode higher than the third.

The method proposed in (**1**) replaces the freedoms of the individual masses by some normal mode shapes of the wings, tailplane, and fuselage under root-fixed conditions, in the matrix for the complete aircraft. In order to justify such a procedure it is first necessary to examine critically the discrete mass method. Certain questions emerge of fundamental importance (**4**). Perhaps the most important concerns the validity of the

dynamical model: whether one may replace a continuous structure possessing infinitely many normal modes by one possessing only a finite number, only the first few of which are representative. Secondly, since the deflexions of the point masses are interpreted as the ordinates of a continuous deflexion curve, to what detail must these discrete ordinates be known in order that the curve may be adequately determined? Thirdly, does the method suggested in (**1**), which makes use of the common idea of truncating infinite series of normal modes to a finite sum, fulfil the conditions of the convergence of the series in such a manner that finite sums are adequate? Finally, having regard to the replacement of subdivisions of the structure having extension by discrete masses, ought the implication of this extension to be taken into account by the use of moments of inertia?

2. Outline of the method of approximate solution

A general answer to the first question is difficult to obtain, but it is instructive to consider the problem of a cantilever beam (**4**). The normal modes are solutions of the integral equation

$$z(x) = \omega^2 \int_0^l F(x,y)\rho(y)z(y)\,dy, \tag{2.1}$$

where

$z(x)$ is the mode shape which may be chosen such that

$$\overline{\lim}\,|z(x)| = 1,$$

ω is the circular frequency appropriate to a given solution.
$\rho(y)$ is the density per unit length, and
$F(x,y)$ is the deflexion at station x due to unit load at station y.

If the beam length is large in relation to its depth, $F(x,y)$ may be determined from

$$F(x,y) = \int_0^x \frac{(v-y)(v-x)}{EI(v)}\,dv, \quad \text{for } x \leqslant y, \tag{2.2}$$

and use of Maxwell's reciprocal theorem $F(x,y) = F(y,x)$. In this expression E is the elastic modulus and $I(v)$ the local value of the second moment of area of the cross-section about the neutral axis.

The definition of the Riemann integral is

$$\int_0^l F(x,y)\rho(y)z(y)\,dy = \lim_{\substack{n\to\infty \\ N(y_r,y_{r+1})\to 0}} \sum_{r=1}^{n} F(x,y_r')\rho(y_r')z(y_r')(y_{r+1}-y_r), \tag{2.3}$$

where $y_{r+1} > y_r' > y_r$ and $N(y_r, y_{r+1})$ is the norm of all intervals (y_r, y_{r+1}).

Accordingly one may write

$$\sum_{r=1}^{n} F(x, y'_r)\rho(y'_r)z(y'_r)(y_{r+1}-y_r) = \epsilon(x)+\int_0^l F(x,y)\rho(y)z(y)\,dy, \tag{2.4}$$

where ϵ is a function of x, n, the distribution of y_r and the order of the function $z(y)$. It is certainly possible to choose n and y_r such that

$$|\epsilon(x)| \leqslant |z(x)|, \tag{2.5}$$

and this being a finite set of intervals the equations

$$z(x_r) = \omega^2 \sum_{s=1}^{n} F(x_r, y_s)z(y_s)\rho(y_s)\delta y_s$$

can be solved to give a finite set of roots, some of which will closely approximate to the corresponding normal modes at the points $x_r = y_r$. A necessary condition for the validity of this approximation to the integral is

(i) that the variation of $F(x,y)\rho(y)z(y)$ in $y_r \leqslant y \leqslant y_{r+1}$ for all r and x is roughly linear.

This condition necessarily rejects all roots whose mode shapes violate this condition. A sufficient set of conditions is

(i*a*) that the variation of $F(x,y)$ in $y_r \leqslant y \leqslant y_{r+1}$ for all r and x is small,

(ii) that the variation of $\rho(y)$ in $y_r \leqslant y \leqslant y_{r+1}$ is small for all r,

(iii) that the variation of $z(y)$ in $y_r \leqslant y \leqslant y_{r+1}$ is small for all r.

Though not necessary, these conditions indicate in what way a dynamical model can be constructed and provide a means of testing for accuracy the roots subsequently extracted. Though the valid range of roots can hardly be known *a priori*, it is certain that, since the number of zeros of $z(y)$ for $0 \leqslant y \leqslant l$ is equal to its order in the infinite set, considerably more discrete masses must be used in the model than the number of roots required.

3. Influence of accuracy of the elastic analysis

In point of fact the function $F(x,y)$ is known only approximately, and if one writes $F'(x,y)$ as this approximate function, then

$$F'(x,y) = F(x,y)+\epsilon_1(x,y). \tag{3.1}$$

Clearly, since an exact elastic analysis is not available, the extent of $\epsilon_1(x,y)$ can never be estimated. It is, however, possible to illustrate the influence on the accuracy of the roots of the numerical accuracy of the elements of the matrix by the simple expedient of comparing the first few roots extracted from a matrix whose elements are expressed to six significant figures with those from the matrix obtained by rounding off the elements to four figures. This has been done for the case of a 5-mass dynamical model of a uniform beam. Comparative tables of the first three vectors are shown in Table 1,

together with the corresponding characteristic root values. These results show that no serious error becomes noticeable until the third root is reached, as might be expected. Although more than five masses should be used for a model from which three roots are required, it is sufficient to regard this as an exercise on a discrete mass system. It is to be expected that these results would be obtained on a model possessing a higher number of degrees of freedom, and therefore the accuracy of the vectors is a function of the accuracy of the matrix elements and not the number of degrees of freedom.

TABLE 1

Comparison of 3 vectors from 2 matrices of differing accuracy†

Mode	1 (6 *figs.*)	1 (4 *figs.*)	2 (6 *figs.*)	2 (4 *figs.*)	3 (6 *figs.*)	3 (4 *figs.*)
y/l \ λ	0·0794142	0·0794124	0·0019312	0·0019326	0·0002266	0·0002352
0·1	0·03371	0·03338	−0·017507	−0·017266	−0·100668	−0·092711
0·3	0·27405	0·27405	−0·098792	−0·101721	−0·29462	−0·337465
0·5	0·68097	0·68129	−0·131154	−0·135655	0·004601	0·022192
0·7	1·18351	1·18336	−0·052909	−0·055104	0·278356	0·294872
0·9	1·72479	1·72479	0·104165	0·107842	−0·144032	−0·155673

4. A comparison of analytical and approximate solutions (ref. 4)

It is difficult to find suitable beam problems from which analytical solutions can be obtained. For this reason the example chosen for comparison between the analytical and approximate solutions is that of the uniform cantilever beam of sufficient length to permit the use of Saint-Venant's principle. Since the beam is uniform, the density $\rho(y)$ and the function $EI(y)$ are constants. The following definitions are used:

$EI(y) = K$,
$\rho(y) = \rho_0$,
l = beam length,
y = distance from root,
$z(y)$ = deflexion function,
$\omega_r = 2\pi \times$ frequency of normal mode r,
α_r = mode parameter defined by $\cosh \alpha_r l \cos \alpha_r l = -1$.

The general solution of the normal mode problem is

$$z(y) = A\Big\{(\cosh \alpha_r l(y/l) - \cos \alpha_r l(y/l)) - \left[\frac{\cosh \alpha_r l + \cos \alpha_r l}{\sinh \alpha_r l + \sin \alpha_r l}\right](\sinh \alpha_r l(y/l) - \sin \alpha_r l(y/l))\Big\} \quad (4.1)$$

† λ is defined in (4.4).

and the frequency is given by

$$\omega_r^2 = \frac{(\alpha_r l)^4 K}{\rho_0 l^4}. \tag{4.2}$$

In passing it should be noticed that

$$\lim_{(y/l)\to 1} \left|\frac{z(y)}{A}\right| = 2, \tag{4.3}$$

and this is the maximum value of z/A for all values of y/l.

An equivalent dynamical model was constructed taking five equal segments of beam (0–0·2), (0·2–0·4), etc., such that five point masses $0{\cdot}2l\rho_0$ could be placed at $(y/l) = 0{\cdot}1, 0{\cdot}3, \ldots, 0{\cdot}9$. This model was then used to derive the first three characteristic roots. Throughout this example λ is defined by

$$\lambda = \frac{K}{\omega^2 l^4 \rho_0}. \tag{4.4}$$

Comparative results of the modal shapes and characteristic root values are shown in Table 2. It should be emphasized that five masses would not be regarded as adequate for the extraction of the first three modes, but this number has been chosen to illustrate the falling off in accuracy fairly quickly. Since the amplitudes of the shapes are arbitrary, the corresponding vectors have been made to coincide at one convenient point in each case.

TABLE 2

Comparison of roots obtained analytically and approximately

Mode	1 (*analyt.*)	1 (5 *mass*)	2 (*analyt.*)	2 (5 *mass*)	3 (*analyt.*)	3 (5 *mass*)
λ / (y/l)	0·080884	0·079414	0·0020597	0·0019312	0·0002627	0·0002266
0·1	0·03354	0·03371	0·18526	0·19053	0·45614	0·47552
0·3	0·27296	0·27405	1·05227	1·07514	1·44900	1·39168
0·5	0·67904	0·68097	1·42733	1·42733	0·03938	−0·02173
0·7	1·18175	1·18351	0·63410	0·57580	−1·31485	−1·31485
0·9	1·72479	1·72479	−1·04750	−1·13361	0·45701	0·68035

5. Discussion of the method on the complete aircraft

If one turns now to the question of the most economical solution of the normal mode problem for the complete aircraft in free space, it is clear that, for any dynamical model, the number of degrees of freedom must be considerably in excess of the number of modes extracted, since each element of the structure must possess at least four times as many point masses in its model as the number of modes required. To illustrate this point more

clearly consider the deformation shape $f(x,y)$ of a wing in a given mode. Let $m_s(x,y)$ denote root-fixed modes of the wing. Then

$$f(x,y) = \sum_1^\infty a_s m_s(x,y), \tag{5.1}$$

a_r being determinate multipliers.

This equation implies convergence of the series so that a finite sum S_n where

$$S_n = \sum_1^n a_s m_s(x,y) \tag{5.2}$$

may be expected to provide an answer whose accuracy increases as n increases. Let it be supposed that a given value of n, say n_0, gives answers adequate for the purposes of the normal mode investigation. Suppose, further, that the dynamical model is so chosen that it can provide normal mode shapes $M_s(x,y)$ such that

$$M_s(x,y) = m_s(x,y)+\epsilon_s(x,y), \tag{5.3}$$

where ϵ_s is small for $$1 \leqslant s \leqslant N. \tag{5.4}$$

Then provided $$N \geqslant n_0 \tag{5.5}$$

the dynamical model will give an adequate approximation to $f(x,y)$.

There must, however, be far more than N degrees of freedom in the dynamical model. By virtue of the two considerations,

(i) that there must be four times as many point masses in the model as the number of normal modes required, and

(ii) that if s normal modes be required from the model, each influence coefficient should possess a percentage accuracy of about $10^{-(s-1)}$ per cent., if the last mode is to be accurate to 10 per cent.,

it usually follows that N is limited, therefore limiting the types of shape $f(x,y)$ rather than vice versa.

Nevertheless, let it be supposed that for a given N the modes can be adequately determined. It then follows that there are $4N$ degrees of freedom on the model, $3N$ of which serve no other purpose than that they are required to ensure accuracy in N of the modes. The method of economizing on the computing labour suggested in (**1**) is as follows:

(*a*) Construct adequate dynamical models for each element of the structure, such as wings, tailplane, front and rear fuselages, and compute such of their root-fixed modes as can be expected to agree with those of the actual structure;

(*b*) Taking these root-fixed mode shapes as degrees of freedom together with rigid displacement modes, construct the usual Lagrangian equations of small vibrations for the complete structure. The usual kinetic

and strain energy terms are, of course, computed from the dynamical models of the parts.

The justification for this procedure is simply that if the matrix were constructed for the complete aircraft using every degree of freedom, only those modes would be extracted which would substantially agree with the foregoing argument. In other words, supposing a given number of modes were required for the complete aircraft, then, for example, the wing dynamical model would have to be adequate for the description of those root-fixed normal modes which would be required in the description of its shape in each of the complete modes. If any more of these modes were required for the description of the vibration shapes this dynamical model would be inadequate in both methods.

The extent of the labour saving is quite obvious. Suppose, for example, the first p modes of the complete aircraft are required. Let the first q modes of the wings enter substantially into the description of the wing shapes in this range of frequency. Let the first r modes of the tailplane, the first s of the rear fuselage, and the first t of the front fuselage enter similarly. Then the total number of degrees of freedom in the iterative matrix for the complete aircraft is $4(q+r+s+t)$.

The total number of multiplications in any iteration is clearly (for the fundamental)

$$N_0 = 16(q+r+s+t)^2. \tag{5.6}$$

The sum of the number of multiplications in an iteration determining the fundamental of each of the elements is simply

$$N_1 = 16(q^2+r^2+s^2+t^2). \tag{5.7}$$

The number of degrees of freedom in the final matrix of the complete aircraft using the method of (**1**) is $(q+r+s+t)$, so that the number of multiplications in an iteration for the fundamental is

$$N_2 = (q+r+s+t)^2. \tag{5.8}$$

Any precise analysis of the computing labour is complicated by the fact that the number of iterations required for the extraction of any mode depends upon the initial guess and the ratio of successive characteristic roots. Further, it is difficult to take account of the zero elements in the matrices which most generally occur. However, it can be seen that the order of labour saving is

$$N_0 - N_2 = 15(q+r+s+t)^2 \tag{5.9}$$

per iteration, for the extraction of the fundamental from the respective complete matrices. As against this, of course, there is the labour of extracting the roots of the elements, but since one can expect q, r, s, and t to be

proportional to p—the number of times the iterative process has to be applied to the final matrices—the general order of labour saving can be regarded (per mode) as being roughly

$$16(q+r+s+t)^2-16(q^2+r^2+s^2+t^2)$$

multiplications per iteration.

There is another equally important implication of the method. Supposing one were limited by the computing machinery available to solving characteristic root matrices no bigger than $N \times N$, then clearly on using the discrete mass matrix for the complete aircraft no more than N masses could be used, thus limiting the accuracy and number of modes which can be extracted. Using the separate normal mode method one may, however, use N discrete masses per element so that in the case of four elements to an aircraft the discrete mass matrix equivalent to that which may now be set up would contain $4N$ degrees of freedom.

6. Consideration of validity of the model under root excitation

Certain questions arise in connexion with this method. Perhaps the most important is connected with the adequacy of a dynamical model constructed under root-fixed conditions which is subject to root excitation. Take, for example, the case of the front fuselage on an aircraft under symmetrical vibrations. The shape of vibration of the front fuselage could be determined from the differential equation subject to the modified boundary conditions at the root

$$z(0) = a, \qquad \frac{dz(0)}{dy} = \theta. \tag{6.1}$$

In general the problem is to decide under what circumstances the dynamical model, represented by a finite set of normal modes, may adequately determine the correct vibration shape when subjected to root excitation.

Consider the solution for a cantilever beam subject to the excitation

$$z(0) = a, \qquad \theta = 0. \tag{6.2}$$

The solution may be expressed as

$$z(y) = a+a\sum_{r=1}^{\infty}\left(\frac{\alpha^4}{\alpha_r^4-\alpha^4}\right)\frac{\int\limits_0^l \rho(y)z_r(y)\,dy}{\int\limits_0^l \rho(y)z_r^2(y)\,dy}\,z_r(y), \tag{6.3}$$

where $z_r(y)$ are the root-fixed normal mode shapes and

$$(\alpha l)^4 = \frac{\rho_0\, l^4\omega^2}{K} \tag{6.4}$$

in the case of a uniform beam (see (4.2)).

The solution can be obtained from the dynamical model of discrete masses by solving a set of simultaneous equations equal in number to the number of masses. However, the solution in terms of a model described by a finite set of normal modes is given by

$$z_s = \sum_{r=1}^{n} q_r z_{rs}, \tag{6.5}$$

where

$$q_r = a\left(\frac{\alpha^4}{\alpha_r'^4 - \alpha^4}\right) \frac{\sum\limits_{s=1}^{n} m_s z_{rs}}{\sum\limits_{s=1}^{n} m_s z_{rs}^2} \tag{6.6}$$

and

z_s = deflexion of point mass m_s,
z_{rs} = deflexion of point mass m_s in the rth mode,
α_r' = the parameter associated with the mode frequency, the prime denoting approximation to the correct value.

Substitution of equation (6.6) in (6.5) gives a result analogous to equation (6.3).

Now, in determining the accuracy of such a method, careful definition is necessary. Quite clearly the shapes z_s will depend upon two distinct sets of numbers, i.e. the set $\alpha^4/(\alpha_r'^4 - \alpha^4)$ and the set $\sum\limits_{s=1}^{n} m_s z_{rs} \Big/ \sum\limits_{s=1}^{n} m_s z_{rs}^2$. If one considers the first set it is clear that values of α which coincide with α_r' (or α_r) cannot be allowed. However, neglecting these singular points, it is quite clear that since it is never likely to be true that $|\alpha_r' - \alpha_r| = 0$ for each and every r, it is quite possible to choose α such that

$$\left|\frac{1}{\alpha_r^4 - \alpha^4} - \frac{1}{\alpha_r'^4 - \alpha^4}\right| = K, \tag{6.7}$$

where K is large. It therefore follows that in prescribing α for an example in which analytical and approximate numerical solutions are compared, due account must be taken of the discrepancies between α_r and α_r'.

This may, on the face of it, seem a trivial point, but it should be remembered that it has a considerable bearing upon the mode shapes for a complete aircraft, for it often happens that the frequencies of the complete modes are close to those of the modes of the separate components. In passing it should be observed that though any uniform shift in the calculated mode frequencies is unimportant, it is essential that the relative distributions of the calculated root-fixed normal mode frequencies of the elements are very accurate, particularly if near coincidence between the modes on two elements occurs.

Considering the second set, ideally one requires that

$$\sum_{s=1}^{n} m_s z_{rs} \Big/ \sum_{s=1}^{n} m_s z_{rs}^2 = \int_0^l \rho(y) z_r(y)\, dy \Big/ \int_0^l \rho(y) z_r^2(y)\, dy \tag{6.8}$$

on referring to equations (6.3), (6.5), and (6.6). Two distinct types of inaccuracy can occur in evaluating this quotient. The first and perhaps the most significant type is due to the fact that the knowledge of a finite set of points on a curve does not constitute a complete specification. To illustrate this point, consider the set of points given by

$$\sin(n\pi x) - x = 0. \tag{6.9}$$

These are the intersections of the two curves given by

$$y = x \tag{6.10}$$

and

$$y = \sin(n\pi x). \tag{6.11}$$

Let it be supposed that one were given this set in the form (x_r, y_r) and required to draw a curve through the points without any reference to their derivation. The curves given by equations (6.10) and (6.11) would be amongst the infinite set of possible graphs. Thus, given any set of points, without reference to the physical nature of the problem, it is impossible to draw a unique curve through them. The degree of uncertainty is, however, considerably diminished if the intervals between successive ordinates are decreased by increasing the number of points.

The second type of error is entirely due to possible inaccuracies in the calculation of the finite sets of ordinates themselves. Reference to the examples shown in Table 2 makes it apparent, however, that if the number and distribution of the points on the deflexion curve is adequate for its description then the calculated values of the ordinates will be sufficiently accurate, provided the elastic analysis is correct.

To conclude this part of the discussion, a worked example on a uniform cantilever beam is shown in which the root is subjected to excitation in the translational sense. The complete analytical solution is known to be

$$\begin{aligned} z(y) = \frac{a}{2(1+\cosh \alpha l \cos \alpha l)} \{ & (1+\cosh \alpha l \cos \alpha l + \sinh \alpha l \sin \alpha l)\cosh \alpha y - \\ & -(\cos \alpha l \sinh \alpha l + \sin \alpha l \cosh \alpha l)\sinh \alpha y + \\ & +(1+\cos \alpha l \cosh \alpha l - \sinh \alpha l \sin \alpha l)\cos \alpha y + \\ & +(\cos \alpha l \sinh \alpha l + \sin \alpha l \cosh \alpha l)\sin \alpha y \}, \end{aligned} \tag{6.12}$$

where

$$(\alpha l)^4 = \frac{\rho_0 \omega^2 l^4}{K}. \tag{6.13}$$

Numerical solutions have been obtained using two dynamical models.

The first comprises five discrete masses and the second uses the first three modes computed from it. The results are shown in Table 3 for $\alpha l = 5$ together with those obtained from equation (6.12).

TABLE 3

Comparison of shapes of vibration with root excitation

y/l	*Deflexion* *Analytical*	*Deflexion* *5-mass model*	*Deflexion* *3-mode model*
0	1·0000	1·0000	1·0000
0·1	0·6465	0·5185	0·5051
0·3	−1·1837	−1·9100	−1·9200
0·5	−2·3263	−3·2325	−3·2189
0·7	−1·2359	−1·4920	−1·4972
0·9	1·6819	2·5469	2·5480

These results show clearly the inadequacy of the numerical approach due to slight errors in the calculated values of the frequency parameters. The associated functions of αl are shown in Table 4. To underline this point, in the final column a value of the parameter αl, say $\alpha^* l$, is chosen for the normal mode model so as to ensure that

$$\frac{(\alpha l)^4}{(\alpha_r l)^4-(\alpha l)^4} = \frac{(\alpha^* l)^4}{(\alpha_r' l)^4-(\alpha^* l)^4} \tag{6.14}$$

when $r = 2$. By this means the mode which contributes most to the shape is given a factor equal to that in the exact solution. It is found necessary to use $\alpha l = 5$ on the analytical model and $\alpha^* l = 5{\cdot}08115$ on the approximate model.

TABLE 4

	$\alpha_r l$	$\alpha_r l$	$\dfrac{(\alpha l)^4}{(\alpha_r l)^4-(\alpha l)^4}$	$\dfrac{(\alpha l)^4}{(\alpha_r' l)^4-(\alpha l)^4}$	$\dfrac{(\alpha^* l)^4}{(\alpha_r' l)^4-(\alpha^* l)^4}$
Mode	*Analytical*	*5-mass model*	$\alpha l = 5$	$\alpha l = 5$	$\alpha^* l = 5{\cdot}08115$
1	1·87514	1·88376	−1·02063	−1·02056	−1·01925
2	4·69409	4·77027	−4·48085	−5·83092	−4·48085
3	7·85475	8·15051	0·19645	0·16499	0·17792

It follows that a relatively small change in the frequency of excitation of the approximate model materially alters its shape of vibration.

Table 5 shows the values of the deflexions in the approximate solutions when $\alpha^* l = 5{\cdot}08115$.

From this table it is clear that the major parts of the discrepancies between these deflexions and those obtained analytically are due to the inadequacy of the approximate integrals as typified in equation (6.8). Undoubtedly a better agreement between the shapes could have been

obtained by taking a value of αl between 5 and 5·08115, but a moment's consideration shows that all the errors would not be absorbed by so doing. Several attempts have been made to improve these results, by the use of interpolation polynomials and by determining from the analytical expression for $F(x, y)$ the complete deformation shapes of the beam when subject to the discrete shear loads (see (2.2)), but in the main the small degree of improvement obtained did not seem to justify the additional labour. It was concluded that the only valid way of improving the answers, using a 3-mode model, would be to employ more discrete masses in the dynamical model.

TABLE 5

y/l	*Deflexion 3-mode model*
0·1	0·62013
0·3	−1·27520
0·5	−2·37204
0·7	−1·15817
0·9	1·87797

Finally it can be seen that the same sort of argument will apply when the root excitation is in the form of rotational vibration rather than translation.

7. Consideration of the validity of superposition

A problem which is introduced when considering the behaviour of a rear fuselage–tailplane combination arises from the method suggested in (1). It was suggested that the first few normal modes of the tailplane root fixed and the first few of the rear fuselage, without the tailplane, be calculated, so that if these modes were freedoms, the shapes of the combination could be calculated, on setting up the usual Lagrangian equations with the cross-coupling terms. The validity of such a procedure must now be considered.

It has already been shown under what circumstances the calculations on a root-excited cantilever beam can give the correct shape. The problem is thus reduced to one of determining the rate of convergence of a series representing a cantilever beam vibrating with constraint added at some point on it.

For the purposes of this study it will be supposed sufficient to consider the determination of the mode shapes of a beam to which a point mass is added, using, as basic data, the normal modes of the beam alone. Provided the solution is considered for both positive and negative values of mass, the reaction of an elastic tailplane can be allowed for.

Let $z_r(y)$ denote the rth mode of the beam alone and let its total mass be M. Let the mass m be added to the beam at $y = y_0$. It can be shown that the normal modes of this structure are obtained from the infinite set of equations

$$M(\omega_r^2-\omega^2)q_r-\omega^2 m z_r(y_0)\sum_{s=1}^{\infty} q_s z_s(y_0) = 0, \tag{7.1}$$

where the amplitudes q_r describe the normal modes of the combination in the form

$$f(y) = \sum_{r=1}^{\infty} q_r z_r(y). \tag{7.2}$$

In equation (7.1), ω_r is the circular frequency of the rth normal mode of the beam alone and ω is the circular frequency of a normal mode of the combination.

Since modes of the combination exist and since they can be represented by the series in (7.2), it follows that this discussion must primarily be concerned with the manner in which it converges. Obviously one is at liberty to choose $f(y)$ fulfilling some prescribed amplitude requirement, say

$$f_r(y_0) = A \tag{7.3}$$

except in a finite number of cases when $f_s(y_0) = 0$. It then follows from equation (7.1) that generally

$$q_r = \frac{m}{M} A\, z_r(y_0)\left(\frac{\omega^2}{\omega_r^2-\omega^2}\right). \tag{7.4}$$

Similarly the basic modes can be chosen to fulfil the requirement

$$z_r(y_0) = B \tag{7.5}$$

except in a finite number of cases. It therefore follows that the series converges in a manner given by

$$q_r = \frac{m}{M} A\, B \frac{\omega^2}{\omega_r^2-\omega^2} \tag{7.6}$$

for any determined value of ω. In particular, in the case of the uniform beam, the convergence depends upon the set of numbers

$$\frac{(\alpha l)^4}{[(r-\frac{1}{2})\pi]^4-(\alpha l)^4} \quad \text{when } r > 3. \tag{7.7}$$

It can be seen that once $(r-\frac{1}{2})\pi > \alpha l$ the convergence will be rapid.

It is worth while considering a numerical example illustrating the problem. The uniform cantilever beam is used again, with normal mode shapes given by equation (4.1). Values of $\alpha_r l$ and $z_r(0{\cdot}9)$ are shown in Table 6 for the first nine modes.

TABLE 6

Values of $\alpha_r l$ and $z_r(0{\cdot}9)$ for the first nine modes

Mode r	$\alpha_r l$	$\frac{z_r}{A}(y/l = 0{\cdot}9)$
1	1·875141	1·72479
2	4·694088	−1·04750
3	7·854752	0·45701
4	10·995565	0·10400
5	13·137167	−0·58802
6	17·278759	0·96644
7	20·420352	−1·21523
8	23·561945	1·31943
9	26·703537	−1·27577

It will be observed that on using these numbers as they stand in the set of equations (7.1), restricted to no more than nine degrees of freedom, the amplitude condition in equation (7.5) is replaced by

$$|z_r(y = l)| = 2. \tag{7.8}$$

The form of equation (7.1) is modified by dividing through by $M(\alpha_r l)^4(\alpha l)^4$, which is equivalent to $M\omega_r^2\omega^2$; and introducing

$$\lambda = \frac{1}{(\alpha l)^4} \tag{7.9}$$

a characteristic root matrix is set up whose elements are

$$a_{rr} = \left[1 + \frac{m}{M}\{z_r^2(0{\cdot}9)\}\right]\frac{1}{(\alpha_r l)^4} - \lambda, \tag{7.10}$$

$$a_{rs} = \frac{m}{M} z_r(0{\cdot}9) z_s(0{\cdot}9) \frac{1}{(\alpha_r l)^4}, \quad r \neq s. \tag{7.11}$$

Two values of m/M are taken, i.e. 0·1 and 10, when m is placed $0{\cdot}9l$ from the root. This distance was chosen because it most nearly represents that which is likely to occur in the aircraft problem.

The solutions obtained for the fundamental mode in the case $m/M = 0{\cdot}1$ using modes 1, 3, 5, 7, and 9 in Table 6 are shown in Table 7. These results indicate that the frequency is the dominant factor conditioning the convergence, but an additional part is played by the variations of $z_r(0{\cdot}9)$ with r. In particular it should be observed that any mode for which $z_r(0{\cdot}9) = 0$ is not affected by the addition of a point mass at $0{\cdot}9l$ from the root.

As expected from the simple theory of infinite series, the rate of convergence to a sum correct to a given accuracy diminishes as the required accuracy is increased. For example, if a two-figure accuracy were required for the fundamental mode in the above problem, certainly no more than the

first two modes would have been necessary. If, however, four-figure accuracy were required, at least the first five modes would be required.

TABLE 7

Approximations to fundamental when $m/M = 0{\cdot}1$ at $y_0 = 0{\cdot}9l$

Basic Mode r	*Amplitudes of basic normal modes in fundamental*			
	3-mode model	*5-mode model*	*7-mode model*	*9-mode model*
1	1·0	1·0	1·0	1·0
2	−0·00362304	−0·00362304	−0·00362312	−0·00362314
3	0·00019816	0·00019816	0·00019816	0·00019816
4	..	0·00001172	0·00001172	0·00001172
5	..	−0·00002424	−0·00002424	−0·00002424
6	..	..	0·00001785	0·00001785
7	..	..	−0·00001150	−0·00001150
8	..	..	..	0·00000704
9	..	..	..	−0·00000413
$\lambda =$	0·10500088	0·10500110	0·10500154	0·1050018

The case when a mass $m = 10M$ is placed at $y_0 = 0{\cdot}9l$ has been solved for the fundamental mode. The amplitude of the component modes are shown in Table 8.

TABLE 8

Basic mode	*Amplitude of basic mode in fundamental*
1	1·0
2	−0·01497880
3	0·00083295
4	0·00004935
5	−0·00010212
$\lambda =$	2·50962535

In this case only the first five modes were used, but it is sufficient to illustrate that, although the influence of m/M increases, it never dominates the convergent tendency created by the frequency factor.

While only the fundamental mode has been considered in this example, it is to be expected from the theory outlined previously that similar results would be obtained from higher modes. Numerical results for these modes have therefore not been included.

It is interesting to consider the two limiting cases, when m/M tends to positive and negative infinity. Reference to equation (7.1) again indicates that for the equation to have any meaning

$$\lim_{m/M \to \pm\infty} \omega^2 \frac{m}{M} z_r(y_0) \sum_{s=1}^{\infty} q_s z_s(y_0) \tag{7.12}$$

must be bounded for all r. This therefore implies that either

$$\omega^2 \to 0 \tag{7.13}$$

or

$$\sum_{s=1}^{\infty} q_s z_s(y_0) \to 0. \tag{7.14}$$

Either case in the limit implies no movement at y_0 although (7.13) implies no movement for every y including y_0, while (7.14) implies that the beam vibrates in such a manner as to have a node at y_0.

In so far as positive values of m/M tend to decrease the frequencies of the modes from those obtained basically, it is clear that negative values will tend to increase them. If m/M is sufficiently negative it is indeed possible for the frequency of the fundamental mode of the combination to lie outside that in which one is interested. The conclusions from these remarks may be summarized as follows:

If one considers the determination of the modal shapes of a tailplane-rear fuselage combination using basic mode data, it is evident that the reaction of the tailplane on the fuselage in any such mode is expressible in terms of some positive or negative mass whose value is so chosen as to be compatible with the shape and frequency of the mode. Since it can be shown that such a combination has shape expressible in terms of rapidly convergent series, the use of a finite set of the basic modes can produce adequate solutions to the problem of their determination.

8. On the introduction of extension of the masses of the model

In discussing the question of the inclusion of the discrete mass extension instead of regarding it as a point, it is instructive to consider again equation (2.1). The dynamical model of a cantilever beam is usually constructed by dividing it into segments (y_r, y_{r+1}) which are represented dynamically by point masses m_r at stations $\bar{x}_r$ where

$$m_r = \int_{y_r}^{y_{r+1}} \rho(y)\, dy \tag{8.1}$$

and

$$\bar{x}_r = \frac{1}{m_r} \int_{y_r}^{y_{r+1}} y\rho(y)\, dy. \tag{8.2}$$

Now one is primarily concerned in finding a good numerical approximation to the expression

$$\int_0^l F(x, y)\rho(y)z(y)\, dy, \tag{8.3}$$

and this is found ideally if y_r' is chosen such that

$$\rho(y_r')F(x, y_r')z(y_r') = \frac{1}{y_{r+1}-y_r} \int\limits_{y_r}^{y_{r+1}} \rho(y)F(x,y)z(y)\,dy. \tag{8.4}$$

But to find y_r' would be equivalent to solving the problem, and the chances of finding a set y_r' fortuitously fulfilling this requirement for any one mode, let alone for all those modes required, would be very small. It therefore follows that the compromise procedure embodied in equations (8.1) and (8.2) is probably as good as any other.

On the face of it the dynamical equivalence between the point mass and beam segment is not very good and the constraints due to the various rotations and moments of inertia should be included. Two ways of including these constraints are possible. Either one may add to the translation freedom of each segment a second due to rotation, or one may apply difference methods to the undetermined values of these rotations. The first method doubles the number of freedoms without generally reducing the mesh of points on the beam, while the second method is equivalent to using approximate values of the derivative of $z(y)$, when in fact the derivative actually required is that of $\rho(y)F(x,y)z(y)$.

In conclusion, if account is to be taken of the extension of the segments of a beam without introducing additional degrees of freedom, it can only be done properly by using difference formulae in a way which cannot be regarded as physically equivalent to the use of moments of inertia.

9. The addition of the torsional freedom

A subject which is of particular interest in the construction of dynamical models for wings is the manner in which the addition of the dimension of depth to a beam already possessing length and thickness affects the problem. With beams whose depth is small in relation to length, it is usually sufficient to regard the curvature of the longitudinal axis as predominant. In other words, the deformations of sections in depth are negligible in comparison with those along the length. This naturally gives rise to the concept of a dynamical model consisting of a light rod possessing flexural and torsional properties to which is attached a series of rigid rods, normal to it, having moments of inertia. This is usually the case with conventional aircraft wings in which the chords are of smaller order than the span. However, delta aircraft depart considerably from such shapes and this treatment of the problem becomes inadequate. To solve the normal mode problem on a delta configuration it therefore becomes necessary to determine structural influence coefficients by a totally different method from

that which has been found adequate hitherto and to adhere rigidly to a discrete mass technique. With the conventional wing, however, use is made of the concept of a flexural axis. Its use can be regarded as giving a semi-rigid representation to the structure, for all sections of the wing normal to this axis are assumed rigid, whereas the wing as a whole is allowed to distort so that any such section can be displaced in a translational or rotational sense.

Consideration of the semi-rigid representation of a conventional wing reveals that any dynamical model which attempts to reproduce the mass distribution must be constructed of a series of rigid rods attached normally to the flexural axis. If an attempt is made to account for the spanwise extension of any segment represented by a rod by giving it a rolling moment of inertia, the same type of problem is encountered which has already been discussed in the previous section on simple cantilever beams. There is, of course, no reason why the extension in the sense of thickness should not be accommodated, but since the aim of all aircraft designers is to make wings as thin as possible, it is a matter of conjecture whether or not this is an important dimension.

With regard to the torsional vibrations of such a structure, it is possible to construct a similar theory to that which is shown for the flexural freedom (cf. (2.1)). For example, a beam possessing torsional freedom only may have modes of vibration whose shapes are solutions of

$$\theta(x) = \omega^2 \int_0^l \Phi(x,y)i(y)\theta(y)\,dy, \tag{9.1}$$

where $\theta(x)$ is the rotation at position x,

$\Phi(x,y)$ is the rotation at x due to unit couple at y,

$i(y)$ is the inertia density distribution, and

ω is circular frequency of vibration.

When both flexural and torsional freedoms are present it is evident that two integral equations containing the integrals of equations (2.1) and (9.1) are necessary, which will be connected by functions denoting the displacement at x due to unit couple at y and the twist at x due to unit force at y. It therefore follows that the requirements for an adequate model of a simple cantilever beam will be identical in form with those for a dynamical model of beams with this additional freedom. In essence, all this amounts to is that the intervals chosen for the approximate evaluation of a definite integral must be sufficiently small, the smallness being governed again by the number of modes required.

10. Conclusion

Recapitulating, the points which have been dealt with are as follows:

(i) the factors governing the adequacy of the discrete mass model;

(ii) the influence of the accuracy of the structural influence coefficients on the calculated shapes of vibration;

(iii) the conditions under which a beam, represented dynamically by its first few root-fixed normal modes, may give correct shapes when subjected to root excitation;

(iv) the conditions under which one may validly superimpose the normal mode models of two structures in computing the composite modes; and

(v) the conditions under which it is possible to compensate for the extensions of the segments of the structure otherwise represented by point masses.

The object of this paper has been to justify and amplify the method of solution outlined in (**1**). The justification has had to rely upon a determination of some of the conditions in which the representation of the derived shapes by an infinite series of basic root-fixed normal modes converges with sufficient rapidity to permit truncation to fewer terms than the number of discrete masses of the associated dynamical model. This has only been done to cover the cases which are likely to arise in the method of reference (**1**); and indeed there must be many other ways in which structural subdivision can be employed, but the conclusions drawn generally are that this method is a valid one.

The range of frequency in which the normal mode model is adequate can be expected to be from zero up to maximum frequency of that element of the complete aircraft whose discrete mass model possesses the smallest range of validity. For example, suppose the wing model were adequate up to 60 c.p.s., the tailplane model from 0 to 70 c.p.s., the rear fuselage from 0 to 100 c.p.s., and the front fuselage from 0 to 75 c.p.s., then the normal mode model constructed of all those modes of each part in these respective ranges can be expected to be adequate up to 60 c.p.s.

When one constructs the dynamical model for any part of the aircraft, the test of adequacy is not simply whether or not the discrete displacements calculated in the modes correspond to those which would be obtained analytically, but also whether or not there are sufficient of these calculated displacements for the kinetic energy in any such mode to be computed with sufficient accuracy. In fulfilling this last requirement the first is usually more than adequately satisfied.

Finally, if one bears in mind the accuracy required from the elastic analysis in computing the higher root-fixed modes of any part of the aircraft, it is concluded that not more than three modes of the flexure type can be expected to agree with experiment so long as Engineer's Theory is retained. It therefore follows that if this method of elastic analysis is used, only those modes of the complete aircraft that can be expressed in terms of the basic root-fixed modes up to the second flexure overtone of each part of the structure can be satisfactorily computed.

REFERENCES

1. B. A. Hunn, 'A method of calculating space free resonance modes of an aircraft', *J. Roy. Aero. Soc.* **57** (1953), 420.
2. A. E. H. Love, *A Treatise on the Mathematical Theory of Elasticity* (Cambridge, 1953).
3. I. T. Minhinnick, 'The determination of normal modes and vibration frequencies', Paper No. 3 of a Symposium on the Flutter Problem in Aircraft Design, M.O.S. Unpublished.
4. W. J. Duncan and A. R. Collar, 'A method for the solution of oscillation problems by matrices', *Phil. Mag.* (7) **17** (1934), 865–909.
5. —— 'A critical examination of the representation of massive and elastic bodies by systems of rigid masses elastically connected', *Quart. J. Mech. and Applied Math.* **5** (1952), 97–108.

THE STRESSES IN AN AEOLOTROPIC CIRCULAR DISK

By H. F. CLEAVES
(*Duke of York's Royal Military School, Dover*)

[Received 29 April 1954]

SUMMARY

This paper is based on the work of Livens and Morris on the use of complex potential theory of two-dimensional elasticity for dealing with the plane strain and associated generalized plane stress in an aeolotropic plate. The stresses are obtained from a complex potential function Ω, which in this work has been found for a circular plate under various edge loadings. These results have been combined to give the most general case where the edge loadings can be expressed in the form of a Fourier series. The paper then deals with the particular material oak and gives the distribution of hoop stress on the boundary of a circular oak disk due to a pair of equal and opposite radial forces at right angles to the grain.

1. Introduction

In recent years several authors have treated the fundamental problems of two-dimensional statical elasticity, viz. the problem of plane strain and the associated generalized plane stress problems, by the use of functions of a complex variable. Such problems have been very thoroughly investigated in the case of isotropic materials, but have received comparatively little attention in the case of aeolotropic materials where solutions of simple problems are far from complete. The results of this paper are based on the method of Livens and Morris (**1**) and Morris (**2**). In (**2**) Morris has dealt with the generalized plane stress problem of the elliptic disk under given edge stresses, but for the particular transformation used in that paper it is not easy to deduce the corresponding results for the circular disk. In any case no details are given for specific problems, as have been given for the isotropic case. This paper gives a comprehensive treatment of the generalized plane stress problem for the circular aeolotropic disk under the most general edge loading. Stevenson (**3**) has solved this problem for an isotropic circular disk in polar coordinates, when the boundary is under a normal pressure over equal and opposite arcs, evaluating the hoop stress at the ends of the two symmetrical diameters at right angles. Rothman (**4**), using Stevenson's methods, treats the isotropic circular disk under the action of a number of isolated forces on the boundary, assuming a balancing force and couple at the origin when necessary. In these isotropic cases these

authors use potentials $\Omega(z)$ and $\omega(z)$, $z = x+iy$, which can be determined from the boundary conditions and the condition that the displacement must be single valued. The connexion between $\Omega(z)$ and $\omega(z)$ is, however, far from simple and Stevenson gives no real indication as to how he arrives at his potential functions. He assumes certain forms of these functions at the beginning of each problem and then shows that they fit the conditions given, provided certain constants involved take on certain definite values. It would appear that the forms of the potentials assumed are arrived at by means of trial and error. This is probably inevitable in the case of isotropic material since the simple relationship between the functions is only brought out in the more general problem of aeolotropic material and, in fact, the whole problem is then interpreted in terms of a single potential function involving the elastic constants of the material, which tend to zero for isotropic material. The relation between parts of this single potential function and the $\Omega(z)$ and $\omega(z)$ of Stevenson is given by Morris and Livens (**1**), section 5.

In addition Okubo (**5**) has dealt with the stress distribution in an aeolotropic circular disk compressed diametrically, and this is, of course, a particular case of the general results given in this paper.

2. General method

The plate considered is assumed to be of uniform thickness in the (x, y)-plane, the normal to the plate being in the direction of the z-axis. The material of the plate has two directions of symmetry at right angles in the (x, y)-plane, and these are taken to be parallel to the x and y axes.

It has been shown (**1**) that the stresses can be obtained from a complex function $\Omega(z)$ by means of the following formulae,

$$\widehat{xx}-\widehat{yy}+2i\widehat{xy} = -\frac{d\Omega}{d\bar{z}},$$

$$\widehat{xx}+\widehat{yy} = \frac{d\Omega}{dz}.$$

The complex function $\Omega(z)$ is made up of four simply related parts, $\Omega_m(z_m)$, $m = 1, 2, 3, 4$, that is,

$$\Omega(z) = \sum_{m=1}^{4} \Omega_m(z_m), \quad \text{where } z_m = z+\lambda_m \bar{z}.$$

The constants involved, λ_m, in this value of $\Omega(z)$ are the roots of the reciprocal quartic

$$(s_{11}+s_{22}-2s_{12}-2s_{66})(\lambda^4+1)-4(s_{11}-s_{22})(\lambda^3+\lambda)+$$
$$+2(3s_{11}+3s_{22}+2s_{12}+2s_{66})\lambda^2 = 0,$$

where s_{11}, etc., are the elastic constants of the material given by Green and Taylor (**6**).

Two of the roots of this equation are the reciprocals of the other two, and if we call the two roots which are less than unity λ_1 and λ_2 then

$$\lambda_3 = \frac{1}{\lambda_1} \quad \text{and} \quad \lambda_4 = \frac{1}{\lambda_2}.$$

This leads to the result that

$$z_3 = z+\lambda_3 \bar{z} = z+\frac{1}{\lambda_1}\bar{z} = \frac{1}{\lambda_1}(\bar{z}+\lambda_1 z) = \frac{1}{\lambda_1}\bar{z}_1$$

and similarly $z_4 = \frac{1}{\lambda_2}\bar{z}_2$ so that, remembering that $\frac{d\Omega}{dz}$ must be real, we derive the following simple form for Ω,

$$\Omega(z) = \Omega_1(z_1)+\Omega_2(z_2)+\frac{1}{\lambda_1}\bar{\Omega}_1(\bar{z}_1)+\frac{1}{\lambda_2}\bar{\Omega}_2(\bar{z}_2),$$

where Ω_2 is derived from Ω_1 by replacing λ_1 by λ_2 and the other two remaining functions are simply the conjugates of the first two. The λ_1 and λ_2 are the γ_1 and γ_2 of Green's analysis. It is thus only necessary to determine $\Omega_1(z_1)$. Then $\Omega_2(z_2)$ is easily obtained by interchanging λ_1 and λ_2 in $\Omega_1(z_1)$, and the conjugates of these give the third and fourth potential functions when divided by λ_1 and λ_2 respectively.

3. Application to the problem of the circular disk

For the problem of the aeolotropic circular disk we follow Livens and Morris (**1**) using curvilinear coordinates ξ and η connected with the rectangular coordinates x and y by the relation

$$z = ae^{-i\zeta} \quad \text{where } \zeta = \xi+i\eta,$$

and which for $\eta \leqslant 0$ gives the space bounded by the circle $|z| = a$. Then, $\eta =$ constant represents a circle, $\widehat{\eta\eta}$ is the outward radial stress, and $\widehat{\eta\xi}$ the tangential stress measured in a clockwise direction at any point on this circle.

We make use of the following results given by Livens and Morris.

When the stress on the boundary is such that $\widehat{\eta\eta}-i\widehat{\eta\xi} = f(\xi)$, the condition for Ω when $\eta = 0$ is

$$\Omega = 2\int^{\xi} f(u)z'(u)\,du.$$

The resultant stress on the boundary has a value

$$X+iY = i\int_c (\widehat{\eta\eta}-i\widehat{\eta\xi})\,dz$$

$$= -i\int_0^{2\pi} (\widehat{\eta\eta}-i\widehat{\eta\xi})\,\frac{dz}{d\xi}\,d\xi.$$

Also Morris (**2**) gives the moment of the resultant couple about the origin as

$$G = \text{re}\int_c (\widehat{\eta\eta}-i\widehat{\eta\xi})\bar{z}\,dz$$

$$= \text{re} - \int_0^{2\pi} (\widehat{\eta\eta}-i\widehat{\eta\xi})\bar{z}\,\frac{dz}{d\xi}\,d\xi.$$

For the disk bounded by $z = ae^{-i\xi}$, $\dfrac{dz}{d\xi} = -iae^{-i\xi}$, giving

$$\Omega_{\eta=0} = -2ia\int^{\xi} f(u)e^{-iu}\,du, \tag{3.1}$$

$$X+iY = -a\int_0^{2\pi} (\widehat{\eta\eta}-i\widehat{\eta\xi})e^{-i\xi}\,d\xi, \tag{3.2}$$

and

$$G = \text{re}\, ia^2\int_0^{2\pi} (\widehat{\eta\eta}-i\widehat{\eta\xi})\,d\xi. \tag{3.3}$$

Following the usual method we now have

$$z = ae^{-i\zeta} \quad\text{and}\quad z_m = ae^{-i\zeta}+\lambda_m ae^{i\bar{\zeta}}$$

so that on the boundary of the disk, where $\eta = 0$, we have

$$z_m = at+\lambda_m\frac{a}{t}$$

where $t = e^{-i\xi}$. This equation in t has two roots: denote that root which reduces to $e^{-i\xi}$ on the boundary by $t = t_m(z_m)$. Then Ω can be expressed in the form

$$\Omega = \sum_{m=1}^{4}\Omega_m(t_m),$$

i.e.

$$\Omega = \Omega_1(t_1)+\Omega_2(t_2)+\frac{1}{\lambda_1}\bar{\Omega}_1(\bar{t}_1)+\frac{1}{\lambda_2}\bar{\Omega}_2(\bar{t}_2). \tag{3.4}$$

Any given boundary stresses are now expressed in a Fourier series in ξ, e.g.

$$(\widehat{\eta\eta}-i\widehat{\eta\xi}) = f(\xi) = \sum_{-\infty}^{\infty} p_n e^{ni\xi}$$

$$= p_0 + \sum_{n=1}^{\infty} (p_n e^{ni\xi} + p_{-n} e^{-ni\xi}). \tag{3.5}$$

If $\Omega_1(t_1)$ is now assumed to be of the form

$$\Omega_1(t_1) = \sum_{n=-\infty}^{\infty} a_{mn} t_1^n$$

then on the boundary where

$$t_1 = t_2 = \frac{1}{\bar{t}_1} = \frac{1}{\bar{t}_2} = e^{-i\xi},$$

Ω reduces to the form

$$\Omega(t) = \sum_{m=1}^{4} \sum_{n=-\infty}^{\infty} a_{mn} e^{-ni\xi},$$

and comparison of this series with that obtained from (3.1), (3.4), and (3.5) will enable us to determine the coefficients a_{mn} and thus obtain the complex potential Ω.

We have ascertained that the application of this method to the case of a circular hole in an aeolotropic plate stressed only at the boundary of the hole gives results identical with those obtained by Holgate (**7**) in sections 5 and 6.

The problem of the disk is not, however, as simple as that of the hole. It has been shown by Livens and Morris (**1**) in sections 8 and 9 that the stresses are functions of $d\Omega/dz$ and $d\Omega/d\bar{z}$ and if $\Omega_m = F_m(t_m)$ we have

$$\frac{d\Omega_m}{dz} = \frac{F'_m(t_m)}{z'_m(t_m)}, \qquad \frac{d\Omega_m}{d\bar{z}} = \frac{\lambda_m F'_m(t_m)}{z'_m(t_m)}$$

and the stresses become infinite when $z'_m(t_m) = 0$, in this case when

$$a - \frac{\lambda_m a}{t_m^2} = 0,$$

i.e. when $\qquad t_m = \pm\sqrt{\lambda_m}$ and $|t_m| < 1$.

These are the branch points of the transformation and lie within the circle $|z| = a$.

In the case of the hole no circuit in the plate can cross the line joining the two branch points so that all potentials and stresses are single valued.

In the case of the disk, however, these two branch points lie within the material and unless the function Ω is chosen in a particular way, it may not be single valued, i.e. it may change in value on crossing the cut. The method used to ensure that Ω is single valued is as follows.

If t_m is the root of the equation $z_m = at+(\lambda_m a/t)$ which reduces to $e^{-i\xi}$ on the boundary, then the other root is $t = \lambda_m/t_m$. We therefore choose Ω_m to be of the form

$$\Omega_m = \sum_{r=-\infty}^{+\infty} a_{mr}\left(t_m^r+\frac{\lambda_m^r}{t_m^r}\right). \tag{3.6}$$

On crossing any cut joining the two branch points the roots are interchanged leaving the expression $t_m^r+(\lambda_m^r/t_m^r)$ and hence Ω_m unchanged.

To determine the hoop stress $\widehat{\xi\xi}$ on the boundary we determine the value of $\widehat{\eta\eta}+\widehat{\xi\xi} = d\Omega/dz$ on the boundary, and since $\widehat{\eta\eta}$ is known this determines $\widehat{\xi\xi}$. Remembering that $z_m = a(t_m+\lambda_m/t_m)$ we have

$$[\widehat{\eta\eta}+\widehat{\xi\xi}]_{\eta=0} = \left[\frac{d\Omega}{dz}\right]_{\eta=0} = 2\,\mathrm{re}\left[\frac{\Omega_1'(t_1)}{z_1'(t_1)}+\frac{\Omega_2'(t_2)}{z_2'(t_2)}\right]_{t_1=t_2=t}. \tag{3.7}$$

We shall now apply the general method outlined above to specific problems of the aeolotropic circular disk under given edge stresses.

4. The simplest case of edge loading, $\widehat{\eta\eta}-i\widehat{\eta\xi} = p_0$ where p_0 is real

The simplest case of edge loading is that in which the stresses are constant and given by $\widehat{\eta\eta}-i\widehat{\eta\xi} = p_0$. Using equations (3.1), (3.2), and (3.3) we obtain

$$\Omega_{\eta=0} = -2ia\int^{\xi} p_0\,e^{-iu}\,du = 2ap_0\,e^{-i\xi} = 2ap_0\,t. \tag{4.1}$$

The resultant boundary stress is

$$X+iY = -a\int_0^{2\pi} p_0\,e^{-i\xi}\,d\xi = 0, \tag{4.2}$$

while the resultant couple G about the origin is

$$\mathrm{re}\,ia^2\int_0^{2\pi} p_0\,d\xi = i\,2\pi a^2 p_0, \tag{4.3}$$

and if $p_0 = P+iQ$, then $G = -2\pi a^2 Q$, and for the boundary stresses to be in equilibrium, p_0 must be real. This is the case we now consider. Let

$$\Omega_m(t_m) = \sum_{n=-\infty}^{\infty} a_{mn}\left(t_m^n+\frac{\lambda_m^n}{t_m^n}\right).$$

Then

$$\Omega = \sum_{-\infty}^{+\infty} \left[a_{1n}\left(t_1^n + \frac{\lambda_1^n}{t_1^n}\right) + a_{2n}\left(t_2^n + \frac{\lambda_2^n}{t_2^n}\right) + \frac{1}{\lambda_1}\bar{a}_{1n}\left(\bar{t}_1^n + \frac{\lambda_1^n}{\bar{t}_1^n}\right) + \frac{1}{\lambda_2}\bar{a}_{2n}\left(\bar{t}_2^n + \frac{\lambda_2^n}{\bar{t}_2^n}\right)\right];$$

on the boundary where $t_1 = t_2 = \bar{t}_1^{-1} = \bar{t}_1^{-1} = t$ this must be equal to $2ap_0 t$, which in this case is $2aPt$.

Comparing the coefficients of t and t^{-1} we get

$$\left.\begin{aligned} a_{11} + a_{21} + \bar{a}_{11} + \bar{a}_{21} &= 2aP \\ \lambda_1 a_{11} + \lambda_2 a_{21} + \frac{1}{\lambda_1}\bar{a}_{11} + \frac{1}{\lambda_2}\bar{a}_{21} &= 0 \end{aligned}\right\}. \tag{4.4}$$

Remembering now that a_{21} is derived from a_{11} by interchange of λ_1 and λ_2 these equations give

$$\left.\begin{aligned} a_{11} &= \frac{\lambda_1(1+\lambda_2^2)}{(1-\lambda_1\lambda_2)(\lambda_1-\lambda_2)}\,aP \\ \text{and} \qquad a_{21} &= -\frac{\lambda_2(1+\lambda_1^2)}{(1-\lambda_1\lambda_2)(\lambda_1-\lambda_2)}\,aP \end{aligned}\right\}. \tag{4.5}$$

All other values of a_{mn} are zero. Also

$$\begin{aligned} [\widehat{\eta\eta} + \widehat{\xi\xi}]_{\eta=0} &= \operatorname{re} 2\left[\frac{\Omega_1'(t_1)}{z_1'(t_1)} + \frac{\Omega_2'(t_2)}{z_2'(t_2)}\right]_{t_1=t_2=t} \\ &= \operatorname{re} 2\left[\frac{a_{11}(1-\lambda_1/t_1^2)}{a(1-\lambda_1/t_1^2)} + \frac{a_{21}(1-\lambda_2/t_2^2)}{a(1-\lambda_2/t_2^2)}\right]_{t_1=t_2=t} \\ &= \operatorname{re} 2\left[\frac{a_{11}+a_{21}}{a}\right] \qquad\qquad (4.6) \\ &= 2P \quad \text{from (4.4).} \end{aligned}$$

As $$[\widehat{\eta\eta}]_{\eta=0} = P \quad \text{then } [\widehat{\xi\xi}]_{\eta=0} = P, \tag{4.7}$$

which is the well-known result for hoop stress.

5. Case when $\widehat{\eta\eta} - i\widehat{\eta\xi} = p_0$ where p_0 is imaginary

When the constant edge loading is purely imaginary, i.e. when

$$\widehat{\eta\eta} - i\widehat{\eta\xi} = iQ,$$

$$\Omega = 2iaQt \tag{5.1}$$

and the resultant stress $$X + iY = 0. \tag{5.2}$$

There is, however, a resultant couple G given by

$$G = -2\pi a^2 Q. \tag{5.3}$$

We consider the case where this is balanced by a couple $-G$ applied at the origin. Morris (**2**), section 5, has shown that the stress potential due to a couple $-G$ applied to a small circle round the origin is

$$\Omega_0 = \frac{iG}{2\pi}\left[\frac{\lambda_1}{z_1}+\frac{\lambda_2}{z_2}-\frac{1}{\bar{z}_1}-\frac{1}{\bar{z}_2}\right].$$

This gives
$$\Omega_{0m} = \frac{iG}{2\pi a}\,\frac{\lambda_m}{(t_m+\lambda_m/t_m)},$$

and in the neighbourhood of the edge of the disk where $|t_m| = 1$ this can be expanded in the form (since $|\lambda_m| < 1$)

$$\begin{aligned}\Omega_{0m} &= -iaQ\frac{\lambda_m}{t_m}\left(1+\frac{\lambda_m}{t_m^2}\right)^{-1}\\ &= -iaQ\frac{\lambda_m}{t_m}\left(1-\frac{\lambda_m}{t_m^2}+\frac{\lambda_m^2}{t_m^4}-\frac{\lambda_m^3}{t_m^6}+\ldots\right)\\ &= iaQ\sum_{n=0}^{\infty}(-)^{n+1}\frac{\lambda_m^{n+1}}{t_m^{2n+1}}.\end{aligned}$$

Therefore

$$\Omega_0 = iaQ\sum_{n=0}^{\infty}(-)^{n+1}\left[\frac{\lambda_1^{n+1}}{t_1^{2n+1}}+\frac{\lambda_2^{n+1}}{t_2^{2n+1}}-\frac{\lambda_1^{n}}{\bar{t}_1^{2n+1}}-\frac{\lambda_2^{n}}{\bar{t}_2^{2n+1}}\right].$$

We form the potential Ω by adding to Ω_0 terms of the type

$$\sum_{n=0}^{\infty} c_{mn}\left(t_m^{2n+1}+\frac{\lambda_m^{2n+1}}{t_m^{2n+1}}\right), \tag{5.4}$$

remembering that Ω must reduce to $2iaQt$ on the boundary. Then

$$\Omega = \Omega_0+\sum_{m=1}^{4}\sum_{n=0}^{\infty} c_{mn}\left(t_m^{2n+1}+\frac{\lambda_m^{2n+1}}{t_m^{2n+1}}\right).$$

Comparing coefficients of t and t^{-1} on the boundary we obtain

$$c_{10}+c_{20}+\bar{c}_{10}+\bar{c}_{20}+2iaQ = 2iaQ,$$

i.e.
$$c_{10}+c_{20}+\bar{c}_{10}+\bar{c}_{20} = 0 \tag{5.5}$$

and
$$\lambda_1 c_{10}+\lambda_2 c_{20}+\frac{1}{\lambda_1}\bar{c}_{10}+\frac{1}{\lambda_2}\bar{c}_{20} = iaQ(\lambda_1+\lambda_2). \tag{5.6}$$

Remembering that c_{20} is formed from c_{10} by interchanging λ_1 and λ_2, these two equations together with the conjugate of (5.6) give

$$\left.\begin{aligned} c_{10} &= -\frac{iaQ\lambda_1(\lambda_1+\lambda_2)}{1-\lambda_1^2}\\ \text{and}\qquad c_{20} &= -\frac{iaQ\lambda_2(\lambda_1+\lambda_2)}{1-\lambda_2^2}\end{aligned}\right\}. \tag{5.7}$$

Comparing the coefficients of t^{2n+1} and $t^{-(2n+1)}$ we obtain

$$\left.\begin{aligned} c_{1n}+c_{2n}+\lambda_1^{2n}\bar{c}_{1n}+\lambda_2^{2n}\bar{c}_{2n} &= (-)^{n+1}iaQ(\lambda_1^n+\lambda_2^n) \\ \frac{1}{\lambda_1}c_{1n}+\frac{1}{\lambda_2}c_{2n}+\lambda_1^{2n+1}\bar{c}_{1n}+\lambda_2^{2n+1}\bar{c}_{2n} &= (-)^{n+1}iaQ(\lambda_1^{n+1}+\lambda_2^{n+1}) \\ \lambda_1^{2n+1}c_{1n}+\lambda_2^{2n+1}c_{2n}+\frac{1}{\lambda_1}\bar{c}_{1n}+\frac{1}{\lambda_2}\bar{c}_{2n} &= (-)^{n}iaQ(\lambda_1^{n+1}+\lambda_2^{n+1}) \\ \lambda_1^{2n}c_{1n}+\lambda_2^{2n}c_{2n}+\bar{c}_{1n}+\bar{c}_{2n} &= (-)^{n}iaQ(\lambda_1^n+\lambda_2^n) \end{aligned}\right\}. \quad (5.8)$$

We denote the determinant of the coefficients of the c's in these equations by Δ_{2n+1} and then by denoting the co-factors of the terms in the first column of Δ_{2n+1} by $\Delta_{2n+1,r}$, $r = 1, 2, 3, 4$, and the same determinants obtained by interchange of λ_1 and λ_2 by $\Delta'_{2n+1,r}$ we derive finally

$$c_{1n} = (-)^{n+1}iaQ\left[\frac{\Delta_{2n+1,1}}{\Delta_{2n+1}}(\lambda_1^n+\lambda_2^n)+\frac{\Delta_{2n+1,2}}{\Delta_{2n+1}}(\lambda_1^{n+1}+\lambda_2^{n+1})-\right.$$
$$\left.-\frac{\Delta_{2n+1,3}}{\Delta_{2n+1}}(\lambda_1^{n+1}+\lambda_2^{n+1})-\frac{\Delta_{2n+1,4}}{\Delta_{2n+1}}(\lambda_1^n+\lambda_2^n)\right], \quad (5.9)$$

$$c_{2n} = (-)^{n+1}iaQ\left[\frac{\Delta'_{2n+1,1}}{\Delta_{2n+1}}(\lambda_1^n+\lambda_2^n)+\frac{\Delta'_{2n+1,2}}{\Delta_{2n+1}}(\lambda_1^{n+1}+\lambda_2^{n+1})-\right.$$
$$\left.-\frac{\Delta'_{2n+1,3}}{\Delta_{2n+1}}(\lambda_1^{n+1}+\lambda_2^{n+1})-\frac{\Delta'_{2n+1,4}}{\Delta_{2n+1}}(\lambda_1^n+\lambda_2^n)\right]. \quad (5.10)$$

It will be noted that the terms with coefficients c_{10} and c_{20} make no contribution to the hoop stress on the boundary since they give

$$\begin{aligned} [\widehat{\eta\eta}+\widehat{\xi\xi}]_{\eta=0} &= \mathrm{re}\, 2\,\frac{c_{10}+c_{20}}{a}, \quad \text{cf. (4.6)}, \\ &= 0, \quad \text{from (5.5)}. \end{aligned} \quad (5.11)$$

If p_0 is complex the solution to the problem can be obtained by superimposing the separate solutions for p_0 real and p_0 imaginary.

6. Variable edge loading: $\widehat{\eta\eta}-i\widehat{\eta\xi} = p_1 e^{i\xi}+p_{-1}e^{-i\xi}$

We next consider the case of variable edge loading defined by

$$\widehat{\eta\eta}-i\widehat{\eta\xi} = p_1 e^{i\xi}+p_{-1}e^{-i\xi}.$$

The boundary condition takes the form

$$\begin{aligned} \Omega_{\eta=0} &= -2ia\int^{\xi}(p_1 e^{iu}+p_{-1}e^{-iu})e^{-iu}\,du \\ &= 2ap_1\log t+ap_{-1}t^2. \end{aligned} \quad (6.1)$$

The force on the boundary is given by

$$X+iY = -a\int_0^{2\pi}(p_1e^{i\xi}+p_{-1}e^{-i\xi})e^{-i\xi}\,d\xi = -2\pi a p_1 \tag{6.2}$$

and the couple by

$$\operatorname{re} ia^2\int_0^{2\pi}(p_1e^{i\xi}+p_{-1}e^{-i\xi})\,d\xi = 0. \tag{6.3}$$

For the applied forces to be in equilibrium we must have $p_1 = 0$.

Considering this case first and assuming Ω to be of the form given by (3.4) and (3.6), since $\Omega_{\eta=0} = ap_{-1}t^2$, we have

$$\left.\begin{aligned} a_{12}+a_{22}+\lambda_1\bar{a}_{12}+\lambda_2\bar{a}_{22} &= ap_{-1}\\ \frac{1}{\lambda_1}a_{12}+\frac{1}{\lambda_2}a_{22}+\lambda_1^2\bar{a}_{12}+\lambda_2^2\bar{a}_{22} &= 0\\ \lambda_1^2a_{12}+\lambda_2^2a_{22}+\frac{1}{\lambda_1}\bar{a}_{12}+\frac{1}{\lambda_2}\bar{a}_{22} &= 0\\ \lambda_1a_{12}+\lambda_2a_{22}+\bar{a}_{12}+\bar{a}_{22} &= a\bar{p}_{-1}\end{aligned}\right\}, \tag{6.4}$$

which give

$$\left.\begin{aligned} a_{12} &= a\left[\frac{\Delta_{2,1}}{\Delta_2}p_{-1}+\frac{\Delta_{2,4}}{\Delta_2}\bar{p}_{-1}\right]\\ \text{and}\quad a_{22} &= a\left[\frac{\Delta'_{2,1}}{\Delta_2}p_{-1}+\frac{\Delta'_{2,4}}{\Delta_2}\bar{p}_{-1}\right]\end{aligned}\right\}. \tag{6.5}$$

When p_1 is not zero but $\widehat{\eta\eta}-i\widehat{\eta\xi} = p_1e^{i\xi}$ the resultant of the boundary stresses is given by

$$X+iY = -2\pi ap_1$$

which passes through the origin as $G = 0$.

We balance this by a force P at the origin in a direction making an angle ϵ with the x-axis. It is shown by Morris (**2**), section 4, that the complex stress potential due to such a force is

$$\Omega_0 = \sum_{m=1}^{4}\Omega_{0m} = \sum_{m=1}^{4}A_m\log z_m,$$

where

$$\left.\begin{aligned} A_1 &= \frac{\lambda_1P}{(\alpha_1-\alpha_2)s_{22}\pi}\left[\frac{s_{12}-\alpha_2s_{22}}{1-\lambda_1}\cos\epsilon+\frac{s_{12}-\alpha_1s_{22}}{1+\lambda_1}i\sin\epsilon\right]\\ \text{and}\quad A_2 &= -\frac{\lambda_2P}{(\alpha_1-\alpha_2)s_{22}\pi}\left[\frac{s_{12}-\alpha_1s_{22}}{1-\lambda_2}\cos\epsilon+\frac{s_{12}-\alpha_2s_{22}}{1+\lambda_2}i\sin\epsilon\right]\end{aligned}\right\}, \tag{6.6}$$

$$A_3 = \frac{\bar{A}_1}{\lambda_1},\quad A_4 = \frac{\bar{A}_2}{\lambda_2}$$

and

$$A_1+A_2-\frac{\bar{A}_1}{\lambda_1}-\frac{\bar{A}_2}{\lambda_2} = \frac{Pe^{i\epsilon}}{\pi}. \tag{6.7}$$

Now
$$\Omega_{0m} = A_m \log a(t_m+\lambda_m/t_m)$$
$$= A_m \log a + A_m \log t_m + A_m \log(1+\lambda_m/t_m^2).$$

Since $\lambda_m < 1$ and $|t_m|$ is in the neighbourhood of 1 near the boundary, we can expand $A_m \log(1+\lambda_m/t_m^2)$ in an infinite series giving

$$\Omega_{0m} = A_m \log a + A_m \log t_m - A_m \sum_{n=1}^{\infty} (-\lambda_m/t_m^2)^n/n.$$

To satisfy the boundary conditions we must add to this potential terms of the type
$$\sum_{n=1}^{\infty} c'_{mn}(t_m^{2n}+\lambda_m^{2n}/t_m^{2n}),$$
giving
$$\Omega = \Omega_0 + \sum_{m=1}^{4} \sum_{n=1}^{\infty} c'_{mn}(t_m^{2n}+\lambda_m^{2n}/t_m^{2n}). \tag{6.8}$$

On the boundary, comparing coefficients of $\log t$, we get

$$A_1+A_2-\frac{\bar{A}_1}{\lambda_1}-\frac{\bar{A}_2}{\lambda_2} = 2ap_1. \tag{6.9}$$

Comparing this with (6.7) shows that $Pe^{i\epsilon}/\pi = 2ap_1$ and
$$Pe^{i\epsilon} = 2\pi a p_1 = -(X+iY),$$
i.e. the force at the origin must balance the resultant of the boundary stresses.

Comparing the coefficients of t^{2n} and t^{-2n} on the boundary we get, for all values of $n \geqslant 1$,

$$\left.\begin{aligned}
c'_{1n}+c'_{2n}+\lambda_1^{2n-1}\bar{c}'_{1n}+\lambda_2^{2n-1}\bar{c}'_{2n} &= \frac{(-)^n}{n}(\lambda_1^{n-1}\bar{A}_1+\lambda_2^{n-1}\bar{A}_2)\\
\frac{1}{\lambda_1}c'_{1n}+\frac{1}{\lambda_2}c'_{2n}+\lambda_1^{2n}\bar{c}'_{1n}+\lambda_2^{2n}\bar{c}'_{2n} &= \frac{(-)^n}{n}(\lambda_1^{n}\bar{A}_1+\lambda_2^{n}\bar{A}_2)\\
\lambda_1^{2n}c'_{1n}+\lambda_2^{2n}c'_{2n}+\frac{1}{\lambda_1}\bar{c}'_{1n}+\frac{1}{\lambda_2}\bar{c}'_{2n} &= \frac{(-)^n}{n}(\lambda_1^{n}A_1+\lambda_2^{n}A_2)\\
\lambda_1^{2n-1}c'_{1n}+\lambda_2^{2n-1}c'_{2n}+\bar{c}'_{1n}+\bar{c}'_{2n} &= \frac{(-)^n}{n}(\lambda_1^{n-1}A_1+\lambda_2^{n-1}A_2)
\end{aligned}\right\}, \tag{6.10}$$

giving

$$c'_{1n} = \frac{(-)^n}{n}\left[\frac{\Delta_{2n,1}}{\Delta_{2n}}(\lambda_1^{n-1}\bar{A}_1+\lambda_2^{n-1}\bar{A}_2)+\frac{\Delta_{2n,2}}{\Delta_{2n}}(\lambda_1^{n}\bar{A}_1+\lambda_2^{n}\bar{A}_2)+\right.$$
$$\left.+\frac{\Delta_{2n,3}}{\Delta_{2,n}}(\lambda_1^{n}A_1+\lambda_2^{n}A_2)+\frac{\Delta_{2n,4}}{\Delta_{2,n}}(\lambda_1^{n-1}A_1+\lambda_2^{n-1}A_2)\right]. \tag{6.11}$$

c'_{2n} is obtained by replacing $\Delta_{2n,1}$, etc., by $\Delta'_{2n,1}$, etc., in this expression for c'_{1n}.

7. Variable edge loading: $\widehat{\eta\eta}-i\widehat{\eta\xi} = p_n e^{ni\xi}+p_{-n}e^{-ni\xi}$

We now consider the case of variable edge loading defined by

$$\widehat{\eta\eta}-i\widehat{\eta\xi} = p_n e^{ni\xi}+p_{-n}e^{-ni\xi}, \quad \text{where } n \geqslant 2.$$

The complex potential on the boundary is given by

$$\begin{aligned} \Omega_{\eta=0} &= -2ia\int^{\xi}(p_n e^{niu}+p_{-n}e^{-niu})e^{-iu}\,du \\ &= -2a\left[\frac{p_n}{(n-1)}t^{-(n-1)}-\frac{p_{-n}}{(n+1)}t^{n+1}\right]. \end{aligned} \tag{7.1}$$

For the resultant of the boundary stresses we have

$$X+iY = -a\int_0^{2\pi}(p_n e^{ni\xi}+p_{-n}e^{-ni\xi})\,d\xi = 0$$

and for the couple about the origin

$$G = \operatorname{re} ia^2\int_0^{2\pi}(p_n e^{ni\xi}+p_{-n}e^{-ni\xi})\,d\xi = 0.$$

This is therefore a case in which the applied forces are in equilibrium.

Using $\Omega_m(t_m) = \sum_{n=-\infty}^{\infty} a_{mn}(t_m^n+\lambda_m^n/t_m^n)$ together with equations (3.4) and (7.1), comparing coefficients of t^{n+1} and $t^{-(n+1)}$ and using the equations obtained together with their conjugates, we have

$$\left.\begin{aligned} a_{1,n+1}+a_{2,n+1}+\lambda_1^n\bar{a}_{1,n+1}+\lambda_2^n\bar{a}_{2,n+1} &= 2a\frac{p_{-n}}{n+1} \\ \frac{1}{\lambda_1}a_{1,n+1}+\frac{1}{\lambda_2}a_{2,n+1}+\lambda_1^{n+1}\bar{a}_{1,n+1}+\lambda_2^{n+1}\bar{a}_{2,n+1} &= 0 \\ \lambda_1^{n+1}a_{1,n+1}+\lambda_2^{n+1}a_{2,n+1}+\frac{1}{\lambda_1}\bar{a}_{1,n+1}+\frac{1}{\lambda_2}\bar{a}_{2,n+1} &= 0 \\ \lambda_1^n a_{1,n+1}+\lambda_2^n a_{2,n+1}+\bar{a}_{1,n+1}+\bar{a}_{2,n+1} &= 2a\frac{\bar{p}_{-n}}{n+1} \end{aligned}\right\}. \tag{7.2}$$

These equations give

$$\left.\begin{aligned} a_{1,n+1} &= \frac{2a}{n+1}\left[\frac{\Delta_{n+1,1}}{\Delta_{n+1}}p_{-n}+\frac{\Delta_{n+1,4}}{\Delta_{n+1}}\bar{p}_{-n}\right] \\ \text{and}\qquad a_{2,n+1} &= \frac{2a}{n+1}\left[\frac{\Delta'_{n+1,1}}{\Delta_{n+1}}p_{-n}+\frac{\Delta'_{n+1,4}}{\Delta_{n+1}}\bar{p}_{-n}\right] \end{aligned}\right\}. \tag{7.3}$$

Similarly comparing the coefficients of t^{n-1} and $t^{-(n-1)}$ we obtain

$$\left.\begin{aligned} a_{1,n-1} &= -\frac{2a}{n-1}\left[\frac{\Delta_{n-1,2}}{\Delta_{n-1}}\bar{p}_n+\frac{\Delta_{n-1,3}}{\Delta_{n-1}}p_n\right] \\ a_{2,n-1} &= -\frac{2a}{n-1}\left[\frac{\Delta'_{n-1,2}}{\Delta_{n-1}}\bar{p}_n+\frac{\Delta'_{n-1,3}}{\Delta_{n-1}}p_n\right] \end{aligned}\right\}. \tag{7.4}$$

All coefficients other than $a_{1,n+1}$, $a_{2,n+1}$, $a_{1,n-1}$, and $a_{2,n-1}$ are zero.

By superimposing the results of sections 4–7 the most general type of edge loading can be dealt with provided $\widehat{\eta\eta}-i\widehat{\eta\xi}$ on the boundary can be expressed in the form of a Fourier series.

8. Derivation of expressions for $\widehat{\eta\eta}+\widehat{\xi\xi}$ on the boundary

We now proceed to obtain an expression for $\widehat{\eta\eta}+\widehat{\xi\xi}$ on the boundary, which will enable us to find the hoop stress $\widehat{\xi\xi}$ when $\widehat{\eta\eta}-i\widehat{\eta\xi}$ on the boundary is known.

We will first consider that part of $\widehat{\eta\eta}+\widehat{\xi\xi}$ on the boundary due to the complex potential

$$\sum_{m=1}^{4} a_{mn}(t_m^n+\lambda_m^n/t_m^n) \quad \text{for } n>1.$$

This is given by the real part of

$$2\left[\frac{\Omega_1'(t_1)}{z_1'(t_1)}+\frac{\Omega_2'(t_2)}{z_2'(t_2)}\right]_{t_1=t_2=t},$$

which reduces to

$$\begin{aligned} &\frac{2n}{aD}\,\mathrm{re}[1-(\lambda_1+\lambda_2)e^{-2i\xi}+\lambda_1\lambda_2 e^{-4i\xi}]\times \\ &\quad\times[(a_{1n}+a_{2n})e^{-(n-1)i\xi}-(\lambda_2 a_{1n}+\lambda_1 a_{2n})e^{-(n-3)i\xi}- \\ &\quad-(\lambda_1^n a_{1n}+\lambda_2^n a_{2n})e^{(n+1)i\xi}+\lambda_1\lambda_2(\lambda_1^{n-1}a_{1n}+\lambda_2^{n-1}a_{2n})e^{(n+3)i\xi}], \end{aligned} \tag{8.1}$$

where
$$D = (1-2\lambda_1\cos 2\xi+\lambda_1^2)(1-2\lambda_2\cos 2\xi+\lambda_2^2). \tag{8.2}$$

That part of $[\widehat{\eta\eta}+\widehat{\xi\xi}]_{\eta=0}$ due to the complex potential

$$\sum_{m=1}^{4}\sum_{n=1}^{\infty} a_{mn}(t_m^n+\lambda_m^n/t_m^n)$$

is the real part of

$$\begin{aligned} &2p_0+\frac{2}{aD}\sum_{n=2}^{\infty} n[1-(\lambda_1+\lambda_2)e^{-2i\xi}+\lambda_1\lambda_2 e^{-4i\xi}]\times \\ &\quad\times[(a_{1n}+a_{2n})e^{-(n-1)i\xi}-(\lambda_2 a_{1n}+\lambda_1 a_{2n})e^{-(n-3)i\xi}- \\ &\quad-(\lambda_1^n a_{1n}+\lambda_2^n a_{2n})e^{(n+1)i\xi}+\lambda_1\lambda_2(\lambda_1^{n-1}a_{1n}+\lambda_2^{n-1}a_{2n})e^{(n+3)i\xi}], \end{aligned} \tag{8.3}$$

that part due to a_{11} and a_{21} being the real part of $2p_0$.

Similarly that part of $[\widehat{\eta\eta}+\widehat{\xi\xi}]_{\eta=0}$ due to the complex potential

$$\sum_{m=1}^{4}\sum_{n=0}^{\infty} c_{mn}(t_m^{2n+1}+\lambda_m^{2n+1}/t_m^{2n+1})$$

is

$$\frac{2}{aD}\,\mathrm{re}\sum_{n=1}^{\infty}(2n+1)[1-(\lambda_1+\lambda_2)e^{-2i\xi}+\lambda_1\lambda_2 e^{-4i\xi}]\times$$

$$\times[(c_{1n}+c_{2n})e^{-2ni\xi}-(\lambda_2 c_{1n}+\lambda_1 c_{2n})e^{-(2n-2)i\xi}-$$

$$-(\lambda_1^{2n+1}c_{1n}+\lambda_2^{2n+1}c_{2n})e^{(2n+2)i\xi}+\lambda_1\lambda_2(\lambda_1^{2n}c_{1n}+\lambda_2^{2n}c_{2n})e^{(2n+4)i\xi}], \quad (8.4)$$

since that part due to c_{10} and c_{20} is zero, from (5.11). Also that part of $[\widehat{\eta\eta}+\widehat{\xi\xi}]_{\eta=0}$ due to the complex potential $\sum_{m=1}^{4}\sum_{n=1}^{\infty} c'_{mn}(t_m^{2n}+\lambda_m^{2n}/t_m^{2n})$ is

$$\frac{2}{aD}\,\mathrm{re}\sum_{n=1}^{\infty}2n[1-(\lambda_1+\lambda_2)e^{-2i\xi}+\lambda_1\lambda_2 e^{-4i\xi}]\times$$

$$\times[(c'_{1n}+c'_{2n})e^{-(2n-1)i\xi}-(\lambda_2 c'_{1n}+\lambda_1 c'_{2n})e^{-(2n-3)i\xi}-$$

$$-(\lambda_1^{2n}c'_{1n}+\lambda_2^{2n}c'_{2n})e^{(2n+1)i\xi}+\lambda_1\lambda_2(\lambda_1^{2n-1}c'_{1n}+\lambda_2^{2n-1}c'_{2n})e^{(2n+3)i\xi}]. \quad (8.5)$$

That part of $[\widehat{\eta\eta}+\widehat{\xi\xi}]_{\eta=0}$ due to the complex potential $\sum_{m=1}^{4}-iaQ\lambda_m/(t_m+\lambda_m/t_m)$ becomes

$$-\frac{2Q}{D_1^2}[(\lambda_1+\lambda_2)(1-\lambda_1\lambda_2)(1+5\lambda_1\lambda_2-\lambda_1^2-\lambda_2^2+\lambda_1^2\lambda_2^2)\sin 2\xi+$$

$$+\lambda_1\lambda_2\{4-\lambda_1^2\lambda_2^2(\lambda_1+\lambda_2)\}\sin 4\xi+\lambda_1\lambda_2(1-\lambda_1\lambda_2)(\lambda_1+\lambda_2)\sin 6\xi], \quad (8.6)$$

where $$D_1=(1+2\lambda_1\cos 2\xi+\lambda_1^2)(1+2\lambda_2\cos 2\xi+\lambda_2^2). \quad (8.7)$$

That part of $[\widehat{\eta\eta}+\widehat{\xi\xi}]_{\eta=0}$ due to the complex potential $\sum_{m=1}^{4}A_m\log a(t_m+\lambda_m/t_m)$ becomes

$$\frac{2}{aD_1}\,\mathrm{re}[1+(\lambda_1+\lambda_2)e^{-2i\xi}+\lambda_1\lambda_2 e^{-4i\xi}][(A_1+A_2)e^{i\xi}+(\lambda_2 A_1+\lambda_1 A_2)e^{3i\xi}]. \quad (8.8)$$

9. Examination of the coefficients $\Delta_{n,1}/\Delta_n$ etc.

The above expressions for $\widehat{\eta\eta}+\widehat{\xi\xi}$ on the boundary given in section 8 are perfectly general and can be used for any aeolotropic material with two axes of symmetry at right angles, by giving λ_1 and λ_2 the appropriate values for the materials concerned.

We shall from now on confine our work to the material oak, and the appropriate values of λ_1 and λ_2 are taken from Holgate's work (**7**). They

are the γ_1 and γ_2 respectively of his Table 1. The constants are chosen so that the grain is parallel to the y-axis and are measured in sq. mm./10^3 kg.

Table 1

The values of $\Delta_{n,1}/\Delta_n$ etc. for $n = 2$ to 12, for oak

n	$\Delta_{n,1}/\Delta_n$	$\Delta_{n,2}/\Delta_n$	$\Delta_{n,3}/\Delta_n$	$\Delta_{n,4}/\Delta_n$
2	1·294	$-3{\cdot}329\times 10^{-2}$	$1{\cdot}315\times 10^{-2}$	$-5{\cdot}393\times 10^{-1}$
3	1·100	$-2{\cdot}860\times 10^{-2}$	$4{\cdot}709\times 10^{-3}$	$-1{\cdot}818\times 10^{-1}$
4	1·075	$-2{\cdot}795\times 10^{-2}$	$1{\cdot}825\times 10^{-3}$	$-7{\cdot}020\times 10^{-2}$
5	1·071	$-2{\cdot}784\times 10^{-2}$	$7{\cdot}185\times 10^{-4}$	$-2{\cdot}762\times 10^{-2}$
6	1·070	$-2{\cdot}783\times 10^{-2}$	$2{\cdot}835\times 10^{-4}$	$-1{\cdot}091\times 10^{-2}$
7	1·070	$-2{\cdot}783\times 10^{-2}$	$1{\cdot}119\times 10^{-4}$	$-4{\cdot}307\times 10^{-3}$
8	1·070	$-2{\cdot}783\times 10^{-2}$	$4{\cdot}424\times 10^{-5}$	$-1{\cdot}701\times 10^{-3}$
9	1·070	$-2{\cdot}783\times 10^{-2}$	$1{\cdot}748\times 10^{-5}$	$-6{\cdot}720\times 10^{-4}$
10	1·070	$-2{\cdot}783\times 10^{-2}$	$6{\cdot}902\times 10^{-6}$	$-2{\cdot}655\times 10^{-4}$
11	1·070	$-2{\cdot}783\times 10^{-2}$	$2{\cdot}727\times 10^{-6}$	$-1{\cdot}048\times 10^{-4}$
12	1·070	$-2{\cdot}783\times 10^{-2}$	$1{\cdot}077\times 10^{-6}$	$-4{\cdot}142\times 10^{-5}$
	Constant for $n \geqslant 6$	Constant for $n \geqslant 6$	$7{\cdot}459\times 10^{-2}\lambda_1^n$ for $n \geqslant 6$	$-2{\cdot}871\lambda_1^n$ for $n \geqslant 6$
n	$\Delta'_{n,1}/\Delta_n$	$\Delta'_{n,2}/\Delta_n$	$\Delta'_{n,3}/\Delta_n$	$\Delta'_{n,4}/\Delta_n$
2	$-8{\cdot}301\times 10^{-2}$	$2{\cdot}810\times 10^{-2}$	$-7{\cdot}310\times 10^{-4}$	$3{\cdot}026\times 10^{-2}$
3	$-7{\cdot}211\times 10^{-2}$	$2{\cdot}786\times 10^{-2}$	$-2{\cdot}640\times 10^{-4}$	$1{\cdot}021\times 10^{-2}$
4	$-7{\cdot}073\times 10^{-2}$	$2{\cdot}784\times 10^{-2}$	$-1{\cdot}024\times 10^{-4}$	$3{\cdot}941\times 10^{-3}$
5	$-7{\cdot}049\times 10^{-2}$	$2{\cdot}783\times 10^{-2}$	$-4{\cdot}033\times 10^{-5}$	$1{\cdot}551\times 10^{-3}$
6	$-7{\cdot}044\times 10^{-2}$	$2{\cdot}783\times 10^{-2}$	$-1{\cdot}592\times 10^{-5}$	$6{\cdot}120\times 10^{-4}$
7	$-7{\cdot}044\times 10^{-2}$	$2{\cdot}783\times 10^{-2}$	$-6{\cdot}288\times 10^{-6}$	$2{\cdot}418\times 10^{-4}$
8	$-7{\cdot}044\times 10^{-2}$	$2{\cdot}783\times 10^{-2}$	$-2{\cdot}484\times 10^{-6}$	$9{\cdot}550\times 10^{-5}$
9	$-7{\cdot}044\times 10^{-2}$	$2{\cdot}783\times 10^{-2}$	$-9{\cdot}811\times 10^{-7}$	$3{\cdot}772\times 10^{-5}$
10	$-7{\cdot}044\times 10^{-2}$	$2{\cdot}783\times 10^{-2}$	$-3{\cdot}875\times 10^{-7}$	$1{\cdot}490\times 10^{-5}$
11	$-7{\cdot}044\times 10^{-2}$	$2{\cdot}783\times 10^{-2}$	$-1{\cdot}531\times 10^{-7}$	$5{\cdot}886\times 10^{-6}$
12	$-7{\cdot}044\times 10^{-2}$	$2{\cdot}783\times 10^{-2}$	$-6{\cdot}045\times 10^{-8}$	$2{\cdot}325\times 10^{-6}$
	Constant for $n \geqslant 6$	Constant for $n \geqslant 6$	$-4{\cdot}190\times 10^{-3}\lambda_1^n$ for $n \geqslant 6$	$1{\cdot}613\times 10^{-1}\lambda_1^n$ for $n \geqslant 6$

The wood is cut from the tree so that the annual layers are parallel to the plane of the plate. The values are

$$\lambda_1 = 0{\cdot}395 \quad \text{and} \quad \lambda_2 = 0{\cdot}026.$$

Using these values we can, in theory, calculate the hoop stress at any point on the boundary of the disk, given the form of $\widehat{\eta\eta} - i\widehat{\eta\xi}$ on the boundary. In practice the work is impossible since, however simple p_n may be, the coefficients $\Delta_{n,1}/\Delta_n$, etc., and $\Delta'_{n.1}/\Delta_n$, etc., are much too complicated for us to sum the series involved. Using the values of λ_1 and λ_2 for oak, however, and calculating these coefficients correct to four significant figures, we find that for $n > 5$ they all become either constant or of the form $k\lambda_1^n$ where k is a constant. Using these values we shall be able to sum the series involved in the expression for $[\widehat{\eta\eta}+\widehat{\xi\xi}]_{\eta=0}$ from $n = 6$ to ∞.

In our calculations we will aim at a result correct to three significant figures and will be free to neglect anything which does not affect the fourth significant figure in our numbers.

We find that

$$\Delta_n = -\frac{(\lambda_1-\lambda_2)^2}{\lambda_1^2\lambda_2^2}\{1+\lambda_1^{2n}\lambda_2^{2n}\}-2(1-\lambda_1^2)(1-\lambda_2^2)\lambda_1^{n-2}\lambda_2^{n-2}+$$
$$+\frac{(1-\lambda_1\lambda_2)^2}{\lambda_1^2\lambda_2^2}\{\lambda_1^{2n}+\lambda_2^{2n}\}, \tag{9.1}$$

$$\Delta_{n,1} = -(\lambda_1-\lambda_2)/\lambda_1\lambda_2^2+\lambda_1^n\lambda_2^{n-2}(1-\lambda_2^2)-\lambda_2^{2n-1}(1-\lambda_1\lambda_2)/\lambda_1, \tag{9.2}$$

$$\Delta_{n,2} = (\lambda_1-\lambda_2)/\lambda_1\lambda_2-\lambda_1^{n-1}\lambda_2^{n-2}(1-\lambda_2^2)+\lambda_2^{2n-2}(1-\lambda_1\lambda_2)/\lambda_1, \tag{9.3}$$

$$\Delta_{n,3} = -\lambda_1^{n-1}\lambda_2^{2n-2}(\lambda_1-\lambda_2)+\lambda_2^{n-2}(1-\lambda_2^2)-\lambda_1^{n-1}(1-\lambda_1\lambda_2)/\lambda_2, \tag{9.4}$$

$$\Delta_{n,4} = \lambda_1^{n-1}\lambda_2^{2n-1}(\lambda_1-\lambda_2)-\lambda_2^{n-2}(1-\lambda_2^2)/\lambda_1+\lambda_1^{n-1}(1-\lambda_1\lambda_2)/\lambda_2^2. \tag{9.5}$$

10. The values of certain expressions for $\widehat{\eta\eta}+\widehat{\xi\xi}$ on the boundary for the particular material oak

Taking first the case when p_n is real, so that both a_{1n} and a_{2n} are also real, we have from consideration of equations (7.3) and (7.4) and superimposing the results, for $n > 1$,

$$a_{1n} = \frac{2a}{n}\left[\left\{\frac{\Delta_{n,1}}{\Delta_n}+\frac{\Delta_{n,4}}{\Delta_n}\right\}p_{-(n-1)}-\left\{\frac{\Delta_{n,2}}{\Delta_n}+\frac{\Delta_{n,3}}{\Delta_n}\right\}p_{n+1}\right], \tag{10.1}$$

$$a_{2n} = \frac{2a}{n}\left[\left\{\frac{\Delta'_{n,1}}{\Delta_n}+\frac{\Delta'_{n,4}}{\Delta_n}\right\}p_{-(n-1)}-\left\{\frac{\Delta'_{n,2}}{\Delta_n}+\frac{\Delta'_{n,3}}{\Delta_n}\right\}p_{n+1}\right], \tag{10.2}$$

so that

$$a_{1n}+a_{2n} = \frac{2a}{n}\left[\left\{\frac{\Delta_{n,1}+\Delta'_{n,1}+\Delta_{n,4}+\Delta'_{n,4}}{\Delta_n}\right\}p_{-(n-1)}-\right.$$
$$\left.-\left\{\frac{\Delta_{n,2}+\Delta'_{n,2}+\Delta_{n,3}+\Delta'_{n,3}}{\Delta_n}\right\}p_{n+1}\right] \tag{10.3}$$

and

$$\lambda_2 a_{1n}+\lambda_1 a_{2n} = \frac{2a}{n}\left[\left\{\frac{\lambda_2\Delta_{n,1}+\lambda_1\Delta'_{n,1}+\lambda_2\Delta_{n,4}+\lambda_1\Delta'_{n,4}}{\Delta_n}\right\}p_{-(n-1)}-\right.$$
$$\left.-\left\{\frac{\lambda_2\Delta_{n,2}+\lambda_1\Delta'_{n,2}+\lambda_2\Delta'_{n,3}+\lambda_1\Delta'_{n,3}}{\Delta_n}\right\}p_{n+1}\right]. \tag{10.4}$$

It can be shown that, correct to four significant figures,

$$(\Delta_{n,1}+\Delta'_{n,1}+\Delta_{n,4}+\Delta'_{n,4})/\Delta_n = 1, \quad \text{for } n > 9, \tag{10.5}$$

$$(\Delta_{n,2}+\Delta'_{n,2}+\Delta_{n,3}+\Delta'_{n,3})/\Delta_n = 0{\cdot}07047\lambda_1^n, \quad \text{for } n > 10, \tag{10.6}$$

$$(\lambda_2\Delta_{n,1}+\lambda_1\Delta'_{n,1}+\lambda_2\Delta_{n,4}+\lambda_1\Delta'_{n,4})/\Delta_n = -0{\cdot}01100\lambda_1^n, \quad \text{for } n > 10, \tag{10.7}$$

$$(\lambda_2\Delta_{n,2}+\lambda_1\Delta'_{n,2}+\lambda_2\Delta_{n,3}+\lambda_1\Delta'_{n,3})/\Delta_n = 0{\cdot}01027, \quad \text{for } n > 5. \tag{10.8}$$

Putting the above values in equations (10.3) and (10.4) we obtain for $n > 10$,

$$a_{1n}+a_{2n} = \frac{2a}{n}[p_{-(n-1)}-0{\cdot}07047\lambda_1^n p_{n+1}], \tag{10.9}$$

and

$$\lambda_2 a_{1n}+\lambda_1 a_{2n} = -\frac{2a}{n}[0{\cdot}011\lambda_1^n p_{-(n-1)}+0{\cdot}01027 p_{n+1}]. \tag{10.10}$$

From consideration of equations (7.2), we see that when the p_n's are real

$$\lambda_1^{n-1}a_{1n}+\lambda_2^{n-1}a_{2n} = \frac{2a}{n}p_{-(n-1)}-(a_{1n}+a_{2n})$$

$$= \frac{2a}{n}[0{\cdot}07047\lambda_1^n p_{n+1}] \tag{10.11}$$

and

$$\lambda_1^n a_{1n}+\lambda_2^n a_{2n} = -\frac{2a}{n}p_{n+1}-\frac{1}{\lambda_1\lambda_2}(\lambda_2 a_{1n}+\lambda_1 a_{2n})$$

$$= -\frac{2a}{n}\left[p_{n+1}-\frac{0{\cdot}011}{\lambda_1\lambda_2}\lambda_1^n p_{-(n-1)}-p_{n+1}\right]$$

$$= \frac{2a}{n}[1{\cdot}071\lambda_1^n p_{-(n-1)}]. \tag{10.12}$$

Substituting these values in expression (8.1) gives that part of $[\widehat{\eta\eta}+\widehat{\xi\xi}]_{\eta=0}$ due to the terms containing a_{1n} and a_{2n} as

$$\left(\frac{2n}{aD}\right)\left(\frac{2a}{n}\right)\mathrm{re}[1-(\lambda_1+\lambda_2)e^{-2i\xi}+\lambda_1\lambda_2 e^{-4i\xi}]\times$$

$$\times[p_{-(n-1)}e^{-(n-1)i\xi}-0{\cdot}07047\lambda_1^n p_{n+1}e^{-(n-1)i\xi}+$$

$$+0{\cdot}011\lambda_1^n p_{-(n-1)}e^{-(n-3)i\xi}+0{\cdot}01027 p_{n+1}e^{-(n-3)i\xi}-$$

$$-1{\cdot}071\lambda_1^n p_{-(n-1)}e^{(n+1)i\xi}+0{\cdot}07047\lambda_1\lambda_2\lambda_1^n p_{n+1}e^{(n+3)i\xi}]. \tag{10.13}$$

Summing the series obtained by taking values of n from 11 to ∞ in (10.13) gives that part of $[\widehat{\eta\eta}+\widehat{\xi\xi}]_{\eta=0}$ due to the terms

$$\sum_{m=1}^{4}\sum_{n=11}^{\infty} a_{mn}(t_m^n+\lambda_m^n/t_m^n)$$

as

$$\frac{4}{D}\operatorname{re}[1-(\lambda_1+\lambda_2)e^{-2i\xi}+\lambda_1\lambda_2 e^{-4i\xi}]\times$$
$$\times\Big[\sum_{n=11}^{\infty} p_{-(n-1)}e^{-(n-1)i\xi}+0{\cdot}01027e^{4i\xi}\sum_{n=11}^{\infty} p_{n+1}e^{-(n+1)i\xi}+$$
$$+0{\cdot}011\lambda_1 e^{2i\xi}\sum_{n=11}^{\infty}\lambda_1^{n-1}p_{-(n-1)}e^{-(n-1)i\xi}-$$
$$-1{\cdot}071\lambda_1 e^{2i\xi}\sum_{n=11}^{\infty}\lambda_1^{n-1}p_{-(n-1)}e^{(n-1)i\xi}-$$
$$-\frac{0{\cdot}07047}{\lambda_1}e^{2i\xi}\sum_{n=11}^{\infty}\lambda_n^{n+1}p_{n+1}e^{-(n+1)i\xi}+$$
$$+0{\cdot}07047\lambda_2 e^{2i\xi}\sum_{n=11}^{\infty}\lambda_1^{n+1}p_{n+1}e^{(n+1)i\xi}\Big].$$

This is equal to

$$\frac{4}{D}\operatorname{re}[1-(\lambda_1+\lambda_2)e^{-2i\xi}+\lambda_1\lambda_2 e^{-4i\xi}]\times$$
$$\times\Big[\sum_{n=10}^{\infty} p_{-n}e^{-ni\xi}+0{\cdot}01027e^{4i\xi}\sum_{n=12}^{\infty} p_n e^{-ni\xi}+$$
$$+0{\cdot}004345e^{2i\xi}\sum_{n=10}^{\infty}\lambda_1^n p_{-n}e^{-ni\xi}-0{\cdot}4321e^{2i\xi}\sum_{n=10}^{\infty}\lambda_1^n p_{-n}e^{ni\xi}-$$
$$-0{\cdot}1784e^{2i\xi}\sum_{n=12}^{\infty}\lambda_1^n p_n e^{-ni\xi}+0{\cdot}001832e^{2i\xi}\sum_{n=12}^{\infty}\lambda_1^n p_n e^{ni\xi}\Big]. \quad (10.14)$$

Also using the appropriate values of λ_1 and λ_2 for oak, expression (8.6) becomes

$$-\frac{Q}{D_1^2}[0{\cdot}7456\sin 2\xi+0{\cdot}08216\sin 4\xi+0{\cdot}00856\sin 6\xi]. \quad (10.15)$$

Again, taking the values

$$\alpha_1 = 5{\cdot}321, \qquad \alpha_2 = 1{\cdot}109, \qquad s_{12} = -0{\cdot}87, \qquad s_{22} = 1{\cdot}72,$$

for oak from Holgate (**7**), Table 1, expressions (6.6) become

$$A_1 = \frac{P}{\pi}[-0{\cdot}2502\cos\epsilon-0{\cdot}3916i\sin\epsilon]$$

and
$$A_2 = \frac{P}{\pi}[0{\cdot}03693\cos\epsilon+0{\cdot}009714i\sin\epsilon].$$

Substituting these values in expression (8.8) we obtain that part of $[\widehat{\eta\eta}+\widehat{\xi\xi}]_{\eta=0}$ due to the complex potential $\sum\limits_{m=1}^{4} A_m \log a(t_m+\lambda_m/t_m)$ as

$$\frac{P}{\pi a D_1}[-0{\cdot}5992\cos\epsilon\cos\xi+1{\cdot}0909\sin\epsilon\sin\xi+$$
$$+0{\cdot}01177\cos\epsilon\cos 3\xi+0{\cdot}02053\sin\epsilon\sin 3\xi]. \quad (10.16)$$

11. Equal and opposite radial forces at right angles to the grain

We now consider the case of a uniform normal stress P over the arcs $-\alpha<\xi<\alpha$ and $\pi-\alpha<\xi<\pi+\alpha$.

On making α small we get results for equal and opposite forces F directed along the positive and negative x-axes.

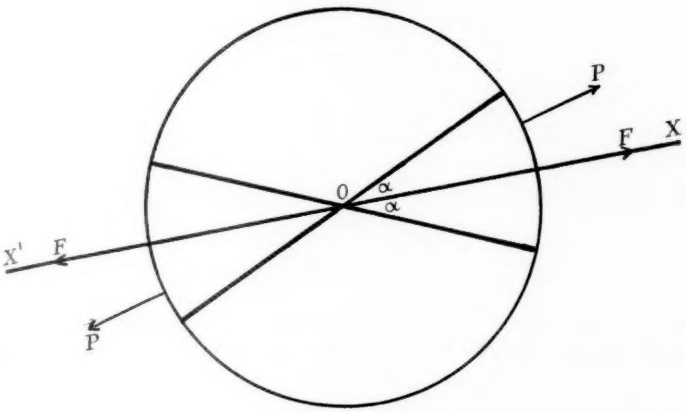

FIG. 1

Assuming that $\widehat{\eta\eta}-i\widehat{\eta\xi}$ can be expressed in the form $\sum\limits_{-\infty}^{+\infty} p_n e^{ni\xi}$ we find that $p_n = \dfrac{P}{\pi}(1+e^{-ni\pi})\dfrac{\sin n\alpha}{n}$.

$$\left.\begin{aligned}
&\text{If } n \text{ is odd,} && p_n = 0\\
&\text{If } n \text{ is even,} && p_n = \frac{2P}{\pi}\frac{\sin n\alpha}{n}\\
&\text{If } n = 0, && p_0 = \frac{2P\alpha}{\pi} = \frac{F}{a\pi}
\end{aligned}\right\}. \quad (11.1)$$

Since p_n is real, on substituting these values in (10.14), that part of $[\widehat{\eta\eta}+\widehat{\xi\xi}]_{\eta=0}$ due to the terms $\sum_{m=1}^{4}\sum_{n=11}^{\infty} a_{mn}(t_m^n+\lambda_m^n/t_m^n)$ becomes

$$\frac{4}{D}\text{re}[1-(\lambda_1+\lambda_2)e^{-2i\xi}+\lambda_1\lambda_2 e^{-4i\xi}]\times$$

$$\times\frac{2P}{\pi}\Big[\sum_{n=5}^{\infty}\frac{\sin 2n\alpha}{2n}e^{-2ni\xi}+0{\cdot}01027e^{4i\xi}\sum_{n=6}^{\infty}\frac{\sin 2n\alpha}{2n}e^{-2ni\xi}+$$

$$+0{\cdot}004345e^{2i\xi}\sum_{n=5}^{\infty}\lambda_1^{2n}\frac{\sin 2n\alpha}{2n}e^{-2ni\xi}-0{\cdot}4231e^{2i\xi}\sum_{n=5}^{\infty}\lambda_1^{2n}\frac{\sin 2n\alpha}{2n}e^{2ni\xi}-$$

$$-0{\cdot}1784e^{2i\xi}\sum_{n=6}^{\infty}\lambda_1^{2n}\frac{\sin 2n\alpha}{2n}e^{-2ni\xi}+0{\cdot}001832e^{2i\xi}\sum_{n=6}^{\infty}\lambda_1^{2n}\frac{\sin 2n\alpha}{2n}e^{2ni\xi}\Big]. \tag{11.2}$$

It can be shown that, when α is small,

$$\sum_{n=t}^{\infty}\lambda_1^{2n}\frac{\sin 2n\alpha}{2n}e^{2ni\theta}=\frac{\alpha\lambda_1^{2t}e^{2ti\theta}}{1-\lambda_1^2 e^{2i\theta}}.$$

Now that part of $[\widehat{\eta\eta}+\widehat{\xi\xi}]_{\eta=0}$ due to the term p_0 is $2p_0$, which is equal to $2F/\pi a$, and on summation all the terms containing λ_1^{2n} in (11.2) are found to be negligible compared with this. Also, when α is small,

$$\sum_{n=t}^{\infty}\frac{\sin 2n\alpha}{2n}e^{2ni\theta}=\frac{i\alpha e^{(2t-1)i\theta}}{2\sin\theta},$$

provided $\theta\pm\alpha\neq n\pi$, a condition with which ξ complies except at the point of application of the forces F, where the stresses are in any case indeterminate.

Expression (11.2) now reduces to the real part of

$$-\left(\frac{8P}{\pi D}\right)\frac{i\alpha}{2\sin\xi}[1-(\lambda_1+\lambda_2)e^{-2i\xi}+\lambda_1\lambda_2 e^{-4i\xi}][e^{-9i\xi}+0{\cdot}01027e^{4i\xi}e^{-11i\xi}]$$

$$=-\frac{2F}{\pi aD\sin\xi}[0{\cdot}01027\sin 7\xi+0{\cdot}9957\sin 9\xi-$$

$$-0{\cdot}4209\sin 11\xi+0{\cdot}01027\sin 13\xi]. \tag{11.3}$$

It now remains to find an expression for $[\widehat{\eta\eta}+\widehat{\xi\xi}]_{\eta=0}$ due to the terms containing a_{13}, a_{23}; a_{15}, a_{25}; a_{17}, a_{27}; a_{19}, a_{29}. The values of $\Delta_{n,1}/\Delta_n$, etc., are taken from Table 1 for $n = 3$, 5, 7, and 9. As α is small, every

$$p_n=\left(\frac{2P}{\pi}\right)\frac{\sin n\alpha}{n}=\frac{2P\alpha}{\pi}=\frac{F}{\pi a}.$$

Substituting the above values in equations (10.3), (10.4), (10.11), and (10.12) and putting the results obtained in equation (8.1) we find that the values of $[\widehat{\eta\eta}+\widehat{\xi\xi}]_{\eta=0}$ for $n = 3, 5, 7$, and 9 respectively are

$$\frac{F}{\pi aD}(0{\cdot}04108+3{\cdot}488\cos 2\xi-1{\cdot}662\cos 4\xi+0{\cdot}04108\cos 6\xi),$$

$$\frac{F}{\pi aD}(0{\cdot}04108\cos 2\xi+3{\cdot}895\cos 4\xi-1{\cdot}678\cos 6\xi+0{\cdot}04108\cos 8\xi),$$

$$\frac{F}{\pi aD}(0{\cdot}04108\cos 4\xi+3{\cdot}9696\cos 6\xi-1{\cdot}6844\cos 8\xi+0{\cdot}04108\cos 10\xi),$$

$$\frac{F}{\pi aD}(0{\cdot}04108\cos 6\xi+3{\cdot}9792\cos 8\xi-1{\cdot}682\cos 10\xi+0{\cdot}04108\cos 12\xi).$$

Summing the last four expressions we obtain

$$\frac{F}{\pi aD}(0{\cdot}04108+3{\cdot}529\cos 2\xi+2{\cdot}274\cos 4\xi+2{\cdot}374\cos 6\xi+$$
$$+2{\cdot}336\cos 8\xi-1{\cdot}641\cos 10\xi+0{\cdot}04108\cos 12\xi),$$

which we shall denote by $FB/\pi aD$.

Expression (11.3) becomes

$$-\frac{F}{\pi aD\sin\xi}(0{\cdot}02054\sin 7\xi+1{\cdot}991\sin 9\xi-0{\cdot}8418\sin 11\xi+0{\cdot}02054\sin 13\xi),$$

which we shall denote by $-\dfrac{FA}{\pi aD}$.

As $\widehat{\eta\eta}$ is zero at all points on the boundary of the disk, except at the points of application of the forces, the hoop stress is the same as the value of $[\widehat{\eta\eta}+\widehat{\xi\xi}]_{\eta=0}$.

TABLE 2

$\pi a\widehat{\xi\xi}/F$ for equal and opposite radial forces at right angles to the grain

$\xi°$	$\pi a\widehat{\xi\xi}/F$	$\xi°$	$\pi a\widehat{\xi\xi}/F$
0	1·656	100	0·843
10	1·607	110	0·884
20	1·465	120	0·948
30	1·310	130	1·033
40	1·160	140	1·160
50	1·033	150	1·310
60	0·948	160	1·465
70	0·884	170	1·607
80	0·843	180	1·656
90	0·827		

For all disks of the same material the expression $\pi a\widehat{\xi\xi}/F$ is independent of the radius and of the magnitude of the applied forces F. Its value is given by the expression $2-(A-B)/D$. Table 2 shows the values of $\pi a\widehat{\xi\xi}/F$ for values of ξ varying from 0° to 180°.

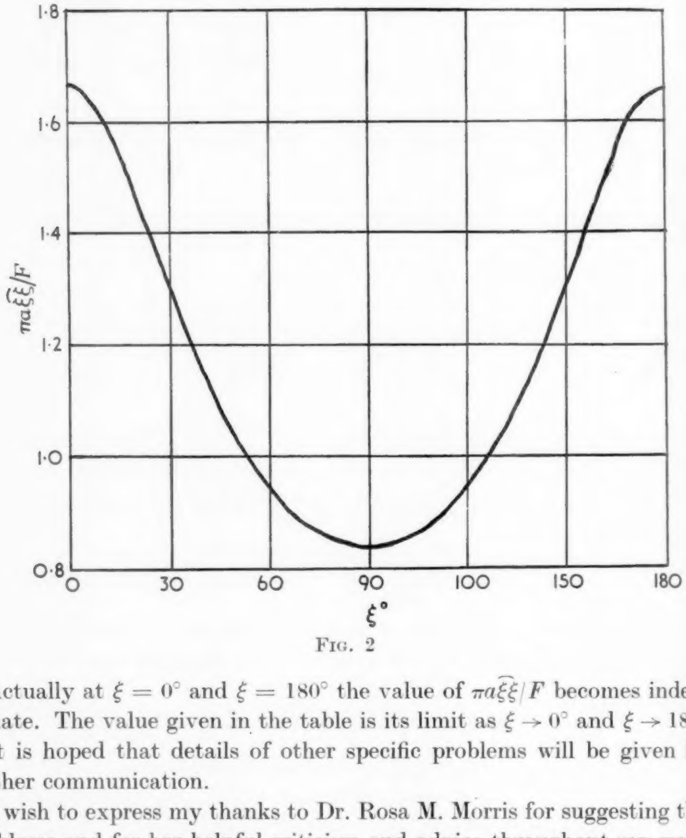

FIG. 2

Actually at $\xi = 0^\circ$ and $\xi = 180^\circ$ the value of $\pi a\widehat{\xi\xi}/F$ becomes indeterminate. The value given in the table is its limit as $\xi \to 0^\circ$ and $\xi \to 180^\circ$.

It is hoped that details of other specific problems will be given in a further communication.

I wish to express my thanks to Dr. Rosa M. Morris for suggesting these problems and for her helpful criticism and advice throughout my work.

REFERENCES

1. G. H. LIVENS and ROSA M. MORRIS, *Phil. Mag.* (7) **38** (1947), 153.
2. ROSA M. MORRIS, *Quart. J. Mech. and Applied Math.* **4** (1951), 248.
3. A. C. STEVENSON, *Phil. Mag.* (7) **34** (1943), 766.
4. M. ROTHMAN, *Quart. J. Mech. and Applied Math.* **3** (1950), 469.
5. H. OKUBO, *Journal of Mathematics and Physics*, **31** (1952), 75.
6. A. E. GREEN and G. I. TAYLOR, *Proc. Roy. Soc.* A, **173** (1939), 162.
7. S. HOLGATE, *Proc. Cambridge Phil. Soc.* **40** (1944), 172.

IMPACT BUCKLING OF DEEP BEAMS IN PURE BENDING

By J. F. DAVIDSON (*Engineering Laboratory, Cambridge*)

[Received 4 March 1954]

SUMMARY

The equations describing lateral instability of a deep beam, first given by Prandtl (**1**) and Michell (**2**), are here extended to the dynamic case in which a beam is suddenly loaded by couples acting in the plane of greatest stiffness. These couples are greater than the first critical moment, and, owing to the slight initial curvature of the beam, their application causes it to deflect exponentially with time until the bending couples are released. For a given value of the bending moment, the period of application is determined by the criterion that the amplitude of the subsequent oscillations shall not be excessive. It is found, in most cases, that the resulting impact time is related to the *longer* of the two gravest component periods of the unloaded beam (torsion and flexure). If the couples are very large, and the gravest component periods widely different, the impact time is fixed by the *shorter* of the component periods.

1. Introduction

THIS paper deals with the behaviour of a slender beam, having slight initial curvature and twist, and bent by impulsive moments of a type tending to produce lateral instability. Various writers have considered the analogous problem of the initially curved strut subjected to an axial load for a short period of time. A survey of this work was given in a previous paper by the author (**3**); the most useful results fall under two headings:

(i) The impulsive axial load may be greater than the Euler load if it is applied for a time of the same order as the first natural period of the strut.

(ii) The axial load which may be applied for an indefinitely long period of time is only slightly less than the allowable static load.

Of these results only the second is immediately applicable to the beam. In attempting to apply the first result, we note that both lateral bending and torsion are involved when the beam becomes unstable, and we have thus to determine whether the period of application is to be compared with the flexural or torsional period.

The present investigations show that if the lateral deflexion, as well as the twist, is limited (by practical considerations) to about twelve times its initial value, then the period of application of the bending action is decided in most cases by the larger of the component periods (flexure and torsion).

To derive the equations governing the behaviour of a deep rectangular section beam, subject both to lateral instability and dynamic effects, we follow the treatment and notation given by Timoshenko (**4**). Thus in Fig. 1 Ox, Oy, Oz are fixed axes and $P'\xi$, $P'\eta$, $P'\zeta$ moving axes, M_ξ, M_η, M_ζ

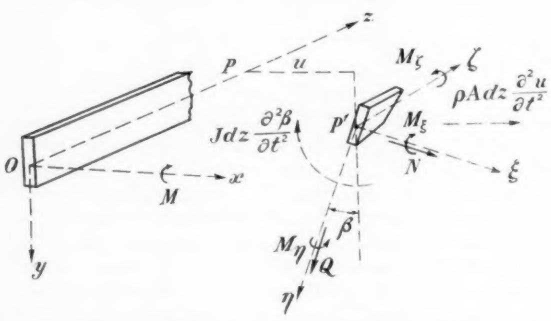

FIG. 1. The stress-couples and mass accelerations for a deep rectangular section beam under pure couples M.

are stress couples, and N and Q are snear forces acting on the element ahead of P'. Also indicated in Fig. 1 are the effective inertia force $\rho A\,dz\,\partial^2 u/\partial t^2$ and the effective inertia couple $J\,dz\,\partial^2\beta/\partial t^2$. Here, ρ is the density of the beam, A its cross-sectional area, and J the moment of inertia per unit length about the central axis; all of these quantities are taken to be uniform.

Taking moments about the axes $P'\xi$, $P'\eta$, $P'\zeta$ for equilibrium of the element of the beam, and noting that M_η and M_ζ are small compared with M_ξ, we get

$$\partial M_\xi/\partial z + Q = 0, \tag{1 i}$$

$$\partial M_\eta/\partial z + M_\xi\,\partial\beta/\partial z - N = 0, \tag{1 ii}$$

$$\partial M_\zeta/\partial z - M_\xi\,\partial^2 u/\partial z^2 = J\,\partial^2\beta/\partial t^2. \tag{1 iii}$$

Also, $Q \gg N$, and for equilibrium of the shearing forces we have

$$-\partial N/\partial z + Q\,\partial\beta/\partial z = \rho A\,\partial^2 u/\partial t^2, \tag{2 i}$$

$$\partial Q/\partial z = 0, \tag{2 ii}$$

where u and β are respectively the lateral shift and twist at any section of the beam and are connected with the stress couples by the equations of deformation, viz.

$$\left.\begin{aligned} M_\eta &= B\,\partial^2(u-u_0)/\partial z^2 \\ M_\zeta &= C\,\partial(\beta-\beta_0)/\partial z \end{aligned}\right\}. \tag{3}$$

B is the smallest flexural rigidity of the beam, and C its torsional rigidity; u_0 and β_0 are small initial values of u and β, due to imperfections in the beam.

2. Effect of pure couples suddenly applied

We now consider a beam of length l, at rest in the position $u = u_0$, $\beta = \beta_0$, to which end moments M, tending to produce pure bending, are suddenly applied at $t = 0$, thereafter remaining constant. It will be shown later that the time taken for these moments to produce substantial lateral deflexion and twist is of the same order as the period of lateral vibration (in the plane Oxz), or the period of torsional vibration. These periods, each referring to the gravest mode, are much longer than the period of flexural vibration in the plane Oyz. This latter period is a measure of the time required for the effect of the end moments to spread along the length of the beam. Thus we may ignore bending waves in the plane Oyz, and put $M_\xi = M$ for all values of z. This result also follows from (2i) and (1i), which were derived by neglecting the vertical accelerations of the beam. The corresponding simplification used in strut work (**3**) is to neglect longitudinal stress waves, thereby assuming a suddenly applied end load to be propagated along the strut with infinite speed.

3. Equations (1), (2), and (3) may now be simplified by putting $M_\xi = M$, $Q = 0$, and eliminating N, M_η, and M_ζ. Then

$$\left.\begin{aligned} B\,\partial^4(u-u_0)/\partial z^4 + M\,\partial^2\beta/\partial z^2 &= -\rho A\,\partial^2 u/\partial t^2 \\ C\,\partial^2(\beta-\beta_0)/\partial z^2 - M\,\partial^2 u/\partial z^2 &= J\,\partial^2\beta/\partial t^2 \end{aligned}\right\}. \tag{4}$$

The initial conditions ($t = 0$) are $u = u_0$, $\beta = \beta_0$, $\partial u/\partial t = \partial\beta/\partial t = 0$. The end conditions are those of simple support, and hence $u = \partial^2 u/\partial z^2 = 0$ at $z = 0$ or l. Finally, twist at the ends is prevented, so that $\beta = 0$ at $z = 0$ or l.

In general, the initial imperfections u_0 and β_0 take the form of a half-range sine series. The higher harmonics in this series have an effect which has been considered, in the case of an impulsively loaded strut, by Lavrentiev and Ishlinsky (**5**). They showed that, if the applied load is not much greater than the gravest critical load, only the first term in the series is important. If, however, the applied load is very much greater, other terms may be more important than the first. This result applies equally well to beams as to struts, and since the treatment of the higher harmonics follows readily from a consideration of the first, we deal only with this latter and write $u_0 = c\sin\pi z/l$, $\beta_0 = d\sin\pi z/l$. The governing equations (4) and the end conditions are then satisfied by $u = u_1\sin\pi z/l$, $\beta = \beta_1\sin\pi z/l$.

Substitution in (4) and the use of the initial conditions then yields the following expressions for the central deflexion u_1 and the central twist β_1,

$$\left.\begin{aligned}\frac{u_1}{c} &= \frac{M^2}{M^2-M_E^2}\left\{\frac{\omega_a^2\cosh\omega_i t+\omega_i^2\cos\omega_a t}{\omega_a^2+\omega_i^2}-\frac{M_E^2}{M^2}+\right.\\&\qquad\left.+\frac{dM_E^2}{cP_E M}\left[\frac{\omega_a^2(1+\omega_i^2/\omega_T^2)\cosh\omega_i t+\omega_i^2(1-\omega_a^2/\omega_T^2)\cos\omega_a t}{\omega_a^2+\omega_i^2}-1\right]\right\}\\\frac{\beta_1}{d} &= \frac{M^2}{M^2-M_E^2}\left\{\frac{\omega_a^2\cosh\omega_i t+\omega_i^2\cos\omega_a t}{\omega_a^2+\omega_i^2}-\frac{M_E^2}{M^2}+\right.\\&\qquad\left.+\frac{cP_E}{dM}\left[\frac{\omega_a^2(1+\omega_i^2/\omega_L^2)\cosh\omega_i t+\omega_i^2(1-\omega_a^2/\omega_L^2)\cos\omega_a t}{\omega_a^2+\omega_i^2}-1\right]\right\}\end{aligned}\right\} \tag{5}$$

where $P_E = \pi^2 B/l^2$ is the Euler load of the beam.

From (5) we see that the deflexion and twist increase exponentially with time, at a rate governed by the 'frequency' ω_i, and that there is a superposed vibration of frequency ω_a. Also ω_i and ω_a are given by

$$\left.\begin{aligned}2\omega_a^2 &= \omega_T^2+\omega_L^2+\sqrt{[(\omega_T^2-\omega_L^2)^2+4\omega_L^2\,\omega_T^2\,M^2/M_E^2]}\\\omega_a^2-\omega_i^2 &= \omega_T^2+\omega_L^2\end{aligned}\right\}, \tag{6}$$

where $\omega_L = \pi^2\sqrt{(B/\rho A)}/l^2$ and $\omega_T = \pi\sqrt{(C/J)}/l$ are the gravest frequencies of flexural and torsional vibration of the free beam; ω_i is real only if M is greater than the first critical moment $M_E = \pi\sqrt{(BC)}/l$. If $M < M_E$, ω_i is imaginary, and the exponential terms in (5) are replaced by harmonic terms.

Similar results are obtained when a pin-ended strut, having a small initial curvature, is subjected to a constant and suddenly applied axial load (**3**). But when this load is greater than the Euler load, the graph of strut deflexion against time contains only exponential terms. In the present case we have both exponential and harmonic components; the extra term will be discussed in a subsequent paper.

4. Numerical results

Calculations based on (6) show that ω_i is of the same order as the smaller of the component frequencies, and ω_a is always greater than either component frequency. This suggests at once that the couples M might be applied for a time decided by the *longer* of the component periods $2\pi/\omega_L$ and $2\pi/\omega_T$. Thus, in (5) we would expect the exponential terms, and therefore $\omega_i t$, to be the governing factor in determining the allowable period of application of the couples M.

5. Complete time history of the beam loaded for a time t_i

This tentative conclusion is confirmed by results shown in Figs. 2, 3, and 4, which give the central deflexion and twist of a beam, bent for a time t_i

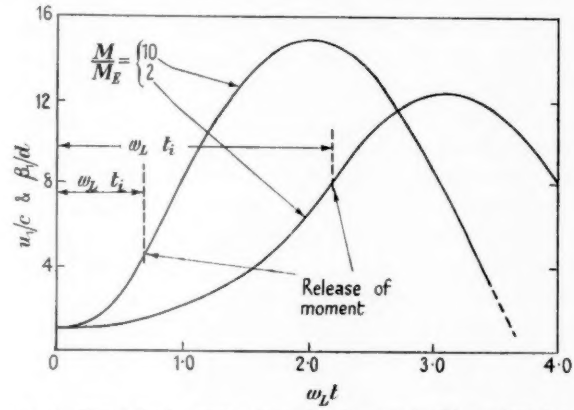

FIG. 2. The deflexion and twist under the couples M, applied for a time t_i, with $\omega_L/\omega_T = 1$.

by pure couples M. Equation (5) is the governing equation for $t < t_i$, and thereafter the beam is in a state of free oscillation about the mean position

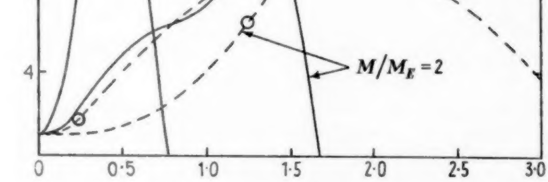

FIG. 3. The deflexion and twist with $\omega_L/\omega_T = 0{\cdot}2$. The full lines show β_1/d and the broken lines u_1/c. ○, times at which the moments are released.

u_0, β_0. The amplitudes of the lateral displacement u_1, and of the twist β_1, depend upon the velocity and displacement when the couples are removed at time t_i.

To compute the curves, it was necessary to have a value for the parameter dM_E/cP_E. A value of unity was adopted, since values of about 0·5 for an I-section, and about 2·0 for a rectangular section, were obtained.

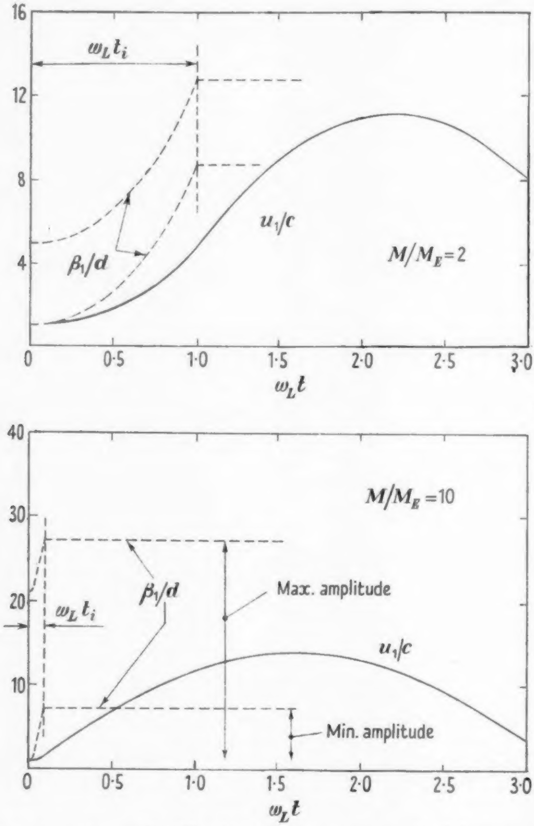

FIG. 4. $\omega_L/\omega_T = 0$. The twist has a component of frequency ω_T when $t < t_i$, the dotted lines showing the limits of movement. When $t > t_i$, vibrations are about a mean position $\beta_1/d = 1$, and the limit of amplitude may be anywhere between the dotted lines.

It was then necessary to have limiting values for the central deflexion u_1 and the central twist β_1. A definite limit can be put on u_1/c, since in practice $l/k < 200$ for a slender beam, k being the least radius of gyration, and u_1/c is then limited by bending stress to a value of about 12. No such definite limit can be imposed on β_1/d, although reasonable values would seem to be $d = 1$ degree and $\beta_1/d < 20$. Using (5), the time of application t_i of the

bending couples M was then adjusted to make either the maximum deflexion or twist, which always occurred after removal of the couples, equal to its limiting value.

Figs. 3 and 4 give results for $\omega_L/\omega_T < 1$. These diagrams also refer to the cases when $\omega_L/\omega_T = 5$ and ∞ respectively, because the symmetry of (5) when $dM_E/cP_E = 1$ enables us to exchange ω_L and ω_T, u_1 and β_1, c and d.

When $\omega_L/\omega_T = 0$, as in Fig. 4, the expression for twist in (5) contains a harmonic component of frequency ω_T. Thus, on the base $\omega_L t$ the harmonic component has infinite frequency, the limits of movement being shown by the dotted lines for $t < t_i$. The final amplitude of the free torsional vibration, about the mean position $\beta_1 = d$, depends upon the exact time of release of the couples, the possible maximum and minimum amplitudes being shown by the dotted lines for $t > t_i$. We note that for $t < t_i$, and when $M/M_E = 10$, the beam has a twist $\beta_1/d = 21$ within a time of order $1/\omega_T$. To keep $\beta_1/d < 21$, therefore, we must apply the couples for a time *less than the smaller of the component periods*.

The results from Figs. 2, 3, and 4 are summarized in the table, which gives values of $\omega_L t_i/2\pi$, the ratio of the impact time to the longer component period.

TABLE

ω_L/ω_T		1	0·2	0
$\omega_L t_i/2\pi$ at	$M/M_E = 2$	0·35	0·20	0·16
	$M/M_E = 10$	0·11	0·04	0

From the comparative constancy of $\omega_L t_i/2\pi$, for varying ω_L/ω_T, we conclude that the period of application of the couples is decided by the *longer* of the component periods, unless the load is very high, and the component periods are widely different.

REFERENCES

1. L. PRANDTL, Diss., Nürnberg (1899).
2. A. G. M. MICHELL, *Phil. Mag.* (5) **48** (1899), 298–309.
3. J. F. DAVIDSON, *J. Mech. Phys. Solids*, **2** (1953), 54–66.
4. S. P. TIMOSHENKO, *Theory of Elastic Stability*, 1st ed. (McGraw-Hill, 1936).
5. M. A. LAVRENTIEV and A. V. ISHLINSKY, *Doklady Acad. Sci. U.S.S.R.* **64** (1949), 779–82.

ON THE STABILITY OF A CIRCULAR TUBE UNDER END THRUST

By E. W. WILKES (*University of Durham, King's College*)

[Received 26 February 1954]

SUMMARY

A circular tube of finite thickness h composed of homogeneous isotropic incompressible material is finitely deformed by end thrust in the direction of its axis so that it changes its length in the ratio $\lambda:1$, and its stability is investigated by considering the equilibrium of a further infinitesimal deformation. A general periodic solution for the displacements in this further deformation is given, but only the special case of radially symmetrical buckling is then considered. The application of the boundary conditions leads to a relation between λ and the frequency of longitudinal rippling $\nu/2\pi$ from which the critical λ, determining the onset of instability, is found. Three examples are chosen: (*a*) thin tube, in which the critical value of λ is derived analytically, (*b*) tube with radius twice the thickness h, (*c*) solid cylinder. The last two examples are treated graphically, a neo-Hookean model being assumed. The longitudinal force required to produce instability is given in each case.

1. Introduction

PROBLEMS of elastic stability have been the centre of considerable interest in recent years, and in particular the stability of such bodies as thin rods, plates, and shells has received much attention. The successful application of theories of stability to special problems usually depends, however, on some dimension of the body being small.

Rivlin and other writers† have solved a variety of problems in finite elasticity, mostly for incompressible materials, by assuming certain forms for the displacements and evaluating the forces required to maintain the assumed deformation. In these theories it has always been recognized, however, that other deformations may be possible under the same set of forces. Green, Rivlin, and Shield (**1**) have developed a theory of small deformations superposed on finite deformations for bodies of both compressible and incompressible materials, and the equations of their paper may be regarded as equations of neutral equilibrium for discussing the stability of the given finite deformation. In deriving these equations, moreover, no restrictions on the size of any of the dimensions of the body have been imposed.

In this paper the stability of a circular tube, of uniform cross-section,

† A list of references may be found in a paper by J. E. Adkins, A. E. Green, and R. T. Shield, *Proc. Roy. Soc.* A, **246** (1953), 181.

composed of homogeneous isotropic incompressible material is examined when the tube is subjected to an end thrust applied parallel to its axis. The tube is not here assumed to be thin, but is taken long enough for end effects to be ignored. Although this problem has already been extensively studied when the thickness of the tube is small, it is known that the classical solution given by Southwell (**2**) and Dean (**3**) for symmetrical buckling produces a value for the critical end thrust which is too high compared with results from experiment, and various proposals have been put forward to overcome this difficulty theoretically. Despite this drawback which has arisen in connexion with the thin cylindrical shell, it appears to be of interest to see if symmetrical (and other types) of buckling are possible when the tube is no longer thin, and in particular when the cylinder is solid.

2. General theory

The results and the notation of the paper of Green, Rivlin, and Shield (loc. cit. **1**) will be used here. A very brief summary of the results required in the present problem is now given, but for details of the notation and for the derivation of these formulae the reader is referred to the original paper. The body in its unstrained, finitely deformed, and second strained states is denoted by B_0, B, B' respectively. The displacement vector of a point is denoted by $\mathbf{v}$ in B, and by $\mathbf{v}+\epsilon\mathbf{w}$ in B', where ϵ is a small arbitrary constant. The base vectors of a curvilinear coordinate system (θ_i) which moves with the body are, in B, $\mathbf{E}_i$ and $\mathbf{E}^i$.

The metric tensors are G_{ik}, G^{ik} in B and $G_{ik}+\epsilon G'_{ik}$, $G^{ik}+\epsilon G'^{ik}$ in B' respectively, where

$$G'_{ik} = w_i\|_k + w_k\|_i, \qquad G'^{ik} = -G^{ir}G^{ks}G'_{rs}; \tag{2.1}$$

whilst the determinant G in B becomes $G+\epsilon G'$ in B' with

$$G' = GG^{ik}G'_{ik}. \tag{2.2}$$

The strain invariants in B' are

$$\left.\begin{aligned} I_1+\epsilon I'_1 &= g^{rs}G_{rs}+\epsilon g^{rs}G'_{rs} \\ I_2+\epsilon I'_2 &= g_{rs}\,G^{rs}I_3+\epsilon g_{rs}(G'^{rs}I_3+G^{rs}I'_3) \\ I_3+\epsilon I'_3 &= \frac{G}{g}+\epsilon G^{rs}G'_{rs}\,I_3 \end{aligned}\right\}. \tag{2.3}$$

In this problem the material is incompressible and isotropic, so that W is a function of $I_1+\epsilon I'_1$ and $I_2+\epsilon I'_2$ only. The stress tensor in B' then becomes

$$\tau^{ik}+\epsilon\tau'^{ik} = \Phi g^{ik}+\Psi B^{ik}+pG^{ik}+\epsilon(\Phi' g^{ik}+\Psi' B^{ik}+\Psi B'^{ik}+p'G^{ik}+pG'^{ik}), \tag{2.4}$$

where
$$\left.\begin{aligned} B^{ik}+\epsilon B'^{ik} &= I_1 g^{ik}-g^{ir}g^{ks}G_{rs}+\epsilon(g^{ik}g^{rs}-g^{ir}g^{ks})G'_{rs} \\ \Phi+\epsilon\Phi' &= 2\frac{\partial W}{\partial I_1}+\epsilon(AI'_1+FI'_2) \\ \Psi+\epsilon\Psi' &= 2\frac{\partial W}{\partial I_2}+\epsilon(FI'_1+BI'_2) \end{aligned}\right\},\tag{2.5}$$
with
$$A = 2\frac{\partial^2 W}{\partial I_1^2},\qquad B = 2\frac{\partial^2 W}{\partial I_2^2},\qquad F = 2\frac{\partial^2 W}{\partial I_1\,\partial I_2}$$

and $p+\epsilon p'$ an unknown hydrostatic pressure. The quantities A, B, F are functions of I_1, I_2 and are evaluated in the strained body B.

The equations of equilibrium in B are $\tau^{ik}\|_i = 0$, and in B' are
$$\tau'^{ik}\|_i+\Gamma'^k_{ir}\tau^{ir}+\Gamma'^r_{ir}\tau^{ik} = 0,\tag{2.6}$$
where
$$\Gamma'^r_{ik} = \tfrac{1}{2}G^{rs}(G'_{si,k}+G'_{sk,i}-G'_{ik,s})+\tfrac{1}{2}G'^{rs}(G_{si,k}+G_{sk,i}-G_{ik,s})\tag{2.7}$$
and covariant differentiation is with respect to coordinates in the body B throughout.

Finally, at the boundary, the components of surface traction must satisfy the relations
$$\gamma\frac{\partial F}{\partial\theta_i}(\tau^{ik}+\epsilon\tau'^{ik}) = P^k+\epsilon P'^k\quad(k = 1, 2, 3),\tag{2.8}$$
where $F(\theta_1,\theta_2,\theta_3) = 0$ is the equation of the surface of the body, and γ is a constant such that $\gamma(\partial F/\partial\theta_i)$ are the components of a unit vector.

3. Application to a tube

The coordinate system θ_i is now chosen to be the cylindrical polar system (r,θ,z) with the axis of z as axis of the tube. The cross-section of the uncompressed tube is the area lying between two concentric circles of radii a_0 and b_0 ($a_0 > b_0$). Then, referred to Cartesian coordinates (x_1, x_2, x_3) with x_3-axis along the axis of the cylinder, the coordinates of a point P_0 in B_0 are taken to be
$$x_1 = r\lambda^{\frac{1}{2}}\cos\theta,\qquad x_2 = r\lambda^{\frac{1}{2}}\sin\theta,\qquad x_3 = z/\lambda\quad(\lambda < 1).$$
The tube is now deformed by an end thrust in such a manner that planes of points initially perpendicular to the axis remain planes perpendicular to the axis and the distance between any pair of planes is diminished in the ratio $\lambda:1$. As a consequence the point P in B, corresponding to P_0 in B_0, has coordinates, referred to the same Cartesian axes,
$$y_1 = r\cos\theta,\qquad y_2 = r\sin\theta,\qquad y_3 = z.$$

The metric tensors for these states are

$$\left.\begin{aligned} G_{ik} &= \begin{pmatrix} 1 & 0 & 0 \\ 0 & r^2 & 0 \\ 0 & 0 & 1 \end{pmatrix}, \qquad G^{ik} = \begin{pmatrix} 1 & 0 & 0 \\ 0 & r^{-2} & 0 \\ 0 & 0 & 1 \end{pmatrix}, \qquad G = r^2 \\ g_{ik} &= \begin{pmatrix} \lambda & 0 & 0 \\ 0 & \lambda r^2 & 0 \\ 0 & 0 & \lambda^{-2} \end{pmatrix}, \qquad g^{ik} = \begin{pmatrix} \lambda^{-1} & 0 & 0 \\ 0 & (\lambda r^2)^{-1} & 0 \\ 0 & 0 & \lambda^2 \end{pmatrix}, \qquad g = r^2 \end{aligned}\right\}; \tag{3.1}$$

from which it is seen that the condition for incompressibility, $I_3 = G/g = 1$, is implied in the choice of coordinates. The invariants and tensor components required for this deformation are given below.

$$\left.\begin{aligned} & I_1 = \frac{2}{\lambda}+\lambda^2, \qquad I_2 = 2\lambda+\frac{1}{\lambda^2} \\ B^{ik} &= \begin{pmatrix} \lambda+\lambda^{-2} & 0 & 0 \\ 0 & r^{-2}(\lambda+\lambda^{-2}) & 0 \\ 0 & 0 & 2\lambda \end{pmatrix} \\ \tau^{ik} &= \begin{pmatrix} \lambda^{-1}\Phi+(\lambda+\lambda^{-2})\Psi+p & 0 & 0 \\ 0 & r^{-2}\tau^{11} & 0 \\ 0 & 0 & \lambda^2\Phi+2\lambda\Psi+p \end{pmatrix} \end{aligned}\right\}. \tag{3.2}$$

The Christoffel symbols for the metric in B take the values

$$\Gamma^1_{22} = -r, \qquad \Gamma^2_{12} = 1/r,$$

all other Γ's being zero.

The additional infinitesimal deformation is now superposed on the previous compression and for this the following quantities are evaluated after writing (u, v, w) for (w_1, w_2, w_3):

$$-I_3' = 2\frac{\partial u}{\partial r}+\frac{2}{r^2}\left(\frac{\partial v}{\partial \theta}+ru\right)+2\frac{\partial w}{\partial z} = 0,$$

giving

$$\frac{1}{r}\frac{\partial}{\partial r}(ru)+\frac{1}{r^2}\frac{\partial v}{\partial \theta}+\frac{\partial w}{\partial z} = 0; \tag{3.3}$$

$$\left.\begin{aligned} I_1' &= \frac{2}{\lambda}\frac{\partial u}{\partial r}+\frac{2}{\lambda r^2}\left(\frac{\partial v}{\partial \theta}+ru\right)+2\lambda^2\frac{\partial w}{\partial z} = -\frac{2}{\lambda}(1-\lambda^3)\frac{\partial w}{\partial z} \\ I_2' &= -2\lambda\frac{\partial u}{\partial r}-\frac{2\lambda}{r^2}\left(\frac{\partial v}{\partial \theta}+ru\right)-\frac{2}{\lambda^2}\frac{\partial w}{\partial z} = -\frac{2}{\lambda^2}(1-\lambda^3)\frac{\partial w}{\partial z} \end{aligned}\right\}; \tag{3.4}$$

where the final expressions for I_1' and I_2' are derived with the aid of (3.3).

Further,

$$
\left.\begin{array}{l}
G'_{11} = -G'^{11} = 2\dfrac{\partial u}{\partial r}, \qquad G'_{22} = -r^4 G'^{22} = 2\left(\dfrac{\partial v}{\partial \theta}+ru\right) \\[2ex]
G'_{33} = -G'^{33} = -\dfrac{B'^{33}}{\lambda} = \dfrac{2\Phi'}{\alpha} = \dfrac{2\Psi'}{\beta} = 2\dfrac{\partial w}{\partial z} \\[2ex]
G'_{23} = -r^2 G'^{23} = -\dfrac{r^2 B'^{23}}{\lambda} = \dfrac{\partial v}{\partial z}+\dfrac{\partial w}{\partial \theta} \\[2ex]
G'_{13} = -G'^{13} = -\dfrac{B'^{13}}{\lambda} = \dfrac{\partial u}{\partial z}+\dfrac{\partial w}{\partial r} \\[2ex]
G'_{12} = -r^2 G'^{12} = -\lambda^2 r^2 B'^{12} = \dfrac{\partial u}{\partial \theta}+\dfrac{\partial v}{\partial r}-2\dfrac{v}{r} \\[2ex]
B'^{11} = -\dfrac{2}{\lambda^2}\dfrac{\partial u}{\partial r}-\dfrac{2}{\lambda^2}(1-\lambda^3)\dfrac{\partial w}{\partial z}, \qquad B'^{22} = \dfrac{2}{r^2}\left(\dfrac{1}{\lambda^2}\dfrac{\partial u}{\partial r}+\lambda\dfrac{\partial w}{\partial z}\right) \\[2ex]
\text{where} \\[1ex]
\alpha = -\dfrac{2}{\lambda^2}(1-\lambda^3)(\lambda A+F), \qquad \beta = -\dfrac{2}{\lambda^2}(1-\lambda^3)(\lambda F+B)
\end{array}\right\}; \tag{3.5}
$$

also

$$
\left.\begin{array}{r@{}l}
\tau'^{11} &{}= \alpha_1\dfrac{\partial w}{\partial z}-2\left(\dfrac{\Psi}{\lambda^2}+p\right)\dfrac{\partial u}{\partial r}+p' \\[2ex]
r^2\tau'^{22} &{}= \alpha_2\dfrac{\partial w}{\partial z}+2\left(\dfrac{\Psi}{\lambda^2}+p\right)\dfrac{\partial u}{\partial r}+p' \\[2ex]
\tau'^{33} &{}= \alpha_3\dfrac{\partial w}{\partial z}+p' \\[2ex]
r^2\tau'^{23} &{}= -(\lambda\Psi+p)\left(\dfrac{\partial v}{\partial z}+\dfrac{\partial w}{\partial \theta}\right) \\[2ex]
\tau'^{13} &{}= -(\lambda\Psi+p)\left(\dfrac{\partial u}{\partial z}+\dfrac{\partial w}{\partial r}\right) \\[2ex]
r^2\tau'^{12} &{}= -\left(\dfrac{\Psi}{\lambda^2}+p\right)\left(\dfrac{\partial u}{\partial \theta}+\dfrac{\partial v}{\partial r}-2\dfrac{v}{r}\right)
\end{array}\right\}; \tag{3.6}
$$

in which

$$
\left.\begin{array}{l}
\alpha_1 = \dfrac{\alpha}{\lambda}+\beta\left(\dfrac{1}{\lambda^2}+\lambda\right)-2\dfrac{\Psi}{\lambda^2}(1-\lambda^3) \\[2ex]
\alpha_2 = \dfrac{\alpha}{\lambda}+\beta\left(\dfrac{1}{\lambda^2}+\lambda\right)+2\lambda\Psi+2p \\[2ex]
\alpha_3 = \lambda^2\alpha+2\lambda\beta-2\lambda\Psi-2p
\end{array}\right\}. \tag{3.7}
$$

Also

$$\left.\begin{aligned}
&\Gamma'^{1}_{11} = \frac{\partial^2 u}{\partial r^2}, \qquad \Gamma'^{1}_{22} = \frac{\partial^2 u}{\partial \theta^2} - \frac{2}{r}\frac{\partial v}{\partial \theta} + r\frac{\partial u}{\partial r} - u, \qquad \Gamma'^{1}_{33} = \frac{\partial^2 u}{\partial z^2}\\
&\Gamma'^{2}_{11} = \frac{1}{r^2}\left[\frac{\partial^2 v}{\partial r^2} - 2\frac{\partial}{\partial r}\left(\frac{v}{r}\right)\right], \qquad \Gamma'^{2}_{22} = \frac{1}{r^2}\frac{\partial^2 v}{d\theta^2} + \frac{2}{r}\frac{\partial u}{\partial \theta} + \frac{1}{r}\frac{\partial v}{\partial r} - 2\frac{v}{r^2}\\
&\Gamma'^{2}_{33} = \frac{1}{r^2}\frac{\partial^2 v}{\partial z^2}, \qquad \Gamma'^{3}_{11} = \frac{\partial^2 w}{\partial r^2}, \qquad \Gamma'^{3}_{22} = \frac{\partial^2 w}{\partial \theta^2} + r\frac{\partial w}{\partial r}\\
&\Gamma'^{3}_{33} = \frac{\partial^2 w}{\partial z^2}, \qquad \Gamma'^{r}_{ir} = \frac{1}{2}\frac{\partial}{\partial \theta_i}\left(\frac{I'_3}{I_3}\right) = 0
\end{aligned}\right\}. \tag{3.8}$$

After substituting the above in the equations of equilibrium (2.6), and after rearranging and making use of the equation of incompressibility, $I'_3 = 0$ (3.3), these equations of equilibrium become

$$\left.\begin{aligned}
&\frac{\partial p'}{\partial r} + L\left(\frac{\partial^2 u}{\partial r^2} + \frac{1}{r}\frac{\partial u}{\partial r} - \frac{u}{r^2}\right) + \frac{N}{r^2}\frac{\partial^2 u}{\partial \theta^2} + M\frac{\partial^2 u}{\partial z^2} + \frac{(L-N)}{r^2}\frac{\partial^2 v}{\partial r \partial \theta} - 2\frac{L}{r^3}\frac{\partial v}{\partial \theta} = 0\\
&\frac{\partial p'}{\partial \theta} + N\frac{\partial^2 v}{\partial r^2} + \frac{L}{r^2}\frac{\partial^2 v}{\partial \theta^2} + M\frac{\partial^2 v}{\partial z^2} + (L-N)\frac{\partial^2 u}{\partial r \partial \theta} + \frac{(L+N)}{r}\frac{\partial u}{\partial \theta} - \frac{N}{r}\frac{\partial v}{\partial r} = 0\\
&\frac{\partial p'}{\partial z} + H\left(\frac{\partial^2 w}{\partial r^2} + \frac{1}{r^2}\frac{\partial^2 w}{\partial \theta^2} + \frac{1}{r}\frac{\partial w}{\partial r}\right) + K\frac{\partial^2 w}{\partial z^2} = 0
\end{aligned}\right\}, \tag{3.9}$$

where

$$\left.\begin{aligned}
&H = \tau^{11} - \lambda\Psi - p, \qquad K = \tau^{33} + \lambda^2\alpha + 2\lambda\beta - \lambda\Psi - p\\
&L = \tau^{11} - \frac{\alpha}{\lambda} - \frac{\beta}{\lambda^2}(1+\lambda^3) - \lambda\Psi - p, \qquad M = \tau^{33} - \lambda\Psi - p\\
&N = \tau^{11} - \frac{\Psi}{\lambda^2} - p
\end{aligned}\right\}, \tag{3.10}$$

and α and β are given in (3.5).

4. Solution

It may be verified that equations (3.9) are satisfied by

$$\left.\begin{aligned}
u &= f_1(r)\cos\nu z\cos\kappa\theta\\
v &= f_2(r)\cos\nu z\sin\kappa\theta\\
w &= f_3(r)\sin\nu z\cos\kappa\theta\\
p' &= \xi(r)\cos\nu z\cos\kappa\theta
\end{aligned}\right\}, \tag{4.1}$$

where

$$\left.\begin{aligned}
f_1(r) &= A_1\left[I_{\kappa+1}(k_1\nu r)+\frac{\kappa}{k_1\nu r}I_\kappa(k_1\nu r)\right]+\\
&\qquad +A_1'\left[K_{\kappa+1}(k_1\nu r)-\frac{\kappa}{k_1\nu r}K_\kappa(k_1\nu r)\right]+\\
&\quad +A_2\left[I_{\kappa+1}(k_2\nu r)+\frac{\kappa}{k_2\nu r}I_\kappa(k_2\nu r)\right]+\\
&\quad +A_2'\left[K_{\kappa+1}(k_2\nu r)-\frac{\kappa}{k_2\nu r}K_\kappa(k_2\nu r)\right]+\frac{\kappa B}{r}I_\kappa(k\nu r)+\frac{\kappa B'}{r}K_\kappa(k\nu r)\\
f_2(r) &= -\frac{\kappa A_1}{k_1\nu}I_\kappa(k_1\nu r)+\frac{\kappa A_1'}{k_1\nu}K_\kappa(k_1\nu r)-\\
&\quad -\frac{\kappa A_2}{k_2\nu}I_\kappa(k_2\nu r)+\frac{\kappa A_2'}{k_2\nu}K_\kappa(k_2\nu r)-B[k\nu rI_{\kappa+1}(k\nu r)+\kappa I_\kappa(k\nu r)]+\\
&\qquad +B'[k\nu rK_{\kappa+1}(k\nu r)-\kappa K_\kappa(k\nu r)]\\
f_3(r) &= -k_1A_1I_\kappa(k_1\nu r)+k_1A_1'K_\kappa(k_1\nu r)-\\
&\qquad -k_2A_2I_\kappa(k_2\nu r)+k_2A_2'K_\kappa(k_2\nu r)\\
\xi(r) &= k_1\nu A_1(K-Hk_1^2)I_\kappa(k_1\nu r)-k_1\nu A_1'(K-Hk_1^2)K_\kappa(k_1\nu r)+\\
&\quad +k_2\nu A_2(K-Hk_2^2)I_\kappa(k_2\nu r)-k_2\nu A_2'(K-Hk_2^2)K_\kappa(k_2\nu r)
\end{aligned}\right\}. \tag{4.2}$$

Here $I_\kappa(k\nu r)$, etc., and $K_\kappa(k\nu r)$, etc., are the modified Bessel functions of the first and second kinds respectively, where for future convenience the functions of the second kind will be defined as in Watson (**4**) and the British Association Tables (**5**). Here A_1, A_1', A_2, A_2', B, B' are arbitrary constants; κ is restricted to integral values; ν is a frequency dependent on the compression ratio λ; $k^2 = M/N$ and k_1^2, k_2^2 are the roots of the equation

$$H\zeta^2-(K+L)\zeta+M = 0. \tag{4.3}$$

When κ takes the value unity, the above solution represents a distortion of the tube with a lateral displacement of planes perpendicular to the axis and corresponds to the Euler strut.

For $\kappa = 0$ the solution (4.1) represents a symmetrical buckling for which

$$\left.\begin{aligned}
u &= f_1(r)\cos\nu z\\
v &= 0\\
w &= f_3(r)\sin\nu z\\
p' &= \xi(r)\cos\nu z
\end{aligned}\right\}, \tag{4.4}$$

with

$$\left.\begin{aligned} f_1(r) &= A_1 I_1(k_1 \nu r)+A_1' K_1(k_1 \nu r)+A_2 I_1(k_2 \nu r)+A_2' K_1(k_2 \nu r) \\ f_3(r) &= -k_1 A_1 I_0(k_1 \nu r)+k_1 A_1' K_0(k_1 \nu r)-k_2 A_2 I_0(k_2 \nu r)+ \\ &\qquad\qquad +k_2 A_2' K_0(k_2 \nu r) \\ \xi(r) &= k_1 \nu A_1(K-Hk_1^2)I_0(k_1 \nu r)-k_1 \nu A_1'(K-Hk_1^2)K_0(k_1 \nu r)+ \\ &\quad +k_2 \nu A_2(K-Hk_2^2)I_0(k_2 \nu r)-k_2 \nu A_2'(K-Hk_2^2)K_0(k_2 \nu r) \end{aligned}\right\}. \tag{4.5}$$

The equations of the curved surfaces of the tube are initially

$$F(r,\theta,z) \equiv r-a_0 = 0 \quad \text{and} \quad F(r,\theta,z) \equiv r-b_0 = 0,$$

so that $(\partial F/\partial\theta_i) = (1,0,0)$ at both inner and outer surfaces. The radii of the tube in its state B are now denoted by a and b respectively, where $a = a_0\lambda^{-\frac{1}{2}}$ and $b = b_0\lambda^{-\frac{1}{2}}$. There are no components of surface traction over the curved surfaces of either B or B', and on using (2.8) this gives rise to the conditions

$$\tau^{11} = \tau'^{11} = \tau'^{12} = \tau'^{13} = 0 \quad (r = a, b). \tag{4.6}$$

Now when $\tau^{11} = 0$, p may be determined from (3.2), and in consequence the following quantities from (3.10) may be put in simplified form:

$$\left.\begin{gathered} p = -\frac{\Phi}{\lambda}-\left(\frac{1}{\lambda^2}+\lambda\right)\Psi, \qquad \tau^{33} = -\frac{(1-\lambda^3)}{\lambda^2}\Theta \\ H = \frac{\Theta}{\lambda^2}, \qquad K = \lambda\Theta+\lambda^2\alpha+2\lambda\beta, \qquad L = \frac{\Theta}{\lambda^2}-\frac{\alpha}{\lambda}-\left(\frac{1}{\lambda^2}+\lambda\right)\beta \\ M = \lambda\Theta, \qquad N = \frac{\Phi}{\lambda}+\lambda\Psi \end{gathered}\right\}, \tag{4.7}$$

where Θ has been written for $\lambda\Phi+\Psi$. On substituting the values of $f_1(r)$, $f_2(r)$, $f_3(r)$, $\xi(r)$ in the expressions for τ'^{11}, τ'^{12}, τ'^{13} from (3.6), and on using the conditions (4.6), the following determinantal equation results after simplification and elimination of the constants A_1, A_1', A_2, A_2', B, B':

$$\begin{vmatrix} P_1(k_1,k_2,a) & Q_1(k_1,k_2,a) & P_1(k_2,k_1,a) & Q_1(k_2,k_1,a) & R_1(a) & S_1(a) \\ P_1(k_1,k_2,b) & Q_1(k_1,k_2,b) & P_1(k_2,k_1,b) & Q_1(k_2,k_1,b) & R_1(b) & S_1(b) \\ P_2(k_1,a) & Q_2(k_1,a) & P_2(k_2,a) & Q_2(k_2,a) & R_2(a) & S_2(a) \\ P_2(k_1,b) & Q_2(k_1,b) & P_2(k_2,b) & Q_2(k_2,b) & R_2(b) & S_2(b) \\ P_3(k_1,a) & Q_3(k_1,a) & P_3(k_2,a) & Q_3(k_2,a) & R_3(a) & S_3(a) \\ P_3(k_1,b) & Q_3(k_1,b) & P_3(k_2,b) & Q_3(k_2,b) & R_3(b) & S_3(b) \end{vmatrix} = 0. \tag{4.8}$$

The elements of this determinant have the following values:

$$\left.\begin{aligned}
P_1(k_s, k_t, r) &= \left[\frac{(1+k_t^2)k_s\nu\Theta}{\lambda^2}+\frac{2\kappa(\kappa-1)N}{k_s\nu r^2}\right]I_\kappa(k_s\nu r)-\frac{2N}{r}I_{\kappa+1}(k_s\nu r)\\
R_1(r) &= \frac{\kappa(\kappa-1)}{r^2}I_\kappa(k\nu r)+\frac{\kappa k\nu}{r}I_{\kappa+1}(k\nu r)\\
P_2(k_s, r) &= \frac{\kappa(\kappa-1)}{k_s\nu r}I_\kappa(k_s\nu r)+\kappa I_{\kappa+1}(k_s\nu r)\\
R_2(r) &= \left[\frac{\kappa(\kappa-1)}{r}+\frac{k^2\nu^2 r}{2}\right]I_\kappa(k\nu r)-k\nu I_{\kappa+1}(k\nu r)\\
P_3(k_s, r) &= \frac{\kappa(1+k_s^2)}{k_s\nu r}I_\kappa(k_s\nu r)+(1+k_s^2)I_{\kappa+1}(k_s\nu r)\\
R_3(r) &= \frac{\kappa}{r}I_\kappa(k\nu r)
\end{aligned}\right\}; \tag{4.9}$$

and Q_1, Q_2, Q_3, S_1, S_2, S_3 are obtained by changing $I_\kappa(\ )$ to $K_\kappa(\ )$ and $I_{\kappa+1}(\ )$ to $-K_{\kappa+1}(\ )$ in the corresponding functions P_1, P_2, P_3, R_1, R_2, R_3. Here s, t take the values 1, 2 and 2, 1, and r the values a, b.

5. Symmetrical buckling

In the special case in which $\kappa = 0$ the buckling of the tube is symmetrical and equation (4.8) reduces to

$$\begin{vmatrix}
P_1'(k_1, k_2, a) & Q_1'(k_1, k_2, a) & P_1'(k_2, k_1, a) & Q_1'(k_2, k_1, a)\\
P_1'(k_1, k_2, b) & Q_1'(k_1, k_2, b) & P_1'(k_2, k_1, b) & Q_1'(k_2, k_1, b)\\
P_3'(k_1, a) & Q_3'(k_1, a) & P_3'(k_2, a) & Q_3'(k_2, a)\\
P_3'(k_1, b) & Q_3'(k_1, b) & P_3'(k_2, b) & Q_3'(k_2, b)
\end{vmatrix} = 0, \tag{5.1}$$

where

$$\left.\begin{aligned}
P_1'(k_s, k_t, r) &= \frac{(1+k_t^2)k_s\nu\Theta}{\lambda^2}I_0(k_s\nu r)-\frac{2N}{r}I_1(k_s\nu r)\\
P_3'(k_s, r) &= (1+k_s^2)I_1(k_s\nu r)
\end{aligned}\right\}; \tag{5.2}$$

and $Q_1'(k_s, k_t, r)$, $Q_3'(k_s, r)$ are obtained by changing $I_0(k_s\nu r)$ to $K_0(k_s\nu r)$ and $I_1(k_s\nu r)$ to $-K_1(k_s\nu r)$ in P_1' and P_3' respectively.

The elements of this determinant are functions of λ and ν, and thus equation (5.1) serves to determine ν when λ is given, or λ when ν is specified. The critical value of λ is given by the least compression which permits buckling of the type (4.4). Thus if ν is regarded as a variable parameter the critical value of λ occurs at its maximum with respect to ν. The equation (5.1) is too complex in general to allow an analytic expression for this maximum to be found, although when the tube is thin the determinant may be expanded as a power series in h, the thickness in the compressed

state ($h = a-b$), and from this an approximate critical value (to the first order in h) derived. This is carried out in the following section.

(i) Thin tube

In order to find the maximum value of λ with respect to ν to the first power in h it is necessary to expand the determinant as far as terms in the second power after extraneous factors have been removed. The Bessel functions $I_0(k_s \nu a)$, $K_0(k_s \nu a)$, etc., can always be removed in factors of the form $I_0(k_s \nu a)K_1(k_s \nu a)+I_1(k_s \nu a)K_0(k_s \nu a)$ irrespective of the power of h at which the series is terminated. After the expansion has been performed and some simplification made, equation (5.1) reduces to

$$\begin{aligned}
&\frac{4N^2\lambda^2}{\Theta}-4N(l+2)+\frac{a^2\nu^2\Theta}{\lambda^2}(l+2)(1-m)+\\
&\quad+\frac{h}{2a}\left[\frac{16N^2\lambda^2}{\Theta}-16N(l+2)+\frac{2a^2\nu^2\Theta}{\lambda^2}(l+2)(1-m)\right]+\\
&\quad+\frac{h^2}{a^2}\left[\frac{2N^2\lambda^2}{\Theta}\left(\frac{13}{2}+\frac{a^2\nu^2 l}{3}\right)-13N(l+2)+\frac{2a^2\nu^2 N}{3}\{1-m-l(l+2)\}+\right.\\
&\qquad\qquad+\frac{13a^2\nu^2\Theta}{12\lambda^2}(l+2)(1-m)-\\
&\qquad\left.-\frac{a^4\nu^4\Theta}{12\lambda^2}\{(1-m)^2-2(1-m)(l+1)(l+2)+(l+2)^2\}\right]=0, \qquad (5.3)
\end{aligned}$$

where

$$l = k_1^2+k_2^2 = 1+\lambda^3-\frac{(\lambda\alpha+\beta)(1-\lambda^3)}{\Theta}, \qquad m = k_1^2 k_2^2 = \lambda^3.$$

On putting $d\lambda/d(a\nu) = 0$ in (5.3), and remembering that $a\lambda^{\frac{1}{2}} = a_0$, $h\lambda^{\frac{1}{2}} = h_0$, the maximum value of λ turns out to be

$$\lambda = 1-\frac{2h_0}{3a_0}, \qquad a_0^2\nu^2 = \frac{3a_0}{h_0}. \qquad (5.4)$$

Then, from (4.7), $$|\tau^{33}| = \frac{(1-\lambda^3)}{\lambda^2}\Theta = \frac{2h_0\Theta_1}{a_0},$$

where $\Theta_1 = \Phi+\Psi$. The total thrust required to bring the cylindrical shell to the state of instability is thus

$$2\pi a h|\tau^{33}| = 4\pi h_0^2\Theta_1, \qquad (5.5)$$

to the first term in h_0.

It will be noticed that this result is in agreement with that of Southwell and Dean (loc. cit. **2**, **3**) when Poisson's ratio is given the value $\frac{1}{2}$ to correspond to the case of the incompressible material assumed here.

(ii) Tubes of finite thickness

In the cases in which the tube is not thin there is difficulty in finding an analytical expression for the maximum value of λ and resort is had to graphical means.

In order to carry out this graphical work it is necessary to make some assumption about the form of the strain energy function, and this is here taken to be neo-Hookean, so that $W = C(I_1-3)$, where C is a constant. With this assumption

$$\left.\begin{aligned} &\Phi = 2C, \qquad \Psi = 0, \\ &\text{and the following simplifications result:} \\ &\Theta = \lambda\Phi = 2\lambda C, \qquad N = \frac{\Phi}{\lambda} = \frac{2C}{\lambda}, \\ &\text{whilst} \qquad k_1 = \lambda^{\frac{3}{2}}, \qquad k_2 = 1 \end{aligned}\right\} \tag{5.6}$$

These quantities are now substituted in (5.1), which then gives, after rearrangement,

$$\begin{vmatrix} av x I_0(avx) & avxK_0(avx) & \dfrac{av(1+x^2)^2}{4} I_0(av) + \dfrac{(1-x^2)}{2} I_1(av) & \dfrac{av(1+x^2)^2}{4} K_0(av) - \dfrac{(1-x^2)}{2} K_1(av) \\ \mu avxI_0(\mu avx) & \mu avxK_0(\mu avx) & \dfrac{\mu av(1+x^2)^2}{4} I_0(\mu av) + \dfrac{(1-x^2)}{2} I_1(\mu av) & \dfrac{\mu av(1+x^2)^2}{4} K_0(\mu av) - \dfrac{(1-x^2)}{2} K_1(\mu av) \\ I_1(avx) & -K_1(avx) & I_1(av) & -K_1(av) \\ I_1(\mu avx) & -K_1(\mu avx) & I_1(\mu av) & -K_1(\mu av) \end{vmatrix} = 0, \tag{5.7}$$

where x has been written for $\lambda^{\frac{3}{2}}$, and μ for b/a $(= b_0/a_0)$.

It is not difficult to show from (5.7) that, as $a\nu \to \infty$, x approaches a value which is the positive root of the equation

$$x^3+x^2+3x-1 = 0,$$

irrespective of the value of μ. This root is $x = 0{\cdot}2956$ or $\lambda = 0{\cdot}444$, and hence all curves of λ against $a\nu$ have this line as asymptote. It may also be shown that when $\nu = 0$ all curves pass through the point $\lambda = -2^{\frac{1}{3}}$, although only those portions of the graphs relevant to the maximum have been plotted.

(*a*) *Case* $a_0 = 2b_0$

In this case the graph of λ against $a\nu$ cuts the axis of $a\nu$ at the value 2·4, rises steeply to a maximum at $a\nu = 4{\cdot}4$, and slowly approaches the asymptote from above. The maximum value of λ is then

$$\lambda = 0{\cdot}645 \quad \text{when } a_0\nu = 3{\cdot}5. \tag{5.8}$$

This leads to an end thrust

$$2\pi|\tau^{33}|\int\limits_{\frac{1}{2}a}^{a} r\,dr = \frac{3\pi a_0^2\,C}{2\lambda^2}(1-\lambda^3) = 8{\cdot}28a_0^2\,C, \tag{5.9}$$

since $a = a_0\lambda^{-\frac{1}{2}}$, and from (4.7) and (5.6), $|\tau^{33}| = \dfrac{2C}{\lambda}(1-\lambda^3)$.

This is not necessarily the actual form of distortion for which instability occurs, as other maxima for λ may arise from equation (4.8) which are of greater value than that calculated here for the symmetrical buckling.

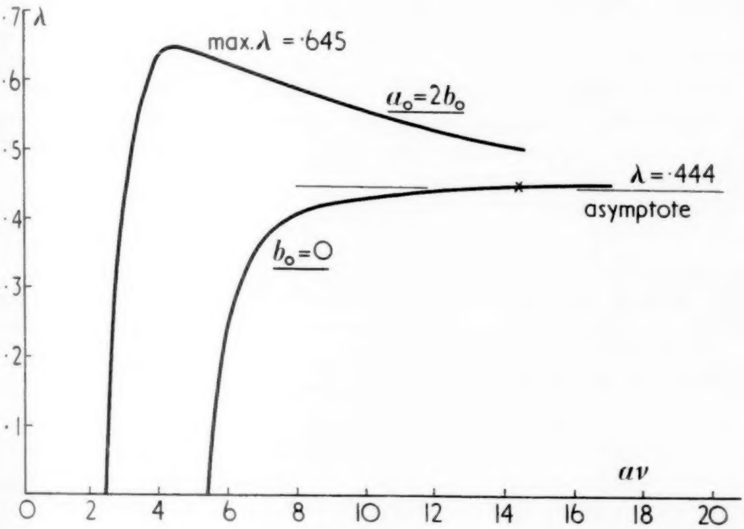

FIG. 1.

(b) Case $b_0 = 0$. The Solid Cylinder

In this case the constants A_1', A_2' of solution (4.5) must be zero and the determinant of (5.7) reduces to one of the second order obtained by omitting the columns in $K_0(avx)$, $K_1(avx)$, etc., and the rows containing μ. When this is developed, it yields

$$av(1+x^2)^2I_0(av)I_1(avx)+2(1-x^2)I_1(av)I_1(avx)-4avxI_1(av)I_0(avx) = 0.$$

It is seen, by plotting some points on the curve of λ against av (Fig. 1) for smaller values of av, that the maximum must occur at a value sufficiently large for asymptotic expansions of the Bessel functions to be used.

From this it may be verified that the curve cuts its asymptote at $a\nu = 14{\cdot}3$ and that it has a maximum at

$$\lambda = 0{\cdot}446 \quad (a\nu = 45 \text{ approx.}). \tag{5.10}$$

The curve is very flat after cutting the asymptote, showing little change in λ for a very wide range of $a\nu$. The value of $a\nu$ corresponding to this critical value of λ has thus only been given approximately, as an accurate location of this quantity does not justify the work involved. The critical λ is, however, correct to the three decimal places given, this being very little greater than the asymptotic value.

The end thrust required to produce this form of instability is

$$2\pi|\tau^{33}|\int\limits_0^a r\,dr = \frac{2\pi a_0^2\,C(1-\lambda^3)}{\lambda^2} = 28{\cdot}80a_0^2\,C. \tag{5.11}$$

Further investigation has not been undertaken, although an examination of other modes of instability would have been desirable for cases in which κ is not zero. The particular value $\kappa = 1$ corresponds to the case of the Euler strut.

REFERENCES

1. A. E. Green, R. S. Rivlin, and R. T. Shield, *Proc. Roy. Soc.* A, **211** (1952), 128.
2. R. V. Southwell, *Phil. Trans.* A, **213** (1914), 187.
3. W. R. Dean, *Proc. Roy. Soc.* A, **107** (1925), 734.
4. G. H. Watson, *A Treatise on the Theory of Bessel Functions*, 2nd edition (Cambridge, 1944).
5. British Association, *Mathematical Tables*, vol. vi (Cambridge, 1950).

CONDUCTION OF HEAT IN A SOLID IN CONTACT WITH A THIN LAYER OF A GOOD CONDUCTOR

By J. C. JAEGER (*Australian National University, Canberra*)

[Received 19 November 1953]

SUMMARY

Boundary conditions and some exact solutions are given for problems on conduction of heat in a solid in contact with a thin layer of a good conductor. Numerical calculations are made for the case of a wire running normally between parallel planes, and the fineness ratio of thermocouple wires necessary to measure transient temperatures accurately in a poor conductor is considered.

1. Introduction

It frequently happens that transient temperatures are measured by a thermocouple inserted into a poor conductor. Physiological measurements are frequently made by a thermocouple mounted in a hypodermic needle, and in the food industry it is common to measure temperatures in cans either in this way or by wires mounted axially in the can. It is important to be able to estimate the errors in such measurements caused by conduction of heat along the wire.

It appears that exact solutions can be obtained for a large class of problems in which a solid with plane or cylindrical boundaries is in contact at some of its boundaries with 'thin' material, the only restriction on this latter being that its temperature is assumed to be constant across its thickness. The results are expressible in terms of functions which arise in one-variable problems in which a solid is in contact at its boundaries with a perfect conductor.

In section 2 the boundary condition is derived and in section 3 the most interesting case, that of a wire running normally between parallel planes, is discussed in detail. Some numerical results for this case are given in section 4. Solutions of some similar problems are given in section 5.

2. Boundary conditions

Suppose that a cylindrical wire of radius a, thermal conductivity K_1, and diffusivity κ_1 is in contact at its surface with a solid of conductivity K and diffusivity κ. The wire is supposed to be a relatively good conductor so that its temperature is uniform over its cross-section. Taking the wire

along the z-axis of cylindrical coordinates, and assuming that there is perfect thermal contact between the wire and the surrounding solid at the boundary $r = a$, the equation of conduction of heat in the wire gives

$$\frac{\partial^2 v}{\partial z^2}+h\frac{\partial v}{\partial r}-\frac{1}{\kappa_1}\frac{\partial v}{\partial t} = 0, \qquad r = a, \tag{1}$$

where
$$h = 2K/aK_1, \tag{2}$$

and v is the temperature in the solid.

This is the boundary condition at $r = a$. If instead of a solid wire there is a thin cylinder of radius a and thickness d, the value of h in (2) is replaced by K/dK_1. Similarly, the general boundary condition for a solid covered by a thin surface skin of a good conductor can be written down. The result may be generalized to the case in which there is a contact resistance between the skin and the solid.

3. A wire running between parallel planes

The problem which will be considered is that of the region $-l < z < l$, $r > a$, with zero initial temperature, the surfaces $z = \pm l$ maintained at unit temperature for $t > 0$, and with the boundary condition (1) at $r = a$.

The differential equation to be solved is

$$\frac{\partial^2 v}{\partial r^2}+\frac{1}{r}\frac{\partial v}{\partial r}+\frac{\partial^2 v}{\partial z^2}-\frac{1}{\kappa}\frac{\partial v}{\partial t} = 0, \quad r > a, \; -l < z < l, \; t > 0 \tag{3}$$

with
$$v = 0, \qquad t = 0, \qquad r > a, \qquad -l < z < l, \tag{4}$$

$$v = 1, \qquad z = \pm l, \qquad r > a, \qquad t > 0. \tag{5}$$

Writing $\bar{v}$ for the Laplace transform of v, so that

$$\bar{v} = \int\limits_0^\infty e^{-pt} v\, dt, \tag{6}$$

it follows by the usual method (**1**) that $\bar{v}$ has to satisfy

$$\frac{\partial^2 \bar{v}}{\partial r^2}+\frac{1}{r}\frac{\partial \bar{v}}{\partial r}+\frac{\partial^2 \bar{v}}{\partial z^2}-\frac{p}{\kappa}\bar{v} = 0, \quad r > a, \; -l < z < l, \tag{7}$$

with
$$\bar{v} = 1/p, \qquad z = \pm l, \qquad r > a \tag{8}$$

and
$$\frac{\partial^2 \bar{v}}{\partial z^2}+h\frac{\partial \bar{v}}{\partial r}-\frac{p}{\kappa_1}\bar{v} = 0, \quad r = a, \; -l < z < l. \tag{9}$$

To solve these, following a method developed for similar problems (**2**), we assume a solution

$$\bar{v} = \frac{\cosh qz}{p\cosh ql} + \sum_{n=0}^{\infty} a_n \cos\frac{(2n+1)\pi z}{2l} K_0(rq_n), \tag{10}$$

where

$$q^2 = p/\kappa, \tag{11}$$

$$q_n^2 = \frac{(2n+1)^2\pi^2}{4l^2} + q^2. \tag{12}$$

This satisfies (7) and (8), and (9) requires

$$\sum_{n=0}^{\infty} a_n \left\{\left(\frac{p}{\kappa_1} + \frac{(2n+1)^2\pi^2}{4l^2}\right)K_0(aq_n) + hq_n K_1(aq_n)\right\} \cos\frac{(2n+1)\pi z}{2l} = \left(\frac{1}{\kappa} - \frac{1}{\kappa_1}\right)\frac{\cosh qz}{\cosh ql}. \tag{13}$$

It follows that

$$a_n = \frac{(-1)^n \pi a^2 (2n+1)(\kappa_1 - \kappa)}{\kappa^2 l^2 q_n^2 \{(a^2 q_n^2 + b_n)K_0(aq_n) + aHq_n K_1(aq_n)\}}, \tag{14}$$

where

$$b_n = \frac{(2n+1)^2\pi^2 a^2(\kappa_1 - \kappa)}{4l^2\kappa}, \qquad H = \frac{\kappa_1 ah}{\kappa} = \frac{2K\kappa_1}{K_1\kappa}. \tag{15}$$

Therefore, finally,

$$\bar{v} = \frac{\cosh qz}{p\cosh ql} + \frac{\pi a^2(\kappa_1 - \kappa)}{\kappa^2 l^2} \sum_{n=0}^{\infty} \frac{(-1)^n (2n+1) K_0(rq_n)\cos(2n+1)\pi z/2l}{q_n^2\{(a^2q_n^2 + b_n)K_0(aq_n) + aHq_n K_1(aq_n)\}}. \tag{16}$$

The derivation of v from $\bar{v}$ follows the usual procedure for the inverse Laplace transformation. The integrals involved have been discussed elsewhere (**3**, **4**). The final result is

$$v = 1 - \frac{2(\kappa_1 - \kappa)a^2}{\kappa l^2} \sum_{n=0}^{\infty} (-1)^n (2n+1) e^{-(2n+1)^2\pi^2\kappa t/4l^2} \cos\frac{(2n+1)\pi z}{2l} \times \int_0^{\infty} e^{-\kappa u^2 t/a^2} \frac{F_n(r,u)\,du}{u\Delta_n(u)}, \tag{17}$$

where

$$F_n(r,u) = J_0(ur/a)[(b_n - u^2)Y_0(u) + uHY_1(u)] - Y_0(ur/a)[(b_n - u^2)J_0(u) + uHJ_1(u)], \tag{18}$$

$$\Delta_n(u) = [(b_n - u^2)J_0(u) + uHJ_1(u)]^2 + [(b_n - u^2)Y_0(u) + uHY_1(u)]^2. \tag{19}$$

The most interesting quantity is the temperature v_0 at the midpoint of the wire, $r = a$, $z = 0$, which is given by

$$v_0 = 1-\frac{4(\kappa_1-\kappa)\kappa_1 a^3 h}{\pi\kappa^2 l^2}\sum_{n=0}^{\infty}(-1)^n(2n+1)e^{-\kappa(2n+1)^2\pi^2 t/4l^2}\int_0^{\infty} e^{-\kappa u^2 t/a^2}\frac{du}{u\Delta_n(u)}. \tag{20}$$

4. Numerical results

The series (20) is rapidly convergent, and the integrals in it are not difficult to evaluate numerically. The parameters involved are $\kappa t/l^2$, which determines the temperature in the solid in the absence of the wire, the

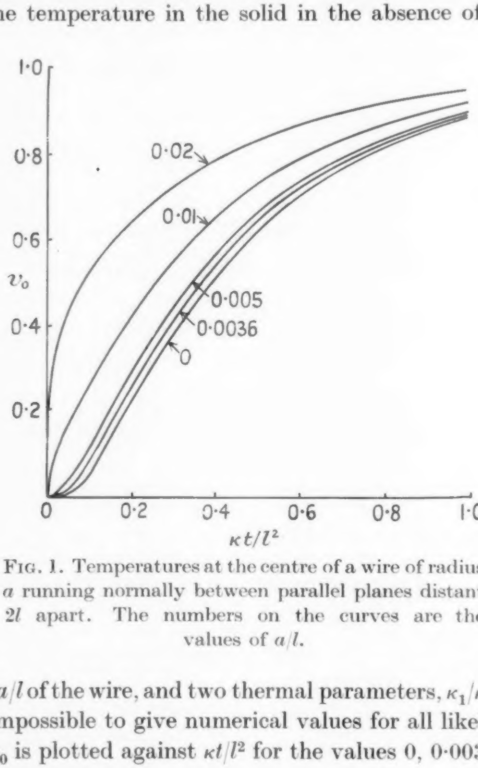

FIG. 1. Temperatures at the centre of a wire of radius a running normally between parallel planes distant $2l$ apart. The numbers on the curves are the values of a/l.

fineness ratio a/l of the wire, and two thermal parameters, κ_1/κ and $K\kappa_1/K_1\kappa$, so that it is impossible to give numerical values for all likely cases.

In Fig. 1, v_0 is plotted against $\kappa t/l^2$ for the values 0, 0·0036, 0·005, 0·01, 0·02 of a/l for the case $K_1 = 0{\cdot}93$, $\kappa_1 = 1{\cdot}14$, $K = \kappa = 0{\cdot}0014$, corresponding to a copper wire in water or biological material. It appears that even for the smallest value, $a/l = 0{\cdot}0036$, there is a substantial difference between the temperature in the wire and that in the solid in the absence of the wire: further, this difference is roughly constant, so that for the smaller values of the time the percentage error will be very large. The

discrepancy will be increased if there is a contact resistance between the wire and the solid, or if the solid is a worse conductor than water. The value $a/l = 0{\cdot}0036$ corresponds roughly to a 28-gauge wire between planes 10 cm. apart or to a 40-gauge wire between planes 3 cm. apart, so it appears that substantially thinner wires than these are needed to give an accurate measurement of temperature.

5. Extensions

A wide variety of problems involving boundary conditions similar to (2) can be solved explicitly. The cases of greatest practical interest are, firstly, that in which the wire of section 3 is heated by electric current, the surfaces $z = \pm l$ being kept at zero temperature, and, secondly, the case of a wire running along the axis of a finite circular cylinder. The solutions of these are given below.

For the region $-l < z < l$, $r > a$, with zero initial temperature, the surfaces $z = \pm l$ maintained at zero temperature for $t > 0$, and the boundary condition at $r = a$

$$\frac{\partial^2 v}{\partial z^2}+h\frac{\partial v}{\partial r}-\frac{1}{\kappa_1}\frac{\partial v}{\partial t} = -\frac{A}{K_1}, \tag{21}$$

where A is the rate of supply of heat to the wire per unit volume, the temperature at the midpoint of the wire, $z = 0$, $r = a$, is given by

$$\frac{16Al^2}{\pi K_1}\sum_{n=0}^{\infty}\frac{(-1)^n K_0\{(n+\frac{1}{2})\pi a/l\}}{(2n+1)^2[(2n+1)\pi^2 K_0\{(n+\frac{1}{2})\pi a/l\}+2\pi lhK_1\{(n+\frac{1}{2})\pi a/l\}]}-$$
$$-\frac{16A\kappa_1^2 a^3 h}{\pi^3 K_1\kappa^2}\sum_{n=0}^{\infty}\frac{(-1)^n}{2n+1}e^{-\kappa(2n+1)^2\pi^2 t/4l^2}\int\limits_0^{\infty}\frac{e^{-\kappa u^2 t/a^2}u\,du}{[u^2+(n+\frac{1}{2})^2\pi^2a^2/l^2]\Delta_n(u)}, \tag{22}$$

where $\Delta_n(u)$ is defined by (19).

For the region $-l < z < l$, $a < r < b$, with zero initial temperature, the surfaces $r = b$ and $z = \pm l$ maintained at unit temperature for $t > 0$, and the boundary condition (2) at $r = a$, the temperature at the midpoint of the wire, $r = a$, $z = 0$, is

$$1-\frac{\pi^2 a^2(\kappa_1-\kappa)}{l^2\kappa}\sum_{n=0}^{\infty}(-1)^n(2n+1)\sum_m F_{m,n}C_0(\alpha_{m,n}, b\alpha_{m,n}/a)\times$$
$$\times\exp\left\{-\frac{\kappa(2n+1)^2\pi^2 t}{4l^2}-\frac{\kappa t}{a^2}\alpha_{m,n}^2\right\}-$$
$$-\frac{8H}{\pi}\sum_{n=0}^{\infty}\frac{(-1)^n}{(2n+1)}\sum_m F_{m,n}\exp\left\{-\frac{\kappa(2n+1)^2\pi^2 t}{4l^2}-\frac{\kappa t}{a^2}\alpha_{m,n}^2\right\}, \tag{23}$$

where $$C_0(\alpha, b\alpha/a) = J_0(\alpha)Y_0(b\alpha/a) - Y_0(\alpha)J_0(b\alpha/a),$$

$$F_{m,n} = [(b_n - \alpha_{m,n}^2)J_0(\alpha_{m,n}) + H\alpha_{m,n} J_1(\alpha_{m,n})]J_0(b\alpha_{m,n}/a) \times$$
$$\times \{[(b_n - \alpha_{m,n}^2)^2 - H(2-H)\alpha_{m,n}^2]J_0^2(b\alpha_{m,n}/a) -$$
$$-[(b_n - \alpha_{m,n}^2)J_0(\alpha_{m,n}) + H\alpha_{m,n} J_1(\alpha_{m,n})]^2\}^{-1},$$

H and b_n are defined in (15), and $\pm\alpha_{m,n}$, $m = 1, 2,\ldots$, are the roots (all real and simple (4)) of

$$[(b_n - \alpha^2)J_0(\alpha) + \alpha H J_1(\alpha)]Y_0(b\alpha/a) - [(b_n - \alpha^2)Y_0(\alpha) + \alpha H Y_1(\alpha)]J_0(b\alpha/a) = 0.$$

REFERENCES

1. H. S. Carslaw and J. C. Jaeger, *Conduction of Heat in Solids* (Oxford, 1947).
2. J. C. Jaeger, *Bull. Amer. Math. Soc.* **47** (1941), 734.
3. —— *Proc. Roy. Soc. N.S.W.* **74** (1940), 342.
4. —— ibid. **75** (1941), 130.

THE PERIODIC SOLUTIONS OF A NON-LINEAR DIFFERENTIAL EQUATION OF THE SECOND ORDER WITH UNSYMMETRICAL NON-LINEAR DAMPING, AND A FORCING TERM

By A. W. GILLIES (*Northampton Polytechnic, London*)

[Received 9 April 1954]

SUMMARY

The equation considered is

$$\ddot{v}-\omega_0(\epsilon+\epsilon^{\frac{1}{2}}kv-\epsilon v^2)\dot{v}+\omega_0^2 v = 2B\omega_1 \sin\omega_1 t$$

with ϵ small, B and $\omega_1-\omega_0$ also small so that both are $O(\epsilon)$. This equation differs from van der Pol's equation by the presence of a relatively large term in v in the damping coefficient. The effect of this is that the solution has to be developed in powers of $\epsilon^{\frac{1}{2}}$, and the equations of the first approximation cannot be obtained without considering the second harmonic. Consequently methods such as those of Kryloff and Bogolinboff or Cartwright's difference equation have to be carried a stage farther than is necessary for the van der Pol equation.

In the present arrangement of the solution the equation of the first approximation is obtained more directly, the form of the series development of the exact periodic solutions is exhibited, and the convergence of the series, for ϵ sufficiently small, is established directly by comparison with a convergent series of positive constants. Variational equations are obtained for the amplitude and phase of the non-periodic solutions, and the stability of the periodic solutions is deduced from the character of the singular points of the variational equations.

The amplitudes of the periodic solutions for different values of B and $(\omega_1-\omega_0)$ are exhibited by resonance curves which are unsymmetrical, and correspond more closely to those obtained experimentally than is the case for the van der Pol resonance curves.

1. Introduction

CONSIDERATION of a simple valve oscillator circuit leads to a differential equation of the form

$$\ddot{v}+(\alpha+\beta v+\gamma v^2+...)\dot{v}+\omega_0^2 v = 2B\omega_1 \sin\omega_1 t. \tag{1}$$

The second term on the left may be written

$$\frac{d}{dt}(\alpha v+\tfrac{1}{2}\beta v^2+\tfrac{1}{3}\gamma v^3+...),$$

the bracket arising from the representation of the valve characteristic by a power series, or approximating polynomial

$$i = \alpha_1 v+\tfrac{1}{2}\beta v^2+\tfrac{1}{3}\gamma v^3+..., \tag{2}$$

the linear term being modified by the linear circuit resistance and by the

effect of 'feed-back'. The coefficient α is positive when there is no feed-back or negative feed-back and the circuit is dissipative and incapable of self-oscillation. With regenerative feed-back α is reduced, becoming zero at critical regeneration and negative when the circuit becomes self-oscillatory.

It has been claimed that the essential features of the behaviour of the system are revealed by using a cubic characteristic, the powers beyond the third contributing more exact quantitative information rather than new qualitative information.

It has been usual also to assume the biasing voltages adjusted so that the quiescent point is at the inflexion of the characteristic so that $\beta = 0$. Equation (1) is thereby reduced to the form

$$\ddot{v} - \epsilon\omega_0(1-v^2)\dot{v} + \omega_0^2 v = 2B\omega_1 \sin\omega_1 t. \tag{3}$$

This is the equation of van der Pol which has been the subject of extensive investigations. Nearly sinusoidal solutions are obtained when ϵ is sufficiently small, i.e. when the electric circuit is sufficiently near to critical regeneration.

Furthermore, it has been shown that if β is not zero, so that the factor multiplying $\dot{v}$ in equation (3) contains a term in the first power of v, and this term is assumed to be of the same order as the other terms in that factor, then its presence does not affect the frequency of the free oscillation ($B = 0$), or the amplitude of free or forced oscillation in the first approximation, to within terms of $O(\epsilon)$.

The latter result, however, derives from the usual practice of characterizing the magnitudes of all the small terms by the first power of a single parameter ϵ, in powers of which the solution is developed. In practice, if one regards equation (2) as giving the Maclaurin expansion of the characteristic one would expect that the terms would be of decreasing orders of magnitude as the index of the power of v increases, i.e. that β would be smaller than α_1, and γ smaller than β, and so on. In fact the operating range of the valve characteristic may conform much more nearly to a square law than to a symmetrical cubic. Thus, unless the circuit is deliberately biased to the inflexion, it is likely that β will often be much larger than γ. The constant term α of equation (1) has, as it were, been artificially reduced by regenerative feed-back compared with α_1 of equation (2), so that near to critical regeneration it is reasonable to assume α to be of the same order as γ. This is, in any case, brought about by normalizing the equation, but in many cases β may be considerably larger. In these circumstances the system may be more closely represented by an equation of the form

$$\ddot{v} - \omega_0(\epsilon + \epsilon^{\frac{1}{2}} kv - \epsilon v^2)\dot{v} + \omega_0^2 v = 2B\omega_1 \sin\omega_1 t. \tag{4}$$

It is the purpose of the present paper to examine the solutions of this equation when ϵ is small, with particular reference to the forced oscillations when ω_1 is near to ω_0 and k is $O(1)$.

2. The method of solution

Periodic solutions of equations such as the present one have usually been developed in powers of the small parameter which in this case must be $\epsilon^{\frac{1}{2}}$, and even the first approximate solution tends to be clumsy when the differential equation involves the small parameter in more than one power. Thus Greaves's (**1**) solution for the free oscillation is clumsy and requires modification in detail if applied to the present equation with $B = 0$ and the method of Kryloff and Bogolinboff (**2**) requires to be carried a stage farther than usual.

The method which will be employed in the present paper proceeds on somewhat different lines. The amplitude $2b$ and phase ϕ of the fundamental component of the periodic forced oscillation are determined by the solution of a non-linear transcendental equation, and the higher harmonics of the solution are then expressed as series in powers of b. It will be found that this arrangement not only allows the first approximation to be obtained more directly, but also enables the convergence of the complete solution to be established by direct comparison with a convergent series of positive constants, and the error resulting from terminating the solution at any point to be related to the remainder after an appropriate number of terms of the comparison series.

To appreciate the logic of the method, which derives from steady state electric circuit theory, it is convenient to distinguish between the small parameter when it occurs in the non-linear terms and when it occurs in the linear damping term. We will therefore write $\epsilon^{\frac{1}{2}} = \mu$ in the non-linear terms so that the equation becomes

$$\ddot{v}-\omega_0(\epsilon+\mu kv-\mu^2v^2)\dot{v}+\omega_0^2\,v = 2B\omega_1\sin\omega_1 t. \tag{5}$$

In the development ϵ and μ will be treated as independent parameters of which μ will always be small.

By a change of time scale equation (5) may be brought to

$$\ddot{v}-(\epsilon+\mu kv-\mu^2v^2)\dot{v}+v = 2B\omega_1\sin\omega_1 t, \tag{6}$$

in which form the equation will be considered.

3. Periodic solution developed in powers of B

If D is used for d/dt, the equation (6) may be rearranged in the form

$$2B\cos\omega_1 t = \left(\epsilon-D-\frac{1}{D}\right)v+\tfrac{1}{2}\mu kv^2-\tfrac{1}{3}\mu^2v^3$$

or

$$2B\cos\omega_1 t = \zeta(D)v+\tfrac{1}{2}\mu kv^2-\tfrac{1}{3}\mu^2v^3, \tag{7}$$

where
$$\zeta(D) = \epsilon - D - \frac{1}{D}. \tag{8}$$

A periodic solution of (7) may be developed in powers of B by treating $\zeta(D)$ in the same way as an impedance operator in circuit theory, i.e. $\zeta(D)\exp i\omega t$ is replaced by $\zeta(i\omega)\exp i\omega t$. Write
$$v = v^{(1)}B + v^{(2)}B^2 + \ldots + v^{(n)}B^n + \ldots \tag{9}$$
in which the $v^{(n)}$ are functions of t to be determined. Substitute (9) into equation (7) and equate coefficients of like powers of B, then equations are obtained from which the $v^{(n)}$ are obtained in succession as periodic functions of t of period $2\pi/\omega_1$. Using exponential notation we thus obtain
$$\left.\begin{aligned} \exp(i\omega_1 t) + \exp(-i\omega_1 t) &= \zeta(D)v^{(1)} \\ 0 &= \zeta(D)v^{(2)} + \tfrac{1}{2}\mu k v^{(1)^2} \\ 0 &= \zeta(D)v^{(3)} + \mu k v^{(1)} v^{(2)} - \tfrac{1}{3}\mu^2 v^{(1)^3} \\ \cdots & \cdots\cdots\cdots \end{aligned}\right\}. \tag{10}$$

From the first of equations (10) we find
$$v^{(1)} = v_1^{(1)} + v_{-1}^{(1)},$$
where
$$v_1^{(1)} = \frac{1}{\zeta(i\omega_1)}\exp(i\omega_1 t),$$
$$v_{-1}^{(1)} = \frac{1}{\zeta(-i\omega_1)}\exp(-i\omega_1 t),$$
the subscript r in $v_r^{(n)}$ indicating that this term contains the exponential factor $\exp(ri\omega_1 t)$, and is therefore an rth harmonic term.

From the second of equations (10) we obtain
$$v^{(2)} = -\frac{1}{\zeta(D)}\tfrac{1}{2}\mu k v^{(1)^2}$$
$$= -\frac{1}{\zeta(D)}\tfrac{1}{2}\mu k (v_1^{(1)^2} + 2v_1^{(1)} v_{-1}^{(1)} + v_{-1}^{(1)^2}). \tag{11}$$
Thus
$$v^{(2)} = v_2^{(2)} + v_0^{(2)} + v_{-2}^{(2)},$$
where
$$v_0^{(2)} = \frac{\mu k v_1^{(1)} v_{-1}^{(1)}}{\zeta(0)} = 0,$$
$$v_2^{(2)} = -\frac{\mu k v_1^{(1)^2}}{2\zeta(2i\omega_1)} = -\frac{\mu k}{2\zeta_1^2 \zeta_2}\exp(2i\omega_1 t),$$
$$v_{-2}^{(2)} = -\frac{\mu k v_{-1}^{(1)^2}}{2\zeta(-2i\omega_1)} = -\frac{\mu k}{2\zeta_{-1}^2 \zeta_{-2}}\exp(-2i\omega_1 t)$$
in which ζ_r is used for $\zeta(ri\omega_1)$. The sum $v_2^{(2)} + v_{-2}^{(2)}$ gives a real second harmonic term.

From the third of equations (10), $v^{(3)}$ is obtained as

$$v^{(3)} = v_3^{(3)} + v_1^{(3)} + v_{-1}^{(3)} + v_{-3}^{(3)},$$

where

$$v_3^{(3)} = -\frac{1}{\zeta_3}(\mu k v_1^{(1)} v_2^{(2)} - \tfrac{1}{3}\mu^2 v_1^{(1)^3}) = -\frac{1}{\zeta_3}\left(\frac{k^2}{2\zeta_2} - \frac{1}{3}\right)\mu^2 v_1^{(1)^3} \tag{12}$$

$$v_1^{(3)} = -\frac{1}{\zeta_1}(\mu k v_{-1}^{(1)} v_2^{(2)} - \mu^2 v_1^{(1)^2} v_{-1}^{(1)}) = -\frac{1}{\zeta_1}\left(\frac{k^2}{2\zeta_2} - 1\right)\mu^2 v_1^{(1)^2} v_{-1}^{(1)}$$

and $v_{-3}^{(3)}$, $v_{-1}^{(3)}$ are the conjugates. $v_3^{(3)} + v_{-3}^{(3)}$ gives a real term of third harmonic frequency and $v_1^{(3)} + v_{-1}^{(3)}$ is a real term of fundamental frequency.

Proceeding in this way the $v^{(n)}$ are determined in succession in the general form

$$v^{(n)} = \sum v_r^{(n)} \tag{13}$$

with r running through the odd (even) integers when n is odd (even) from $-n$ to $+n$, $r = 0$ being omitted when n is even, since $v_0^{(n)}$ is always zero. The series (9) then gives a formal solution of the equation (6).

4. Convergence of the solution in powers of B

An interval of assured convergence for the series (9) may be obtained by considering the equation

$$\xi = N\eta - \tfrac{1}{2}\mu_1 k_1 \eta^2 - \tfrac{1}{3}\mu_1^2 \eta^3, \tag{14}$$

in which N, μ_1, and k_1 are positive constants chosen so that

$$\left.\begin{aligned} \mu &< \mu_1 \\ |k| &< k_1 \\ \text{and} \qquad |\zeta(\pm ri\omega_1)| &\geqslant N \quad (r = 1, 2, 3, \ldots) \end{aligned}\right\}. \tag{15}$$

If ω_1 has values near to unity (i.e. near to ω_0 on the original time scale), the third condition requires $N = |\epsilon|$.

Equation (14) has the solution $\eta = 0$ when $\xi = 0$ and since $N \neq 0$ it has a solution for η as a function of ξ, vanishing when $\xi = 0$, which is analytic in a certain neighbourhood of $\xi = 0$. This solution can therefore be expanded in powers of ξ, the expansion converging in a circle extending to the singularity nearest to the origin on the ξ-plane, which will be one of the branch points determined by $d\xi/d\eta = 0$, i.e.

$$0 = N - \mu_1 k_1 \eta - \mu_1^2 \eta^2.$$

Let this branch point be $\xi = R$, $\eta = S$, then we may obtain

$$R = \frac{1}{12\mu_1}[(4N + k_1^2)^{\frac{3}{2}} - 6k_1 N - k_1^3], \tag{16}$$

$$S = \frac{1}{2\mu_1}[(4N + k_1^2)^{\frac{1}{2}} - k_1]. \tag{17}$$

The series for η in powers of ξ will therefore converge if

$$|\xi| < R.$$

Now if this series is obtained by setting

$$\eta = \eta^{(1)}\xi + \eta^{(2)}\xi^2 + \ldots + \eta^{(n)}\xi^n + \ldots, \tag{18}$$

substituting in (14) and equating coefficients of like powers of ξ to determine the $\eta^{(n)}$ in succession, a set of equations is obtained which corresponds term by term with equations (10), such that if $2B \leqslant \xi < R$ and the inequalities (15) are satisfied then (9) is dominated by (18) in the sense that

$$|v^{(n)}B^n| \leqslant \sum |v_r^{(n)}| B^n \leqslant \eta^{(n)}\xi^n. \tag{19}$$

Thus the series (9) will then converge absolutely and uniformly with respect to t. Since its terms are analytic in t its sum is an analytic function, which, from the manner in which it was derived, must satisfy the differential equation (6). Moreover its terms may be rearranged according to frequency to give the Fourier expansion of the solution, each harmonic being represented as a power series in B.

It may be noted that $v^{(n)}$ contains μ only in the factor μ^{n-1} so that the series may be regarded equally as a development in powers of μ.

5. Inadequacy of the solution in powers of B

The series (9) provides a solution of the differential equation for any k and μ less than k_1 and μ_1 respectively, and for $B < \frac{1}{2}R$, where R is given by (16). If ϵ were negative and not small, i.e. the circuit had appreciable positive linear damping, this solution would have an adequate interval of convergence, and would determine the steady response of the non-linear system to the applied e.m.f.

The interval of convergence of the dominating series (18) will be wider the larger the value which may be chosen for N, the other parameters being fixed, since N occurs as a divisor in determining the $\eta^{(n)}$. But N must be less than the corresponding divisors, the $\zeta(\pm ri\omega_1)$ which occur in the determination of the $v^{(n)}$. Thus, in the case envisaged in the present paper, when $\epsilon = \mu^2$ is small, the interval of convergence is restricted however small μ_1 may be. In fact, for a fixed $k_1 \neq 0$, R approximates to $\mu_1^3/(2k_1)$ as $\mu_1 \to 0$, or if $k_1 = 0$ then $R = \frac{2}{3}\mu_1^2$, for $\epsilon = \mu_1^2$.

We observe firstly that this restriction on the interval of convergence arises through the occurrence of $\zeta(\pm i\omega_1)$ as a small divisor in the determination of the $v^{(n)}$. If this can be avoided then a better choice of N may be possible. Secondly, the $v^{(n)}$ are expressed in the first place, as in equations

(11) and (12), in powers of $v_1^{(1)}$ and $v_{-1}^{(1)}$, and the relationship between the $v^{(n)}$ and the $\eta^{(n)}$ will remain valid so long as

$$B\{|v_1^{(1)}|+|v_{-1}^{(1)}|\} < \eta^{(1)}\xi < \frac{R}{N}, \tag{20}$$

the conditions (15) being also satisfied. These observations suggest a modification of the method which gives an entirely adequate interval of convergence. It is known that if B is sufficiently small at least one periodic solution certainly exists. Therefore let the fundamental term in the Fourier expansion of such a periodic solution be $2b\cos(\omega_1 t+\phi)$. It will be shown that the harmonics above the first may be expressed by series in powers of b, while b and ϕ are determined by an auxiliary equation.

6. Periodic solution in powers of b

To do this replace (9) by

$$v = v^{(1)}b+v^{(2)}b^2+...+v^{(n)}b^n+... \tag{21}$$

with $$v^{(1)} = 2\cos(\omega_1 t+\phi),$$

i.e. $$v_1^{(1)} = \exp i(\omega_1 t+\phi), \qquad v_{-1}^{(1)} = \exp(-i(\omega_1 t+\phi)), \tag{22}$$

so that $v^{(1)}b$ is the fundamental of the periodic solution. Substitute (21) into (7) and choose the $v^{(n)}$ in succession, to annul all terms of other than fundamental frequency. The $v^{(n)}$ are then given by the same expressions as before, with the omission of the terms $v_1^{(n)}$ and $v_{-1}^{(n)}$ when n is odd, and the omission of terms which arise from these in the higher orders. Thus $v^{(2)}$ is still given by (11) while $v^{(3)}$ contains only $v_3^{(3)}$ and $v_{-3}^{(3)}$ with $v_3^{(3)}$ given by (12).

The terms which were formerly cancelled by $v_1^{(n)}$ and $v_{-1}^{(n)}$ now remain to form an equation containing only terms with $\exp(i\omega_1 t)$ or $\exp(-i\omega_1 t)$, which will be satisfied if the terms containing $\exp(i\omega_1 t)$ are equal on the two sides, since those containing $\exp(-i\omega_1 t)$ are the conjugates of the former. This gives the equation

$$\begin{aligned} B\exp(i\omega_1 t) &= \zeta(D)v_1^{(1)}b-\left(\frac{k^2}{2\zeta_2}+1\right)\mu^2 v_1^{(1)^2}v_{-1}^{(1)}b^3+... \\ &= \zeta(i\omega_1)v_1^{(1)}b-\left(\frac{k^2}{2\zeta_2}+1\right)\mu^2 v_1^{(1)^2}v_{-1}^{(1)}b^3+..., \end{aligned} \tag{23}$$

the right-hand side being an infinite series of the form

$$\sum_{n=0}^{\infty} A_{2n+1}\mu^{2n}v_1^{(1)n+1}v_{-1}^{(1)n}b^{2n+1},$$

where the A_{2n+1} are functions of k and of the values of the $\zeta(\pm ri\omega_1)$ for $r = 2, 3,..., 2n$, and $n > 0$, while $A_1 = \zeta(i\omega_1)$.

If we substitute for $v_1^{(1)}$ and $v_{-1}^{(1)}$ from (22) and divide by $\exp i(\omega_1 t+\phi)$, equation (23) becomes

$$B\exp(-i\phi) = \zeta(i\omega_1)b-\left(\frac{k^2}{2\zeta_2}+1\right)\mu^2b^3+\dots. \tag{24}$$

The right side of (24) is an infinite series which along with (21) must converge for the process to have any significance. If, however, a positive b and ϕ can be found, for which the series converge, and which satisfy (24), then with these values for b and ϕ, (21) provides a periodic solution of the differential equation. Equation (24) thus determines the amplitude and phase (it is equivalent to two real equations) of the periodic forced oscillation. It will therefore be described as the amplitude equation.

7. Convergence of the solution in powers of b

Comparing the present procedure with that of section 3 it is clear that in terms of $v_1^{(1)}$ and $v_{-1}^{(1)}$ we have simply omitted from the $v^{(n)}$ certain terms, namely $v_1^{(n)}$ and $v_{-1}^{(n)}$ for n odd, which were formerly included, and the relationship to the series for η in powers of ξ remains, in the form

$$|v^{(n)}b^n| < \sum |v_r^{(n)}|b^r < \eta^{(n)}\xi^n,$$

provided $$(|v_1^{(1)}|+|v_{-1}^{(1)}|)b < \eta^{(1)}\xi,$$

i.e. $$2b \leqslant \xi/N < R/N,$$

together with (15), with the important difference that the last inequality in (15) need not now be satisfied for $r = \pm 1$. Since

$$\zeta(ri\omega_1) = \epsilon-i\left(r\omega_1-\frac{1}{r\omega_1}\right)$$

this means that if ω_1 is restricted to values near to 1, N may take a value near to $\frac{3}{2}$ which is independent of ϵ.

Furthermore, the terms in b^n which remain to form the amplitude equation will have the sum of their moduli less than $N\eta^{(n)}\xi^n$ so that the series (24) will be dominated by the comparison series (18) multiplied by N.

It is also clear from (16), since N is now independent of ϵ, that given k_1 and b_1 we may choose μ_1, so that $R/N \geqslant 2b_1$. We then have the theorem:

Given constants b_1 and k_1, the series (21) and (24) will converge absolutely and uniformly with respect to t, for any $b \leqslant b_1$ and any $k \leqslant k_1$ provided $\mu \leqslant \mu_1$ and ω_1 is near to 1, this statement being valid whether we set $\epsilon = \mu^2$ in the linear damping term or continue to regard ϵ as an independent parameter.

These conditions being satisfied, the possibility of (21) providing a periodic solution of the differential equation depends on the existence of a solution of the amplitude equation with $b < b_1$.

In discussing this we cease to treat ϵ and μ as independent parameters

and μ^2 will be replaced by ϵ. Since $v^{(n)}$ contains μ^{n-1}, i.e. $\epsilon^{(n-1)/2}$, as a factor, the series (21) proceeds in powers of $\epsilon^{\frac{1}{2}}$ as well as in powers of b, whilst (24) is of the form $\sum_{n=0}^{\infty} A_{2n+1} v_1^{(1)^{n+1}} v_{-1}^{(1)^n} \epsilon^n b^{2n+1}$ and proceeds in powers of ϵ, the series converging provided $\epsilon < \epsilon_1 = \mu_1^2$. Both series may thus be regarded as developments in powers of $\epsilon^{\frac{1}{2}}$ and ϵ respectively, the coefficients of which are also functions of ϵ through the $\zeta(\pm ri\omega_1)$.

Since the interval of convergence $b < b_1$ has been fixed it is necessary to regard ϵ as determining the relative orders of magnitude of the terms; and when considering an approximate solution in which only the first few terms of the series are retained, with ϵ sufficiently small for higher powers to be neglected, terms arising from the coefficients which are of higher order in ϵ may be omitted.

8. Solution of the amplitude equation

It is now assumed that B, as well as $\omega_1 - 1$, is small of $O(\epsilon)$ and we will set

$$\epsilon F = B,$$

$$\epsilon x = \omega_1 - \frac{1}{\omega_1} \doteqdot 2(\omega_1 - 1).$$

We then have
$$\zeta(i\omega_1) = \epsilon(1-ix)$$
and the amplitude equation (24), after cancelling the common factor ϵ, becomes

$$F\exp(-i\phi) = (1-ix)b - \left(\frac{k^2}{2\zeta_2} + 1\right)b^3 + \epsilon R_1, \tag{25}$$

where ϵR_1 denotes the sum of the terms beyond that containing b^3, and $|\epsilon R_1|$ is certainly less than N/ϵ times the remainder after the third term in the expansion of η in powers of ξ with $\mu = \epsilon^{\frac{1}{2}}$ replacing μ_1. Since $\eta^{(n)}$ then contains μ^{n-1} as a factor, the other factors being constants, this can be made as small as we please by making ϵ sufficiently small.

With $\epsilon = 0$ equation (25) has solutions determined by

$$F\exp(-i\phi) = (1-ix)b - \left(\frac{k^2}{2\zeta_2} + 1\right)b^3, \tag{26}$$

and we may use implicit function theory to show that if ϵ is sufficiently small (25) has solutions near to those of (26) and which differ from the latter by a quantity at most of $O(\epsilon)$.

The solutions of (26) are independent of ϵ and the constant b_1 may be chosen so that the roots of (26) for b are less than b_1; ϵ_1 may then be chosen so that the series converge for $b < b_1$ and $\epsilon < \epsilon_1$. Thus if ϵ is sufficiently small the solution of (25) near to any solution of (26) will be within the

interval of convergence and for such values of b and ϕ the series (21) converges and gives a periodic solution of the original differential equation.

If $B = 0$, i.e. there is no external forcing term in the differential equation, ω_1 may be replaced by ω, and b by a throughout, and equation (25) with $B = 0$ will then determine the frequency ω and amplitude a of a free oscillation. Thus if (25) so modified can be satisfied by positive values of a and ω, then for ϵ sufficiently small (21), with a instead of b and ω instead of ω_1, will give a periodic solution of the differential equation with $B = 0$, of period $2\pi/\omega$ and fundamental amplitude $2a$.

It is not necessary to specify any particular method of solving (25), but clearly if ϵ is sufficiently small the solutions will be approximated by those of (26), which may therefore be regarded as the equation of the first approximation.

9. Error in an approximate solution

Suppose that the amplitude equation is cut off at the term containing $\mu^{2n}b^{2n+1}$, that is $\epsilon^n b^{2n+1}$, terms beyond this being omitted, and that b and ϕ are chosen to satisfy exactly the curtailed equation. Suppose that with these values of b and ϕ the series (21) is carried as far as the terms containing the same powers of μ and b. A comparison of the solutions of (7) and of the comparison series shows that the sum of the moduli of the residual terms when this curtailed series is substituted for v in (7) is certainly less than

$$N[\eta^{(2n+2)}\xi^{2n+2}+\eta^{(2n+3)}\xi^{2n+3}+\ldots],$$

i.e. less than N times the remainder after the same number of terms of the comparison series. Since $\eta^{(n)}$ contains μ_1^{n-1} as a factor, this remainder is of the form μ_1^{2n+1} times a bounded factor and may certainly be made as small as we please by taking μ_1 sufficiently small. Thus the residual when the approximate solution is substituted in (7) is less than $C\epsilon^{n+\frac{1}{2}}$ where C is independent of ϵ.

10. The equations of the first approximation

We have
$$\zeta_2 = \zeta(2i\omega_1) = \epsilon - i\left(2\omega_1 - \frac{1}{2\omega_1}\right)$$
$$= -\tfrac{3}{2}i + O(\epsilon)$$

when ω_1 is near to 1.

We may therefore replace ζ_2 by $-\frac{3}{2}i$ in equation (26), and separating real and imaginary parts we have

$$\left.\begin{aligned} F\cos\phi &= b(1-b^2) \\ F\sin\phi &= b(x+\nu b^2) \end{aligned}\right\}, \tag{27}$$

where ν is written for $\frac{1}{3}k^2$. These are the equations giving the first approximation for b and ϕ.

For the free oscillation they become

$$0 = a(1-a^2),$$
$$0 = a(x+\nu a^2),$$

and, rejecting $a = 0$, they have the solution $a = 1$, $x = -\nu a^2 = -\nu$. Thus a free oscillation must have the real amplitude $2a = 2$ and frequency given by $2(\omega-1) = x\epsilon = -\nu\epsilon$, i.e. $\omega = 1-\frac{1}{2}\nu\epsilon = 1-\frac{1}{6}k^2\epsilon$.

Comparing with van der Pol's equation with $k = 0$, it appears that a non-zero value of k does not affect the amplitude of free oscillation in the first approximation, but causes its frequency to deviate below $\omega_0 = 1$. This is associated with the relatively large second harmonic whose amplitude is $O(\epsilon^{\frac{1}{2}})$, whereas in the van der Pol case the second harmonic does not occur, and the third is $O(\epsilon)$, and is in accordance with the well-known relationship between frequency and harmonic content (**3**, **4**).

Turning now to the forced oscillations, squaring and adding equations (27) gives

$$F^2 = b^2[(1-b^2)^2+(x+\nu b^2)^2],$$

or, writing $y = b^2$,

$$F^2 = y[(1-y)^2+(x+\nu y)^2]. \tag{28}$$

The curves representing y against x for fixed F are the resonance curves. For $\nu = 0$ they are the van der Pol resonance curves. If $P'(x', y)$ is a point on a van der Pol curve, the point $P(x, y)$ with $x = x'-\nu y$ lies on the curve for the same F on the resonance curve figure for ν. Thus the general figure may be obtained from the van der Pol figure by displacing all points to the left by an amount proportional to the ordinate, so that the maxima of the resonance curves lie on the straight line $x = -\nu y$ instead of on the y-axis. This gives the unsymmetrical resonance curves as shown in Figs. 1 and 2.

Double roots of (28) satisfy

$$0 = (1-y)(1-3y)+(x+\nu y)(x+3\nu y). \tag{29}$$

This is the locus of points of contact of tangents to the resonance curves which are parallel to the y-axis. This curve, denoted by $\mathscr{E}$, is an ellipse for $\nu < \sqrt{3}$ (Fig. 1), a parabola for $\nu = \sqrt{3}$, and a branch of a hyperbola for $\nu > \sqrt{3}$ (Fig. 2).

A triple root of (28) must satisfy (29) and also

$$3(1+\nu^2)y+2(\nu x-1) = 0. \tag{30}$$

This determines two points for $\nu < \sqrt{3}$, at each of which a resonance curve is tangential to $\mathscr{E}$. The right-hand point is at $x = (1-\sqrt{3}\nu)/(\sqrt{3}+\nu)$, the left-hand point is at $x = -(1+\sqrt{3}\nu)/(\sqrt{3}-\nu)$, in each case with y given by (30) and F^2 by (28). The second value of x tends to $-\infty$ as $\nu \to \sqrt{3}$,

and is no longer on the figure when $\nu > \sqrt{3}$. For $\nu = 0$ these points are $x = \pm 1/\sqrt{3}$, $y = \frac{2}{3}$, $F^2 = \frac{8}{27}$.

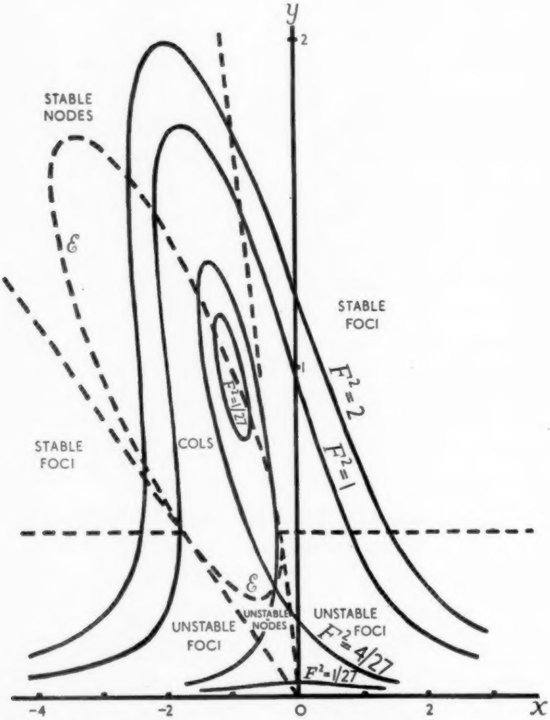

FIG. 1. Resonance curves for $\nu = 1$. The values of F^2 are shown against each curve. The broken lines divide the plane into regions; points in each region correspond to singularities of the variational equations of the types indicated.

For $F^2 = \frac{4}{27}$ the resonance curve has a double point at $x = -\frac{1}{3}\nu$, $y = \frac{1}{3}$. For $F^2 < \frac{4}{27}$ it has a loop surrounding $x = -\nu$, $y = 1$, which point represents the free oscillation, together with a branch extending from $x = -\infty$ to $x = +\infty$, asymptotic to the x-axis in both directions. For $F^2 > \frac{4}{27}$ the curve has a single branch extending from $x = -\infty$ to $x = +\infty$ asymptotic to the x-axis again on both sides. The stationary points of the resonance curves all lie on $x = -\nu y$.

When $\nu < \sqrt{3}$, for a sufficiently large F the resonance curve passes above $\mathscr{E}$ and there is never more than one y (i.e. one periodic solution) for any x. If, however, $\nu > \sqrt{3}$, every resonance curve intersects $\mathscr{E}$ on the left, giving

an interval of values of x in which there are three values of y (i.e. three periodic solutions) for each x.

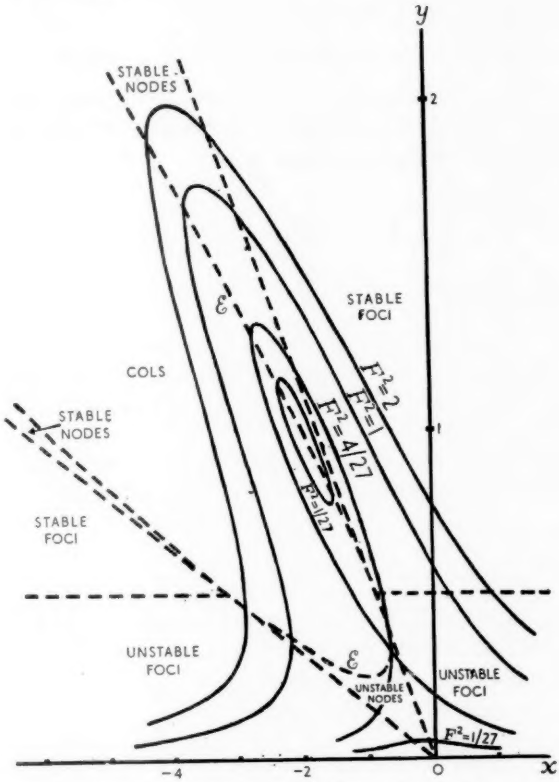

FIG. 2. Similar to Fig. 1, but with $\nu = 2$.

11. Stability of the periodic solutions

Since only stable periodic solutions are physically significant the stability of the possible periodic solutions must be considered.

Let the formal solution (21) be denoted by $K(b, \phi, t)$, i.e.

$$K(b, \phi, t) = \sum v^{(n)} b^n.$$

The terms of the amplitude equation together with their conjugates are the residual terms when the formal solution is substituted for v in equation (7). Bringing these on to the left-hand side they are

$$2B\cos\omega_1 t - 2\,\mathrm{re}\left[\zeta(i\omega_1)v_1^{(1)} b - \left(\frac{k^2}{2\zeta_2}+1\right)\epsilon v_1^{(1)^2} v_{-1}^{(1)} b^3 + O(\epsilon^2)\right],$$

or with the assumptions regarding B and ω_1

$$2\epsilon[F\cos\omega_1 t - b(1-b^2)\cos(\omega_1 t+\phi) - b(x+\nu b^2)\sin(\omega_1 t+\phi) + O(\epsilon)].$$

Denote this expression by $2H(b,\phi,t)$, so that

$$H(b,\phi,t) = \epsilon[F\cos\omega_1 t - b(1-b^2)\cos(\omega_1 t+\phi) - b(x+\nu b^2)\sin(\omega_1 t+\phi) + O(\epsilon)].$$

Since the differential equation (6) is obtained by differentiating (7), the residual terms when the formal solution is substituted for v in (6) will be $2(\partial H/\partial t)$ when the equation is written as

$$\frac{d^2v}{dt^2} - (\epsilon+\epsilon^{\frac{1}{2}}kv-\epsilon v^2)\frac{dv}{dt} + v - 2B\omega_1\sin\omega_1 t = 0. \tag{31}$$

Thus
$$\frac{\partial^2 K}{\partial t^2} - (\epsilon+\epsilon^{\frac{1}{2}}kK-\epsilon K^2)\frac{\partial K}{\partial t} + K - 2B\omega_1\sin\omega_1 t = 2\frac{\partial H}{\partial t}. \tag{32}$$

Furthermore, since real b and ϕ are chosen to satisfy the amplitude equation, the conjugate equation being satisfied by the same values, it follows that such values will cause both H and $\partial H/\partial t$ to vanish for all values of t.

In order to discuss the stability of the periodic solutions we now introduce b and ϕ as new independent variables defined by

$$v = K(b,\phi,t), \tag{33}$$

$$\frac{dv}{dt} = \frac{\partial K(b,\phi,t)}{\partial t} - H(b,\phi,t). \tag{34}$$

Equations (33) and (34) require

$$\frac{\partial K}{\partial b}\dot{b} + \frac{\partial K}{\partial \phi}\dot{\phi} + H = 0. \tag{35}$$

It we now substitute from (33) and (34) into the differential equation (31) and use (32) we obtain

$$\frac{\partial}{\partial b}\left(\frac{\partial K}{\partial t} - H\right)\dot{b} + \frac{\partial}{\partial \phi}\left(\frac{\partial K}{\partial t} - H\right)\dot{\phi} + L = 0, \tag{36}$$

where
$$L = \frac{\partial H}{\partial t} + (\epsilon+\epsilon^{\frac{1}{2}}K-\epsilon K^2)H.$$

Solving (35) and (36) for $\dot{b}$ and $\dot{\phi}$ gives

$$\dot{b} = (1/\Delta)\left[L\frac{\partial K}{\partial \phi} - H\frac{\partial}{\partial \phi}\left(\frac{\partial K}{\partial t} - H\right)\right], \tag{37}$$

$$\dot{\phi} = (1/\Delta)\left[-L\frac{\partial K}{\partial b} + H\frac{\partial}{\partial b}\left(\frac{\partial K}{\partial t} - H\right)\right], \tag{38}$$

with $$\Delta = \frac{\partial K}{\partial b}\frac{\partial}{\partial \phi}\left(\frac{\partial K}{\partial t} - H\right) - \frac{\partial K}{\partial \phi}\frac{\partial}{\partial b}\left(\frac{\partial K}{\partial t} - H\right).$$

Equations (37) and (38) determine the variation of amplitude and phase. If b and ϕ satisfy the amplitude equation, H, $\partial H/\partial t$, and therefore also L, all vanish, so that $\dot{b}$ and $\dot{\phi}$ also vanish. Thus b and ϕ remain constant and (33) determines a periodic solution.

Evaluating the right-hand sides of (37), (38) as far as terms of $O(\epsilon)$ gives

$$\frac{2\dot{b}}{\epsilon} = -F\cos\phi + b(1-b^2) + O(\epsilon^{\frac{1}{2}}), \tag{39}$$

$$\frac{2b\dot{\phi}}{\epsilon} = F\sin\phi - b(x+\nu b^2) + O(\epsilon^{\frac{1}{2}}). \tag{40}$$

If arbitrary initial values are given for v and dv/dt, equations (33), (34) with $\epsilon = 0$ have a unique solution

$$b = \frac{1}{2}\sqrt{\left[v^2 + \frac{1}{\omega_1^2}\left(\frac{dv}{dt}\right)^2\right]}$$

and ϕ in $-\pi < \phi \leqslant \pi$, the jacobian $\Delta = -4b\omega_1 + O(\epsilon^{\frac{1}{2}})$ not vanishing except for $v = dv/dt = 0$, and then $b = 0$ and ϕ is indeterminate. For ϵ small they will therefore have a unique solution for b and ϕ with values near to those for $\epsilon = 0$ provided

$$\sqrt{\left[v^2 + \frac{1}{\omega_1^2}\left(\frac{dv}{dt}\right)^2\right]} < 2b_1'$$

where b_1' is less than b_1 by a quantity of $O(\epsilon^{\frac{1}{2}})$, so that $b < b_1$ for convergence. These values of b and ϕ provide initial conditions for the system (39), (40) corresponding to which this system has a unique solution for b and ϕ as functions of t, which in turn through (33) determines a solution of (31). Thus, within $b < b_1$, the system (39), (40) is altogether equivalent to the original differential equation.

Moreover for ϵ sufficiently small an integral curve of (39), (40) will in any finite interval of time run close to the integral curve through the same initial point of the system

$$\frac{2\dot{b}}{\epsilon} = -F\cos\phi + b(1-b^2), \tag{41}$$

$$\frac{2b\dot{\phi}}{\epsilon} = F\sin\phi - b(x+\nu b^2) \tag{42}$$

obtained by omitting the terms of $O(\epsilon^{\frac{1}{2}})$ from (39) and (40). The approximate variational equations (41), (42) are therefore sufficient to determine the stability of the periodic solutions, as well as forming the equations of the first approximation for the transient solutions.

These variational equations may be deduced from Cartwright's difference equations (**5**). Alternatively, if it be assumed that non-periodic solutions can be represented by allowing b and ϕ to vary slowly, so that $\dot{b}$ and $\dot{\phi}$ are $O(\epsilon)$, the variational equations may be deduced from the amplitude equation by a simple symbolic procedure. For this purpose the amplitude equation (23) is written

$$B\exp(i\omega_1 t) = \zeta(D)b\exp i(\omega_1 t+\phi)+\epsilon A_3 v_1^{(1)^2} v_{-1}^{(1)} b^3+O(\epsilon^{\frac{3}{2}}), \tag{43}$$

any effect arising from variation of b and ϕ in the terms after the first on the right being of order higher than $O(\epsilon)$. In the first term on the right set

$$\begin{aligned}\zeta(D)b\exp i(\omega_1 t+\phi) &= \exp(i\omega_1 t)\zeta(i\omega_1+D)b\exp(i\phi)\\ &= \exp(i\omega_1 t)[\zeta(i\omega_1)+\zeta'(i\omega_1)D+M(D)]b\exp(i\phi),\end{aligned}$$

where $M(D)$ contains D^2 as a factor, and operating on $b\exp(i\phi)$ is assumed to give terms of higher order than $O(\epsilon)$. We then have

$$\zeta(D)b\exp i(\omega_1 t+\phi) = \exp i(\omega_1 t+\phi)[\zeta(i\omega_1)b+\zeta'(i\omega_1)(\dot{b}+ib\dot{\phi})]$$

within $O(\epsilon^{\frac{3}{2}})$. Within the same order $\zeta'(i\omega_1)$ may be replaced by $\zeta'(i) = -2$, and on substituting back into (43) and separating real and imaginary parts the variational equations (41) and (42) are obtained. This method does not give the exact equations (39) and (40), but it may be verified by direct substitution that if b and ϕ satisfy the approximate equations the differential equation for v will be satisfied within $O(\epsilon^{\frac{3}{2}})$.

12. The variational equations

By a further change of time scale the variational equations may be brought to the form

$$\dot{b} = -F\cos\phi+b(1-b^2), \tag{44}$$

$$b\dot{\phi} = F\sin\phi-b(x+\nu b^2). \tag{45}$$

b and ϕ are taken as polar coordinates on a plane with (b_1, b_2) as cartesian coordinates, so that if P is a representative point on an integral curve, $\overrightarrow{OP}$ may be regarded as the representative vector of the fundamental oscillation of v. Since b and ϕ vary only by $O(\epsilon)$ in the period $2\pi/\omega_1$, the non-periodic solutions for v are represented as nearly sinusoidal oscillations of slowly varying amplitude and phase.

The singular points of the system represent the periodic solutions and, when stable, give the synchronized oscillations of the physical system. Stable limit cycles represent combination oscillations in which free and forced oscillations are present simultaneously. Other integral curves represent transient responses of the physical system, which, apart from possible unstable limit cycles, must approach either a stable singularity or a stable limit cycle as $t \to \infty$; as is evident since $\dot{b}$ is negative for $b > 1+\frac{1}{2}F$, i.e. the

integral curves cross any sufficiently large circle on the (b, ϕ) plane inwards as t increases. Thus, however excited, the physical system settles down ultimately to a synchronized oscillation or to a combination oscillation.

Since the equations are unaltered if the signs of ν, x, and ϕ are reversed it is only necessary to consider positive values of ν, and this is in fact the case since $\nu = \frac{1}{3}k^2$.

13. Distribution of the singular points on the (b, ϕ) plane

The number and radii of the singular points for any values of F, x, and ν are shown on the resonance curve diagram. Their positions on the (b, ϕ)-plane are most easily obtained as the intersections of the curves on which $\dot{b}$ and $\dot{\phi}$ vanish. The first of these has the equation

$$F\cos\phi = b(1-b^2)$$

and depends only on F. It therefore has exactly the same form as in the van der Pol case and need not be described in detail. It has a double point when $F^2 = \frac{4}{27}$, has two separate loops when $F^2 < \frac{4}{27}$, and a single loop when $F^2 > \frac{4}{27}$.

The second curve $\dot{\phi} = 0$ has the equation

$$F\sin\phi = b(x+\nu b^2).$$

This may be rearranged as

$$F\sqrt{\left(\frac{\nu}{-x^3}\right)}\sin\phi = -b\sqrt{\left(\frac{\nu}{-x}\right)}\left[1-b^2\left(\frac{\nu}{-x}\right)\right],$$

which becomes $$\mathscr{F}\cos\varphi = \beta(1-\beta^2)$$

if $$\mathscr{F} = F\sqrt{\left(\frac{\nu}{-x^3}\right)}, \qquad \beta = b\sqrt{\left(\frac{\nu}{-x}\right)}, \qquad \varphi = \phi+\tfrac{1}{2}\pi.$$

Thus for $x < 0$ it has the same form as a $\dot{b} = 0$ curve turned through a right angle in the negative sense. It has a double point on the negative b_2-axis when $\mathscr{F}^2 = -F^2\nu/x^3 = \frac{4}{27}$, it has two loops when $0 < \mathscr{F}^2 < \frac{4}{27}$ and one loop for $\mathscr{F}^2 > \frac{4}{27}$. When $x > 0$ it has a single loop above the b_1-axis.

At some distance from the origin the direction of the integral curves as t increases is inwards and clockwise, cutting the radii from the origin at an angle γ, given by $\tan\gamma = \nu$. Within the curve $\dot{\phi} = 0$, when it has a single loop, the direction is anticlockwise; when it has two loops the direction of the integral curves is clockwise again within the inner loop. When curve $\dot{b} = 0$ has a single loop the direction of the integral curves within it is outwards from the origin, $\dot{b}$ positive; while if it has two loops, $\dot{b}$ becomes negative again within the inner loop.

If we follow a resonance curve, i.e. if x is varied with F and ν fixed, the $\dot{\phi} = 0$ curve changes through its complete sequence of forms, the singu-

larities moving round the fixed $\dot{b} = 0$ curve. The two curves have always at least one intersection other than the origin. A second-order singular point occurs when the curves are tangential, such a singular point corresponding to a point where the resonance curve crosses $\mathscr{E}$. A triple singular point occurs when the two curves have contact of the second order. In this case the singular point corresponds to a point on the resonance curve diagram at which a resonance curve is tangential to $\mathscr{E}$.

The sequence of forms of the $\dot{\phi} = 0$ curves is shown in Figs. 3 and 4.

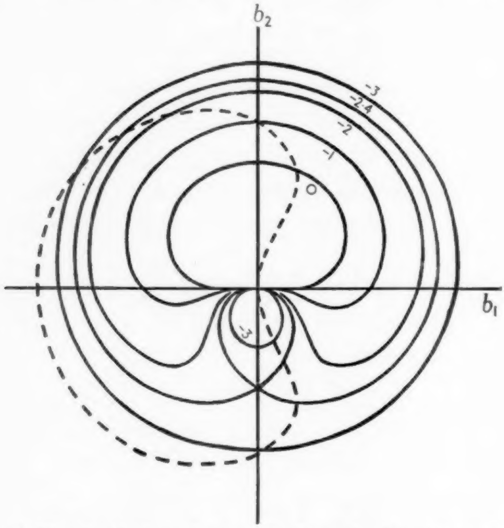

FIG. 3. The (b,ϕ)-plane for $\nu = \frac{1}{4}$, $F^2 = \frac{2}{27}$. The broken curve is $\dot{b} = 0$. The continuous curves are the $\dot{\phi} = 0$ curves for different values of x, the value of x being marked on each curve.

14. Character of the singular points

The variational equations in cartesian coordinates are

$$\dot{b}_1 = b_1(1-b^2)+b_2(x+\nu b^2)-F,$$
$$\dot{b}_2 = b_2(1-b^2)-b_1(x+\nu b^2).$$

If (b_0, ϕ_0) are the polar coordinates and (b_{10}, b_{20}) the cartesian coordinates of a singular point, while (B_1, B_2) are cartesian coordinates of a general point referred to this singularity as a new origin we may transform the variational equations to the form

$$\dot{B}_1 = P(B_1, B_2),$$
$$\dot{B}_2 = Q(B_1, B_2),$$

where P and Q are polynomials of the third degree.

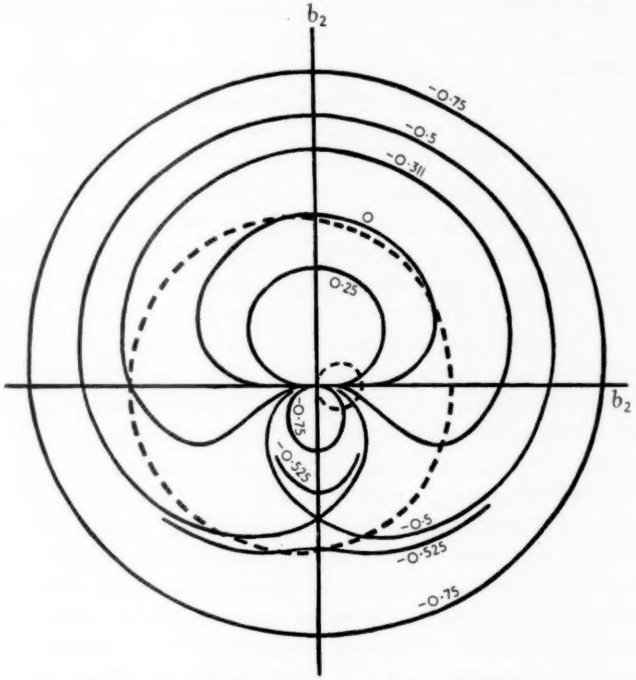

FIG. 4. Similar to Fig. 3, but with $\nu = 2$, $F^2 = 1$.

If the first-degree terms are

$$\dot{B}_1 = pB_1 + qB_2 + \dots,$$
$$\dot{B}_2 = rB_1 + sB_2 + \dots,$$

we obtain

$$p = 1 - b_0^2 + 2\nu b_{10} b_{20} - 2b_{10}^2,$$
$$q = x + \nu b_0^2 + 2\nu b_{20}^2 - 2b_{10} b_{20},$$
$$r = -x - \nu b_0^2 - 2b_{10} b_{20} - 2\nu b_{10}^2,$$
$$s = 1 - b_0^2 - 2\nu b_{10} b_{20} - 2b_{20}^2.$$

The characteristic equation

$$\lambda^2 - (p+s)\lambda + ps - qr = 0$$

becomes

$$\lambda^2 - 2(1-2y)\lambda + \mathscr{E}(x,y) = 0,$$

where $y = b_0^2$ refers to the singular point, and

$$\mathscr{E}(x,y) = (1-y)(1-3y) + (x+y)(x+3y).$$

Thus the singularity is a col if $\mathscr{E}(x,y)$ is negative, i.e. if it corresponds to a point within $\mathscr{E}$ on the resonance curve figure. If it corresponds to a point

outside $\mathscr{E}$, then $\mathscr{E}(x,y)$ is positive and it is a node or focus, stable if $2y-1$ is positive, i.e. $y > \frac{1}{2}$, and unstable if $y < \frac{1}{2}$.

The singularity is a node if the discriminant of (39) is positive, a focus if the discriminant is negative. The discriminant is

$$(1-2y)^2-\mathscr{E}(x,y),$$

which may be written

$$[\mathscr{P}(x,y)]^2-\mathscr{E}(x,y)\mathscr{E}(0,0),$$

where $\mathscr{P}(x,y) = 0$ is the polar of the origin with respect to $\mathscr{E}$. Thus the discriminant vanishes for singularities represented in the resonance curve diagram by points on the tangents from the origin to $\mathscr{E}$, which meet $\mathscr{E}$ on $y = \frac{1}{2}$ at $x = -\nu \pm \frac{1}{2}\sqrt{(1+\nu^2)}$. The discriminant is positive for singularities represented by points between these tangents, such singularities are therefore nodes. We thus obtain the scheme of singular points shown in Figs. 1 and 2. Only those parts of the resonance curves which are outside $\mathscr{E}$ and above $y = \frac{1}{2}$ represent stable and therefore physically realizable oscillations.

When there is no stable singularity there must be at least one stable limit cycle representing a combination oscillation, but the general consideration of limit cycles is rather involved and will be reserved for another paper.

The curve $\dot{b} = 0$ is the contact locus for circles with centre at the origin, and the points of any limit cycle at extreme radii from the origin must lie on this curve. When a singularity corresponds to the maximum of a resonance curve it is at the maximum radius of this locus and hence no limit cycle can enclose it. If it is the only singular point, then there can be no limit cycle, and the corresponding periodic solution of the original equation is its only stable solution to which all other solutions approach as $t \to \infty$. If three singularities exist, it is possible that in some ranges of the parameters a stable limit cycle may surround the unstable focus.

15. General remarks and conclusion

The differential equation considered is of interest from two points of view. Physically it gives a better approximation to the behaviour of real oscillators than the van der Pol equation. Unsymmetrical resonance curves resembling those shown in Figs. 1 and 2 are in fact obtained experimentally (**6**). Mathematically it shows in the first approximation the frequency deviation associated with the presence of higher harmonics, and the first approximations for both the free and forced oscillations cannot be obtained without considering the second harmonic.

Consequently, to obtain the equations of the first approximation by the methods of Kryloff and Bogolinboff or by Cartwright's difference equation the calculation has to be carried a stage farther than is necessary in the case of van der Pol's equation.

The method used in this paper gives the exact periodic solutions as convergent series, convergence being established directly by a comparison series of positive constants, the error due to using only a finite number of terms being dominated by the appropriate remainder of the comparison series. If convergence is assumed, the equations of the first approximation are obtained more directly.

Greaves's method for the free oscillation gives the exact solution, but convergence is established indirectly without any estimate of the error in retaining a finite number of terms. It requires modification when applied to the present equation and, like the other methods mentioned, has to be carried a stage farther to obtain the equations of the first approximation. Both methods derive from Lindstedt to the extent that secular terms are avoided in the calculation of the successive orders but the selection of the 'steady solution' of the present method seems more direct than Greaves's choice of integration constants, when it is not very obvious that a different choice would not lead to a different solution.

Finally, it is evident that the solution in powers of B which tends to zero with B must give the unstable oscillation of smaller amplitude when ω_1 is near to 1, though when ω_1 is not too near to 1 it may have an interval of convergence extending into the region of stable oscillations, $y > \frac{1}{2}$. It could be recovered from the more general solution by a reversion of the amplitude equation to develop the fundamental in powers of B. The exact interval of convergence will be determined near resonance by the branch point of b, considered as a function of B represented by points on the lower boundary of $\mathscr{E}$, on the resonance curve figure.

16. Acknowledgements

The author wishes to thank Mr. A. Geary and Dr. M. L. Cartwright for the interest they have shown in this work, and Dr. M. L. Cartwright for helpful suggestions regarding presentation.

REFERENCES

1. E. V. Appleton and W. M. H. Greaves, 'On the solution of the representative differential equation of the triode oscillator', *Phil. Mag.* (6) **45** (1923), 401, and W. M. H. Greaves, 'On a certain family of periodic solutions of differential equations with an application to the triode oscillator', *Proc. Roy. Soc.* A, **103** (1923), 516.
2. N. Kryloff and N. Bogolinboff, 'Introduction to non-linear mechanics', *Ann. Math. Studies*, No. 11 (Princeton, 1947).
3. ——— ——— loc. cit., p. 39.

4. J. Groskowski, 'The interdependence of frequency variations and harmonic content, and the problem of constant frequency oscillators', *Proc. Inst. Radio Eng.* **21** (1933), 958.

5. M. L. Cartwright, 'Contributions to the theory of non-linear oscillations', *Ann. Math. Studies*, No. 20 (Princeton, 1950), 202 et seq.

6. D. G. Tucker, 'Forced oscillations in oscillator circuits and the synchronization of oscillators', *J. Inst. E.E.* **92** (1946), 226.

RELAXATION METHODS APPLIED TO DETERMINE THE MOTION, IN TWO DIMENSIONS, OF A VISCOUS FLUID PAST A FIXED CYLINDER

By D. N. DE G. ALLEN (*Imperial College*) and
R. V. SOUTHWELL (*Cambridge*)

[Received 13 May 1954]

SUMMARY

In this paper relaxational techniques are applied to the general case of steady laminar motion of an incompressible viscous fluid past a stationary cylinder: that is, to motion at speeds such that neither inertia nor viscosity can be neglected. The governing equation is

$$[u\,\partial/\partial x+v\,\partial/\partial y-\nu\nabla^2]\zeta = 0,$$

where $\nabla^2 \equiv \partial^2/\partial x^2+\partial^2/\partial y^2$, u and v are the component velocities, ν is the kinematic viscosity, and ζ (the vorticity) $= \partial v/\partial x-\partial u/\partial y$. It must be solved in conjunction with the equation of continuity

$$\partial u/\partial x+\partial v/\partial y = 0,$$

which permits the introduction of a stream-function ψ such that

$$u = \partial\psi/\partial y, \qquad v = -\partial\psi/\partial x, \qquad \zeta = -\nabla^2\psi.$$

The numerical computations relate to a *circular* cylinder, but the methods are applicable to any shape (an initial conformal transformation changes the independent variables from x and y to α and β, the irrotational velocity-potential and stream-function for flow past the specified cylinder). The flow-patterns (contours of ψ and ζ) change as the 'Reynolds number' R increases; but an introduction of variables involving R makes the change relatively slow, and thereby (e.g.) the accepted solution for $R = 10$ is made a good starting assumption for $R = 100$.

Fig. 6 relates computed values of the total drag with experimental and other theoretical estimates.

1. Introduction. This paper treats two-dimensional (laminar) motion of an incompressible viscous fluid in the most general case—viz. when neither inertia nor viscosity can be neglected. The governing equations are the equation of continuity

$$\frac{\partial u}{\partial x}+\frac{\partial v}{\partial y}+\frac{\partial w}{\partial z} = 0 \tag{1}$$

and the dynamical conditions

$$\left[\frac{\partial}{\partial t}+u\frac{\partial}{\partial x}+v\frac{\partial}{\partial y}+w\frac{\partial}{\partial z}\right](u,v,w)$$
$$= -\frac{1}{\rho}\left[\frac{\partial}{\partial x},\frac{\partial}{\partial y},\frac{\partial}{\partial z}\right]p+(X,Y,Z)+\nu\nabla^2(u,v,w), \tag{2}$$

in which

$$\left.\begin{array}{l} u,\ v,\ w \text{ are the components of velocity,} \\ X,\ Y,\ Z \text{ are the components of body-force,} \\ p \text{ is the 'mean normal pressure',} \\ \rho \text{ is the density and} \\ \nu \text{ is the 'kinematic viscosity' of the fluid (\textit{both taken}} \\ \quad \text{\textit{here as constant}), and} \\ \nabla^2 \text{ stands for } \partial^2/\partial x^2+\partial^2/\partial y^2+\partial^2/\partial z^2. \end{array}\right\} \tag{3}$$

In two-dimensional motion $w = Z = 0$ and u, v, X, Y, p are independent of z, so (1) reduces to

$$\frac{\partial u}{\partial x}+\frac{\partial v}{\partial y} = 0 \tag{4}$$

and (2) to

$$\left[\frac{\partial}{\partial t}+u\frac{\partial}{\partial x}+v\frac{\partial}{\partial y}\right](u,v) = -\frac{1}{\rho}\left[\frac{\partial}{\partial x},\frac{\partial}{\partial y}\right]p+(X,Y)+\nu\nabla^2(u,v), \tag{5}$$

∇^2 now standing for $\qquad \partial^2/\partial x^2+\partial^2/\partial y^2. \qquad (6)$

We postulate that the body-forces are conservative so that

$$\frac{\partial X}{\partial y}-\frac{\partial Y}{\partial x} = 0, \tag{7}$$

and on that understanding, having regard to (4), we eliminate p from (5) to obtain for *steady* motion (independent of t)

$$[u\,\partial/\partial x+v\,\partial/\partial y]\zeta = \nu\nabla^2\zeta, \tag{8}$$

where ∇^2 has the significance stated in (6) and

$$\zeta \text{ (the vorticity)} = \partial v/\partial x-\partial u/\partial y. \tag{9}$$

2. In relation to plane two-dimensional motion (4), (8), and (9) have to be satisfied in conjunction with appropriate boundary conditions. This paper treats in detail flow past a rigid cylinder (with axis parallel to Oz) of a stream which otherwise (i.e., in the absence of the cylinder) would have uniform velocity U. When, as here, the cylinder is kept stationary, the conditions to be satisfied at its surface are

$$u = v = 0. \tag{10}$$

Other conditions (at infinity) will receive attention later.

3. Even when thus reduced to (4), (8), and (9) the general equations have hitherto proved intractable, except by approximate methods and as relating to fairly small velocities. High-speed solutions have been attained only by the introduction—by L. Prandtl in 1904—of assumptions based on the notion of a 'boundary layer' and of a 'wake' within which the effects of viscosity are confined; and even so it is necessary to *postulate*

the distribution of the pressure on the cylinder, which strictly should emerge as a result of computation. The only treatment known to us which dispenses with this postulate (**1**) relates to rather slow flow past a circular cylinder.† It has some points of similarity with our relaxational treatment (e.g. its evaluation of the stream-function ψ at discrete nodal points of a square-mesh net).

4. Here, too, flow past a *circular* cylinder is discussed, for the reasons (i) that both in theory and in experiment this shape has received more attention than others and (ii) that it is sufficiently 'bluff' to exemplify difficulties which such shapes may oppose to computation. Actually an initial step in the relaxational treatment makes the shape a matter of relatively small concern: namely, a conformal transformation which changes the independent variables from x and y to α and β, the velocity-potential and stream-function for irrotational steady flow past the given cylinder. Thereby the field of computation is transformed into an infinite plane containing a rectilinear slit, so computation can be effected on square-mesh nets having no 'irregular stars': the shape affects them only in that the transformed equations involve h, the modulus of transformation.

With a view to the numerical computations, all quantities are made 'non-dimensional'; and in consequence U (the velocity at infinity) appears in a numerical parameter

$$R = UL/\nu \tag{11}$$

(the Reynolds number of the motion) conjoined with ν and L, a representative dimension of the inserted cylinder. A further transformation which replaces β by $\beta'' = \beta R^{\frac{1}{2}}$ gives to the equations forms such that a solution found for some particular speed U_1 can be made a starting assumption from which, with relatively little computation, the solution for another speed U_2 can be derived. In sections 14–16 yet another transformation (devised by Allen) is employed to derive equations which, as involving exponentials, are not closely represented by the customary approximations in finite differences.

5. Results are presented in Figs. 1–7, of which their legends provide sufficient explanation. Figs. 1–5 exhibit, by contours of the 'non-dimensional' stream-function (ψ) and vorticity (ζ), the general characteristics of the flow when $R = 0, 1, 10, 10^2, 10^3$. Fig. 6 compares computed values of total 'drag' with experimental and with other theoretical estimates. Fig. 7 shows how the computed pressure-distribution alters with Reynolds number.

† Another treatment, also for fairly slow flow past a circular cylinder, has recently been reported by Kawaguti (**2**).

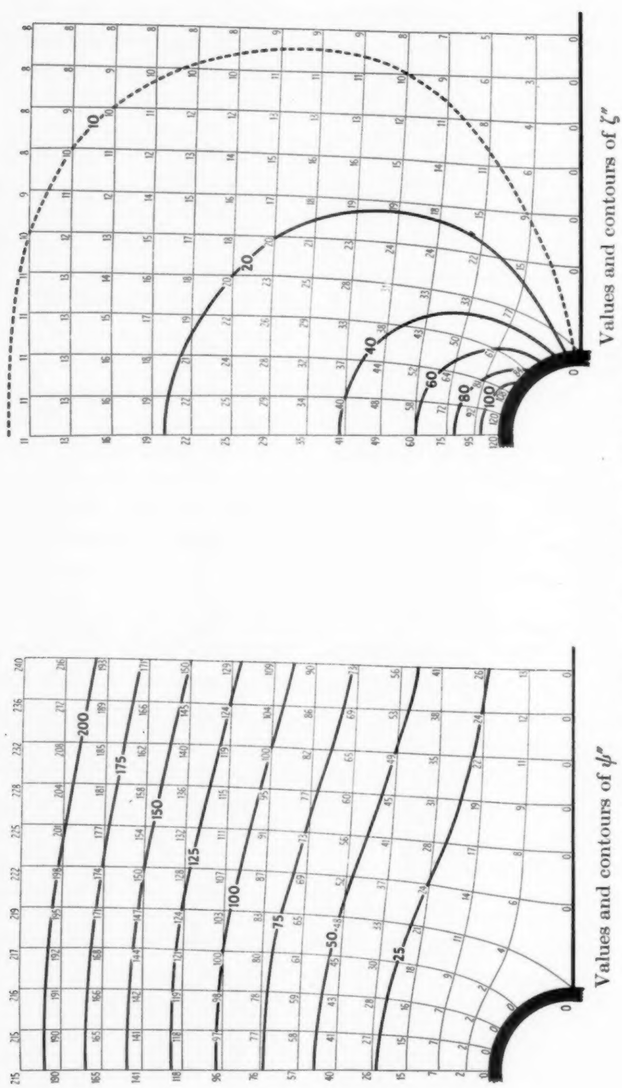

(N.B. For $R = 0$, only relative values are significant)

FIG. 1. Stream-function (ψ) and vorticity (ζ'') for Reynolds number $R = 0$.

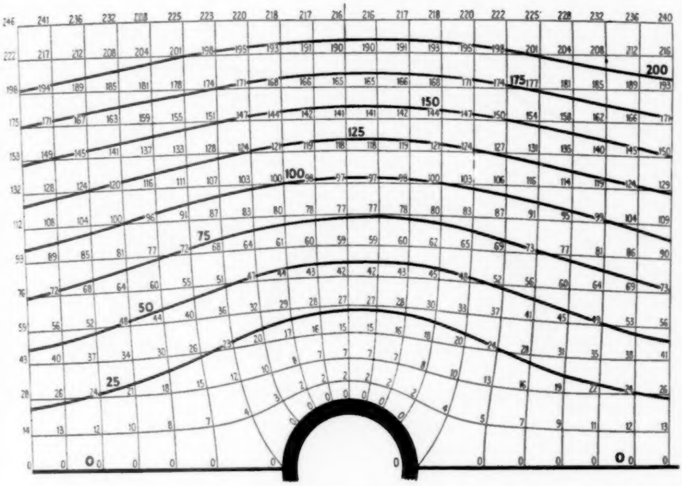

Values and contours of $100\psi''$

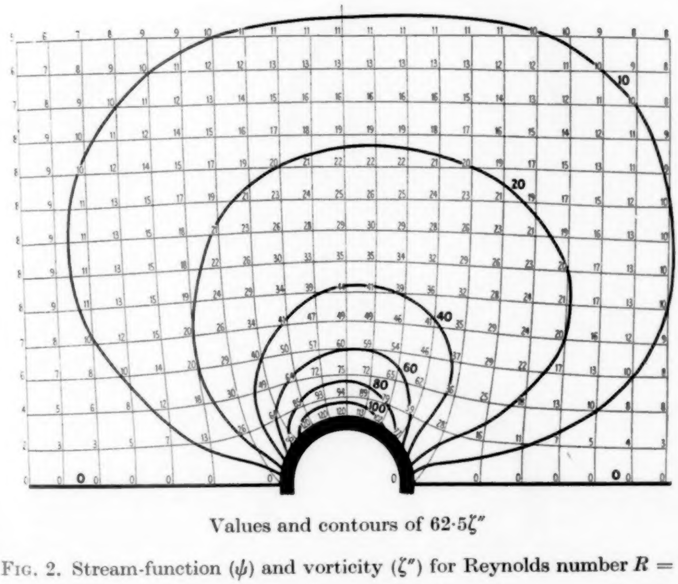

Values and contours of $62{\cdot}5\zeta''$

FIG. 2. Stream-function (ψ) and vorticity (ζ'') for Reynolds number $R = 1$.

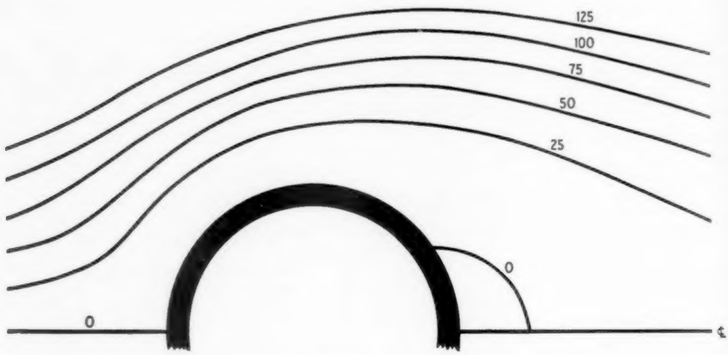

FIG. 3 (*a*). Stream-function ($100\psi''$) for $R = 10$.

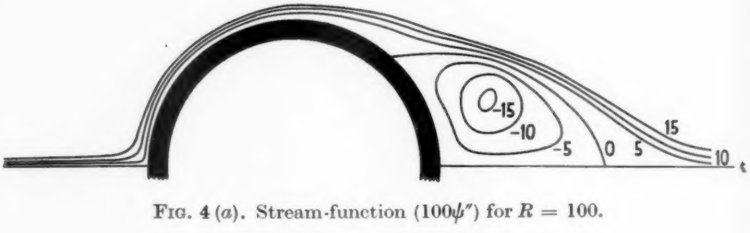

FIG. 4 (*a*). Stream-function ($100\psi''$) for $R = 100$.

FIG. 5 (*a*). Stream-function ($100\psi''$) for $R = 1000$.

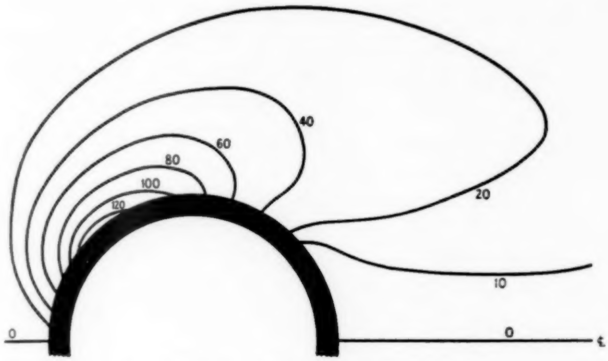

FIG. 3 (*b*). Vorticity ($62{\cdot}5\zeta''$) for $R = 10$.

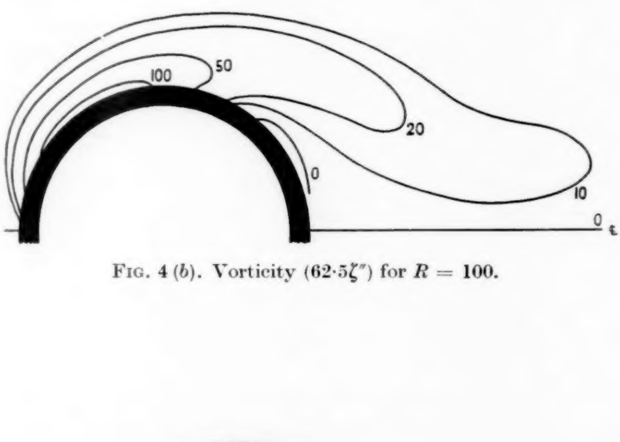

FIG. 4 (*b*). Vorticity ($62{\cdot}5\zeta''$) for $R = 100$.

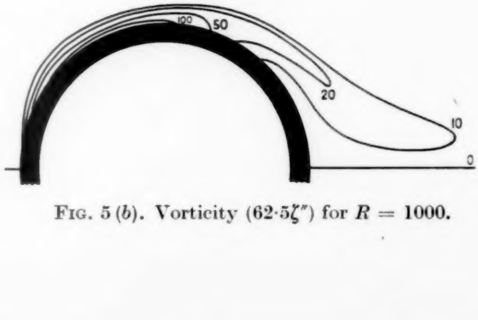

FIG. 5 (*b*). Vorticity ($62{\cdot}5\zeta''$) for $R = 1000$.

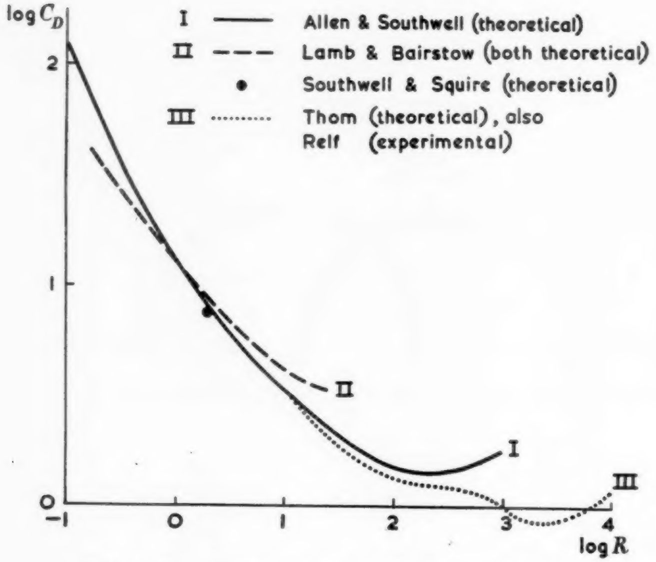

FIG. 6. Drag-coefficient (C_D) as a multiple of $\frac{1}{2}\rho U^2 L$.

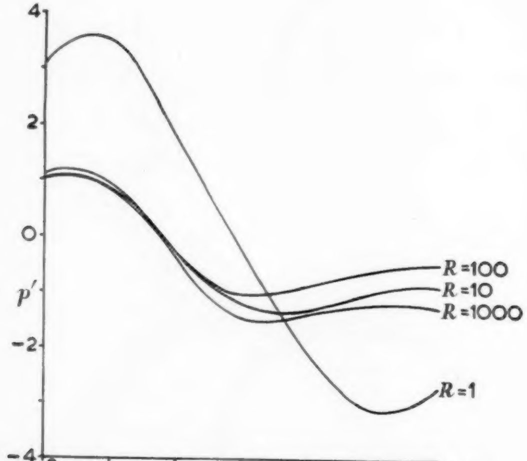

FIG. 7. Pressure (p') as a multiple of $\frac{1}{2}\rho U^2$.

6. In this connexion a word should be said about ***stability***. It is the essence of the relaxational technique that it starts from solutions which, being inexact, would require body-forces for their maintenance, and thereafter systematically corrects the flow-pattern until the body-forces have been 'liquidated' (rendered negligible). Such treatment, though it does not contemplate instability, will normally detect any tendency of a solution to diverge, and in this way will indicate the occurrence of instability, though it cannot precisely determine the point of transition. It seems worth while to record that in this problem the flow appeared to be stable for $R = 10$, but a distinct impression of instability was gained in the computation for $R = 100$; for (Goldstein *et al.* **3**, p. 419) 'the value of R at which the unsteady régime commences . . . is probably about 50'.†

The instability entailed no computational difficulty: that is to say, steady régimes could be computed for $R = 100$ and for $R = 1000$ which in experiment would not be realizable because the smallest disturbance would upset them.

7. **The governing equations.** For two-dimensional flow the governing equations are (4)–(9), and the conditions (10) have to be satisfied at the boundary of the inserted cylinder. The relation (4) permits expression of u and v in terms of a stream-function ψ by

$$u = \partial\psi/\partial y, \qquad v = -\partial\psi/\partial x, \tag{12}$$

and then, according to (9), $\quad \zeta = -\nabla^2\psi \quad$ (13)

where ∇^2 has the significance stated in (6). At the boundary of the inserted cylinder ψ must satisfy conditions derived from (10)—viz.

$$\partial\psi/\partial x = 0, \qquad \partial\psi/\partial y = 0. \tag{14}$$

As 'conditions at infinity' we shall assume that

$$\psi \to Uy, \quad \text{so that} \quad \zeta \to 0. \tag{15}$$

8. **Reduction of the equations to 'non-dimensional' form.** Using L to denote some representative dimension (e.g. the diameter) of the cylinder, and U to denote the velocity at infinity, we now write

$$x = Lx', \quad y = Ly', \quad u = Uu', \quad v = Uv', \quad \psi = UL\psi'. \tag{16}$$

Then, according to (13),

$$\zeta = \frac{U}{L}\zeta', \quad \text{where} \quad -\zeta' = \nabla'^2\psi', \tag{17}$$

† Kawaguti (**2**) found no evidence of instability in his calculations for $R = 40$.

and according to (8)

$$R\left(u'\frac{\partial\zeta'}{\partial x'}+v'\frac{\partial\zeta'}{\partial y'}\right) = \nabla'^2\zeta', \tag{18}$$

where R (the Reynolds number of the motion) $= UL/\nu$ (11) *bis*

and $$\nabla'^2 \equiv \partial^2/\partial x'^2+\partial^2/\partial y'^2. \tag{19}$$

Also, by (12) and (16),

$$u' = \partial\psi'/\partial y', \qquad -v' = \partial\psi'/\partial x',$$

so the boundary conditions (14) and (15) become

$$\left.\begin{array}{l} u' = 0,\ v' = 0, \text{ at the surface of the inserted cylinder,} \\ u' = 1,\ v' = 0, \text{ far away from the inserted cylinder.} \end{array}\right\} \tag{20}$$

9. First change of independent variables (to avoid 'irregular stars'). We can avoid 'irregular stars' in the relaxational computations by changing the variables from x' and y' to α and β, the velocity-potential and stream-function for irrotational flow past the cylinder under discussion.† Far up-stream

$$\alpha \to x'+\text{constant}, \quad \beta \to y', \tag{21}$$

and on the surface of the cylinder (and in the plane of symmetry)

$$\beta = 0. \tag{22}$$

Here α and β are conjugate plane-potential functions such that $(\alpha+i\beta)$ is a function of $(x'+iy')$. Accordingly

$$\frac{\partial\alpha}{\partial x'} = \frac{\partial\beta}{\partial y'}, \qquad -\frac{\partial\alpha}{\partial y'} = \frac{\partial\beta}{\partial x'}, \tag{23}$$

and writing $$h^2 \equiv \left(\frac{\partial\alpha}{\partial x'}\right)^2+\left(\frac{\partial\alpha}{\partial y'}\right)^2 = \left(\frac{\partial\beta}{\partial x'}\right)^2+\left(\frac{\partial\beta}{\partial y'}\right)^2 \tag{24}$$

we have $$\frac{\partial}{\partial x'} \equiv \frac{\partial\alpha}{\partial x'}\frac{\partial}{\partial\alpha}+\frac{\partial\beta}{\partial x'}\frac{\partial}{\partial\beta}, \qquad \frac{\partial}{\partial y'} \equiv \frac{\partial\alpha}{\partial y'}\frac{\partial}{\partial\alpha}+\frac{\partial\beta}{\partial y'}\frac{\partial}{\partial\beta},$$

therefore $$\left.\begin{array}{l} \nabla'^2 \equiv h^2[\partial^2/\partial\alpha^2+\partial^2/\partial\beta^2] = h^2\nabla^2_{\alpha\beta} \text{ (say),} \\ u'\dfrac{\partial}{\partial x'}+v'\dfrac{\partial}{\partial y'} \equiv h^2\left[\dfrac{\partial\psi'}{\partial\beta}\dfrac{\partial}{\partial\alpha}-\dfrac{\partial\psi'}{\partial\alpha}\dfrac{\partial}{\partial\beta}\right]. \end{array}\right\} \tag{25}$$
(and)

Consequently (17) transforms to

$$-\zeta' = h^2\nabla^2_{\alpha\beta}\psi', \tag{26}$$

and (18) transforms to

$$R\left(\frac{\partial\psi'}{\partial\beta}\frac{\partial\zeta'}{\partial\alpha}-\frac{\partial\psi'}{\partial\alpha}\frac{\partial\zeta'}{\partial\beta}\right) = \nabla^2_{\alpha\beta}\zeta'. \tag{27}$$

† This device was employed by Thom (**1**). Kawaguti (**2**) employs an iterative process generally similar to Thom's, but a different transformation (into a *finite* rectangle).

The transformed boundary conditions are

$$\left.\begin{array}{l} \psi' = \dfrac{\partial\psi'}{\partial\beta} = 0 \text{ on that part of the } \alpha\text{-axis } (\beta = 0) \text{ which} \\ \qquad\qquad \text{corresponds with the inserted cylinder,} \\ \psi' = \zeta' = 0 \text{ (by symmetry) on all other parts of the } \alpha\text{-axis,} \\ \dfrac{\partial\psi'}{\partial\alpha} \to 0, \quad \dfrac{\partial\psi'}{\partial\beta} \to 1, \quad \zeta' \to 0 \quad \text{as } (\alpha^2+\beta^2) \to \infty. \end{array}\right\} \tag{28}$$

10. Second change of variables (to facilitate approximate treatment). The product terms in (26) and (27) imply that the flow-pattern alters with the Reynolds number. But it is evident, even when we envisage 'break-away', that the α-gradients of ψ' and ζ' will not be large, whereas their β-gradients may attain high values; and on that account a further transformation is advantageous.

If β, ψ', ζ' are replaced by β'', ψ'', ζ'', where

$$\beta = R^{-\frac{1}{2}}\beta'', \qquad \psi' = R^{-\frac{1}{2}}\psi'', \qquad \zeta' = R^{\frac{1}{2}}\zeta'', \tag{29}$$

(26) is transformed to

$$-\zeta'' = h^2\nabla''^2\psi'', \tag{30}$$

and (27) to

$$\nabla''^2\zeta'' = \frac{\partial\zeta''}{\partial\alpha}\frac{\partial\psi''}{\partial\beta''} - \frac{\partial\zeta''}{\partial\beta''}\frac{\partial\psi''}{\partial\alpha}, \tag{31}$$

where

$$\nabla''^2 \equiv \frac{1}{R}\nabla^2_{\alpha\beta} \equiv \frac{1}{R}\frac{\partial^2}{\partial\alpha^2} + \frac{\partial^2}{\partial\beta''^2}. \tag{32}$$

Also from (27) and (28) it follows that

$$\left.\begin{array}{l} \psi'' = \dfrac{\partial\psi''}{\partial\beta''} = 0 \text{ on that part of the } \alpha\text{-axis } (\beta'' = 0) \text{ which} \\ \qquad\qquad \text{corresponds with the inserted cylinder,} \\ \psi'' = \zeta'' = 0 \text{ on all other parts of the } \alpha\text{-axis,} \\ \dfrac{\partial\psi''}{\partial\alpha} \to 0, \quad \dfrac{\partial\psi''}{\partial\beta''} \to 1, \quad \zeta'' \to 0, \quad \text{as } (R\alpha^2+\beta''^2) \to \infty. \end{array}\right\} \tag{33}$$

Thus R now disappears from the equations, excepting as it enters into ∇''^2; and on the assumption that the derivatives of ψ'' and ζ'' with respect to α and to β'' are comparable, when R is large a close approximation to (32) is

$$\nabla''^2 \doteqdot \partial^2/\partial\beta''^2, \tag{34}$$

which makes the distribution both of ψ'' and of ζ'' independent of R, and thereby greatly reduces the labour of a relaxational treatment. This aims at systematic elimination of residuals which express the errors of a trial solution; and now the errors entailed when the solution for $R = 10$ (say)

is taken as a trial solution for $R = 100$ are small enough to require but little adjustment. Then the solution for $R = 100$ may be utilized, similarly, as a trial solution for $R = 1000$; and so on. (R may be either increased or decreased in successive solutions. Our sequence was $R = 1000$, 100, 0, 1, 10.)

11. Introduction of the relaxation technique. We now describe the application to our present problem of the relaxational techniques which have been explained in earlier papers. They are not required for the transformation of section 9 in relation to a *circular* cylinder, since the known solution can be utilized. It is

$$\left.\begin{aligned}\alpha &= x'\left\{1+\frac{1}{4(x'^2+y'^2)}\right\}\\ \beta &= y'\left\{1-\frac{1}{4(x'^2+y'^2)}\right\}\\ h^2 &= 1+\frac{1-8(x'^2-y'^2)}{16(x'^2+y'^2)^2}\end{aligned}\right\}, \tag{35}$$

when Ox, Oy pass through the axis and when L—the representative dimension—is the diameter of the cylinder. With a use of these expressions the transformation is easy (Fig. 8).

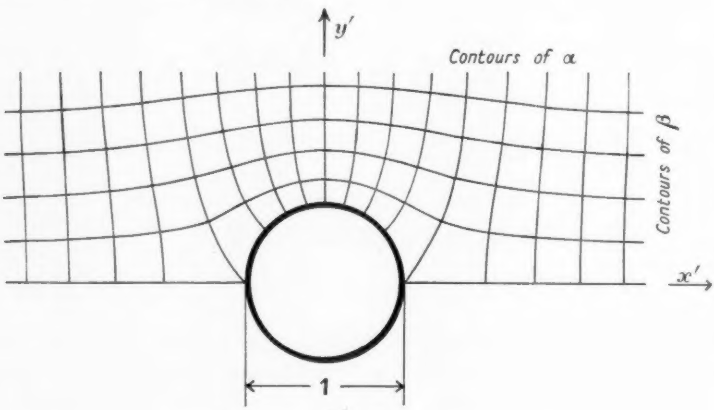

FIG. 8.

12. *Hereafter we shall give to β, ψ, ζ the meanings which in section* 10 *were attached to β'', ψ'', ζ''.* On that understanding (30) will now be written as

$$\frac{\partial^2\psi}{\partial\beta^2}+\frac{1}{R}\frac{\partial^2\psi}{\partial\alpha^2} = -\frac{\zeta}{h^2}, \tag{36}$$

and (31), after some rearrangement, as

$$\frac{\partial^2\zeta}{\partial\beta^2}+\left(\frac{\partial\psi}{\partial\alpha}\right)\frac{\partial\zeta}{\partial\beta}+\frac{1}{R}\left\{\frac{\partial^2\zeta}{\partial\alpha^2}-R\frac{\partial\psi}{\partial\beta}\frac{\partial\zeta}{\partial\alpha}\right\}=0. \tag{37}$$

It is not necessary to rewrite the boundary conditions (33).

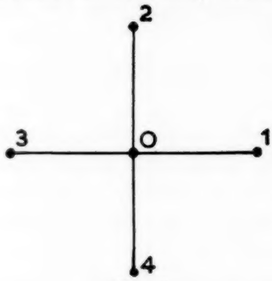

FIG. 9.

For a relaxational treatment, (36) and (37) must be replaced by approximations in finite differences. Since (36) is linear, it presents no difficulty: in the notation of 'residuals' (4) its approximation is

$$(F_\psi)_0 \equiv \psi_2+\psi_4-2\psi_0+\frac{1}{R}(\psi_1+\psi_3-2\psi_0)+a^2(\zeta/h^2)_0=0, \tag{38}$$

the suffixes 0, 1, 2, 3, and 4 denoting points so numbered in Fig. 9;

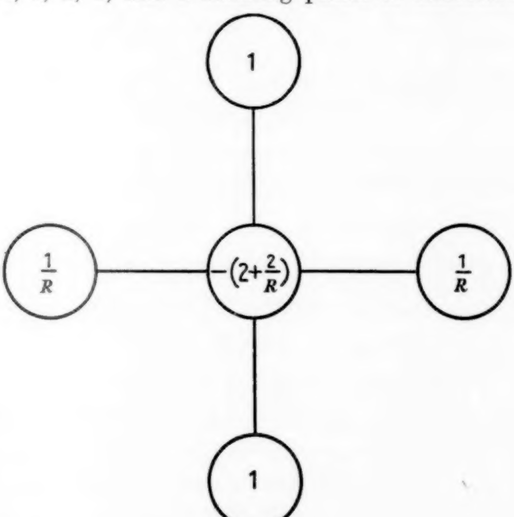

FIG. 10.

and from (38) it is easy to deduce the standard 'pattern' shown in Fig. 10, for the effect on the F_ψ's of an increment $\Delta\psi = 1$ at 0, Fig. 9.

13.† Equation (37) presents a harder problem, and being non-linear yields a 'pattern' which alters as the work proceeds. But it has been shown in earlier papers that inaccurate patterns can be used to liquidate residuals, provided that an exact account of these is kept; and here a simple pattern represents sufficiently a relation of rather complicated form.

We contemplate a 'two-diagram technique' in which ψ and ζ are modified alternately. At the end of a stage of ζ-relaxation the F_ψ's will have altered in accordance with the last term of (38), and the ψ's must be altered so as (temporarily) to liquidate them: then, with the altered values given to ψ, the ζ's must be modified in accordance with a finite-difference approximation to (37). This we proceed to derive.

14. The two quantities which together make up (37)—namely,

$$\left.\begin{aligned} &(a) \quad \frac{\partial^2\zeta}{\partial\beta^2}+\frac{\partial\psi}{\partial\alpha}\frac{\partial\zeta}{\partial\beta} \\ \text{and} \qquad &(b) \quad \frac{\partial^2\zeta}{\partial\alpha^2}-R\frac{\partial\psi}{\partial\beta}\frac{\partial\zeta}{\partial\alpha} \end{aligned}\right\} \tag{39}$$

—can be treated similarly in a way we now explain in relation to (a). Writing

$$\kappa \equiv \frac{\partial\psi}{\partial\alpha}, \qquad A \equiv \frac{\partial^2\zeta}{\partial\beta^2}+\kappa\frac{\partial\zeta}{\partial\beta}, \tag{40}$$

we have as the solution of the second of (40) *when κ and A are invariant*

$$\kappa\zeta = A\beta+P+Qe^{-\kappa\beta},$$

P and Q being constants of integration. Then, 2, 0 and 4 denoting adjacent nodes on a β-line of the α–β net (so that

$$\beta_2 = \beta_0+a, \qquad \beta_4 = \beta_0-a$$

when a, as is usual, denotes the mesh-length), we have

$$\kappa(\zeta_2-\zeta_0) = Aa+Qe^{-\kappa\beta_0}(e^{-\kappa a}-1),$$

$$\kappa(\zeta_4-\zeta_0) = -Aa+Qe^{-\kappa\beta_0}(e^{\kappa a}-1),$$

therefore $$\kappa\{e^{\kappa a}(\zeta_2-\zeta_0)+\zeta_4-\zeta_0\} = Aa(e^{\kappa a}-1).$$

We thus have an expression for A—i.e. for (a) of (39); and a like expression may be formed in the same way for (b). The values of κ $(\equiv \partial\psi/\partial\alpha)$ and of λ $(\equiv -R\,\partial\psi/\partial\beta)$, the corresponding quantity in the expression for (b), will of course not be known until the solution has been completed; but they may be treated as known when ψ has been *temporarily* determined,

† It should be recorded that the technique described in Sections 13–16 is entirely due to Allen (R.V.S.).

and values appropriate to the point 0 may be computed from finite-difference expressions of normal form: viz. from

$$2\kappa a = \psi_1 - \psi_3, \qquad 2\lambda a = -R(\psi_2 - \psi_4).$$

We then have as an expression for the typical ζ-residual, defined as the finite-difference approximation to $a^2 \times$[left-hand side of (37)]:

$$(F_\zeta)_0 \equiv \kappa_0 a\{e^{\kappa_0 a}(\zeta_2 - \zeta_0) + \zeta_4 - \zeta_0\}/(e^{\kappa_0 a} - 1) +$$
$$+ \lambda_0 a\{e^{\lambda_0 a}(\zeta_1 - \zeta_0) + \zeta_3 - \zeta_0\}/R(e^{\lambda_0 a} - 1). \quad (41)$$

(It is the latent exponentials in the solution, revealed in (41), which necessitate this special treatment. Except within a very narrow range, an exponential is not closely represented by a polynomial; and on that account the customary expression in finite differences for the second term in (39), (*a*) or (*b*), has insufficient accuracy when κ_0 and/or λ_0 is not small.)

15. Regard must be paid, in liquidation, to the boundary conditions (33), section 10. Rewritten in accordance with section 12, and with

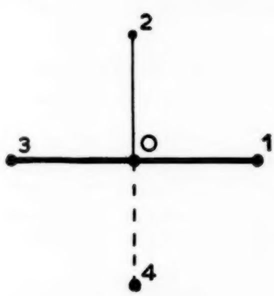

FIG. 11.

derivatives replaced by their approximations in finite differences, these become

at all nodes on the α-axis except the 'slit' (i.e. that part which corresponds with the inserted cylinder):

$$\psi = \zeta = 0;$$

at nodes far away from the 'slit' (where $\alpha^2 + \beta^2 \to \infty$): (42)

$$\psi \to \beta, \qquad \zeta \to 0;$$

at nodes on the 'slit' (typified by 0, Fig. 11, in which the node 4 is 'fictitious'):

$$\psi_0 = 0, \qquad \psi_2 = \psi_4.$$

Only the last of (42) needs special notice. Combined with (38) of section 12 (which here reduces to

$$\psi_2+\psi_4+\frac{a^2}{h_0^2}\zeta_0 = 0$$

because $\psi_3 = \psi_0 = \psi_1 = 0$), it becomes

$$\zeta_0 = -2h_0^2\psi_2/a^2, \tag{43}$$

so permits, at the start of each stage of 'ζ-relaxation', a specification of ζ at all nodes on the α-axis.

16. Except in its use of 'patterns' which alter as the work proceeds and which call for a use of exponential tables, the relaxational procedure follows normal lines; 'residuals' of the types $\mathbf{F}_\psi$ and $\mathbf{F}_\zeta$ being liquidated *alternately, in stages.* Small changes made in ζ-values were found to alter ψ-values largely, and on that account the F_ζ's were liquidated more or less completely; but the stages of 'ψ-relaxation' were made short because the F_ψ's became smaller almost automatically by reason of the changes made in the ζ's.

17. When acceptable distributions have been found for ψ and ζ as functions of α and β—that is, in the notation of section 10, for ψ'' and ζ'' as functions of α and β''—the transformations (29) will yield ψ' and ζ' in terms of α and β, which have the expressions (35) in terms of x' and y'. Contours of ψ'' and ζ'' can then be plotted on the rectangular (x', y') net. Figs. 1–5 were thus derived.

For Figs. 6 and 7, expressions for the boundary tractions were required. It can be shown (cf., e.g., (**5**), sections 325–6) that the normal pressure on the circular cylinder is

$$-p_{nn}\ (\text{say}) = p-2\nu\rho\cos 2\theta\frac{\partial^2\psi}{\partial x\partial y}+\nu\rho\sin 2\theta\left[\frac{\partial^2}{\partial y^2}-\frac{\partial^2}{\partial x^2}\right]\psi$$

and the tangential traction (upstream) on the cylinder is (44)

$$p_{ns}\ (\text{say}) = \nu\rho\cos 2\theta\left[\frac{\partial^2}{\partial y^2}-\frac{\partial^2}{\partial x^2}\right]\psi+2\nu\rho\sin 2\theta\frac{\partial^2\psi}{\partial x\partial y}$$

at a point whose angular distance from the upstream stagnation-point is θ. At points on the boundary $\left(\text{where } \psi = \frac{\partial\psi}{\partial\alpha} = \frac{\partial^2\psi}{\partial\alpha^2} = 0, \text{ so } \zeta = h^2\frac{\partial^2\psi}{\partial\beta^2}\right)$

$$\frac{\partial^2\psi}{\partial x\partial y} \equiv \frac{\partial^2\alpha}{\partial x^2}\frac{\partial\psi}{\partial\beta}+\frac{\zeta}{h^2}\frac{\partial\alpha}{\partial x}\frac{\partial\alpha}{\partial y}+\left\{\left(\frac{\partial\alpha}{\partial x}\right)^2-\left(\frac{\partial\alpha}{\partial y}\right)^2\right\}\frac{\partial^2\psi}{\partial\alpha\partial\beta},$$

$$\frac{\partial^2\psi}{\partial y^2}-\frac{\partial^2\psi}{\partial x^2} \equiv \zeta\left\{1-\frac{2}{h^2}\left(\frac{\partial\alpha}{\partial x}\right)^2\right\}+2\frac{\partial^2\alpha}{\partial x\partial y}\frac{\partial\psi}{\partial\beta}+4\frac{\partial\alpha}{\partial x}\frac{\partial\alpha}{\partial y}\frac{\partial^2\psi}{\partial\alpha\partial\beta},$$

and p, the 'mean normal pressure' (section 1), is related with p_s, the 'static pressure at infinity', by

$$p_s - p = \tfrac{1}{2}\rho h^2\left(\frac{\partial\psi}{\partial\beta}\right)^2 + \mu \int_{-\infty} \frac{\partial\zeta}{\partial\beta}\,d\alpha. \tag{45}$$

Consequently

$$\left.\begin{aligned} -p_{nn} &= p_s - \rho U^2 \int_{-\infty} \frac{\partial\zeta''}{\partial\beta''}\,d\alpha \\ p_{ns} &= \rho U^2 \zeta''/R^{\frac{1}{2}} \end{aligned}\right\}, \tag{46}$$

at a point on the boundary (where, by (35), $\alpha = 2x' = -\cos\theta$, $\beta = 0$). From (45) and (46) the 'drag' (Fig. 6) and pressure-distribution (Fig. 7) were computed: Fig. 6 by integration of

$$-(p_{ns}\sin\theta + p_{nn}\cos\theta).$$

18. This investigation, started in 1944, was frequently interrupted on account of pressure of more immediately urgent problems. An interim account of it was presented at the International Congress of Applied Mechanics (London) in 1948.

Work done since 1948 has been aided financially by a benefaction which the Worshipful Company of Clothworkers made to Imperial College in 1945 for the promotion of relaxational research. We gratefully acknowledge this assistance.

REFERENCES

1. A. Thom, *Proc. Roy. Soc.* A, **141** (1933), 651–69.
2. M. Kawaguti, *J. Phys. Soc. Japan*, **8** (1953), 747–57.
3. S. Goldstein *et al.*, *Modern Developments in Fluid Dynamics* (1st ed.) (Oxford, 1948).
4. R. V. Southwell, *Relaxation Methods in Theoretical Physics* (1st ed.) (Oxford, 1946).
5. H. Lamb, *Hydrodynamics* (6th ed.) (Cambridge, 1932).

ROTATORY AND LONGITUDINAL OSCILLATIONS OF AXI-SYMMETRIC BODIES IN A VISCOUS FLUID

By R. P. KANWAL (*Indian Institute of Technology, Kharagpur*)

[Received 29 April 1954]

SUMMARY

The Stokes stream function is used to obtain the perturbations arising from the slow rotatory and longitudinal oscillations of axi-symmetrical bodies in an infinite mass of viscous fluid which is at rest at infinity. The bodies considered in this paper are a sphere, an infinite circular cylinder, a prolate spheroid, an oblate spheroid, and a circular disk. The case of the circular disk is deduced as a limiting case of the oblate spheroid. The paper has been divided into two parts. Part I deals with the rotatory oscillations and Part II with the longitudinal ones.

1. Introduction

THE perturbations arising from the longitudinal vibrations of a sphere along a diameter in an infinite mass of viscous fluid at rest have been considered by the author (**1**) by applying the idea of periodic singular points, and the results are found to agree with those found by Lamb (**2**). The rotatory oscillations of a sphere about a diameter, in an infinite mass of viscous fluid at rest, have been discussed by Lamb (**2**). The object of this paper is to utilize the Stokes stream function to obtain the motion of the fluid due to the rotatory and longitudinal oscillations of certain axi-symmetric bodies in a viscous fluid. The slow motion, in which the inertia terms in the equations of motion are neglected, is considered in the case when the bodies are in the form of a sphere, an infinite circular cylinder, a prolate spheroid, an oblate spheroid, and a circular disk. The rotatory oscillations are about a diameter in the case of a sphere, about its axis in the case of an infinite circular cylinder, about their axes of symmetry in the cases of spheroids, and about the normal axis through its centre in the case of a circular disk. The case of the circular disk has been discussed as a limiting case of the oblate spheroid. The longitudinal oscillations are along the same axes about which the rotatory oscillations of respective bodies have been considered. Some of the results obtained agree with results already known, while others appear to be new. For spheroids it is found that we have to use spheroidal wave functions discussed by Stratton, Morse, Chu, and Hutner (**3**). The notation given by them will be used throughout this paper.

2. Equations of motion

Let α, β, γ be the general orthogonal coordinates and let the elements of length at the point (α, β, γ) in the directions of α, β, γ increasing, respectively, be $e_1\,d\alpha$, $e_2\,d\beta$, and $e_3\,d\gamma$, such that

$$ds^2 = e_1^2(d\alpha)^2+e_2^2(d\beta)^2+e_3^2(d\gamma)^2.$$

Let u, v, w be respectively the components of the velocity in the directions of α, β, γ increasing. For motion symmetrical about an axis (**4**) we take α and β to be the general orthogonal coordinates in a meridian plane and γ the azimuthal angle ϕ, so that e_3 will be the distance from the axis of revolution. All quantities are supposed to be independent of ϕ. The equation of continuity then takes the form

$$\frac{\partial}{\partial\alpha}(e_2 e_3 u)+\frac{\partial}{\partial\beta}(e_3 e_1 v) = 0, \tag{1}$$

so that there is a stream-function ψ such that

$$e_3 u = \frac{1}{e_2}\frac{\partial\psi}{\partial\beta}, \qquad e_3 v = -\frac{1}{e_1}\frac{\partial\psi}{\partial\alpha}. \tag{2}$$

This is true whether the velocity w round the axis is zero or not so long as it is independent of ϕ. In the case when there is an azimuthal velocity w, we put

$$e_3 w = \Omega;$$

then ξ, η, ζ, the components of vorticity, are given by

$$\xi = \frac{1}{e_2 e_3}\frac{\partial\Omega}{\partial\beta}, \qquad \eta = -\frac{1}{e_3 e_1}\frac{\partial\Omega}{\partial\alpha},$$

and $$\zeta = -\frac{1}{e_1 e_2}\left[\frac{\partial}{\partial\alpha}\left(\frac{e_2}{e_3 e_1}\frac{\partial\psi}{\partial\alpha}\right)+\frac{\partial}{\partial\beta}\left(\frac{e_1}{e_3 e_2}\frac{\partial\psi}{\partial\beta}\right)\right] = -\frac{1}{e_3}D^2\psi,$$

where $$D^2 = \frac{e_3}{e_1 e_2}\left[\frac{\partial}{\partial\alpha}\left(\frac{e_2}{e_3 e_1}\frac{\partial}{\partial\alpha}\right)+\frac{\partial}{\partial\beta}\left(\frac{e_1}{e_3 e_2}\frac{\partial}{\partial\beta}\right)\right].$$

The equations of motion give

$$\frac{\partial}{\partial t}(D^2\psi)+\frac{2\Omega}{e_1 e_2 e_3^2}\frac{\partial(\Omega, e_3)}{\partial(\alpha,\beta)}-\frac{1}{e_1 e_2 e_3}\frac{\partial(\psi, D^2\psi)}{\partial(\alpha,\beta)}+\frac{2D^2\psi}{e_1 e_2 e_3^2}\frac{\partial(\psi, e_3)}{\partial(\alpha,\beta)} = \nu D^4\psi,$$

which, if we neglect the second-order terms, becomes

$$\frac{\partial}{\partial t}(D^2\psi) = \nu D^4\psi, \tag{3}$$

which is the equation for ψ; likewise, the equation for Ω is

$$\frac{\partial\Omega}{\partial t}-\frac{1}{e_1 e_2 e_3}\frac{\partial(\psi, \Omega)}{\partial(\alpha,\beta)} = \nu D^2\Omega. \tag{4}$$

(*a*) *Rotatory oscillations.* In this case

$$u = 0, \qquad v = 0, \qquad e_3 w = \Omega.$$

Thus $\psi = 0$ and the equation (3) is automatically satisfied. The motion is given by the equation (4), which reduces to

$$\frac{\partial\Omega}{\partial t} = \nu D^2\Omega. \tag{5}$$

(*b*) *Longitudinal oscillations.* In this case

$$e_3 u = \frac{1}{e_2}\frac{\partial\psi}{\partial\beta}, \qquad e_3 v = -\frac{1}{e_1}\frac{\partial\psi}{\partial\alpha}, \qquad w = 0.$$

Hence $\Omega = 0$, the equation (4) is satisfied, and the motion is given by the equation (3), which now may be written as

$$D^2\left(D^2 - \frac{1}{\nu}\frac{\partial}{\partial t}\right)\psi = 0. \tag{6}$$

If ψ_1 and ψ_2 be two functions satisfying the equations

$$D^2\psi_1 = 0, \tag{7}$$

$$\left(D^2 - \frac{1}{\nu}\frac{\partial}{\partial t}\right)\psi_2 = 0, \tag{8}$$

a solution of the equation (6) may be written as

$$\psi = \psi_1 + \psi_2. \tag{9}$$

Thus we have to solve the equations (7) and (8). The superposition of their solutions will give the required stream function.

To satisfy the conditions at the surface of the body in this case we take the origin (2) at the mean position of the centre of the body.

Part I: Rotatory Oscillations

I. *Sphere oscillating about a diameter*

3. Taking spherical polar coordinates R, θ, ϕ for α, β, γ respectively, we get

$$e_1 = 1, \qquad e_2 = R, \qquad e_3 = R\sin\theta,$$

and

$$u = 0, \qquad v = 0, \qquad w = \Omega/R\sin\theta.$$

The equation of motion for harmonic oscillations of period $2\pi/\sigma$ is

$$\frac{\partial^2\Omega_1}{\partial R^2} + \frac{\sin\theta}{R^2}\frac{\partial}{\partial\theta}\left(\frac{1}{\sin\theta}\frac{\partial\Omega_1}{\partial\theta}\right) + h^2\Omega_1 = 0, \tag{10}$$

where

$$\Omega = \Omega_1 e^{i\sigma t}, \qquad h^2 = -i\sigma/\nu.$$

The solution satisfying the boundary condition at infinity is

$$\Omega_1 = Ae^{-ihR}\left(1 + \frac{1}{ihR}\right)\sin^2\theta, \tag{11}$$

and the angular velocity ω is given as

$$\omega = \frac{Ae^{-ihR}}{R^2}\left(1+\frac{1}{ihR}\right)e^{i\sigma t}. \tag{12}$$

Applying the boundary condition at $R = a$, viz.

$$\omega = \omega_0 e^{i\sigma t}, \tag{13}$$

we find
$$A = \frac{ih\omega_0 e^{iha}a^3}{(1+iha)}. \tag{14}$$

4. The couple required to maintain the motion

The tangential stress on the surface $R =$ constant and in the direction of ϕ increasing is

$$T = \frac{\mu\omega_0(3+3iha-h^2a^2)}{(1+iha)}\sin\theta\, e^{i\sigma t}. \tag{15}$$

The couple G is thus given by

$$G = -\left\{\tfrac{8}{3}\pi\mu a^3\omega_0 \frac{3+3iha-h^2a^2}{1+iha}\right\}e^{i\sigma t}, \tag{16}$$

which agrees with the result obtained otherwise by Lamb (**2**).

II. *Circular cylinder oscillating about its axis*

5. For cylindrical polar coordinates we take α as z and β as r. Then the equation of motion for harmonic oscillations reduces to

$$\frac{d^2\Omega_1}{dr^2}-\frac{1}{r}\frac{d\Omega_1}{dr}-ik^2\Omega_1 = 0, \tag{17}$$

where
$$k^2 = \sigma/\nu \quad\text{and}\quad \Omega = \Omega_1 e^{i\sigma t}.$$

Its appropriate solution is given in terms of modified Bessel function as

$$\Omega_1 = ArK_1(\sqrt{i}\,kr), \tag{18}$$

and the angular velocity ω is given by

$$\omega = \frac{AK_1(\sqrt{i}\,kr)}{r}e^{i\sigma t}. \tag{19}$$

The boundary condition at $r = a$, viz. $\omega = \omega_0 e^{i\sigma t}$, gives

$$A = \frac{\omega_0 a}{K_1(\sqrt{i}\,ka)}. \tag{20}$$

6. The couple required to maintain the motion

The tangential stress T on the surface $r = a$ and in the direction of ϕ increasing is given by

$$T = \frac{-\mu\omega_0\sqrt{i}\,kaK_2(\sqrt{i}\,ka)}{K_1(\sqrt{i}\,ka)}e^{i\sigma t}. \tag{21}$$

So the couple per unit length of the cylinder is

$$G = -2\pi\mu\omega_0 a^2 \frac{\sqrt{i}\,kaK_2(\sqrt{i}\,ka)}{K_1(\sqrt{i}\,ka)} e^{i\sigma t}. \tag{22}$$

III. *Prolate spheroid oscillating about its axis of revolution*

7. In this case we use the prolate spheroidal coordinates defined by

$$z+ir = c\cosh(\alpha+i\beta),$$

$$e_1 = e_2 = c\sqrt{(\cosh^2\alpha-\cos^2\beta)}, \qquad e_3 = c\sinh\alpha\sin\beta.$$

The equation of motion is $\qquad \dfrac{\partial\Omega}{\partial t} = \nu D^2\Omega,$

where

$$D^2 = \left\{\frac{1}{c^2(\cosh^2\alpha-\cos^2\beta)}\left(\frac{\partial^2}{\partial\alpha^2}+\frac{\partial^2}{\partial\beta^2}-\coth\alpha\frac{\partial}{\partial\alpha}-\cot\beta\frac{\partial}{\partial\beta}\right)\right\}.$$

Writing $\Omega_1 e^{i\sigma t} = \Omega$ in the equation of motion, we get

$$D^2\Omega_1 = \frac{i\sigma}{\nu}\Omega_1 = ik^2\Omega_1, \tag{23}$$

where $k^2 = \sigma/\nu$, or

$$\left[\frac{\partial^2}{\partial\alpha^2}+\frac{\partial^2}{\partial\beta^2}-\coth\alpha\frac{\partial}{\partial\alpha}-\cot\beta\frac{\partial}{\partial\beta}-ik^2c^2(\cosh^2\alpha-\cos^2\beta)\right]\Omega_1 = 0. \tag{24}$$

Putting

$$\Omega_1 = \sinh\alpha\sin\beta\, S(\beta)R(\alpha),$$

$$\cosh\alpha = \xi, \qquad \cos\beta = \eta,$$

equation (24) separates into the two following equations:

$$\frac{d}{d\eta}\left\{(\eta^2-1)\frac{dS}{d\eta}\right\}+\left\{\lambda-ik^2c^2\eta^2-\frac{1}{\eta^2-1}\right\}S = 0, \tag{25}$$

$$\frac{d}{d\xi}\left\{(\xi^2-1)\frac{dR}{d\xi}\right\}+\left\{\lambda-ik^2c^2\xi^2-\frac{1}{\xi^2-1}\right\}R = 0, \tag{26}$$

where λ is the constant of separation. Equations (25) and (26) are identical with the equations obtained by Stratton and others (**3**) in the discussion of the prolate spheroidal wave functions. Such equations contain a third parameter m and have solutions for the suitably related values of the parameter in series of associated Legendre functions or Bessel functions of half order. In our case m is unity. Thus, for various characteristic values of λ, there are 'angular solutions' $S^1_{1l}(\sqrt{i}\,kc,\eta)$ of (25) which are finite throughout the range $-1 \leqslant \eta \leqslant 1$ and are expressed as infinite series of associated Legendre functions in the form

$$S^1_{1l}(\sqrt{i}\,kc,\eta) = \sum_{n=0,1}{}' d^l_n P^1_{n+1}(\eta), \tag{27}$$

where the prime indicates summation over even or odd values of n according as n is even or odd, and

$$\sum_{n=0}^{\infty}{}' i^{n-l} d_n^l \frac{\{\frac{1}{2}(n+1)\}!}{(\frac{1}{2}n)!} = \frac{\{\frac{1}{2}(l+1)\}!}{(\frac{1}{2}l)!}, \quad l \text{ even},$$

$$\sum_{n=1}^{\infty}{}' i^{n-l} d_n^l \frac{\{\frac{1}{2}(n+2)\}!}{\{\frac{1}{2}(n-1)\}!} = \frac{\{\frac{1}{2}(l+2)\}!}{\{\frac{1}{2}(l-1)\}!}, \quad l \text{ odd}.$$

Since Ω is to be expressed ultimately as the sum of series of products $S(\beta)R(\alpha)$, the boundary condition $\Omega \to 0$ as $\xi \to \infty$ determines at once the appropriate 'radial solution' of (26). The function which satisfies this condition is $R_{1l}^3(\sqrt{i}\,kc, \xi)$, which is given, for large values of $\sqrt{i}\,kc\xi$, as

$$R_{1l}^{(3)}(\sqrt{i}\,kc, \xi) = \frac{(\xi^2-1)^{\frac{1}{2}}\sqrt{(\pi/2\sqrt{i}\,kc\xi^3)}\sum_{n=0,1}^{\infty}{}' i^{l-n} d_n^l (n+1)(n+2) K_{n+\frac{3}{2}}(\sqrt{i}\,kc\xi)}{\sum_{n=0,1}^{\infty}{}' d_n^l (n+1)(n+2)} \tag{28}$$

$$\to \frac{1}{\sqrt{i}\,kc\xi} e^{i\{\sqrt{i}\,kc\xi - \frac{1}{2}(l+2)\pi\}}. \tag{29}$$

The complete solution of equation (24) is

$$\Omega_1 = c \sinh\alpha \sin\beta \sum_{l=0}^{\infty} A_l R_{1l}^3(\alpha) S_{1l}^1(\beta). \tag{30}$$

Therefore
$$\omega = \sum_{l=0}^{\infty} A_l R_{1l}^3(\alpha) S_{1l}^1(\beta) e^{i\sigma t} \tag{31}$$

and the angular velocity is

$$\omega = \frac{1}{c \sinh\alpha \sin\beta} \sum_{l=0}^{\infty} A_l R_{1l}^3(\alpha) S_{1l}^1(\beta) e^{i\sigma t}. \tag{32}$$

The boundary condition requires

$$\omega = \omega_0 e^{i\sigma t} \quad \text{at } \alpha = \alpha_0.$$

Therefore
$$\omega_0 c \sinh\alpha_0 \sin\beta = \sum_{l=0}^{\infty} A_l R_{1l}^3(\alpha_0) S_{1l}^1(\beta). \tag{33}$$

Using the orthogonal property of $S_{1l}^1(\beta)$, we have

$$\omega_0 c \sinh\alpha_0 \int_0^{\pi} \sin^2\beta\, S_{1l}^1(\beta)\, d\beta = A_l q_l R_{1l}^3(\alpha_0), \tag{34}$$

where
$$q_l = 2 \sum_{n=0,1}^{\infty}{}' \frac{(n+1)(n+2)}{(2n+3)} (d_n^l)^2. \tag{35}$$

To integrate $$\int_0^{\pi} \sin^2\beta \, S^1_{1l}(\beta)\, d\beta = \int_{-1}^{+1} \sqrt{(1-\eta^2)}\, S^1_{1l}(\eta)\, d\eta,$$
where $$\eta = \cos\beta,$$
we notice that $$S^1_{1l}(\eta) = \sum_{n=0,1}^{\infty}{}' d^l_n \, P^1_{n+1}(\eta),$$
and assume the validity of the interchange of the operations of integration and summation. We have

$$\int_{-1}^{+1} \sqrt{(1-\eta^2)} P^1_{n+1}(\eta)\, d\eta = -\int_{-1}^{+1} P^1_1(\eta) P^1_{n+1}(\eta)\, d\eta = \begin{cases} -\frac{4}{3} & \text{for } n = 0, \\ 0 & \text{for } n > 0. \end{cases}$$

So the equation (34) gives

$$\left.\begin{aligned} A_l &= \frac{-4\omega_0 c \sinh\alpha_0}{3q_l R^3_{1l}(\alpha_0)} && \text{for } l \text{ even} \\ A_l &= 0 && \text{for } l \text{ odd} \end{aligned}\right\}. \tag{36}$$

8. The couple required to maintain the motion

The tangential stress T on the surface $\alpha = \alpha_0$ and in the direction of ϕ increasing is given by

$$\begin{aligned} T &= \mu\left\{\frac{e_3}{e_1}\left[\frac{\partial}{\partial\alpha}\left(\frac{\omega}{e_3}\right)\right]\right\}_{\alpha=\alpha_0} \\ &= \frac{\mu \sinh\alpha_0}{c(\cosh^2\alpha_0 - \cos^2\beta)^{\frac{1}{2}}}\left[\frac{\partial}{\partial\alpha}\left\{\frac{\sum_{l=0}^{\infty} A_l R^3_{1l}(\alpha) S^1_{1l}(\beta)}{\sinh\alpha}\right\}\right]_{\alpha=\alpha_0} e^{i\sigma t} \\ &= -\left\{\frac{\mu\omega_0 \cosh\alpha_0 \sin\beta}{(\cosh^2\alpha_0 - \cos^2\beta)^{\frac{1}{2}}} + \frac{4\mu\omega_0 \sum_{l=0}^{\infty} \{R^{3\prime}_{1l}(\alpha_0)/q_l R^3_{1l}(\alpha_0)\} S^1_{1l}(\beta)}{3(\cosh^2\alpha_0 - \cos^2\beta)^{\frac{1}{2}}}\right\} e^{i\sigma t}. \end{aligned} \tag{37}$$

The required couple G is given as

$$\begin{aligned} G &= -e^{i\sigma t}\Big[2\pi\mu\omega_0 c^3 \sinh^2\alpha_0 \cosh\alpha_0 \int_0^{\pi} \sin^3\beta \, d\beta + \\ &\qquad + \tfrac{8}{3}\pi\mu\omega_0 c^3 \sinh^2\alpha_0 \sum_{l=0}^{\infty} \{R^{3\prime}_{1l}(\alpha_0)/q_l R^3_{1l}(\alpha_0)\} \int_0^{\pi} \sin^2\beta \, S^1_{1l}(\beta)\, d\beta\Big] \\ &= \Big[-\cosh\alpha_0 + \tfrac{4}{3}\sum_{l=0}^{\infty} \{R^{3\prime}_{1l}(\alpha_0)/q_l R^3_{1l}(\alpha_0)\}\Big] \tfrac{8}{3}\pi\mu\omega_0 c^3 \sinh^2\alpha_0 \, e^{i\sigma t}, \end{aligned} \tag{38}$$

where a dash denotes differentiation with respect to α.

IV. *Oblate spheroid oscillating about its axis of revolution*

For an oblate spheroid we introduce a system of coordinates defined by

$$z+ir = c\sinh(\alpha+i\beta),$$

$$\phi = \gamma.$$

We then get

$$e_1 = e_2 = c\sqrt{\{\sinh^2\alpha+\cos^2\beta\}}, \qquad e_3 = c\cosh\alpha\sin\beta.$$

The equation of motion $\qquad \dfrac{\partial\Omega}{\partial t} = \nu D^2\Omega$

transforms into

$$\left[\frac{\partial^2}{\partial\alpha^2}+\frac{\partial^2}{\partial\beta^2}-\tanh\alpha\frac{\partial}{\partial\alpha}-\cot\beta\frac{\partial}{\partial\beta}-ik^2c^2(\sinh^2\alpha+\cos^2\beta)\right]\Omega_1 = 0, \tag{39}$$

where $\qquad \Omega = \Omega_1 e^{i\sigma t}, \qquad k^2 = \sigma/\nu.$

Putting

$$\Omega_1 = \cosh\alpha\sin\beta\, S(\beta)R(\alpha),$$

$$\sinh\alpha = \xi, \quad \text{and} \quad \cos\beta = \eta,$$

equation (39) separates into the following two equations,

$$\frac{d}{d\eta}\left[(\eta^2-1)\frac{dS}{d\eta}\right]+\left[\lambda+ik^2c^2\eta^2-\frac{1}{\eta^2-1}\right]S = 0, \tag{40}$$

$$\frac{d}{d\xi}\left[(\xi^2+1)\frac{dR}{d\xi}\right]+\left[\lambda-ik^2c^2\xi^2+\frac{1}{\xi^2+1}\right]R = 0, \tag{41}$$

where λ is a constant of separation. Equation (40) can be obtained from (25) by changing $\sqrt{i}\,k$ to $i\sqrt{i}\,k$. The equation (41) can be obtained from equation (26) by changing $\sqrt{i}\,k$ to $i\sqrt{i}\,k$ and ξ to $-i\xi$. Therefore the solutions of the equations (40) and (41) can be obtained from those of the equations (25) and (26) by changing $\sqrt{i}\,k$ to $-i\sqrt{i}\,k$ and ξ to $i\xi$. Thus the angular solution is given by

$$S^1_{1l}(-i\sqrt{i}\,k,\eta) = \sum_{n=0,1}^{\infty}{}' f^l_n P^1_{n+1}(\eta), \tag{42}$$

where the coefficients f^l_n are different in value from the coefficients d^l_n of the prolate case, but are obtained in the same way (**5**). The radial solutions are given by

$$R^3_{1l}(-i\sqrt{i}\,kc, i\xi)$$

$$= \frac{(1+\xi^2)^{\frac{1}{2}}\sqrt{\{\pi/(-2\sqrt{i}\,kc\xi^3)\}}\sum_{n=0,1}^{\infty}{}' i^{l-n}f^l_n(n+1)(n+2)K_{n+\frac{3}{2}}(\sqrt{i}\,kc\xi)}{\sum_{n=0,1}^{\infty}{}' f^l_n(n+1)(n+2)}. \tag{43}$$

The required solution in this case is

$$\Omega = c\cosh\alpha\sin\beta\sum_{l=0}^{\infty} A_l\, R^3_{1l}(\alpha)S^1_{1l}(\beta)e^{i\sigma t}, \tag{44}$$

$$w = \sum_{l=0}^{\infty} A_l\, R^3_{1l}(\alpha)S^1_{1l}(\beta)e^{i\sigma t}, \tag{45}$$

$$\omega = \frac{1}{c\cosh\alpha\sin\beta}\sum_{l=0}^{\infty} A_l\, R^3_{1l}(\alpha)S^1_{1l}(\beta)e^{i\sigma t}. \tag{46}$$

The boundary condition gives

$$\omega_0\, c\cosh\alpha_0\sin\beta = \sum_{l=0}^{\infty} A_l\, R^3_{1l}(\alpha_0)S^1_{1l}(\beta). \tag{47}$$

Employing the orthogonal property of $S^1_{1l}(\beta)$, we get, as in equation (33),

$$\left.\begin{aligned} A_l &= \frac{-4\omega_0\, c\cosh\alpha_0}{3q_l\, R^3_{1l}(\alpha_0)} && \text{for } l \text{ even}\\ A_l &= 0 && \text{for } l \text{ odd}\end{aligned}\right\}, \tag{48}$$

where $$q_l = 2\sum_{n=0,1}^{\infty}{}' \frac{(n+1)(n+2)}{(2n+3)}(f^l_n)^2.$$

9. The couple required to maintain the motion

T, the tangential stress on the surface $\alpha = \alpha_0$ and in the direction of ϕ increasing, is

$$\begin{aligned} T &= \mu\frac{e_3}{e_1}\left[\frac{\partial}{\partial\alpha}\left(\frac{w}{e_3}\right)\right]_{\alpha=\alpha_0}\\ &= \frac{\mu\cosh\alpha_0}{c(\sinh^2\alpha_0+\cos^2\beta)^{\frac{1}{2}}}\left[\frac{\partial}{\partial\alpha}\left\{\operatorname{sech}\alpha\sum_{l=0}^{\infty} A_l\, R^3_{1l}(\alpha)S^1_{1l}(\beta)\right\}e^{i\sigma t}\right]_{\alpha=\alpha_0}. \end{aligned} \tag{49}$$

The required couple is given as

$$\begin{aligned} G &= \left[2\pi\mu c^2\cosh^2\alpha_0\sum_{l=0}^{\infty} A_l\, R^{3\prime}_{1l}(\alpha_0)\int_0^{\pi}\sin^2\beta\, S^1_{1l}(\beta)\,d\beta - \right.\\ &\qquad\left. -2\pi\mu c^3\omega_0\cosh^2\alpha_0\sinh\alpha_0\int_0^{\pi}\sin^3\beta\,d\beta\right]e^{i\sigma t}\\ &= \left[\tfrac{32}{9}\pi\mu\omega_0 c^3\cosh^3\alpha_0\sum_{l=0}^{\infty}\frac{R^{3\prime}_{1l}(\alpha_0)}{q_l\, R^3_{1l}(\alpha_0)} - \tfrac{8}{3}\pi\mu\omega_0 c^3\cosh^2\alpha_0\sinh\alpha_0\right]e^{i\sigma t}, \end{aligned} \tag{50}$$

where a dash denotes differentiation with respect to α.

V. *Circular disk oscillating about its axis*

The motion due to rotatory oscillations of a circular disk about the normal through its centre can be obtained from the motion of the oblate spheroid as a limiting case. If we take the expression of the function $R^3_{1l}(\xi)$,

the 'radial solution' found in the case of the oblate spheroid, near $\xi = 0$, the required expression is an infinite series of associated Legendre functions. The appropriate form of the function (**5**), apart from a constant factor, may be written as $F_l(k, \xi)$, where, for even values of l,

$$F_l(k,\xi) = e^{i\pi l/2}\left\{\sum_{n=0}^{\infty} f^l_{2n} Q^1_{1+2n}(\sqrt{i}\,\xi) + f^l_{-2}\, Q^1_{-1}(\sqrt{i}\,\xi) + \right.$$

$$\left. + \sum_{n=2}^{\infty}\left(\frac{f^l_{-2n}}{\rho}\right) P^1_{2n-2}(\sqrt{i}\,\xi) - i\epsilon_l\, S^1_{1l}(k, \sqrt{i}\,\xi)\right\} \tag{51}$$

and
$$\epsilon_l = \tfrac{1}{6}\pi c f^l_0 f^l_{-2}\left\{\frac{(\frac{1}{2}l)!}{[\frac{1}{2}(l+1)]!}\right\}^2,$$

while for odd values of l,

$$F_l(k,\xi) = e^{i\pi l/2}\left[\sum_{n=1}^{\infty} f^l_{2n-1} Q^1_{2n}(\sqrt{i}\,\xi) + f^l_{-1}\, Q^1_{0}(\sqrt{i}\,\xi) + \right.$$

$$\left. + \sum_{n=1}^{\infty}\left(\frac{f^l_{-2n-1}}{\rho}\right) P^1_{2n-1}(\sqrt{i}\,\xi) - i\epsilon_l\, S^1_{1l}(k, \sqrt{i}\,\xi)\right] \tag{52}$$

and
$$\epsilon_l = \tfrac{1}{40}\pi c^3 f^l_{+1} f^l_{-1}\left\{\frac{\{\frac{1}{2}(l-1)\}!}{\{\frac{1}{2}(l+2)\}!}\right\}^2.$$

Having proved that $A_l = 0$ for odd values of l, we shall be concerned with the expression in (51).

The expression for Ω is now given as

$$\Omega = c\cosh\alpha\sin\beta\sum_{l=0}^{\infty} A_{2l} F_{2l}(\alpha) S^1_{1,2l}(\beta) e^{i\sigma t}, \tag{53}$$

where
$$A_{2l} = -\frac{4\omega_0 c\cosh\alpha_0}{3q_l F_{2l}(\alpha_0)}.$$

In the limiting case when $\alpha_0 \to 0$, A_{2l} takes the value

$$A_{2l} = -\frac{4\omega_0 c}{3q_{2l} F_{2l}(0)}.$$

Proceeding as before, we get the couple on the oblate spheroid as

$$G = e^{i\sigma t}\left[\tfrac{32}{9}\mu\omega_0 c^3\cosh^3\alpha_0 \sum_{l=0}^{\infty}\left\{\frac{F'_{2l}(\alpha_0)}{q_{2l} F_{2l}(\alpha_0)}\right\} - \tfrac{8}{3}\pi\mu\omega_0 c^3\cosh^2\alpha_0\sinh\alpha_0\right].$$

The couple in the case of the circular disk is given by the limit of G as $\alpha_0 \to 0$, viz.

$$\tfrac{32}{9}\pi\mu\omega_0 c^3\sum_{l=0}^{\infty}\frac{F'_{2l}(0)}{q_{2l}F_{2l}(0)} e^{i\sigma t}. \tag{54}$$

The values of $F_{2l}(0)$ and $F'_{2l}(0)$ are given as

$$\left.\begin{aligned} F_{2l}(0) &= (-1)^l \pi^{\frac{1}{2}}\left[(1+2\epsilon_{2l}/\pi)\sum_{n=0}^{\infty}(-1)^n\frac{(n+\frac{1}{2})!}{n!}f^{2l}_{2n}\right] \\ F'_{2l}(0) &= (-1)^l\left[2\sum_{n=0}^{\infty}(-1)^{n+1}\frac{(n+1)!\,(-\frac{1}{2})!}{(n-\frac{1}{2})!}f^{2l}_{2n}-f^{2l}_{-2}+\right. \\ &\qquad\left.+4\sum_{n=2}^{\infty}(-1)^{n+1}\frac{(n-\frac{1}{2})!}{(n-2)!\,(-\frac{1}{2})!}\left(\frac{f^{2l}_{-2n}}{\rho}\right)\right] \end{aligned}\right\}. \tag{55}$$

Part II. Longitudinal Oscillations

VI. *Sphere oscillating along a diameter*

The sphere is oscillating longitudinally along a diameter. The equations governing such a motion are

$$D^2\psi_1 = 0,$$

$$\left\{D^2-\frac{1}{\nu}\frac{\partial}{\partial t}\right\}\psi_2 = 0.$$

Taking the spherical polar coordinates R, θ, ϕ and writing $\psi_1 = \psi'_1 e^{i\sigma t}$, $\psi_2 = \psi'_2 e^{i\sigma t}$, the above equations reduce to

$$\frac{\partial^2\psi'_1}{\partial R^2}+\frac{\sin\theta}{R^2}\frac{\partial}{\partial\theta}\left(\frac{1}{\sin\theta}\frac{\partial\psi'_1}{\partial\theta}\right) = 0 \tag{56}$$

and
$$\frac{\partial^2\psi'_2}{\partial R^2}+\frac{\sin\theta}{R^2}\frac{\partial}{\partial\theta}\left(\frac{1}{\sin\theta}\frac{\partial\psi'_2}{\partial\theta}\right)+h^2\psi'_2 = 0, \tag{57}$$

where
$$h^2 = -i\sigma/\nu.$$

The boundary conditions are

$$\psi_{R=a} = -\tfrac{1}{2}w_0 a^2\sin^2\theta\, e^{i\sigma t},$$

$$\left(\frac{\partial\psi}{\partial R}\right)_{R=a} = -w_0 a\sin^2\theta\, e^{i\sigma t},$$

$$u = v = 0 \quad \text{at infinity},$$

where $w_0 e^{i\sigma t}$ is the velocity of the sphere along the diameter.

With the behaviour of the motion at infinity in view, the solution of the equations (56), (57) is

$$\psi'_1 = A\frac{\sin^2\theta}{R}, \tag{58}$$

$$\psi'_2 = Be^{-ihR}\left\{1+\frac{1}{ihR}\right\}\sin^2\theta. \tag{59}$$

Therefore
$$\psi = \left\{\frac{A}{r}+Be^{-ihR}\left(1+\frac{1}{ihR}\right)\right\}\sin^2\theta\, e^{i\sigma t}. \tag{60}$$

The boundary conditions give

$$A = \{\tfrac{3}{2}+\tfrac{3}{2}iha-\tfrac{1}{2}h^2a^2\}\frac{w_0 a}{h^2},$$

$$B = \frac{3}{2}\frac{w_0 a e^{iha}}{ih}.$$

The velocity components are given by

$$u = \frac{1}{R^2 \sin\theta}\frac{\partial\psi}{\partial\theta}, \qquad v = -\frac{1}{R\sin\theta}\frac{\partial\psi}{\partial R}, \qquad w = 0,$$

which when calculated agree with results already obtained by different methods (**1**, **2**).

VII. *Prolate spheroid oscillating along its axis of revolution*

As in Part I we introduce the prolate spheroidal coordinates α, β, γ such that

$$z+ir = c\cosh(\alpha+i\beta),$$

$$\phi = \gamma,$$

$$e_1 = e_2 = c\sqrt{(\cosh^2\alpha-\cos^2\beta)}, \qquad e_3 = c\sinh\alpha\sin\beta.$$

The equations of motion (7)–(8) are transformed into

$$\left\{\frac{\partial^2}{\partial\alpha^2}+\frac{\partial^2}{\partial\beta^2}-\coth\alpha\frac{\partial}{\partial\alpha}-\cot\beta\frac{\partial}{\partial\beta}\right\}\psi_1 = 0, \tag{61}$$

$$\left[\left\{\frac{\partial^2}{\partial\alpha^2}+\frac{\partial^2}{\partial\beta^2}-\coth\alpha\frac{\partial}{\partial\alpha}-\cot\beta\frac{\partial}{\partial\beta}\right\}-\frac{c^2(\cosh^2\alpha-\cos^2\beta)}{\nu}\frac{\partial}{\partial t}\right]\psi_2 = 0. \tag{62}$$

Writing $\psi_1 = \psi_1' e^{i\sigma t}$, $\psi = \psi_2' e^{i\sigma t}$, and $k^2 = \sigma/\nu$, equations (61)–(62) reduce to

$$\left\{\frac{\partial^2}{\partial\alpha^2}+\frac{\partial^2}{\partial\beta^2}-\coth\alpha\frac{\partial}{\partial\alpha}-\cot\beta\frac{\partial}{\partial\beta}\right\}\psi_1' = 0 \tag{63}$$

and

$$\left[\frac{\partial^2}{\partial\alpha^2}+\frac{\partial^2}{\partial\beta^2}-\coth\alpha\frac{\partial}{\partial\alpha}-\cot\beta\frac{\partial}{\partial\beta}-ik^2c^2(\cosh^2\alpha-\cos^2\beta)\right]\psi_2' = 0. \tag{64}$$

Putting

$$\psi_1' = \sinh\alpha\sin\beta\,\theta(\alpha)\phi(\beta),$$

$$\xi = \sinh\alpha, \qquad \eta = \cos\beta,$$

equation (63) separates into the following two equations with λ as the separation constant:

$$\frac{d}{d\eta}\left\{(\eta^2-1)\frac{d\phi}{d\eta}\right\}+\left\{\lambda-\frac{1}{\eta^2-1}\right\}\phi = 0, \tag{65}$$

$$\frac{d}{d\xi}\left\{(\xi^2-1)\frac{d\theta}{d\xi}\right\}+\left\{\lambda-\frac{1}{\xi^2-1}\right\}\theta = 0, \tag{66}$$

which are the particular cases of the associated Legendre differential equation. Thus the appropriate solution of (63), keeping in view the boundary condition at infinity, is

$$\psi_1' = \sinh\alpha \sin\beta \sum_{n=0}^{\infty} A_n\, Q^1_{1+n}(\alpha) P^1_{1+n}(\beta). \tag{67}$$

The solution of (64), as already found in Part I, is

$$\psi_2' = \sinh\alpha \sin\beta \sum_{l=0}^{\infty} B_l\, R^3_{1l}(\alpha) S^1_{1l}(\beta), \tag{68}$$

where
$$S^1_{1l}(\beta) = \sum_{n=0,1}^{\infty}{}' d^l_n\, P^1_{1+n}(\beta)$$
and
$$R^3_{1l}(\sqrt{i}\,kc,\xi) = \frac{(\xi^2-1)^{\frac{1}{2}}\sqrt{(\pi/2\sqrt{i}\,kc\xi^3)}\,\sum\limits_{n=0,1}^{\infty}{}' i^{l-n} d^l_n (n+1)(n+2) K_{n+\frac{3}{2}}(\sqrt{i}\,kc\xi)}{\sum\limits_{n=0,1}^{\infty}{}' d^l_n (n+1)(n+2)}.$$

The complete solution of the problem is

$$\psi = \sinh\alpha \sin\beta \Big[\sum_{n=0}^{\infty} A_n\, Q^1_{1+n}(\alpha) P^1_{1+n}(\beta) + \sum_{l=0}^{\infty} B_l\, R^3_{1l}(\alpha) S^1_{1l}(\beta)\Big] e^{i\sigma t}. \tag{69}$$

10. Determination of the constants of integration A_n and B_l

The constants of integration A_n and B_l can be determined from the boundary conditions at the surface of the prolate spheroid, viz.

$$u = -\frac{w_0 \sinh\alpha_0 \cos\beta}{(\cosh^2\alpha_0 - \cos^2\beta)^{\frac{1}{2}}} e^{i\sigma t} = \left\{\frac{1}{e_2 e_3}\frac{\partial\psi}{\partial\beta}\right\}_{\alpha=\alpha_0},$$

$$v = \frac{w_0 \cosh\alpha_0 \sin\beta}{(\cosh^2\alpha_0 - \cos^2\beta)^{\frac{1}{2}}} e^{i\sigma t} = -\left\{\frac{1}{e_1 e_3}\frac{\partial\psi}{\partial\alpha}\right\}_{\alpha=\alpha_0},$$

which require

$$(\psi)_{\alpha=\alpha_0} = -\tfrac{1}{2} w_0 c^2 \sinh^2\alpha_0 \sin^2\beta\, e^{i\sigma t},$$

$$\left(\frac{\partial\psi}{\partial\alpha}\right)_{\alpha=\alpha_0} = -w_0 c^2 \sinh\alpha_0 \cosh\alpha_0 \sin^2\beta\, e^{i\sigma t},$$

where $w_0 e^{i\sigma t}$ is the velocity of the body along the axis of symmetry.

Now ψ and $\partial\psi/\partial\alpha$ are given as

$$\psi = \Big[\sum_{n=0}^{\infty} A_n \sinh\alpha\, Q^1_{1+n}(\alpha) P^1_{1+n}(\beta)\sin\beta + \sum_{l=0}^{\infty} B_l \sinh\alpha\, R^3_{1l}(\alpha) S^1_{1l}(\beta)\sin\beta\Big] e^{i\sigma t}, \tag{70}$$

$$\frac{\partial\psi}{\partial\alpha} = \Big[\sum_{n=0}^{\infty} A_n\{\cosh\alpha\, Q^1_{1+n}(\alpha) + \sinh\alpha\, Q^{1\prime}_{1+n}(\alpha)\} P^1_{1+n}(\beta)\sin\beta +$$
$$+ \sum_{l=0}^{\infty} B_l\{\cosh\alpha\, R^3_{1l}(\alpha) + \sinh\alpha\, R^{3\prime}_{1l}(\alpha)\} S^1_{1l}(\beta)\sin\beta\Big] e^{i\sigma t}, \tag{71}$$

where a dash denotes differentiation with respect to α.

We rewrite these expressions in forms which are suitable for fitting the boundary conditions at the surface of the body. For this purpose we expand the right-hand sides of (70) and (71) into associated Legendre functions. Let us introduce functions $f_n(\alpha)$ and $F_{l,n}(\alpha)$ such that

$$\left.\begin{aligned} f_n(\alpha) &= Q^1_{1+n}(\alpha)\sinh\alpha \\ \text{and}\qquad \sum_{n=0}^{\infty} F_{l,n}(\alpha)P^1_{1+n}(\beta) &= \sinh\alpha\, R^3_{1l}(\alpha)S^1_{1l}(\beta) \end{aligned}\right\}. \tag{72}$$

Equating the coefficients of the associated Legendre functions of the same order on both sides, we get

$$F_{l,n}(\alpha) = \sinh\alpha\, R^3_{1l}(\alpha)d^l_n. \tag{73}$$

The boundary conditions take the form

$$\left.\begin{aligned} \tfrac{1}{2}w_0 c^2\sinh^2\alpha_0\, P^1_1(\beta) &= \sum_{n=0}^{\infty}\Big[A_n f_n(\alpha_0)+\sum_{l=0}^{\infty} B_l F_{l,n}(\alpha_0)\Big]P^1_{1+n}(\beta) \\ w_0 c^2\sinh\alpha_0\cosh\alpha_0\, P^1_1(\beta) &= \sum_{n=0}^{\infty}\Big[A_n f'_n(\alpha_0)+\sum_{l=0}^{\infty} B_l F'_{l,n}(\alpha_0)\Big]P^1_{1+n}(\beta) \end{aligned}\right\}, \tag{74}$$

which yield

$$\left.\begin{aligned} A_n f_n(\alpha_0)+\sum_{l=0}^{\infty} B_l F_{l,n}(\alpha_0) &= \begin{cases} \tfrac{1}{2}w_0 c^2\sinh^2\alpha_0 & \text{for } n=0 \\ 0 & \text{for } n>0 \end{cases} \\ A_n f'_n(\alpha_0)+\sum_{l=0}^{\infty} B_l F'_{l,n}(\alpha_0) &= \begin{cases} w_0 c^2\sinh\alpha_0\cosh\alpha_0 & \text{for } n=0 \\ 0 & \text{for } n>0 \end{cases} \end{aligned}\right\}. \tag{75}$$

Eliminating A_n, we get

$$\sum B_l\{F_{l,n}(\alpha_0)f'_n(\alpha_0)-F'_{l,n}(\alpha_0)f_n(\alpha_0)\}$$
$$= \begin{cases} w_0 c^2\sinh\alpha_0\{\tfrac{1}{2}\sinh\alpha_0 f'_n(\alpha_0)-\cosh\alpha_0 f_n(\alpha_0)\} & \text{for } n=0, \\ 0 & \text{for } n>0. \end{cases} \tag{76}$$

The B_l can be determined by solving this system of simultaneous linear algebraic equations. Tomotika and Aoi (**6**) have made some suggestions for the solution of a similar set of equations. In our case it is not possible to give similar expansions at this stage as the values of the coefficients d^l_n which have been tabulated to date are of little use to us here.

The stream function is thus completely determined.

VIII. *Oblate spheroid oscillating along its axis of revolution*

For an oblate spheroid the system of coordinates is

$$z+ir = c\sinh(\alpha+i\beta),$$

$$\phi = \gamma,$$

$$e_1 = e_2 = c(\sinh^2\alpha+\cos^2\beta)^{\frac{1}{2}}, \qquad e_3 = c\cosh\alpha\sin\beta.$$

The equations of motion when transformed into these coordinates become

$$\left(\frac{\partial^2}{\partial\alpha^2}+\frac{\partial^2}{\partial\beta^2}-\tanh\alpha\frac{\partial}{\partial\alpha}-\cot\beta\frac{\partial}{\partial\beta}\right)\psi_1 = 0, \tag{77}$$

$$\left\{\frac{\partial^2}{\partial\alpha^2}+\frac{\partial^2}{\partial\beta^2}-\tanh\alpha\frac{\partial}{\partial\alpha}-\cot\beta\frac{\partial}{\partial\beta}-\frac{c^2}{\nu}(\sinh^2\alpha+\cos^2\beta)\frac{\partial}{\partial t}\right\}\psi_2 = 0. \tag{78}$$

Writing $\psi_1 = \psi_1' e^{i\sigma t}$, $\psi_2 = \psi_2' e^{i\sigma t}$, and $k^2 = \sigma/\nu$, we get

$$\left(\frac{\partial^2}{\partial\alpha^2}+\frac{\partial^2}{\partial\beta^2}-\tanh\alpha\frac{\partial}{\partial\alpha}-\cot\beta\frac{\partial}{\partial\beta}\right)\psi_1' = 0, \tag{79}$$

$$\left\{\frac{\partial^2}{\partial\alpha^2}+\frac{\partial^2}{\partial\beta^2}-\tanh\alpha\frac{\partial}{\partial\alpha}-\cot\beta\frac{\partial}{\partial\beta}-ik^2c^2(\sinh^2\alpha+\cos^2\beta)\right\}\psi_2' = 0. \tag{80}$$

To solve equation (79) we put

$$\psi_1' = \cosh\alpha\sin\beta\,\theta(\alpha)\phi(\beta),$$

$$\sinh\alpha = \xi, \qquad \cos\beta = \eta.$$

The equation separates into

$$\frac{d}{d\eta}\left[(\eta^2-1)\frac{d\phi}{d\eta}\right]+\left[\lambda-\frac{1}{\eta^2-1}\right]\phi = 0 \tag{81}$$

and

$$\frac{d}{d\xi}\left[(\xi^2+1)\frac{d\theta}{d\xi}\right]+\left[\lambda+\frac{1}{\xi^2+1}\right]\theta = 0, \tag{82}$$

where λ is a constant of separation.

The required solution of (79) is therefore

$$\psi_1' = \cosh\alpha\sin\beta\sum_{l=0}^{\infty} A_n\, Q^1_{1+n}(i\sinh\alpha)P^1_{1+n}(\cos\beta). \tag{83}$$

The solution of (80), as already obtained in Part I, is

$$\psi_2' = \cosh\alpha\sin\beta\sum_{l=0}^{\infty} B_l\, R^3_{1l}(\alpha)S^1_{1l}(\beta). \tag{84}$$

The superposition of these two solutions gives the complete solution

$$\psi = \cosh\alpha\sin\beta\left[\sum_{n=0}^{\infty} A_n\, Q^1_{1+n}(\alpha)P^1_{1+n}(\beta)+\sum_{l=0}^{\infty} B_l\, R^3_{1l}(\alpha)S^1_{1l}(\beta)\right]e^{i\sigma t}. \tag{85}$$

11. Determination of the constants of integration A_n and B_l

The boundary conditions, in this case, are

$$u = -\frac{w_0\cosh\alpha_0\cos\beta}{(\sinh^2\alpha_0+\cos^2\beta)^{\frac{1}{2}}}e^{i\sigma t} = \left(\frac{1}{e_2 e_3}\frac{\partial\psi}{\partial\beta}\right)_{\alpha=\alpha_0},$$

$$v = -\frac{w_0\sinh\alpha_0\sin\beta}{(\sinh^2\alpha_0+\cos^2\beta)^{\frac{1}{2}}}e^{i\sigma t} = -\left(\frac{1}{e_1 e_3}\frac{\partial\psi}{\partial\alpha}\right)_{\alpha=\alpha_0},$$

which reduce to

$$\left.\begin{aligned}(\psi)_{\alpha=\alpha_0} &= -\tfrac{1}{2}w_0\,c^2\cosh^2\alpha_0\sin^2\beta\,e^{i\sigma t}\\ \left(\frac{\partial\psi}{\partial\alpha}\right)_{\alpha=\alpha_0} &= -w_0\,c^2\cosh\alpha_0\sinh\alpha_0\sin^2\beta\,e^{i\sigma t}\end{aligned}\right\}. \tag{86}$$

Proceeding as in the case of the prolate spheroid, we introduce functions $g_n(\alpha)$ and $G_{l,n}(\alpha)$ such that

$$\left.\begin{aligned}g_n(\alpha) &= \cosh\alpha\,Q^1_{1+n}(\alpha)\\ \sum_{n=0}^{\infty} G_{l,n}(\alpha)P^1_{1+n}(\beta) &= \cosh\alpha\,R^3_{1l}(\alpha)S^1_{1l}(\beta)\end{aligned}\right\}. \tag{87}$$

Equating the coefficients of the associated Legendre functions of the same order, we get

$$G_{l,n}(\alpha) = \cosh\alpha\,R^3_{1l}(\alpha)f'_n. \tag{88}$$

The boundary conditions take the form

$$\left.\begin{aligned}\tfrac{1}{2}w_0\,c^2\cosh^2\alpha_0\,P^1_1(\beta) &= \sum_{n=0}^{\infty}\Big[A_n\,g_n(\alpha_0)+\sum_{l=0}^{\infty}B_l\,G_{l,n}(\alpha_0)\Big]P^1_{1+n}(\beta)\\ w_0\,c^2\cosh\alpha_0\sinh\alpha_0\,P^1_1(\beta) &= \sum_{n=0}^{\infty}\Big[A_n\,g'_n(\alpha_0)+\sum_{l=0}^{\infty}B_l\,G'_{l,n}(\alpha_0)\Big]P^1_{1+n}(\beta)\end{aligned}\right\}, \tag{89}$$

where dashes denote differentiation with respect to α.

Equations (89) yield

$$\left.\begin{aligned}A_n\,g_n(\alpha_0)+\sum_{l=0}^{\infty}B_l\,G_{l,n}(\alpha_0) &= \begin{cases}\tfrac{1}{2}w_0\,c^2\cosh^2\alpha_0 & \text{for } n=0\\ 0 & \text{for } n>0\end{cases}\\ A_n\,g'_n(\alpha_0)+\sum_{l=0}^{\infty}B_l\,G'_{l,n}(\alpha_0) &= \begin{cases}w_0\,c^2\cosh\alpha_0\sinh\alpha_0 & \text{for } n=0\\ 0 & \text{for } n>0\end{cases}\end{aligned}\right\}. \tag{90}$$

Eliminating A_n, we get a set of algebraic equations

$$\sum B_l\{G_{l,n}(\alpha_0)g'_n(\alpha_0)-G'_{l,n}(\alpha_0)g_n(\alpha_0)\}$$
$$= \begin{cases}w_0\,c^2\cosh\alpha_0[\tfrac{1}{2}\cosh\alpha_0\,g'_n(\alpha_0)-\sinh\alpha_0\,g_n(\alpha_0)] & \text{for } n=0\\ 0 & \text{for } n>0\end{cases} \tag{91}$$

to determine the values of the constants B_l. These equations involve the coefficients f^l_n, and those so far tabulated only are of no use to us here.

IX. *Circular disk oscillating along the normal axis at its centre*

For deducing the stream function for the motion of the disk as a limiting case of the oblate spheroid we take the expression of the function $R^3_{1l}(\xi)$ for values of ξ near $\xi = 0$. The required expression, as in Part I, is $F_l(k,\xi)$,

which, apart from a constant factor, is given for even values of l as

$$F_l(k,\xi) = e^{i\pi l/2}\Big\{\sum_{n=0}^{\infty} f_{2n}^l\, Q_{1+2n}^1(\sqrt{i}\,\xi)+f_{-2}^l\, Q_{-1}^1(\sqrt{i}\,\xi)+$$
$$+\sum_{n=2}^{\infty}\Big(\frac{f_{-2n}^l}{\rho}\Big)P_{2n-1}^1(\sqrt{i}\,\xi)-i\epsilon_l\, S_{1l}^1(k,\sqrt{i}\,\xi)\Big\},$$

while, for odd values of l,

$$F_l(k,\xi) = e^{i\pi l/2}\Big\{\sum_{n=1}^{\infty} f_{2n-1}^l\, Q_{2n}^1(\sqrt{i}\,\xi)+f_{-1}^l\, Q_0^1(\sqrt{i}\,\xi)+$$
$$+\sum_{n=1}^{\infty}\Big(\frac{f_{-2n-1}^l}{\rho}\Big)P_{2n-1}^1(\sqrt{i}\,\xi)-i\epsilon_l\, S_{1l}^1(k,\sqrt{i}\,\xi)\Big\}.$$

The expression for the stream function for an oblate spheroid is now given as

$$\psi = \cosh\alpha\sin\beta\Big[\sum_{n=0}^{\infty} A_n\, Q_{1+n}^1(\alpha)P_{1+n}^1(\beta)+\sum_{l=0}^{\infty} B_l\, F_l(\alpha)S_{1l}^1(\beta)\Big]e^{i\sigma t}. \tag{92}$$

A_n and B_l are determined by the equations

$$\left.\begin{aligned} A_n\, g_n(\alpha_0)+\sum_{l=0}^{\infty} B_l\, H_{l,n}(\alpha_0) &= \begin{cases}\tfrac{1}{2}w_0\, c^2\cosh^2\alpha_0 & \text{for } n=0\\ 0 & \text{for } n>0\end{cases}\\ A_n\, g_n'(\alpha_0)+\sum_{l=0}^{\infty} B_l\, H_{l,n}'(\alpha_0) &= \begin{cases}w_0\, c^2\cosh\alpha_0\sinh\alpha_0 & \text{for } n=0\\ 0 & \text{for } n>0\end{cases}\end{aligned}\right\}, \tag{93}$$

where the function $H_{l,n}(\alpha)$, being defined in the same way as $G_{l,n}(\alpha)$, is

$$H_{l,n}(\alpha) = \cosh\alpha\, F_l(\alpha)d_n^l. \tag{94}$$

In the limiting case when $\alpha_0 \to 0$, A_n and B_l are given by

$$\left.\begin{aligned} A_n\, g_n(0)+\sum_{l=0}^{\infty} B_l\, H_{l,n}(0) &= \begin{cases}\tfrac{1}{2}w_0\, c^2 & \text{for } n=0\\ 0 & \text{for } n>0\end{cases}\\ A_n\, g_n'(0)+\sum_{l=0}^{\infty} B_l\, H_{l,n}'(0) &= 0 \qquad \text{for all } n\end{aligned}\right\}. \tag{95}$$

Elimination of A_n yields us a set of algebraic equations

$$\sum_{l=0}^{\infty} B_l\{H_{l,n}(0)g_n'(0)-H_{l,n}'(0)g_n(0)\} = \begin{cases}\tfrac{1}{2}w_0\, c^2 g_n'(0) & \text{for } n=0\\ 0 & \text{for } n>0\end{cases} \tag{96}$$

for the determination of the B_l. They are similar to the equations (91).

In conclusion I wish to thank Professor B. R. Seth for his guidance in the course of the preparation of this paper. My thanks are also due to Professor L. Rosenhead and Mr. L. Sowerby for their helpful suggestions.

REFERENCES

1. R. P. KANWAL, 'Generalized periodic singular points with applications to flow problems' (to be published).
2. H. LAMB, *Hydrodynamics* (Dover, New York, 1945), pp. 642–4.
3. J. A. STRATTON, P. M. MORSE, L. J. CHU, and R. A. HUTNER, *Elliptic Cylinder and Spheroidal Wave Functions* (New York, 1941).
4. S. GOLDSTEIN, *Modern Developments in Fluid Dynamics* (Oxford, 1938), pp. 114–15.
5. L. SOWERBY, 'Couple on a rotating spheroid in a slow stream', *Proc. Camb. Phil. Soc.* **49** (1935), 327–32.
6. S. TOMOTIKA and T. AOI, 'The steady flow of a viscous fluid past an elliptic cylinder and a flat plate at small Reynolds numbers', *Quart. J. Mech. and Applied Math.* **6** (1953), 295.

ON THE DIFFUSION OF LOAD FROM A STIFFENER INTO A SHEET

By W. T. KOITER (*Laboratory of Applied Mechanics, Technological University, Delft, Netherlands*)

[Received 31 August 1954]

SUMMARY

A rigorous solution is obtained for the diffusion of load from a semi-infinite stiffener into an infinite or a semi-infinite sheet. A Mellin transformation, applied to the basic singular integro-differential equation of the problem, yields a difference equation in a strip of the complex plane which is solved by means of Laplace transforms. The final solution is obtained in the form of an inverse Mellin integral which is evaluated by contour integration.

1. Introduction

THE diffusion of load from a stiffener into a sheet is a fundamental problem of aircraft stress analysis. It occurs in many forms and it has been discussed by many authors, but so far very few if any rigorous solutions have been obtained. It is the object of the present paper to give the *rigorous* solution of this problem for an *infinite* or *semi-infinite sheet* with a *semi-infinite stiffener* of *constant* cross-section.

A semi-infinite sheet with a semi-infinite edge stiffener of constant cross-section has been investigated by Buell (**1**) by means of a complex stress function for the sheet. Although his solution is entirely adequate for all practical purposes, it is not rigorous because the convergence of his process of successive approximations to an infinite system of equations has not been established. Benscoter (**2**) has discussed an infinite sheet with a finite stiffener, starting from the integro-differential equation for the shear stress between stiffener and sheet. He observed that this equation is formally identical with Prandtl's equation for the aerodynamic load distribution over a wing of finite span, and therefore amenable to the same (approximate) methods of solution. Our rigorous solution for a semi-infinite stiffener is also based on this equation—which, apart from a different scale factor, also applies to a semi-infinite sheet with an edge stiffener—but the method of solution, i.e. the application of Mellin transforms, is quite different. It may be observed that our solution is likewise applicable to the aerodynamic load distribution over a semi-infinite wing.

2. The integro-differential equation

We consider an infinite or semi-infinite sheet (Figs. 1 and 2), loaded by

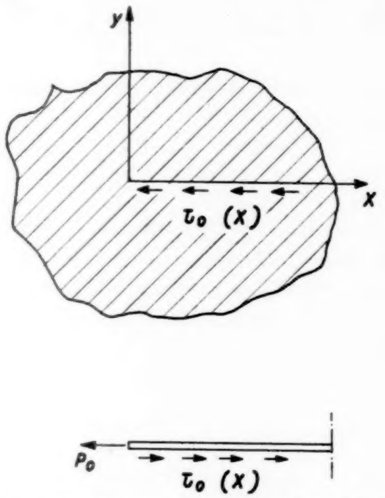

FIG. 1. Infinite sheet with semi-infinite stiffener.

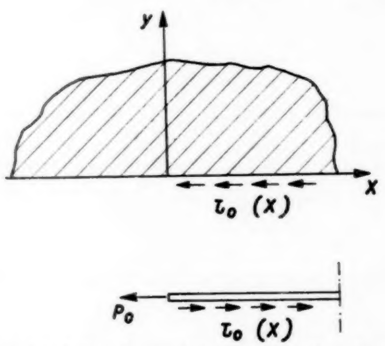

FIG. 2. Semi-infinite sheet with semi-infinite edge stiffener.

a system of continuously distributed forces over the positive x-axis and directed along the negative x-axis; these loads are applied by the stiffener and their reactions act on the stiffener together with the end load P_0. The direct strain ϵ_x along the x-axis in the sheet in the case of an *infinite sheet* is given by (**2**)

$$(\epsilon_x)_{y=0} = -\frac{(3-\nu)(1+\nu)}{4\pi E}\int\limits_0^\infty \frac{\tau_0(\xi)}{\xi-x}\,d\xi, \tag{1}$$

where the integral is defined as Cauchy's principal value, and in the case of a *semi-infinite* sheet by (3)

$$(\epsilon_x)_{y=0} = -\frac{2}{\pi E}\int\limits_0^\infty \frac{\tau_0(\xi)}{\xi-x}\,d\xi, \tag{2}$$

where E is Young's modulus and ν is Poisson's ratio. The axial strain in the stiffener is given by

$$\epsilon_{xs} = \frac{1}{E_s A_s}\Big[P_0 - h\int\limits_0^x \tau_0(\xi)\,d\xi\Big], \tag{3}$$

where E_s is Young's modulus for the stiffener, A_s is the area of the cross-section, and h is the sheet thickness. Equating expressions (1) and (3) (or (2) and (3) for a semi-infinite sheet) yields the integro-differential equation for the shear stress $\tau_0(x)$ between stiffener and sheet.

The integro-differential equation may be written in non-dimensional form by the following substitutions for an *infinite* sheet

$$\left.\begin{aligned} x &= \tfrac{1}{8}(3-\nu)(1+\nu)\frac{E_s A_s}{Eh}\bar{x}, \qquad \xi = \tfrac{1}{8}(3-\nu)(1+\nu)\frac{E_s A_s}{Eh}\bar{\xi} \\ \tau_0 &= \frac{8}{(3-\nu)(1+\nu)}\frac{P_0 E}{E_s A_s}\bar{\tau}_0 \end{aligned}\right\}, \tag{4}$$

the corresponding substitutions for a *semi-infinite* sheet are

$$x = \frac{E_s A_s}{Eh}\bar{x}, \qquad \xi = \frac{E_s A_s}{Eh}\bar{\xi}, \qquad \tau_0 = \frac{P_0 E}{E_s A_s}\bar{\tau}_0. \tag{5}$$

Dropping the bars over the non-dimensional variables, the basic integro-differential equation now reads

$$-\frac{2}{\pi}\int\limits_0^\infty \frac{\tau_0(\xi)}{\xi-x}\,d\xi + \int\limits_0^x \tau_0(\xi)\,d\xi - 1 = 0. \tag{6}$$

The additional requirement that all stresses vanish at infinity is expressed by the equation

$$\int\limits_0^\infty \tau_0(\xi)\,d\xi = 1. \tag{7}$$

3. Solution of the integro-differential equation

We multiply both sides of (6) by x^{s-1} and integrate from $x = 0$ to $x = \infty$, obtaining

$$-\frac{2}{\pi}\int\limits_0^\infty x^{s-1}\,dx\int\limits_0^\infty \frac{\tau_0(\xi)}{\xi-x}\,d\xi + \int\limits_0^\infty x^{s-1}\,dx\Big[\int\limits_0^x \tau_0(\xi)\,d\xi - 1\Big] = 0. \tag{8}$$

Formal inversion of the order of integration in the first term and integration by parts of the second term results in

$$-\frac{2}{\pi}\int_0^\infty \xi^{s-1}\tau_0(\xi)\,d\xi \int_0^\infty \frac{\eta^{s-1}}{1-\eta}\,d\eta - \frac{1}{s}\int_0^\infty x^s\tau_0(x)\,dx = 0. \tag{9}$$

Introducing the Mellin transforms (**4**)

$$T_0(s) = \int_0^\infty x^{s-1}\tau_0(x)\,dx, \tag{10}$$

$$H(s) = \int_0^\infty \frac{x^{s-1}}{1-x}\,dx, \tag{11}$$

this equation is written in the form of a difference equation with variable coefficients for the transform $T_0(s)$

$$T_0(s+1) = -\frac{2}{\pi}sH(s)T_0(s). \tag{12}$$

The foregoing formal analysis may be justified if the following assumptions are made on the behaviour of $\tau_0(x)$:

(*a*) $\tau_0(x)x^{\lambda-1}$ is $L(0,\infty)$ for all λ in a range $b < \lambda < 1$, where $0 < b < 1$;

(*b*) $|\tau_0(\xi)-\tau_0(x)| \leqslant F(x)|\xi-x|$ for all $|\xi-x| < \epsilon x$, where $\epsilon < 1$ is an arbitrarily small positive number and $F(x)x^\lambda$ is $L(0,\infty)$ for all λ in the range $b < \lambda < 1$;

(*c*) $$x^\lambda\Big[\int_0^x \tau_0(\xi)\,d\xi - 1\Big] \to 0 \quad \text{and} \quad x^\lambda\int_x^\infty |\tau_0(\xi)|\,d\xi \to 0$$

for $x \to \infty$ and $b < \lambda < 1$.

These assumptions may be verified once the solution has been obtained.

It is now obvious that integration by parts of the second term in (8) is justified by assumption (*c*) in the strip $b < \operatorname{re} s < 1$. In order to justify the inversion of the order of integration in the first term we write†

$$\int_0^\infty x^{s-1}\,dx \int_0^\infty \frac{\tau_0(\xi)}{\xi-x}\,d\xi$$

$$= \lim_{A\to\infty}\Bigg\{\int_0^A x^{s-1}\,dx \int_0^{x(1-\epsilon)} \frac{\tau_0(\xi)}{\xi-x}\,d\xi + \int_0^A x^{s-1}\,dx \int_{x(1-\epsilon)}^{x(1+\epsilon)} \frac{\tau_0(\xi)}{\xi-x}\,d\xi +$$

$$+ \int_0^A x^{s-1}\,dx \int_{x(1+\epsilon)}^{A(1+\epsilon)} \frac{\tau_0(\xi)}{\xi-x}\,d\xi + \int_0^A x^{s-1}\,dx \int_{A(1+\epsilon)}^\infty \frac{\tau_0(\xi)}{\xi-x}\,d\xi\Bigg\}, \tag{13}$$

† The author is indebted to his colleague Professor S. C. van Veen for helpful criticism of this inversion

where $0 < \epsilon < 1$. Bearing in mind that the inner integral in (8) is defined as a principal value, the inner integral in the second term is also defined as a principal value, and it follows from assumption (*b*) that the second term in (13) is bounded and of order ϵ in the strip $b < \operatorname{re} s < 1$. The last term tends to zero for $A \to \infty$ in the strip $b < \operatorname{re} s < 1$ on account of the inequality

$$\left| \int_0^A x^{s-1}\,dx \int_{A(1+\epsilon)}^{\infty} \frac{\tau_0(\xi)}{\xi - x}\,d\xi \right| < \int_0^A |x^{s-1}|\,dx \int_{A(1+\epsilon)}^{\infty} |\tau_0(\xi)|\,\frac{d\xi}{A\epsilon}$$

$$< \frac{1}{A\epsilon}\,\frac{1}{\sigma}\,A^{\sigma} \int_A^{\infty} |\tau_0(\xi)|\,d\xi, \tag{14}$$

where $\sigma = \operatorname{re} s$. In the two remaining terms the order of integration may be inverted (cf. Fig. 3). Putting $x/\xi = \eta$, we write

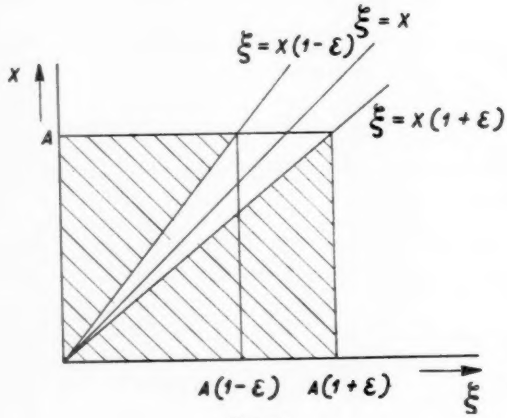

FIG. 3.

$$\lim_{A\to\infty} \left\{ \int_0^A x^{s-1}\,dx \int_0^{x(1-\epsilon)} \frac{\tau_0(\xi)}{\xi - x}\,d\xi + \int_0^A x^{s-1}\,dx \int_{x(1+\epsilon)}^{A(1+\epsilon)} \frac{\tau_0(\xi)}{\xi - x}\,d\xi \right\}$$

$$= \lim_{A\to\infty} \left\{ \int_0^{A(1-\epsilon)} \tau_0(\xi)\,d\xi \int_{\xi/(1-\epsilon)}^{A} \frac{x^{s-1}}{\xi - x}\,dx + \int_0^{A(1+\epsilon)} \tau_0(\xi)\,d\xi \int_0^{\xi/(1+\epsilon)} \frac{x^{s-1}}{\xi - x}\,dx \right\}$$

$$= \lim_{A\to\infty} \left\{ \int_0^{A(1-\epsilon)} \xi^{s-1}\tau_0(\xi)\,d\xi \int_{1/(1-\epsilon)}^{A/\xi} \frac{\eta^{s-1}}{1-\eta}\,d\eta + \int_0^{A(1+\epsilon)} \xi^{s-1}\tau_0(\xi)\,d\xi \int_0^{1/(1+\epsilon)} \frac{\eta^{s-1}}{1-\eta}\,d\eta \right\}. \tag{15}$$

The limit of the second term may be written down immediately. In order to obtain the limit of the first term, we write, with $0 < B < A$,

$$\int_0^{A(1-\epsilon)} \xi^{s-1}\tau_0(\xi)\,d\xi \int_{1/(1-\epsilon)}^{A/\xi} \frac{\eta^{s-1}}{1-\eta}\,d\eta$$

$$= \int_0^{B(1-\epsilon)} \xi^{s-1}\tau_0(\xi)\,d\xi \int_{1/(1-\epsilon)}^{A/\xi} \frac{\eta^{s-1}}{1-\eta}\,d\eta + \int_{B(1-\epsilon)}^{A(1-\epsilon)} \xi^{s-1}\tau_0(\xi)\,d\xi \int_{1/(1-\epsilon)}^{A/\xi} \frac{\eta^{s-1}}{1-\eta}\,d\eta.$$

Because $A/\xi \geqslant 1/(1-\epsilon)$, the inner integral exists, and it remains bounded for $A \to \infty$ in the strip $b < \operatorname{re} s < 1$. Therefore

$$\lim_{A\to\infty} \int_0^{A(1-\epsilon)} \xi^{s-1}\tau_0(\xi)\,d\xi \int_{1/(1-\epsilon)}^{A/\xi} \frac{\eta^{s-1}}{1-\eta}\,d\eta$$

$$= \int_0^{B(1-\epsilon)} \xi^{s-1}\tau_0(\xi)\,d\xi \int_{1/(1-\epsilon)}^{\infty} \frac{\eta^{s-1}}{1-\eta}\,d\eta + \text{remainder term},$$

where

$$|\text{remainder term}| < \int_{B(1-\epsilon)}^{\infty} |\xi^{s-1}\tau_0(\xi)|\,d\xi \int_{1/(1-\epsilon)}^{\infty} \left|\frac{\eta^{s-1}}{1-\eta}\right| d\eta.$$

If we now let B tend to infinity, the remainder term tends to zero. Hence we may write (13) in the form

$$\int_0^\infty x^{s-1}\,dx \int_0^\infty \frac{\tau_0(\xi)}{\xi-x}\,d\xi$$

$$= \int_0^\infty \xi^{s-1}\tau_0(\xi)\,d\xi \left\{ \int_0^{1/(1+\epsilon)} \frac{\eta^{s-1}}{1-\eta}\,d\eta + \int_{1/(1-\epsilon)}^{\infty} \frac{\eta^{s-1}}{1-\eta}\,d\eta \right\} + O(\epsilon)$$

$$= \int_0^\infty \xi^{s-1}\tau_0(\xi)\,d\xi \left\{ \int_0^{1-\epsilon} \frac{\eta^{s-1}}{1-\eta}\,d\eta + \int_{1+\epsilon}^{\infty} \frac{\eta^{s-1}}{1-\eta}\,d\eta \right\} + O(\epsilon). \qquad (16)$$

This result holds for ϵ arbitrarily small. If we let ϵ tend to zero, we obtain, for $b < \operatorname{re} s < 1$,

$$\int_0^\infty x^{s-1}\,dx \int_0^\infty \frac{\tau_0(\xi)}{\xi-x}\,d\xi = \int_0^\infty \xi^{s-1}\tau_0(\xi)\,d\xi \int_0^\infty \frac{\eta^{s-1}}{1-\eta}\,d\eta = T_0(s)H(s), \qquad (17)$$

where the integral $H(s)$ is again defined by Cauchy's principal value.

In order to evaluate the integral $H(s)$, we write

$$H(s) = \int_0^\infty \frac{\eta^{s-1}}{1-\eta}\,d\eta = \lim_{\epsilon\to 0} \left\{ \int_0^{1-\epsilon} \frac{\eta^{s-1}}{1-\eta}\,d\eta + \int_{1+\epsilon}^{\infty} \frac{\eta^{s-1}}{1-\eta}\,d\eta \right\}$$

and change the variable in the second integral into $\xi = 1/\eta$:

$$H(s) = \lim_{\epsilon\to 0}\left\{\int\limits_0^{1-\epsilon} \frac{\eta^{s-1}}{1-\eta}\,d\eta - \int\limits_0^{1/(1+\epsilon)} \frac{\zeta^{-s}}{1-\zeta}\,d\zeta\right\}$$

$$= \lim_{\epsilon\to 0}\left\{\int\limits_0^{1-\epsilon} \frac{\eta^{s-1}-\eta^{-s}}{1-\eta}\,d\eta - \int\limits_{1-\epsilon}^{1/(1+\epsilon)} \frac{\zeta^{-s}}{1-\zeta}\,d\zeta\right\} = \int\limits_0^1 \frac{\eta^{s-1}-\eta^{-s}}{1-\eta}\,d\eta. \quad (18)$$

Applying Legendre's formula (**5**, p. 260)

$$\int\limits_0^1 \frac{x^{s-1}-1}{x-1}\,dx = \frac{d\log\Gamma(s)}{ds}+\gamma, \quad (19)$$

where γ is the Euler–Mascheroni constant ($= 0{\cdot}5772157...$), we obtain finally

$$H(s) = -\frac{d\log\Gamma(s)}{ds}-\frac{d\log\Gamma(1-s)}{ds} = \pi\cot\pi s, \quad (20)$$

holding for $0 < \operatorname{re} s < 1$.

The difference equation (12) may now be written in the explicit form

$$T_0(s+1) = -2s\cot\pi s\, T_0(s), \quad (21)$$

holding for $b < \operatorname{re} s < 1$. The solution of this equation has to satisfy the condition that $T_0(s)$ is acceptable as the Mellin transform of $\tau_0(x)$, i.e. $T_0(s)\to 0$ for $|s|\to\infty$ in the strip $b < \operatorname{re} s < 1$. The solution obviously contains an arbitrary constant factor which may be determined from the 'boundary' condition (7), viz. $T_0(1) = 1$.

It may now be observed that $T_0(s)$, which is regular in the strip

$$b < \operatorname{re} s < 1$$

on account of assumption (a), is also regular in the wider strip

$$b < \operatorname{re} s < 2.$$

This statement is proved by considering the inverse transform in the second term of (6),

$$\int\limits_0^x \tau_0(\xi)\,d\xi - 1 = -\frac{1}{2\pi i}\int\limits_{c-i\infty}^{c+i\infty} \frac{1}{s}T_0(s+1)x^{-s}\,ds,$$

where $b < c < 1$. On the other hand, we may write

$$\int\limits_0^x \tau_0(\xi)\,d\xi = \int\limits_0^x \frac{1}{2\pi i}\int\limits_{c-i\infty}^{c+i\infty} T_0(s)\xi^{-s}\,ds = -\frac{1}{2\pi i}\int\limits_{c-i\infty}^{c+i\infty}\frac{1}{s-1}T_0(s)x^{-s+1}\,ds.$$

Writing

$$1 = \frac{1}{2\pi i}\int\limits_{c+1-i\infty}^{c+1+i\infty}\frac{1}{s-1}x^{-s+1}\,ds - \frac{1}{2\pi i}\int\limits_{c-i\infty}^{c+i\infty}\frac{1}{s-1}x^{-s+1}\,ds,$$

we may obtain the equation

$$-\frac{1}{2\pi i}\int\limits_{c-i\infty}^{c+i\infty}\frac{1}{s-1}[T_0(s)-1]x^{-s+1}\,ds = -\frac{1}{2\pi i}\int\limits_{c-i\infty}^{c+i\infty}\frac{1}{s}T_0(s+1)x^{-s}\,ds + $$
$$+\frac{1}{2\pi i}\int\limits_{c+1-i\infty}^{c+1+i\infty}\frac{1}{s-1}x^{-s+1}\,ds.$$

Writing $s+1 = s'$ in the first integral in the right-hand member and $s = s'$ in the second integral, this equation becomes

$$\int\limits_{c-i\infty}^{c+i\infty}\frac{1}{s-1}[T_0(s)-1]x^{-s+1}\,ds = \int\limits_{c+1-i\infty}^{c+1+i\infty}\frac{1}{s'-1}[T_0(s')-1]x^{-s'+1}\,ds'.$$

From a general theorem† given by Titchmarsh (**4**, art. 9.9) it now follows that $\frac{1}{s-1}[T_0(s)-1]$ is regular in the strip $c \leqslant \operatorname{re} s \leqslant c+1$ and the proof that $T_0(s)$ is regular in the strip $b < \operatorname{re} s < 2$ has been completed.

Finally, it may be stated here that the problem may also be attacked without recourse to the integro-differential equation (6). The state of stress in the sheet is governed by a stress function which satisfies the biharmonic equation. Applying the Mellin transform to this biharmonic equation and its boundary conditions ultimately results in the same difference equation (21) for the Mellin transform of the shear stress between stiffener and sheet. This alternative approach may also be used in similar problems where the kernel of the integro-differential equation is not known beforehand, e.g. for a wedge-shaped sheet with a semi-infinite stiffener. We may return to this more general problem in a later paper.

4. Solution of difference equation (21)

In order to simplify (21) we write

$$T_0(s) = 2^s\Gamma(s)\frac{1}{\sin\frac{1}{2}\pi s}y(s). \tag{22}$$

Substitution into (21) yields the equation

$$y(s+1) = \frac{\cos\pi s}{\cos\pi s-1}y(s) \tag{23}$$

with the 'boundary' condition $y(1) = \frac{1}{2}$. The factor $2^s\Gamma(s)$ in (22) has been introduced for obvious reasons. The factor $(\sin\frac{1}{2}\pi s)^{-1}$ serves to make the

† Titchmarsh formulates his theorem for Fourier transforms; its analogue for Mellin transforms is then nearly obvious.

cofactor of $y(s)$ in (23) tend to 1 as $\operatorname{im} s \to \pm\infty$ in the strip $b < \operatorname{re} s < 1$. Taking the logarithmic derivative of (23), we obtain

$$x(s+1)-x(s) = \frac{\pi \sin \pi s}{\cos \pi s(\cos \pi s - 1)} = f(s), \tag{24}$$

where

$$x(s) = \frac{1}{y(s)} \frac{dy(s)}{ds}. \tag{25}$$

Equation (24) is much simpler than (21) because it is a difference equation with *constant* coefficients and it is solved by Laplace transforms.† Assuming that $x(\sigma+i\tau)e^{\mu\tau}$ is $L(-\infty,\infty)$ in the strip $b < \sigma = \operatorname{re} s < 1$ for all μ in the range $-\pi < -d < \mu < d < \pi$, we may introduce the transforms

$$X(w) = \int\limits_{c-i\infty}^{c+i\infty} x(s)e^{sw}\, ds, \tag{26}$$

$$F(w) = \int\limits_{c-i\infty}^{c+i\infty} f(s)e^{sw}\, ds = \int\limits_{c-i\infty}^{c+i\infty} \frac{\pi \sin \pi s}{\cos \pi s(\cos \pi s - 1)} e^{sw}\, ds, \tag{27}$$

where $b < c < 1$ and $-d < v = \operatorname{im} w < d$. Equation (24) is now transformed into

$$(e^{-w}-1)X(w) = F(w)$$

with the solution

$$X(w) = -\frac{e^w}{e^w-1} F(w). \tag{28}$$

The solution of (24) is now obtained by means of the inverse transformation

$$x(s) = \frac{1}{2\pi i} \int\limits_{-\infty}^{\infty} X(w)e^{-ws}\, dw = -\frac{1}{2\pi i} \int\limits_{-\infty}^{\infty} \frac{e^w}{e^w-1} F(w)e^{-ws}\, dw, \tag{29}$$

where $b < \operatorname{re} s < 1$. It may be observed that $w = 0$ is *not* a pole of (28) because

$$F(0) = \int\limits_{c-i\infty}^{c+i\infty} \frac{d}{ds}\left[\log \frac{\cos \pi s}{\cos \pi s - 1}\right] ds = 0.$$

In fact, this is the reason why we introduced the factor $(\sin \frac{1}{2}\pi s)^{-1}$ in (22).

The general solution of (24) is now obtained by adding to (29) any function with period 1. However, such a function cannot satisfy the simultaneous requirements that it tends to zero for $|s| \to \infty$ in the strip $b < \operatorname{re} s < 1$ and that it is regular in the strip $b < \operatorname{re} s < 2$, and it must therefore be omitted.

The evaluation of $F(w)$ (27) and $x(s)$ (29) is performed by standard methods of the calculus of residues. The results are

$$F(w) = -2\pi i \frac{e^{\frac{3}{2}w}(e^{\frac{1}{2}w}-1)}{(e^{\frac{1}{2}w}+1)(e^w+1)}, \tag{30}$$

† The author is indebted to his collaborator Mr. J. B. Alblas for the suggestion that a homogeneous difference equation may take a more convenient form by applying logarithmic differentiation.

in agreement with $F(0) = 0$, and

$$x(s) = \frac{\pi}{2\sin\pi s} + \frac{\pi(3-2s)}{\sin 2\pi s}. \tag{31}$$

It is easily verified that $x(s)$ is regular in the strip $\frac{1}{2} < \operatorname{re} s < 2\frac{1}{2}$ and that it satisfies the assumptions made with the introduction of its Laplace transform. A solution of (21) with the 'boundary' condition $T_0(1) = 1$ is now given by

$$T_0(s) = \frac{2^{s-1}\Gamma(s)}{\sin\frac{1}{2}\pi s}\exp\left[\int\limits_1^s \left\{\frac{\pi}{2\sin\pi z} + \frac{\pi(3-2z)}{\sin 2\pi z}\right\} dz\right], \tag{32}$$

where $\frac{1}{2} < \operatorname{re} s < 2$ and the line of integration lies in this strip. The exponential factor is bounded for $|s| \to \infty$ in this strip and its cofactor tends to zero exponentially. Our result therefore satisfies all requirements on $T_0(s)$.

It should be noted that the solution of (21) with 'boundary' condition $T_0(1) = 1$ is not unique. In fact, alternative solutions are obtained by multiplying (32) by any function $Q(s)$ of period 1 which is regular in the strip $b < \operatorname{re} s < 2$ and equal to unity for $s = 1$. However, such a function is at least of order $e^{2\pi|s|}$ for $|s| \to \infty$ in this strip, and the alternative solutions therefore violate the requirement $T_0(s) \to 0$ for $|s| \to \infty$ in this strip. Hence (32) is the *only* solution which satisfies *all* requirements on $T_0(s)$.

The exponential factor in (32) may be expressed in Alexeiewsky's G-function, defined by (**5**, p. 264),

$$G(z+1) = (2\pi)^{\frac{1}{2}z} e^{-\frac{1}{2}z(z+1)-\frac{1}{2}\gamma z^2} \prod_{n=1}^{\infty} \left\{\left(1+\frac{z}{n}\right)^n e^{-z+z^2/2n}\right\}, \tag{33}$$

where γ is again the Euler–Mascheroni constant. We write

$$\int\limits_1^s \left\{\frac{\pi}{2\sin\pi z} + \frac{\pi(3-2z)}{\sin 2\pi z}\right\} dz$$

$$= \frac{1}{2}\int\limits_1^s \left\{\frac{\pi}{\sin\pi z} + \pi(3-2z)(\cot\pi z + \tan\pi z)\right\} dz$$

$$= \frac{1}{2}\int\limits_1^s \left\{\frac{\pi}{\sin\pi z} - 2\pi(z-1)\cot\pi z + \pi\cot\pi z + 2\pi(z-\tfrac{3}{2})\cot\pi(z-\tfrac{1}{2})\right\} dz$$

$$= \frac{1}{2}\int\limits_1^s \left\{\frac{\pi(1+\cos\pi z)}{\sin\pi z} - 2\pi(z-1)\cot\pi(z-1) + 2\pi(z-\tfrac{3}{2})\cot\pi(z-\tfrac{3}{2})\right\} dz$$

$$= \int\limits_1^s \tfrac{1}{2}\pi\frac{\cos\frac{1}{2}\pi z}{\sin\frac{1}{2}\pi z}\, dz - \int\limits_0^{s-1} \pi z'\cot\pi z'\, dz' + \int\limits_{-\frac{1}{2}}^{s-\frac{3}{2}} \pi z''\cot\pi z''\, dz'',$$

where in the second integral we have written $z-1 = z'$ and in the third integral $z-\frac{3}{2} = z''$. Applying the formula (**5**, p. 264)

$$\int_0^s \pi z \cot \pi z \, dz = \log \frac{G(1-s)}{G(1+s)} + s \log 2\pi, \tag{34}$$

we obtain after a simple reduction

$$\int_1^s \left\{ \frac{\pi}{2 \sin \pi z} + \frac{\pi(3-2z)}{\sin 2\pi z} \right\} dz = \log \left\{ \sin \tfrac{1}{2}\pi s \, \frac{G(\frac{1}{2})G(s)G(\frac{5}{2}-s)}{G(\frac{3}{2})G(2-s)G(-\frac{1}{2}+s)} \right\}. \tag{35}$$

The result (35) remains valid for all s in the complex s-plane except when the line of integration in the left-hand member passes through or ends in one of the poles of $x(s)$ defined in (31), viz. $s = 0$ or $s = 1 \pm n$ ($n = 2, 3, 4,...$) or $s = \frac{3}{2} \pm k$ ($k = 1, 2, 3,...$). Using the recurrence relation (**5**, p. 264)

$$G(z+1) = \Gamma(z)G(z), \tag{36}$$

expression (32) may now be simplified into

$$T_0(s) = \frac{2^{s-1}}{\Gamma(\frac{1}{2})} \frac{G(s+1)G(\frac{5}{2}-s)}{G(s-\frac{1}{2})G(2-s)}. \tag{37}$$

It is now easily verified that (37) indeed satisfies (21) in virtue of (36) and the gamma function formula

$$\Gamma(z)\Gamma(1-z) = \frac{\pi}{\sin \pi z}.$$

It may be observed that $T_0(s)$ is a *meromorphic* function because $G(z+1)$ is an *integral* function with n-tuple zeros $z = -n$ ($n = 1, 2, 3,...$). The poles of $T_0(s)$ are n-tuple poles $s = n+1$ ($n = 1, 2, 3,...$) and k-tuple poles $s = \frac{3}{2}-k$ ($k = 1, 2, 3,...$).

The required non-dimensional shear stress distribution between the stiffener and the sheet is now obtained by means of the inverse Mellin transform

$$\tau_0(x) = \frac{1}{2\pi i} \int_{c-i\infty}^{c+i\infty} T_0(s) x^{-s} \, ds = \frac{1}{2\pi i} \int_{c-i\infty}^{c+i\infty} \frac{2^{s-1}}{\Gamma(\frac{1}{2})} \frac{G(s+1)G(\frac{5}{2}-s)}{G(s-\frac{1}{2})G(2-s)} x^{-s} \, ds, \tag{38}$$

where $\frac{1}{2} < c < 2$. The axial load $P(x)$ in the stiffener is given by

$$\frac{P(x)}{P_0} = 1 - \int_0^x \tau_0(\xi) \, d\xi = 1 - \frac{1}{2\pi i} \int_{c-i\infty}^{c+i\infty} \frac{T_0(s)}{1-s} x^{1-s} \, ds$$

$$= 1 - \frac{1}{2\pi i} \int_{c-i\infty}^{c+i\infty} \frac{2^{s-1}}{\Gamma(\frac{1}{2})(1-s)} \frac{G(s+1)G(\frac{5}{2}-s)}{G(s-\frac{1}{2})G(2-s)} x^{1-s} \, ds, \tag{39}$$

where $\frac{1}{2} < c < 1$ and x is the non-dimensional coordinate.

5. Evaluation of solution

Evaluation of (38) and (39) by numerical integration is cumbersome. However, it will be shown that the line of integration may be closed in the left half-plane $\operatorname{re} s < c$ if the contour does not pass through any pole of (37). We take a rectangular contour with sides $\operatorname{re} s = c$, $\operatorname{re} s = -k+\frac{3}{4}$, where k is a large integer, and $\operatorname{im} s = \pm\tau$, where $\tau \to \infty$. It is easily seen from the bounds on the exponential factor in (32) that the contributions of the sides $\operatorname{im} s = \pm\tau$ tend to zero for $\tau \to \infty$. Furthermore, we write

$$\begin{aligned} T_0(s) &= \frac{2^{s-1}\Gamma(s)}{\Gamma(\frac{1}{2})}\frac{G(s)G(\frac{5}{2}-s)}{G(2-s)G(s-\frac{1}{2})} \\ &= \frac{2^{s-1}\Gamma(s)}{\Gamma(\frac{1}{2})}\exp\Bigl\{-\int_0^{s-1}\pi z\cot\pi z\,dz+(s-1)\log 2\pi+ \\ &\qquad\qquad +\int_0^{s-\frac{3}{2}}\pi z\cot\pi z\,dz-(s-\tfrac{3}{2})\log 2\pi\Bigr\} \\ &= \frac{2^{s-1}\Gamma(s)}{\Gamma(\frac{1}{2})}\exp\Bigl\{-\int_{s-\frac{3}{2}}^{s-1}\pi z\cot\pi z\,dz+\tfrac{1}{2}\log 2\pi\Bigr\}, \end{aligned} \tag{40}$$

where the exponential factor is seen to be $O(e^k)$ on the line $\operatorname{re} s = -k+\frac{3}{4}$. It is now obvious from the asymptotic expansion of the gamma function that the contribution of the side $\operatorname{re} s = -k+\frac{3}{4}$ of the rectangular contour tends to zero for $k \to \infty$.

The solution may now be written in the form of the series

$$\tau_0(x) = \sum_{k=1}^{\infty} \text{residues of } [T_0(s)x^{-s}] \text{ in } s = -k+\tfrac{3}{2}, \tag{41}$$

$$\frac{P(x)}{P_0} = 1-\sum_{k=1}^{\infty} \text{residues of } \left[\frac{T_0(s)}{1-s}x^{1-s}\right] \text{ in } s = -k+\tfrac{3}{2}, \tag{42}$$

where $T_0(s)$ is given by (37), and the series are convergent for all $x > 0$. Because $s = -k+\frac{3}{2}$ is a k-tuple pole, these series may be written in the form

$$\tau_0(x) = \sum_{k=1}^{\infty}\frac{1}{(k-1)!}\left\{\frac{d^{k-1}}{ds^{k-1}}[(s+k-\tfrac{3}{2})^k T_0(s)x^{-s}]\right\}_{s=-k+\frac{3}{2}}, \tag{43}$$

$$\frac{P(x)}{P_0} = 1-\sum_{k=1}^{\infty}\frac{1}{(k-1)!}\left\{\frac{d^{k-1}}{ds^{k-1}}\left[(s+k-\tfrac{3}{2})^k\frac{T_0(s)}{1-s}x^{1-s}\right]\right\}_{s=-k+\frac{3}{2}}. \tag{44}$$

The first few terms of the series (43) and (44) may be calculated in a straightforward manner, using the formulae

$$\frac{d}{ds}f(s) = f(s)\frac{d}{ds}\log f(s),$$

$$\frac{d^2}{ds^2}f(s) = f(s)\left[\frac{d^2}{ds^2}\log f(s)+\left\{\frac{d}{ds}\log f(s)\right\}^2\right], \quad \text{etc.}$$

By means of the recurrence relation (36) the final result for the stiffener load is obtained after some elementary but tedious algebra:

$$\begin{aligned}\frac{P(x)}{P_0} &= 1-\sqrt{\left(\frac{2x}{\pi}\right)}+\frac{x}{3\pi}\sqrt{\left(\frac{2x}{\pi}\right)}[\tfrac{5}{3}+\log 2+\psi(\tfrac{3}{2})-\log x]- \\ &\quad -\frac{x^2}{30\pi^2}\sqrt{\left(\frac{2x}{\pi}\right)}[-\tfrac{1}{2}\pi^2+\tfrac{4}{25}-\psi'(\tfrac{5}{2})+\{\tfrac{7}{5}+\log 2+\psi(\tfrac{5}{2})-\log x\}^2]+\dots \\ &= 1-\sqrt{\left(\frac{2x}{\pi}\right)}[1-x(0{\cdot}25425-0{\cdot}10610\log x)+ \\ &\quad +x^2\{0{\cdot}0086265-0{\cdot}018888\log x+0{\cdot}0033774(\log x)^2\}+\dots], \qquad (45)\end{aligned}$$

where $\psi(z)$ is the logarithmic derivative of the gamma function, and dashes denote differentiations.

The series in (45) is rapidly convergent when x is not too large, say $x < 2$, as may be seen from Fig. 4, where the curves a, b, c show the result by taking consecutively 1, 2, or 3 terms of the series between brackets in (45). It should be noted that between x around 0·5 and x around 1·5 the curve c lies below curve b, the maximum difference being approximately 2 per cent., and that from a value of x slightly above 1·5 curve c lies above curve b, the difference becoming important for $x > 2$. For large x the convergence is slow and the series (43) and (44) are not convenient for numerical computations. In fact, it appears that for x between, say, 2·5 and 5 the approximation by three terms between brackets in (45), curve c, shows even larger errors than the approximation by two terms, curve b.

However, a useful approximation for large x is obtained from the asymptotic expansion, deduced from (39) by contour integration in the half-plane re $s > c$. The first few terms of this expansion are readily written down as the residues in the simple poles $s = 1$ and $s = 2$ and in the double pole $s = 3$. The resulting asymptotic approximation for large x is

$$\frac{P(x)}{P_0} = \frac{2}{\pi x}-\frac{4}{\pi^2 x^2}(\log 2-\gamma-\log x)+\dots. \qquad (46)$$

This result, retaining one or two terms in (46), is also depicted in Fig. 4 (curves d and e), and it is obvious that a satisfactory result for all $x > 0$ is obtained by linking the convergent expansion for small and moderate x with the asymptotic expansion for large x. This link has been drawn in Fig. 4 (curve f); the maximum possible error is estimated to be at most a few per cent.

A comparison with Buell's results shows very satisfactory agreement. Buell's curve for the stiffener load agrees with curve f in Fig. 4 within a few per cent. Our solution may serve to judge whether the number of unknown coefficients $b_n/\overline{P}$ (notation of (1)) retained by Buell is adequate.

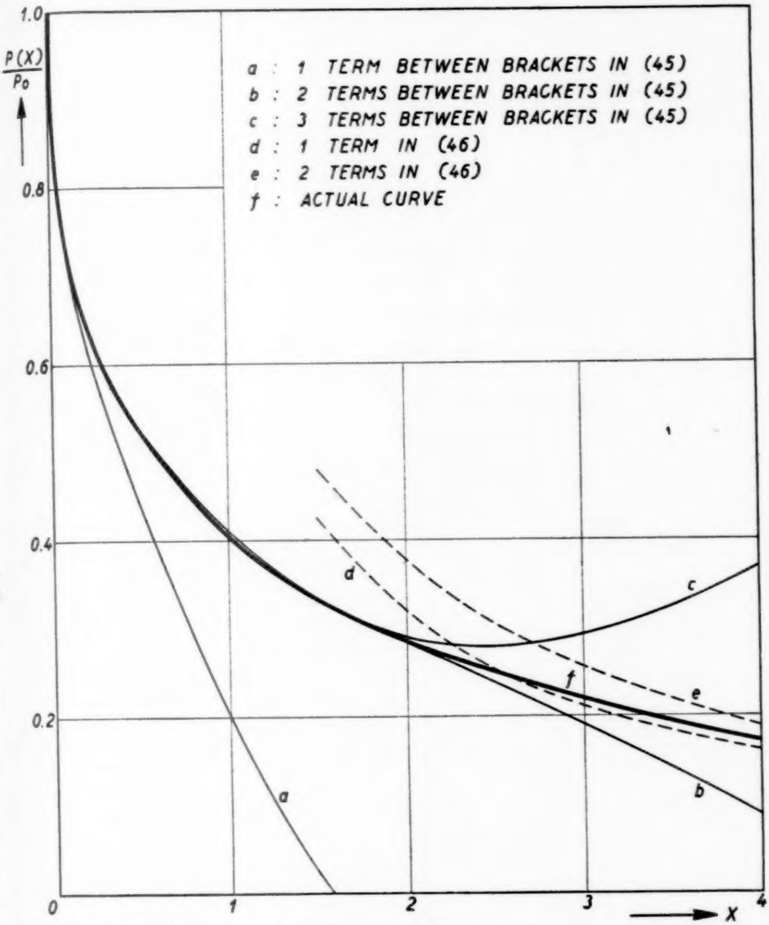

FIG. 4. The stiffener load as a function of the non-dimensional coordinate.

According to his solution the first two terms corresponding with our expansion (45) are (**1**, equation (42))

$$\frac{P(x)}{P_0} = 1-\sqrt{x}\left[\frac{2}{\pi}+\frac{2}{\pi}\sum_{n=1}^{\infty}\frac{n\pi b_n}{\overline{P}}\right]. \tag{47}$$

The equivalence of (47) with the first two terms in (45) requires

$$\sum_{n=1}^{\infty}\frac{n\pi b_n}{\overline{P}} = \sqrt{(\tfrac{1}{2}\pi)}-1 = 0{\cdot}253314. \tag{48}$$

Buell has solved his infinite system of equations approximately by retaining at most six equations and the first six coefficients. His result yields

$$\sum_{n=1}^{6} \frac{n\pi b_n}{P} = 0{\cdot}247108,$$

indicating an error in the verification of (48) of around 2·5 per cent.

Finally it may be remarked that the numerical work required for evaluation of the present rigorous solution is negligible in contrast to Buell's approximate solution. Howevei, this reduction in numerical computations has been bought at the expense of considerably more analytical work, involving more advanced methods.

Note added 8 March 1955

A. Pflüger ('Halbscheibe mit Randglied', *Zeitschr. f. angew. Math. u. Mech.* 25/27 (1947), 177) has also observed, independently from Benscoter, that the basic integro-differential equation is formally identical with Prandtl's equation.

REFERENCES

1. E. L. Buell, 'On the distribution of plane stress in a semi-infinite plate with partially stiffened edge', *J. Math. and Phys.* **26** (1948), 223.
2. S. U. Benscoter, 'Analysis of a single stiffener on an infinite sheet', *J. Applied Mech.* **16** (1949), 242.
3. S. Timoshenko and J. N. Goodier, *Theory of Elasticity*, 2nd ed. (McGraw-Hill, 1951), art. 33.
4. E. C. Titchmarsh, *Theory of Fourier Integrals* (Oxford, 1937).
5. E. T. Whittaker and G. N. Watson, *Modern Analysis*, 4th ed. (Cambridge, 1927).

ng

for
to
om-
ical

. *u.*
ter,
vith

with

plied

-Hill,

idge,